

**Design, Synthesis and Pharmacological
Evaluation of Chromone Hydrazones and their
Transition Metal Complexes**

Thesis submitted to
Cochin University of Science and Technology
in partial fulfillment of the requirements
for the award of the degree of
Doctor of Philosophy
in
Chemistry
Under the Faculty of Science

by

Jessica Elizabeth Philip
(Reg. No: 4359)



Department of Applied Chemistry
Cochin University of Science and Technology
Kochi - 22

April 2018

Design, Synthesis and Pharmacological Evaluation of Chromone Hydrazones and their Transition Metal Complexes

Ph.D. Thesis under the Faculty of Science

By

Jessica Elizabeth Philip

Research Fellow

Department of Applied Chemistry

Cochin University of Science and Technology

Kochi, India 682022

Email: jessicaep25@gmail.com.

Supervising Guide

Dr. P.V. Mohanan

Assistant Professor

Department of Applied Chemistry

Cochin University of Science and Technology

Kochi, India 682022

Email: *pvmohanan@gmail.com, mohan@cusat.ac.in*

Department of Applied Chemistry

Cochin University of Science and Technology

Kochi, India 682022

April 2018

**DEPARTMENT OF APPLIED CHEMISTRY
COCHIN UNIVERSITY OF SCIENCE AND TECHNOLOGY
KOCHI - 682022, INDIA**

Dr. P. V. Mohanan
Assistant Professor



Ph: 0484-2575804
Fax: 0484-2577595
E-mail: pvmohanan@gmail.com
mohan@cusat.ac.in

Certificate

This is to certify that the thesis entitled “**Design, Synthesis and Pharmacological Evaluation of Chromone Hydrazones and their Transition Metal Complexes**” submitted by **Mrs. Jessica Elizabeth Philip**, in partial fulfillment of the requirements for the degree of Doctor of Philosophy, to the Cochin University of Science and Technology, Kochi-22, is an authentic record of the original research work carried out by her under my guidance and supervision. The results embodied in this thesis, in full or in part, have not been submitted for the award of any other degree. All the relevant corrections and modifications suggested by the audience and recommended by the doctoral committee of the candidate during the presynopsis seminar have been incorporated in the thesis.

Kochi-22
07/04/2018


Dr. P. V. Mohanan
(Supervising Guide)

Declaration

I hereby declare that the work presented in this thesis entitled “**Design, Synthesis and Pharmacological Evaluation of Chromone Hydrazones and their Transition Metal Complexes**” is entirely original and was carried out by me independently under the supervision of **Dr. P. V. Mohanan**, Department of Applied Chemistry, Cochin University of Science and Technology and has not been included in any other thesis submitted previously for the award of any other degree.

Kochi-22
07/04/2018

Jessica Elizabeth Philip



The LORD is my strength and shield.
I trust him with all my heart.
He helps me, and my heart is filled with joy.
I burst out in songs of thanksgiving.

Psalm 28:7

*“I Command You
Be Strong and Courageous!
Do not be Afraid or Discouraged
For the Lord your God is with you
Wherever you Go”*

[Joshua 1:9]

Dedicated to Jesus Christ.....

Acknowledgement

*This research work could be conducted only by cooperation and blessings of many people who have come along my life. I take this opportunity with much pleasure to remember all those people who have helped me through the course of my journey towards bringing out this thesis. First of all I stoop before my **Lord Almighty** for paving my way into the field of research and for the grace shown to me for completing this work. Thank you for sharing all those wonderful people with me and for showing me your love and care through them.*

*The person to whom I am greatly indebted is my supervising guide **Dr. P. V. Mohanan** for providing me an opportunity to work in his group. According to my conception, the most important factor in research is to get a right person as a guide. I being fortunate enough to have a guide like him would thank him for his inspiration, motivation, guidance and valuable suggestions. Apart from my research, it was a great learning experience for me. Which I am sure, will be useful in different stages of my life. His simplicity, patience, management skills, behaviour towards colleagues and students inspired me a lot. Sir, I consider it as a blessing to work under you with heart full of sincerity and love I extend my gratitude towards you. I shall always cherish this association.*

I would like to express my sincere gratitude to Prof. K. Girish Kumar (Head of the Department), my doctoral committee member, for his timely suggestions and support. I am very much obliged to Prof. K. Sreekumar and Dr. N. Manoj Former Heads for providing me the research facilities in the Department.

My studies would not have become fruitful without the helping hand of Prof. M. R. Prathapachandra Kurup has offered unreserved help and suggestions. I remember with gratitude Dr. K. K. Muhamad Yusuff, Dr. S. Sugunan, Dr. S. Prathapan, Dr. P. M. Sabura Begum, Dr. P. A. Unnikrishnan, Dr. Suja Haridas, Dr. Sebastian Nybin Remello, Dr. Susmita De, Dr. R. Kala and Dr. R. Leena for their valuable suggestions and constructive criticism. I am really thankful for the cooperation received from all the Faculty members. At this stage I cannot forget the services of the non-teaching staff of this Department. I also

extend my gratitude to UGC for providing me the financial assistance for carrying out the research work. I thank Sophisticated Test and Instrumentation Centre (STIC), CVSAT and IIT Bombay to aid in various analysis.

Research work is always a concerted effort. I would like to thank Dr. Toms C. Joseph, Principal Scientist, Microbiology, fermentation & Biotechnology Department, and Joshy chetten, Scientist, Fish Processing Department, Central Institute of Fisheries Technology, Indian Council of Agricultural Research (ICAR) Kochi, for providing me the facilities to carry out the antimicrobial studies of our samples without any delay. I owe my thanks to Dr. K. G. Raghu, Principal Scientist, Agro-Processing and Technology Division, National Institute for Interdisciplinary Science and Technology (NIIST), Council of Scientific & Industrial Research (CSIR) Trivandrum, for helping me in executing cytotoxicity studies.

It has been an exciting, fruitful and enjoyable experience for me to spend at the Bioinorganic Chemistry lab. I am sure it will become one of the most treasured memories of my life. No words can suffice to acknowledge the friendly and stimulating atmosphere created by my labmates. My sincere thanks to all my seniors Dr. Priya and Dr. Navya, they helped me at the initial stage of my research through their mentoring and caring. I expand my thanks to my lab colleagues Shanty chechi, Divya chechi, Maria chechi, sneha, Bindu chechi, Geetha, Liz, Savitha and Anjaly, for creating a stimulating and fun filled environment.

A person who is not your blood relation, but who cares for you, hears you, supports you and fights with you - Sneha, you're more like a sister for me. Our discussions on research topics, friendly fighting and debates - when I think that these are going to end, fills me with a deep sense of pain. I have had many highs and lows especially during the last phase of my research life and every time I needed a shoulder to bank, you were there for me. You're just great. I'm sure my job would not take its final shape without Sneha's team effort.

I especially thank Shanty chechi (Dr. Shanty) for her encouragement, valuable suggestions and moral support. I admire her loving and helping nature. I gratefully recall the countless splendid memories of Mrs. Vineetha, Mrs. Ligi,

Midhun chetten and research scholars of polymer lab for supporting me to complete my research work, I also remember with affection the support and help from Ms. Letcy. I would extend my heartfelt thanks to my dear Letcy.

There are two important persons in my life – Friends who squeezed time in between their busy schedule just to comfort me; friends who always wanted and wished the best for me; who have confidence in me; who rendered their hand whenever needed, whom I can call at any time; with whom I need not be conscious while conversing – my besties, dearest Sariqa (SIF CUSAT) and Nayana (Biotechnology CUSAT)... your presence made the hostel hours worth remembering. You are my left and right, who balanced me throughout to reach my goal.

Where would I be without my family? My Mummy and Daddy who deserve special mention for their unconditional love and support, for giving life in the first place, for educating me, with all the opportunities they could provide to explore my potentials and pursue my dreams ever since I was a child. As a typical parent, they worked industriously to support the family and did not spare any effort to provide the best possible environment for educating me. Mummy being my first teacher sincerely has put the fundamental learning character, showing me the joy of intellectual pursuit ever since I was a child. She laid a strong foundation with utmost care. My amazing brothers and sister in law are always a source of love and energy. They have also given me so many happy and beautiful memories throughout this journey. My brothers have been my best friends all my life and I thank them for their support. And I specially thank my younger brother, Justin (Unnikuttan) for understanding the awe and agony that underpins the doctoral life span. Thanks a lot for teaching me the important lessons of life. Words cannot express how grateful I am to my in laws, for all the love, sacrifice and caring that has made on my behalf.

Words are insufficient to express my gratitude to my beloved husband, Tonychayan for his endless love, all-out support and understanding. His motivation and encouragement helped me a lot to complete this journey. His careful editing and inspiring suggestions contributed enormously to the formation of this thesis. Completion of this thesis would not have been possible without the encouragement and understanding of my family. I am so blessed to be a part of such a family.

This script of acknowledgement would be incomplete if I don't make a special mention of my baby who is waiting to step into this world soon. Words won't be enough to explain my happiness and his presence has made me comfortable to carve my thesis into the best possible way.

Finally, I would like to thank everyone who is important to the successful realization of thesis, as well as expressing my apology that I could not mention personally one by one.

*Above all my deepest gratitude to **God** for continuously looking after me despite my flaws and guide me through.*

Jessica Elizabeth Philip

||| Preface |||

In recent years, the field of metal-based drug has experienced an impressive renaissance. The chemistry of the transition elements is largely concerned with the study of their coordination compounds. Academic and industrial research in coordination chemistry is flourishing and the output of research papers and reviews is growing exponentially. In addition to the various applications in the applied science, 'Complex Chemistry' plays vital roles in the chemistry of living matter. The work performed presents a comprehensive analysis of the chemistry of some transition metals like Ni, Cu & Zn (II) complexes of novel ligands 3-formyl chromone hydrazones that are of interest as biological point of view. In the present investigation, new ligands and their transition metal complexes are prepared and characterized. The characterization and elucidation of the structure of the prepared compounds were performed by elemental analysis, FTIR, $^1\text{H}/^{13}\text{C}$ -NMR, electronic, AAS, EPR, ESI-MS data and thermo gravimetric analyzes, as well as conductivity and magnetic susceptibility measurements. Ni, Cu & Zn (II) are the metal ions used for the complexation. The procedure for carrying out the biological activities like antibacterial and antifungal studies and their methodology were also discussed. Preliminary *in vitro* antimicrobial activities of the ligands and their metal complexes have been carried out in order to understand the toxicity of ligands and metal complexes against microbes, 3T3-L1 normal cells. The materials, methods and instruments used for the cytotoxicity study, α -amylase and α -glucosidase inhibition, and DNA binding were described.

For the sake of brevity, symbols have been used in this thesis, which is given in the abbreviations at the end of thesis. A detailed list of references arranged in serial order is given at the end of each chapter. The research work presented in this thesis has partly been published/ under publication as indicated at the end of thesis.

The aim of this work was the development of new Ni, Cu & Zn (II) complexes and we interested the interaction of metal (II) complexes with different derivatives of 3-formyl chromones. We have been interested in the relationship between compounds (ligands and their metal complexes) because large numbers of flavones are exhibit anti-proliferative effects against breast cancer cells.

In the present study, we synthesized eight different 3-formyl chromone hydrazones and their transition metal complexes showing antimicrobial activities, α -amylase and α -glucosidase inhibition and DNA binding.

The first chapter introduces the historical background of metal-based drugs, anticancer agents based on metal complexes and 3-formyl chromones are explained in detail. In the second chapter, a detailed account full characterization of all ligands using elemental analysis, FTIR, $^1\text{H}/^{13}\text{C}$ -NMR, ESI-MS and UV-Vis techniques. In third chapter, a detailed account full characterization of metal complexes using elemental analysis, FTIR, $^1\text{H}/^{13}\text{C}$ -NMR, electronic, AAS, EPR and thermo gravimetric analyzes, as well as conductivity and magnetic susceptibility measurements. Chapter IV deals with the antimicrobial activities of ligands and their metal (II) complexes. Chapter V contains DNA interaction studies by absorption titration and viscosity measurements of newly synthesized metal (II) complexes of 3-formyl chromones. Chapter VI includes Study of *in-vitro* Inhibition of α -amylase and α -glucosidase by chromone hydrazones and their Ni (II), Cu (II) and Zn (II) complexes. In chapter VII consists of cytotoxicity studies of all metal complexes and their ligands.

Contents

Chapter 1

A Brief Prologue to Chromone Hydrazones and their Transition Metal Complexes 01 - 56

1.1	Introduction.....	01
1.2	Outline of the systems employed in our study.....	02
1.2.1	Hydrazones	02
1.2.1.1	Bonding and diversity in the chelating behavior of hydrazones	05
1.2.2	Chromone hydrazones	08
1.2.3	Choice of Metals	10
1.3	Application of metal complexes of chromone hydrazones	12
1.3.1	Pharmacological activities of the chromone analogs.....	12
1.3.1.1	Anti-cancer agents.....	13
1.3.1.2	Anti-HIV agents	13
1.3.1.3	Anti-oxidant agents	14
1.3.1.4	Anti-tubercular agents	16
1.3.1.5	Anti-inflammatory and Analgesic agents	16
1.3.1.6	Anti-microbial agents	17
1.3.1.7	Anti-diabetic agents.....	19
1.3.2	DNA binding of metal complexes	20
1.3.2.1	Covalent binding	23
1.3.2.2	Electrostatic binding.....	24
1.3.2.3	Groove binding.....	24
1.3.2.4	Intercalation.....	25
1.3.3	Enzyme inhibition studies.....	27
1.3.3.1	Factors affecting enzyme activity.....	28
1.3.3.1.1	Substrate concentration	28
1.3.3.1.2	Enzyme concentration	28
1.3.3.1.3	Product concentration	29
1.3.3.1.4	Temperature	29
1.3.3.1.5	Hydrogen ion concentration (pH)	29
1.3.3.1.6	Presence of activators	30
1.3.3.1.7	Presence of inhibitors.....	30
1.3.3.2	Why are enzyme inhibitors important?	30
1.3.3.3	The active site.....	31
1.3.3.4	How to determine K_m and V_{max} : Lineweaver-Burk Plot	34
1.3.3.5	Classification of enzyme inhibitors	35
1.3.3.5.1	Reversible inhibitors.....	36
1.3.3.5.1.1	Competitive inhibitors.....	37
1.3.3.5.1.2	Noncompetitive inhibitors	38

1.4	Scope and objectives of the present study	40
1.5	Physical measurements.....	41
1.5.1	Elemental analysis.....	41
1.5.2	Conductivity measurements	42
1.5.3	Magnetic susceptibility measurements	42
1.5.4	Infrared spectroscopy	43
1.5.5	Electronic spectroscopy	43
1.5.6	NMR spectroscopy.....	45
1.5.7	Mass spectroscopy.....	45
1.5.8	EPR spectroscopy.....	46
1.5.9	Thermal analysis	47
	References.....	49

Chapter 2

Synthesis and Spectral Characterization of ONO/NO Donor Chromone Hydrazones 57 - 85

2.1	Introduction.....	58
2.2	Materials and Methods	59
2.2.1	Synthesis of 3-formyl chromone hydrazones.....	59
2.2.1.1	Synthesis of hydrazone derived from 3-formyl chromone and benzhydrazide (FB)	59
2.2.1.2	Synthesis of hydrazone derived from 3-formyl chromone and 4-hydroxybenzhydrazide (FBH)	60
2.2.1.3	Synthesis of hydrazone derived from 3-formyl chromone and nicotinic hydrazide (FN).....	60
2.2.1.4	Synthesis of hydrazone derived from 3-formyl chromone and isonicotinic hydrazide (FIN).....	61
2.2.1.5	Synthesis of hydrazone derived from 6-methyl-3- formyl chromone and benzhydrazide (FMB)	61
2.2.1.6	Synthesis of hydrazone derived from 6-methyl-3- formyl chromone and 4-hydroxybenzhydrazide (FMBH)	62
2.2.1.7	Synthesis of hydrazone derived from 6-methyl-3- formyl chromone and nicotinic hydrazide (FMN).....	62
2.2.1.8	Synthesis of hydrazone derived from 6-methyl-3- formyl chromone and isonicotinic hydrazide (FMIN)	63
2.3	Result and Discussion.....	64
2.3.1	Characterizations of 3-formyl chromone hydrazones.....	64
2.3.1.1	Elemental analysis.....	64
2.3.1.2	Mass spectra	65
2.3.1.3	FT-Infrared spectra.....	68
2.3.1.4	Electronic spectra	70

2.3.1.5 NMR spectra.....	72
2.3.1.5.1 ¹ H NMR spectra	72
2.3.1.5.2 ¹³ C NMR spectra	78
2.4 Conclusion	83
References.....	83

Chapter 3

Synthesis and Spectral Characterization of Ni (II), Cu (II) & Zn (II) complexes of ONO/NO

Donor Chromone Hydrazones.....87 - 146

3.1 Introduction.....	88
3.1.1 Importance of Ni (II), Cu (II) and Zn (II) complexes	88
3.2 Materials and Methods	91
3.2.1 Materials	91
3.2.2 Synthesis of ligands	91
3.2.3 Synthesis of complexes	92
3.3 Result and Discussion.....	92
3.3.1 Elemental analysis and AAS.....	92
3.3.2 Molar conductivity and magnetic susceptibility measurements.....	95
3.3.3 FT-Infrared spectra.....	98
3.3.4 Electronic spectra	106
3.3.5 Electron paramagnetic resonance spectra	116
3.3.6 Thermo gravimetric analysis.....	123
3.3.7 ¹ H NMR spectra	132
3.3.8 Geometry of the complexes	137
3.4 Conclusion	141
References.....	141

Chapter 4

Antimicrobial Activity of Chromone Hydrazones

and their Ni (II), Cu (II) and Zn (II) Complexes 147 - 177

4.1 Introduction.....	148
4.1.1 Metal (II) Complexes used for study - Ni, Cu and Zn.....	150
4.1.2 Bacterial and Fungal Species used for study.....	151
4.1.2.1 <i>Staphylococcus aureus</i>	151
4.1.2.2 <i>Bacillus subtilis</i>	152
4.1.2.3 <i>Pseudomonas aeruginosa</i>	152
4.1.2.4 <i>Escherichia coli</i>	153
4.1.2.5 <i>Candida albicans</i>	154
4.2 Materials and Methods	154

4.2.1	Bacterial and Fungal cultures	154
4.2.2	Maintenance of cultures.....	155
4.2.3	Growth conditions and media	155
4.2.4	<i>In Vitro</i> Antimicrobial evaluation	155
4.2.4.1	Agar diffusion method.....	155
4.2.4.2	Time Kill Kinetic studies.....	156
4.2.4.3	Minimum Inhibitory Concentration (MIC) - Resazurin based Microtiter Dilution Assay (RMDA)	157
4.3	Result and Discussion.....	158
4.4	Conclusion	174
	References.....	174

Chapter 5

DNA Interaction Studies by Absorption Titration and Viscosity Measurements 179 - 204

5.1	Introduction.....	180
5.2	Materials and Methods	183
5.2.1	Preparation of DNA stock solution	183
5.2.2	DNA binding experiments	183
5.2.2.1	Electronic absorption spectral titration	183
5.2.2.2	Viscosity measurement	185
5.3	Result and Discussion.....	186
5.3.1	Electronic absorption studies	186
5.3.2	Viscosity measurement	197
5.4	Conclusion	201
	References.....	201

Chapter 6

Study of *In Vitro* Inhibition of α -Amylase and α -Glucosidase by Chromone hydrazones and their Ni (II), Cu (II) and Zn (II) complexes 205 - 231

6.1	Introduction.....	206
6.1.1	Importance α -amylase enzyme in the body	210
6.1.2	Importance of α -glucosidase enzyme in the body	211
6.1.3	α -Amylase inhibitors	211
6.1.4	α -Glucosidase inhibitors	211
6.2	Materials and Methods	212
6.2.1	Determination of enzyme activity	213
6.2.1.1	Alpha-amylase inhibition assay	213
6.2.1.1.1	Alpha-amylase enzyme solution	213

6.2.1.1.2	Sodium phosphate buffer (0.02 M), pH 6.90 with 0.006 M sodium chloride	213
6.2.1.1.3	Dinitrosalicylic acid (DNSA) reagent	214
6.2.1.1.4	1% starch solution	214
6.2.1.1.5	Determination of alpha-amylase inhibitory activity	214
6.2.1.1.6	Determination of kinetic parameters	215
6.2.1.2	Alpha-glucosidase inhibition Assay	216
6.2.1.2.1	Alpha-glucosidase enzyme solution	216
6.2.1.2.2	0.02M sodium phosphate buffer (pH 6.90)	216
6.2.1.2.3	5mM p-nitrophenyl-D-glucopyranoside substrate solution	216
6.2.1.2.4	Determination of alpha-glucosidase inhibitory activity	216
6.2.1.2.5	Determination of kinetic parameters.....	217
6.3	Result and Discussion.....	218
6.3.1	Antidiabetic activity-Enzyme Inhibition of α -amylase & α -glucosidase	218
6.3.2	Mode of enzyme inhibition	223
6.4	Conclusion	229
	References.....	229

Chapter 7

Cytotoxicity studies of Chromone hydrazones

and their Ni (II), Cu (II) and Zn (II) Complexes..... 233 - 245

7.1	Introduction.....	234
7.1.1	Importance of MTT assay.....	237
7.2	Materials and Methods	238
7.2.1	Materials	238
7.2.2	MTT Assay	238
7.3	Result and Discussion.....	240
7.4	Conclusion	243
	References.....	243

Chapter 8

Summary and Conclusion..... 247 - 253

Publications 255 - 258

Abbreviations 259 - 261

Chapter 1

A BRIEF PROLOGUE TO CHROMONE HYDRAZONES AND THEIR TRANSITION METAL COMPLEXES

<i>Contents</i>	1.1 <i>Introduction</i>
	1.2 <i>Outline of the systems employed in our study</i>
	1.3 <i>Application of metal complexes of chromone hydrazones</i>
	1.4 <i>Scope and objectives of the present study</i>
	1.5 <i>Physical measurements</i>

1.1 Introduction

The present study of coordination compounds commences with Alfred Werner, first inorganic chemist, awarded the Noble prize for chemistry in 1913[1]. It is continuously matured as bioinorganic chemistry. These days, coordination complexes are involved in a wide range of applications as homo/ heterogeneous catalysts, [2] semiconductor film precursors and nano particles [3]. In the field medicine they are used as image-fixing and chemotherapeutic agents [4] etc. The combinatorial approach to the discovery of new chemotherapeutic agents and catalysts is currently an innovative and exciting field of research. Metals play an essential role in a large number of expansively diverse biological activities. Some of these processes are rather specific in their metal ion requirements, only some metal ions in specific oxidation states can meet

the essential catalytic structural requirements. Processes associated to metal ions are found throughout the science and differ enormously in their function and complexity. Now we realize that metal ions manage a wide range of processes in biology. Numerous innovative and breathtaking developments in the area of biochemistry have created attention in inorganic chemists to introducing in the new field called “Bioinorganic Chemistry”. Biomedical inorganic chemistry is a new important area of chemistry offers a new design for potential diagnostic and therapeutic agents. Bioinorganic chemistry is to discover new methods and design for coenzyme with properties to mimic the functional properties of natural metalloproteins [5]. Metal ions are present in vitamins, proteins and enzymes having macromolecular ligands. The chemistry of metal complexes with multidentate ligands having delocalized orbitals, such as Schiff bases, hydrazones or porphyrins has recently gained more attention due to their use as models in biological systems.

1.2 Outline of the Systems Employed in our Study

1.2.1 Hydrazones

Coordination complexes are formed by ligands that have various donor sites generally heterocyclic rings, for example: NNO or NNS. Among the ligands hydrazone playing a significant role since coordination complexes of these compounds are at present extensively used for the treatment of numerous diseases, in analytical and synthetic chemistry as heterogeneous catalysts in the oxidation-reduction reaction process and a variety of chemical, photochemical reactions as well as different industrial significance in the field of science and technology [6-10].

Hydrazones are obtained by the condensation reaction of carbonyl compounds such as ketones or aldehydes with hydrazides. The substituted hydrazones are formed from the reaction between substituted carbonyl compounds and hydrazides. The general formula for an acylhydrazone is shown in Figure 1.1.

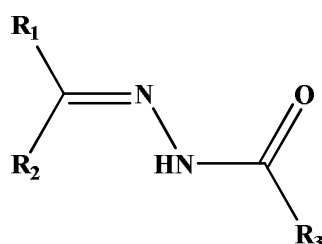
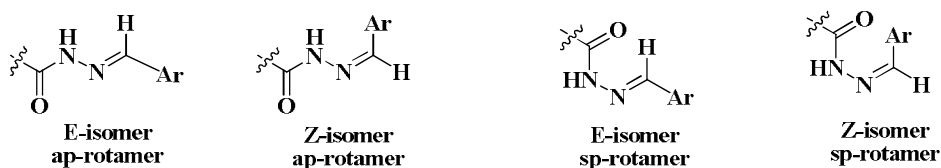


Figure 1.1 General formula for an acylhydrazone.

Hydrazones are an extremely old category of compounds, firstly reported in 1850 [11] by the synthesis of N-acylhydrazone. Now large number of mono or di substituted hydrazones are common. Hydrazones are extremely reactive nitrogen containing versatile compound, used as intermediates and precursors of many organic molecules such as pharmaceuticals, heterocycles, polymers and photographic products, etc. [12]. A huge number of cyclic or acyclic hydrazones shows chemiluminescence [13]. Due to wide variety of biological and promising pharmacological activities of hydrazones, they are extensively studied in the current scenario [14-17]. They are formed by simply refluxing different carbonyl compounds with acid hydrazide (AH) in methanol or ethanol. Because of these simpler reaction conditions, expanded chemical libraries can be created to discover numerous prospective bioactive molecules. In hydrazones newly formed C=N bond constitute to the geometric isomeric form such as syn and anti. Geometric isomerism can

have a choice of vital functions in the bioactivity of hydrazones, so their studies are tremendously essential for developing synthetic methods for the selective synthesis of a particular isomer.

N-acylhydrazones having general formula $\text{ArCONHN}=\text{C}(\text{R})\text{Ar}'$. Hydrazones containing azomethine $-\text{CH}=\text{NNH}-$ hydrogen are formed from the reaction of carbonyl compounds with acid hydrazide or in different solvents or in solvent-free conditions. Most of all, the acylhydrazone derivatives can exist in four possible forms because of the collective effect of the configurational stereochemistry E and Z as well as of conformational stereoisomers or rotamers i.e antiperiplaner (ap) and syn periplaner conformers (sp).

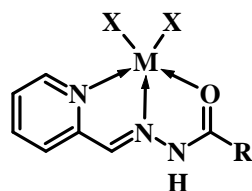


The substituted hydrazones have an extensive variety of biological applications, such as antimicrobial, anti-convulsant, analgesic, anti-inflammatory, anti-tuberculosis, anti-platelet, antiviral, anti-HIV and anti-tumor activity [18-19]. An Isonicotinic acid hydrazide (INH) derivative is used as anti-tuberculosis medicine in deterrence or treatment and also has an antidepressant effect. It was one of the first antidepressants discovered. It has high *in vivo* inhibitory activities against *M. tuberculosis* H37Rv. INH hydrazones have inhibitory activity in mice infected with various *M. tuberculosis* strains. Hydrazones show less toxicity than hydrazides because the $-\text{NH}_2$ group is blocked. These findings further support the

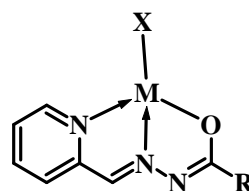
increasing significance of the synthesis of hydrazide-hydrazones compound [20-22]. Nifuroxazide (INN), 4-hydroxy-*N'*-[(5-nitrofur-2-yl)methylene] benzohydrazide is an oral hydrazone based nitrofuran antibiotic used to treat colitis and diarrhea.

1.2.1.1 Bonding and diversity in the chelating behaviour of hydrazones

The coordination mode present in hydrazones are depend on numerous factors such as reaction conditions, tautomerism, the stability of the complex formed and the number or type of substituent present in hydrazones. The donor sites present in hydrazones are amide oxygen and azomethine nitrogen. In addition to this, if the carbonyl part contains a hetero atom, the hetero atom can coordinate with the center to form a tridentated ligand. Because of the tautomerism in the hydrazones, the amide oxygen can be in the form of keto (Structure I) or in enol form (Structure II).



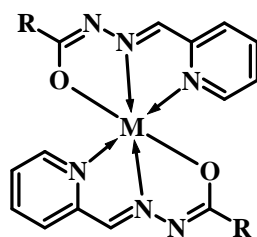
Structure (I)



Structure (II)

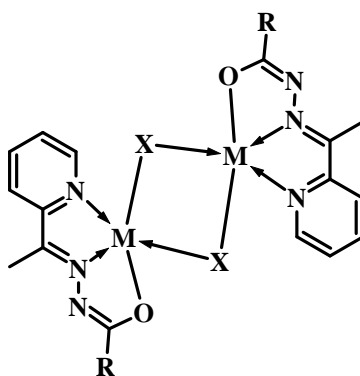
The actual ionization state depends on the condition and the metallic salts used. In the basic solution the amide is deprotonated and coordinates the center of the metal in an enol form while the strongly acidic conditions favour the compounds formulated with a neutral ligand.

In some cases there is a possibility in which two deprotonated ligands coordinate at the same metal center giving rise to six coordinate distorted octahedral complexes. These types of complexes have greater stability due to chelation.



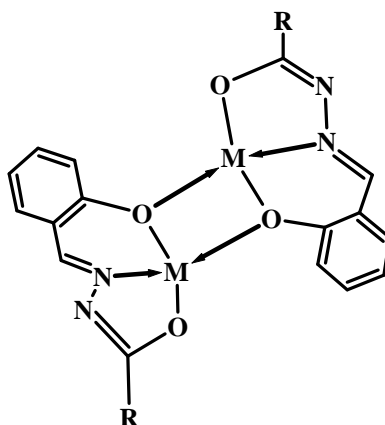
Structure (III)

In number of cases hydrazones appeared as bridged complexes. It is due to that an atom or group of atom may act as bridging ligand which leads to the formation of dimer. Usually halogens, azide and thiocyanate ligands can act as these types of bridges.



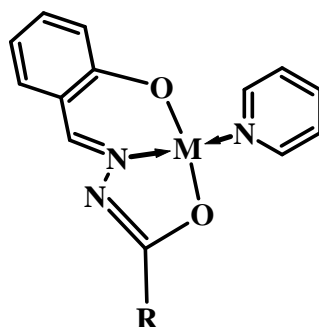
Structure (IV)

In the case of hydrazones (ONO donor) having phenolic group. The phenolate oxygen atom can form a bridge between the metal centers leads to the formation of a dimer.



Structure (V)

Presence of extra donor sites in the ketonic part may lead to the formation of multinuclear complexes. Another possibility is that hetero atom present in the hydrazide part of hydrazones it can also take part in bonding. Another possibility is that hetero atom presents in the hydrazide part of hydrazones, it can also take part in bonding.



Structure (VI)

1.2.2 Chromone hydrazones

Chromone (or 1, 4-benzopyrone) is a derivative of benzopyran (Figure 1.2) with a substituted keto group on the pyran ring. Chromones are one of the important classes of naturally occurring compounds and interest in their chemistry continues because of their usefulness as biologically active agents [23]. The chromone structure is an important part of several flavonoids.

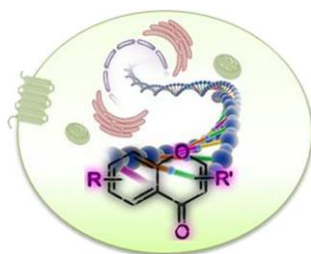


Figure 1.2 Structure of chromone

The chromone moiety forms an important pharmacophore of a large number of biologically active synthetic as well as natural compounds having medicinal usefulness. The famous anti-asthmatics, such as cromolyn sodium (or cromolyn) and nedocromil, are commonly grouped together as chromones (also called cromoglycates). These chromones are potent in preventing both early and late responses to inhaled allergens, such as pollen, and reducing airway reactivity to a range of inhaled irritants, such as sulfur dioxide and cold air [24].

Chromones have drawn considerable interest from synthetic organic and medicinal chemists [25], mainly 3-formylchromone has emerged as a valuable synthon for incorporation of the chromone moiety into a number of molecular frameworks [26]. However, its synthetic utility is limited due to

ease of opening of the chromone ring [27-28] and strategies are being worked out to deal with this problem [29]. Reaction of 3-formylchromones with aromatic amino acids has also been studied by Groweiss et al. [30]. The synthetic significance of 4-oxo-4*H*-[1]-benzopyran-3-carboxaldehydes (4-oxochromene-3-carboxaldehydes, 3-formylchromones) (Figure 1.3) comes from their usefulness as reactive agents and valuable precursors for many different heterocycles.

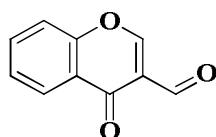


Figure 1.3 Structure of 3-formylchromones

There are lots of reasonable mechanisms whereby fruits and vegetables intake can prevent carcinogenesis. Plant foods have an extensive variety of anticancer phytochemicals with several potential bioactivities that can diminish susceptibility to cancer [31]. Flavonoids and isoflavonoids are particularly promising candidates for cancer prevention [32]. Flavonoids are secondary metabolites of plants, present in all terrestrial vascular plants. Flavonoids are chemically defined as substances composed of a common phenylchromone (C6-C3-C6) structure with one or more hydroxyl substituent. In recent years, particular attention has been paid to understanding the mechanism of their ability to inhibit the cell cycle [33], cell proliferation and oxidative stress and to detoxification enzymes, apoptosis and the immune system. In view of a greater interest in the biological effects of flavonoids and isoflavonoids, it is appropriate to review the present knowledge of epidemiology, anti-carcinogenic activity, bioavailability and the potential mechanisms of action of flavonoids and

isoflavinoids. Building on this basis will facilitate the development of new strategies and approaches for cancer control.

Chromones are omnipresent in nature, particularly in plants. It forms a numerous biologically active molecules of synthetic and natural origin as antitumor, anti-inflammatory, antimicrobial and pesticide agents [34]. It is also a precious synthon for a number of molecular structures; it has aroused significant interest as a precursor of the drug. On the other hand several functional groups have proven to be especially valuable in promoting mesomorphic properties in imine group [35].

1.2.3 Choice of Metals

The DNA interaction studies of metal complexes are an emerging research area, in addition to their use as potential therapeutic agents. Metals are capable to interact (covalently or non-covalently) with DNA through the electron-donating DNA bases and phosphate groups producing both intra or inter-strand interactions and among others. In addition to the coordinated atoms/groups in metal complexes contribute specific abilities ie. hydrogen bonding, intercalation, electrostatic interaction leading to the global effects [36]. Chemotherapy is the use of chemicals/drugs to an invading organism without damage to the host organism. A combined approach of new compounds is necessary to recognize the metabolism of metal-based drugs. Especially target interactions may not be as a significant in distinguishing drug action as part of metabolism and deactivation. The crucial role of transition metal ions in biological systems is well known [37]. In this thesis reassess the advancement of transition metal complexes as pharmacophores. While designing new metal complexes for therapeutic use the subsequent actions

require to be considered are hydrolysis, protein binding membrane transports are molecular target. Hydrolysis of metal complexes is significant since the aqueous milieu of biological systems, but the hydrophobic nature of cell membranes, vesicles and enzyme active sites need to consideration of lipophilic ligands in the development of new complexes. So, design of metallo-drugs requires bringing together organometallic chemistry with traditional aqueous coordination chemistry, a merger that is in its infancy [38].

The chemistry of Nickel is much simpler than that of other first row transition elements. The only oxidation state of importance is Ni (II) and these compounds are stable. Ni (II) has d^8 configuration and is able to form square planar complexes as well as octahedral ones. Ligands with large crystal fields favor square planar coordination because of the more favorable CFSE.

Copper (II) is an important and spectroscopically well examined metal ion in biological systems. Due to the Jahn-Teller distortion the structural properties which are not in a priori expected by the classical molecular mechanics approach. Cytochrome C oxidase and superoxide dismutase are copper containing metalloenzymes. These enzymes are used to be determinants in diabetes by their roles in regulating oxidant status. Cu (II) complexes are observed as the most hopeful alternatives to cisplatin as anticancer drug after Ru(II) complexes. Copper (II) is take part in an important role in biological systems as well as pharmacological agents. Synthetic Cu (II) complexes have been reported to act as potential anticancer and cancer inhibiting agents [39] Recently, the ligand Cu(II)

complexes of diimines could bind and cleave DNA and exhibit anticancer activity that is more efficient than that of cisplatin [40].

Zinc is a bluish grey metal. It is an essential element to life. The most common oxidation state of zinc is +2. It is a d^{10} system and is very stable. Zinc complexes are predominantly four coordinated and tetrahedral. In the field of coordination chemistry, zinc has importance. Zn (II) ion has been found in several metalloenzymes such as zinc-peptidases, human carbonic anhydrase, and alkalinephosphatase [41]. Today more than 200 different zinc proteins are known [42]. Metallothioneins, proteins containing zinc remain unique in character and are encountered both in animals and microorganisms [43-44]. The emerging importance of Zn (II) in neurological signaling and some proposed functions in biological systems have generated an urgent demand for the development of Zn (II)-specific molecular probes, and many Zn (II) fluorescent sensors have been reported, exhibiting high selectivity and sensitivity over other biologically essential metal ions in specific ranges of concentration [45-47].

1.3 Application of Metal Complexes of Chromone Hydrazones

1.3.1 Pharmacological activities of the chromone analogs

Chromones are a group of naturally occurring compounds that are ubiquitous in nature especially in plants. Molecules containing the chromone skeleton have extensive biological applications including antimycobacterial, antifungal, anticancer, antioxidant, antihypertensive, and anti-inflammatory applications and tyrosinase and protein kinase C inhibitors [48-57]. Chromone and its analogs are important pharmacophores and privileged structures in medicinal chemistry and have featured in a number of clinically

used drugs. The most relevant and recent studies have revealed that chromones derivatives have a broad spectrum of pharmacological activities which can be classified into the following categories:

1.3.1.1 Anti-cancer agents

Cancer is a burning issue under investigation which refers to the uncontrolled and rapid abnormal cell division that can invade nearby tissue. In 2015 about 90.5 million people were cancer carrying and even its number is increasing every year. A number of hydarzone derivatives have been developed with anticancer properties. R. M. Mohareb et al. reported the synthesis of a number of hydrazide-hydrazone derivatives from ring D modification of pregnenolone [58]. These compounds were evaluated for anticancer activity and were reported highly effective against breast cancer, lung cancer and CNS cancer compared to the reference drug doxorubicin. A new Schiff base obtained from 3-formylchromone and benzohydrazide (Hfcbh) and its Ru (II), Ru (III), Pd (II), Pt (II) and Ag (I) complexes were synthesized and evaluated as anticancer agents against the human breast cancer (MDA-MB231) and human ovarian cancer (OVCAR-8) cell lines. The [Ag(fcbh)(PPh₃)] complex shows the highest efficacy with a mean IC₅₀ values of 1.0 (MDA-MB231) and 0.87 (OVCAR-8) μM, respectively[59].

1.3.1.2 Anti-HIV agents

New Schiff base ligands derived from 5-amino-4-phenyl-4H-1, 2, 4-triazole-3-thiol and substituted benzaldehydes as well as their metal complexes with Cu (II), Fe (II), Au (III), and Mn (II) have been synthesized by Al-Masoudi et al. and assayed for anti-HIV-1 and HIV-2 activity by examination of their inhibition of HIV-induced cytopathogenicity in MT-4

cells. Copper complexes were found to be the most active inhibitors in cell culture ($EC_{50}=12.2 \mu\text{g/mL}$ ($SI=4$) and $>2.11 \mu\text{g/mL}$ ($SI=>1$), respectively) against HIV-1, and also showed inhibition against HIV-2 of $EC_{50}>10.2 \mu\text{g/mL}$ with $SI=9$, which provided a good lead for further optimization [60].

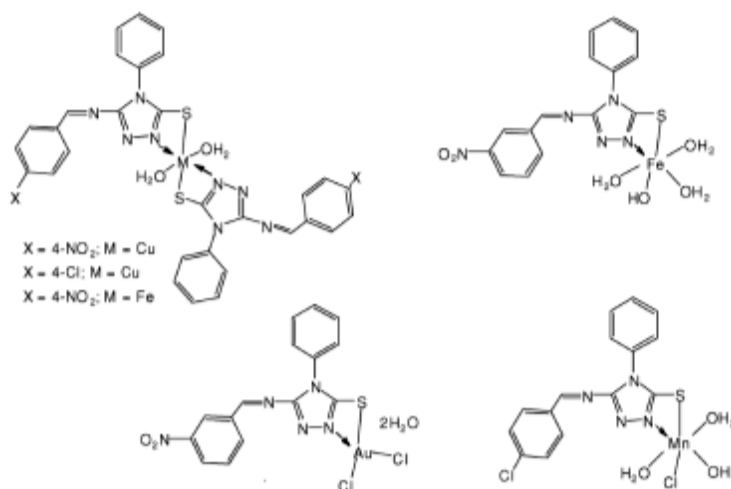


Figure 1.4 Example of metal (II) complexes showing anti-HIV activity [Ref: 60]

1.3.1.3 Anti-oxidant agents

Free radical production occurs continuously in all cells as part of normal cellular function. However, excess free radical production originating from endogenous or exogenous sources might play a role in many diseases. Antioxidants stop free radical induced tissue damage by preventing the formation of radicals, scavenging them, or by promoting their decomposition. Sathyadevi et al. have been synthesised bivalent transition metal hydrazone complexes of $[\text{Ni}(\text{L}_1)_2]$, $[\text{Co}(\text{L}_1)_2]$, $[\text{Ni}(\text{L}_2)_2]$ and $[\text{Co}(\text{L}_2)_2]$ from the reactions of $[\text{MCl}_2(\text{PPh}_3)_2]$ (where $\text{M}=\text{Ni}$ or Co) with hydrazones derived from 2-acetyl pyridine and carboxylic acid

hydrazides of benzhydrazide (HL₁) or thiophene-2-carboxylic acid hydrazide (HL₂) showed good antioxidant activity [61]. Three new hydrazone complexes [Cu(L)(neocuprin)]NO₃·H₂O, [Cu(L)(HL)]ClO₄, and [Cu₂(2-(2-pyridyl)benzimidazole)₂(L)₂]ClO₄ (L = *N'*-[(*E*)-phenyl (pyridin-2-yl)methylidene]furan-2-carbohydrazide) have been synthesized and studied their antioxidant activity. The experimental values (antioxidant SOD activity data) are indicative of the promising application of these complexes into the bioinorganic chemistry of superoxide dismutase [62].

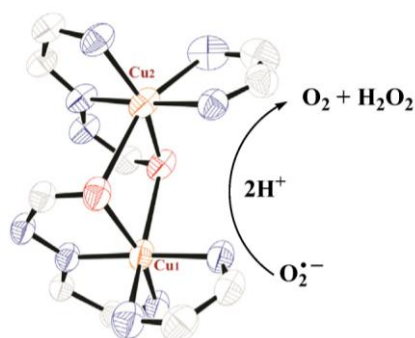


Figure 1.5 Example of Cu (II) complexes showing antioxidant activity [Ref: 62]

Chang et al. synthesised [Zn(L)(HL)(ClO₄)]·H₂O and [Ni(L)(HL)(ClO₄)]·H₂O (HL=2-acetylpyridine isonicotinohydrazone), complexes. They are active scavengers for O₂^{•-} and HO[•], exerting superior activities compared to the free ligand [63]. Zheng et al. synthesised Ln(III) complexes with hesperetin-4-one-(benzoyl) hydrazone. The antioxidant activity of the ligand and Ln(III) complexes was determined by superoxide and hydroxyl radical scavenging method *in vitro*, which indicate that the ligand and Ln(III) complexes have the activity to suppress O₂^{•-} and HO[•] and the Ln(III) complexes exhibit more effective antioxidant activity than the ligand alone [64].

1.3.1.4 Anti-tubercular agents

Tuberculosis (TB) is a chronic bacterial infection, spread through the air, and caused by a bacterium called *Mycobacterium tuberculosis* (MTB). Indoline-2,3-dione (isatin) derivatives are reported to show anti-tubercular activities, accordingly, isatin is a versatile lead molecule for designing of potential anti-tubercular agent. Hunoor et al. synthesised Co (II), Ni (II), Cu (II) and Zn (II) complexes with heterocyclic Schiff base formed by the condensation of isonicotinoylhydrazide and 3-acetylcoumarin and evaluate anti-tuberculosis. Upon complexation with Co (II) and Ni (II) ions, anti-TB activity of the ligand has enhanced [65].

1.3.1.5 Anti-inflammatory and Analgesic agents

Inflammation refers to a commonly used broad term for a local response to cellular injury characterized by pain, capillary dilatation, odema, heat, redness and loss of function. To date, a number of hydrazone derivatives has been efficiently synthesized and evaluated for the analgesic and anti-inflammatory activities. It is important to mention that COX-I and COX-II have an important role in the inflammation. Structure modification of the parent bioactive molecule which is a common practice over the years may further enhance its biological importance. Kajal et al. synthesised a series of 6-substituted-3(2H)-pyridazinone-2-acetyl-2(p-substituted/nonsubstituted benzal) hydrazine and evaluated for their analgesic and anti-inflammatory activity. The results revealed that 6-substituted-3(2H)-pyridazinone-2-acetyl-2(nonsubstitutedbenzal) hydrazones, were found to be most potent anti-inflammatory agents and 6-[4-(3-chlorophenyl)piperazine]-3(2H)-pyridazinone-2-acetyl-2(p-substituted/nonsubstituted

benzal)hydrazine, was found to be slightly better than standard drug indomethacin[66]. Five-coordinate transition metal complexes of pyridine-2-ethyl-(3-carboxylideneamino)-3-(2-phenyl)-1,2-dihydroquinazolin-4(3H)-one were synthesized by Hoonur et al and studied anti-inflammatory activity[67].

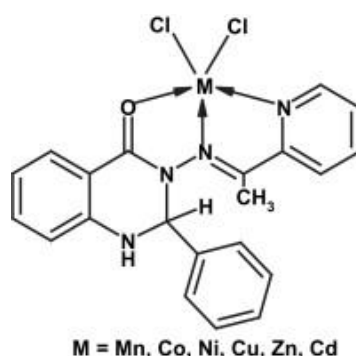


Figure 1.6 Example of metal (II) complexes showing anti-inflammatory activity [Ref: 67]

Hunoor et al. were synthesized 3-[1-(2-hydroxyphenyl)ethylideneamino]-2-phenyl-3,4-dihydroquinazolin-4(3H)-one and its metal complexes. Anti-inflammatory activity was observed for Ni (II), Cu (II) and Zn(II) complexes. The analgesic activity of the ligand was greater than the standard at 60 min. and at a 10 mg kg^{-1} dose, whereas the activity of Ni (II) and Cu (II) complexes at 10 mg kg^{-1} dose was comparable with the standard used [68].

1.3.1.6 Anti-microbial agents

The development of bacterial resistance to presently available antibiotics has necessitated the need to search for new antibacterial agents. Most of the hydrazones and their metal complexes are significant

compounds in medicinal and pharmaceutical area because of their biological activities. Therefore the development of new and effective antibiotics remains a challenging area for the researchers. Complexes $[\text{Ag}(\text{HCrPh})_2]\text{NO}_3 \cdot 2\text{H}_2\text{O}$ and $[\text{Ag}(\text{HCrpClPh})_2]\text{NO}_3$ were obtained with 3-formyl-6-methylchromone-phenyl hydrazone (HCrPh) and 3-formyl-6-methylchromone-*para*-chloro-phenyl hydrazone (HCrpClPh). Silver complexes showed antifungal activity against several *Candida* strains [69]. Shebl et al. synthesized a tridentate ONS donor ligand by the condensation of 2-aminochromone-3-carboxaldehyde with thiosemicarbazide. The ligand and most of its metal complexes showed antibacterial activity towards Gram-positive bacteria (*Staphylococcus aureus* and *Bacillus subtilis*), Gram-negative bacteria (*Salmonella typhimurium* and *Escherichia coli*), yeast (*Candida albicans*) and fungus (*Aspergillus fumigatus*)[70].

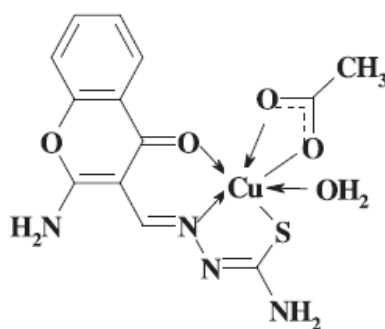


Figure 1.7 Example of Cu (II) complexes showing antimicrobial activity [Ref: 70]

Altintop et al. synthesized novel hydrazone derivatives through the addition-elimination reaction of 2-[(1-methyl-1H-tetrazol-5-yl)thio]acetohydrazide and aromatic aldehydes/ketones [71]. Compounds were subsequently investigated and were observed to have significant

antifungal potential. A series of 2-thiazolylhydrazones were developed by Chimenti et al. that exhibit potent antifungal activity against various *Candida* species [72].

1.3.1.7 Anti-diabetic agents

S. A. Iqbal et al. synthesised metal complexes of manganese (II) and cobalt (II) complexes active hypoglycemic agent (glimepiride), an oral antidiabetic drug [73]. A. Levina et al. synthesised complexes of V(V/IV), Cr(III), Mo(VI), W(VI), Zn(II), Cu(II), and Mn(III) as potential oral drugs against type 2 diabetes [73]. The chromium (III) metformin hydrochloride complex act as an antidiabetic drug was synthesised by the chemical reaction between chromium (III) chloride hexahydrate and metformin HCl (Mfn.HCl) in methanol solvent. The chromium (III) metformin HCl complex was recorded successful efficiency in the decreasing blood glucose level and HbA1C against diabetic rats. The Cr(III)-2Mfn.HCl complex has succeeded to great extent as antidiabetic drug with enhanced the antioxidant defence system as well as act as pronounced efficient hypoglycaemic agent compared to metformin HCl free drug [74].

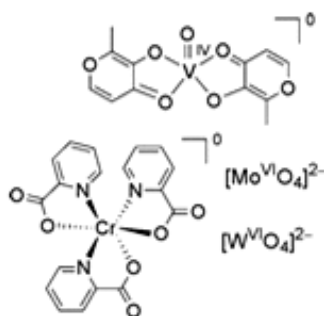


Figure 1.8 Example of complexes showing antidiabetic activity [Ref: 74]

1.3.2 DNA binding of metal complexes

In present situation, several researchers have continued on the studies of interaction of small molecules with DNA [75-80]. DNA is commonly the primary intracellular target of anticancer drugs, so the interaction between DNA and small molecules can cause DNA damage in cancer cells, blocking the division of cancer cells and causing cell death [81-82]. Studies on the interaction of transition metal complexes with DNA continue to catch the attention of the researcher's interest due to their importance in the design and development of new chemotherapeutic drugs, DNA cleavage agents, synthetic restriction enzymes, DNA printing agents and DNA "molecular light switch" [83-85]. The attention in the mode of combination of the metal complex to DNA has been motivated not merely by the desire to be aware of the basic concepts of these modes of interaction but also by the improvement of metal complexes in antibacterial, antifungal, anticancer reagents or anti-inflammatory agents [86].

Structure of Deoxyribonucleic acid (DNA)

Deoxyribonucleic acid, or DNA, is the carrier of genetic information in our cells. It consists of two strands of polymer that intertwine on each other in a right handed helix. The polymer strands consist of four different building blocks, the nucleotides, which include the molecular information that carries the DNA molecule. Each nucleotide consists of a phosphoric acid that is esterified with a deoxyribose sugar, which in turn is covalently linked to one of the four different DNA bases: adenine (A), guanine (G), thymine (T) or cytosine (C) (Figure 1.9 A). A and G are two-ring bases and are referred to as purines, while T and C are pyrimidines to a ring. Each nucleotide is attached to its neighbour via phosphodiester bonds

from the 5' carbon of the first nucleotide to the 3' carbon of the other, with the result that single-stranded DNA (ssDNA). The ssDNA usually forms a double helix with a second strand of DNA. The double helix of DNA can have different conformations and the most known are the A, B and Z form, where the form B is the most common conformation in physiological conditions (Figure 1.9B). In B-DNA, the helix is right-handed, with the bases positioned centrally and positioned perpendicular to the phosphate backbone, like the steps of a spiral staircase. The DNA bases show a unique hydrogen bonding pattern, resulting in A combining with T and G with C. As a consequence of this, the two strands of DNA in the double helix are complementary to each other, thus bringing the same information. The C-G base pair contains three hydrogen bonds, compared to only two in the A-T base pair, so C-G rich base pair sequences are more stable than A-T rich base pairs. At physiological pH, the phosphate backbone of DNA carries a negative charge per nucleotide. The repulsive charges between the two strands in the double-stranded DNA (dsDNA) are overcome by stabilizing the contributions from the hydrogen bonds and hydrophobic interactions between the aromatic DNA bases that are stacked on top of each other in the center of the helix, as well as the neutralizing contribution of the counterions present in the solvent. In B-DNA, the pitch (number of bases to complete a turn) is 10.5, with a helical increase of 3.4 Å. Two grooves run along the B-DNA helix, one on each side of the base pairs in the center. These grooves are called the major and the minor groove and, as the names indicate, the major groove is wider than the minor groove (11nm and 6 nm, respectively), but have similar depths (4nm and 5nm, respectively) [87].

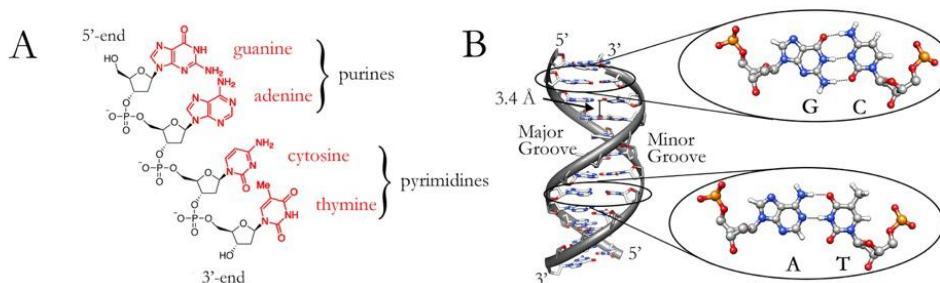


Figure 1.9 The molecular structure of DNA (A). Deoxyribose and phosphoric acid make up the backbone of the DNA, while the nucleobases adenine (A), guanine (G), thymine (T) and cytosine (C) protrude from the backbone. A B-form DNA is shown in (B) where two polymer chains are linked to each other via hydrogen bonds between the DNA bases; A base-pairs with T, and G base-pairs with C. The minor and major grooves of the B-DNA helix are also marked in the figure

DNA is a critical therapeutic target that is responsible for, and the focus of, a wide variety of intracellular interactions [88]. Each of the complementary strands of DNA are stabilized by hydrogen bonding between adenine and thymine (A-T) and guanine and cytosine (G-C) nucleic acids [89]. In B-DNA, the most common DNA form, the strands are held in the anti-parallel double helix by stacking interactions between parallel oriented bases [90]. The formation of this helix results in the presence of a major and minor groove which provides sites for the binding of small molecules [91]. The major and minor groove differs significantly in size, shape, hydration, electrostatic potential and position of hydrogen bonding sites [92].

DNA provides a wide range of binding modes and binding sites for non-covalent and covalent interactions (Figure 1.9). The non-covalent interactions include intercalation, partial intercalation, groove bindings

and electrostatic binding with metal complexes, in which the later two are the non-classical intercalative binding modes.

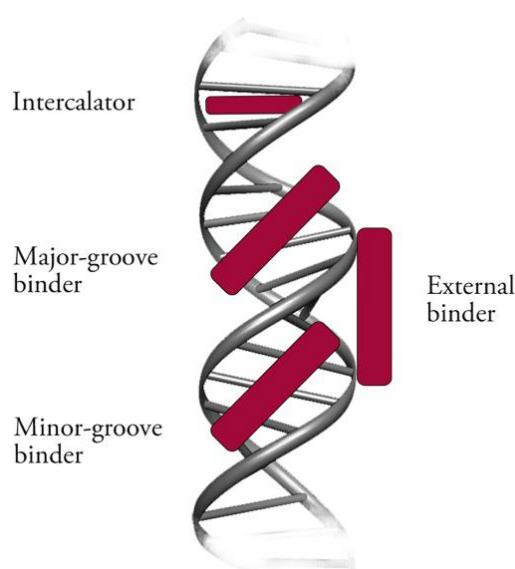


Figure 1.10 Binding modes of DNA

1.3.2.1 Covalent binding

Metal complexes have labile ligands that can be readily substituted by covalent attachment to nitrogenous DNA bases. The complex interact to DNA through covalent binding mode (Figure 1.11), usually resulting in hyperchromism (increased absorption intensity) with bathochromic change. The presence of red shift with hyperchromism (decreased absorption intensity) indicates the coordination of the complex with DNA through the N7 position of guanine. The hyperchromism is the result of the decomposition of the secondary structure of the DNA due to the fact that the phosphate group can provide the appropriate anchors for coordination with the complexes.

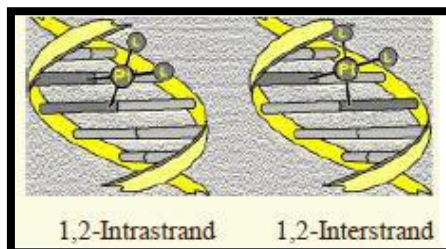


Figure 1.11 Covalent binding of cis-platin to DNA

1.3.2.2 Electrostatic binding

When cationic or anionic complexes are bound to the anionic surface of DNA, such an interaction occurs (Figure 1.11). Complex hyperchromism may be due to external interaction with DNA, or the complex may open the helical structure of DNA and expose more DNA-embedded bases. Ions and charged metal complexes such as Na^+ , Mg^{+2} , Ru^{+2} electronically associate with DNA. And forming ionic or hydrogen bonds along the outside of the double helix. This type of interaction do not show bathochromism [93-94].

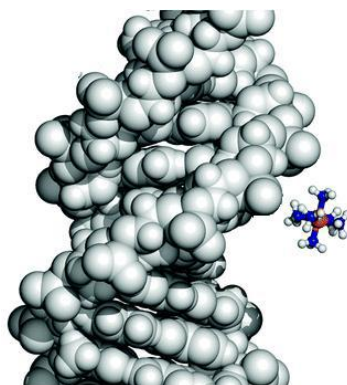


Figure 1.12 $[\text{Ru}(\text{NH}_3)_6]^{3+}$ binds electrostatically to DNA

1.3.2.3 Groove binding

There are two types of groove binding (1) major and (2) minor (Figure 1.13). Groove binding, unlike intercalation, does not induce large

conformational changes in DNA and can be considered as to standard lock and key models for ligand-macromolecular binding [95]. Groove binders are normally crescent-shaped molecules that bind to the minor groove region of DNA. They are stabilized by intermolecular interactions and typically have binding constants larger than the intercalators (approximately 10^{11} M^{-1}), since a free energy cost is not required for the creation of the binding site [96]. Groove binders also have a demonstrated clinical utility as antibacterial and anticancer agents.

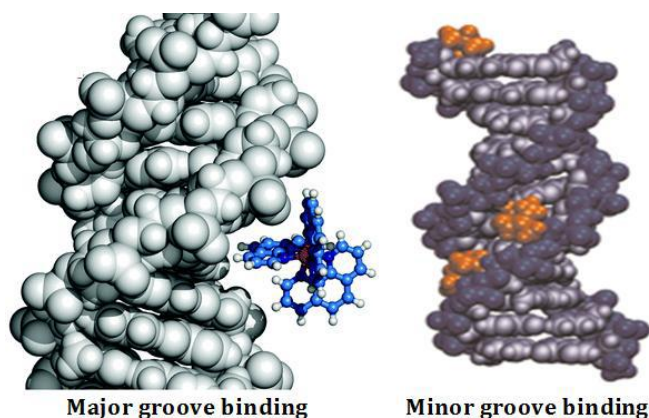


Figure 1.13 Major and minor groove binding

1.3.2.4 Intercalation

Intercalation involves the insertion of a planar molecule between DNA base pairs, which results in a decrease in the DNA helical twist and lengthening of the DNA (Figure 1.14) [97]. Although there is a considerable free energy cost for the establishment of the intercalation centre (approximately 4 kcal mol^{-1}), favorable contributions (hydrophobic, ionic, hydrogen bonding, and van der Waals) result in association constants of 10^5 to 10^{11} M^{-1} [98]. Although intercalation has been traditionally associated with

molecules containing fused bi/tricyclic ring structures, a typical intercalators with nonfused ring systems may be more prevalent than previously recognized [99]. DNA intercalators have been widely used as antitumor, antineoplastic, antimalarial, antibiotic and antifungal agents.

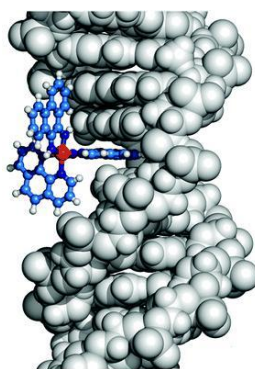


Figure 1.14 Complex intercalation between bases of DNA

Several methods have been employed to study the binding of small molecules to DNA ie electronic absorption spectroscopy, viscosity measurement etc.

Absorption spectroscopy is one of the most important techniques to study the interaction of metal complexes with DNA. This method is universally employed to examine the binding strength and binding mode of DNA with the metal complex. The extent of the binding strength of the complexes is quantitatively determined by calculating the intrinsic binding constants K_b of the complexes. The binding with DNA through intercalation usually results in hyperchromism or hypochromism [100]

The viscosity of a fluid is an important property in the analysis of liquid behavior and fluid motion near solid boundaries. The viscosity is the

fluid resistance to shear or flow and is a measure of the adhesive/cohesive or frictional fluid property. The resistance is caused by intermolecular friction exerted when layers of fluids attempt to slide by one another. In short, viscosity is a measure of a fluids resistance to flow. Optical or photophysical probes generally provide necessary, but not sufficient clues to confirm how complex interacts with DNA i.e. the binding mode. To further investigate the binding abilities of the compounds with DNA, viscosity measurements were carried out on CT DNA by varying the concentrations of the added compounds; gives information about coordination of transition metal complexes to DNA.

1.3.3 Enzyme Inhibition Studies

Enzymes are biological catalysts formed by a cell and responsible for "high speed" and specificity of one or more intracellular or extracellular biochemical reactions. Enzymes are protein catalysts accountable for supporting almost all chemical reactions that maintain animal homeostasis [101-105]. Enzymatic reactions are always reversible. The substance on which an enzyme acts is called a substrate. Enzymes are involved in converting the substrate into the product. Most of the enzymes are globular proteins consisting of a single polypeptide or two or more polypeptides held together (in a quaternary structure) by non-covalent bonds. The enzymes do nothing but accelerate the rates at which the equilibrium positions of the reversible reactions are reached. In terms of thermodynamics, enzymes reduce the activation energies of reactions, allowing them to present themselves much more easily at low temperatures, essential for biological systems [106-107]. The basic characteristics of enzymes include

Almost all enzymes are proteins and follow the physical and chemical reactions of proteins

- Enzymes are sensitive and labile to heat
- Enzymes are soluble in water
- Enzymes could be precipitated by protein precipitating agents such as ammonium sulfate and trichloroacetic acid.
- The rate or rate of enzymatic reaction is evaluated by the rate of change in concentration of the substrate or product in a given period of time.

1.3.3.1 Factors affecting enzyme activity

1.3.3.1.1 Substrate concentration

The rate of a reaction increases with presence of enzyme and increasing in the concentration of the substrate. The velocity (V) is expressed in micromoles of substrate is converted per minute. As the substrate concentration increases, the rate of a reaction increases. The continuous increase in the concentration of the substrate can lead to a reduction in the speed of the reaction and leads to the flattened curve. The maximum velocity obtained by an enzymatic reaction is called V_{\max} . V_{\max} represents the maximum reaction speed possible in the presence of excess substrate [108-110].

1.3.3.1.2 Enzyme concentration

As there is optimal substrate concentration, rate of an enzymatic reaction or velocity (V) is directly proportional to the enzyme concentration. Presence of excess substrate and an increase in the enzyme

concentration may cause several restrictions. It is worthy of note that the enzymes are saturated with substrates under physiological conditions [108-110].

1.3.3.1.3 Product concentration

According to law of mass action the rate of reaction is slow down at equilibrium, for a reversible enzyme catalyzed reaction. So reaction rate is slowed, stopped or even reversed with enhance in product concentration [108-110].

1.3.3.1.4 Temperature

Velocity of enzymatic reaction increases with temperature of the medium. The temperature at which maximum rate of the reaction is termed as optimum temperature. As temperatures increases it leads to denaturation; i. e. due to the molecular arrangement loss the active sites of the enzyme surfaces and results in a loss of efficiency [108-110].

1.3.3.1.5 Hydrogen ion concentration (pH)

Like temperature, all enzymes have an optimum pH, at which the enzymatic activity will be at maximum. Majority of the enzymes are more efficient in the region of pH 6-7, which is the cell pH. Outside this pH range, enzyme activity decreases awfully. Diminishing in the efficiency leads to pH change; it affects the degree of ionization of the substrate and enzyme. Highly alkaline or acidic conditions may cause denaturation and subsequent loss of activity. Some exceptions such as pepsin (with optimum pH 1-2), alkaline phosphatase (with optimum pH 9-10) and acid phosphatase (with optimum pH 4-5) are even noticed [108-110].

1.3.3.1.6 Presence of activators

Presence of certain inorganic ions increases the activity of enzymes. The best examples are chloride ions activated salivary amylase and calcium activated lipases.

1.3.3.1.7 Presence of inhibitor

The catalytic activity of enzyme can be reduced by substances that prevent the formation of a normal enzyme-substrate complex. The amount of inhibition therefore depends completely on the relative concentrations of the true substrate and inhibitor. This inhibition, which depends on competition with the substrate for active sites of the enzyme, is called competitive inhibition. In other cases, the inhibitor combines with the enzyme-substrate complex to form an inactive enzyme-substrate-inhibitor complex, which cannot undergo further reactions to give the usual product. This is called non-competitive inhibition. Non competitive inhibition is the combination of the inhibitor with the enzyme or the enzyme substrate complex, as a result an inactive complexes. In this case, the inhibitor binds to the sites, other than the active site of an enzyme leads to deformation of the enzyme molecule. Therefore the rate of formation of the enzyme-substrate complex is slow down [108-110].

1.3.3.2 Why are enzyme inhibitors important?

Although enzymes are enormously very important for life, an abnormally elevated enzyme activity can lead to diseases. Therefore, active enzymes are attractive targets for the improvement of inhibitory molecules to alleviate pathologies. The exploitation of enzyme catalysis with inhibitors is significant for the deterrence of infectious diseases, cell

growth and activation of the cell cycle, management of hypertension, control of inflammatory response and others. In addition to acting as therapeutic agents, inhibitors also play important roles in biological and clinical research.

1.3.3.3 The active site

Enzymes are specific in catalyzing reactions: each enzyme generally acts on a single substrate or a pair of substrates (in the case of bimolecular reactions). But, a few enzymes are able to act on directly related substrate molecule, often with various efficiencies. Enzymes have a small region (usually only about 20 amino acids), known as an active site, where the reaction takes place. Enzymes catalyze most of the biological reactions by binding the substrate to the active site. These bond modify the allocation of electrons in the chemical bonds of the substrate, reducing the activation energy of the substrate reaction and allowed to form the final product. This product is free from the active site, allowing the enzyme to regenerate for another reaction cycle. The substrate can interact with the active site through ionic interactions, hydrogen bonding, non-polar hydrophobic interactions and covalent coordination with a metal ion activator [111].

The active site is complementary to that of the substrate molecule, which only allows a substrate to bind to the site. Nevertheless, in several cases, similar molecules can also act as substrates, but with less than optimal kinetics. This is known as the lock-and-key model. However, not all reactions can be explained by the type of lock and key model (Figure 1.15).

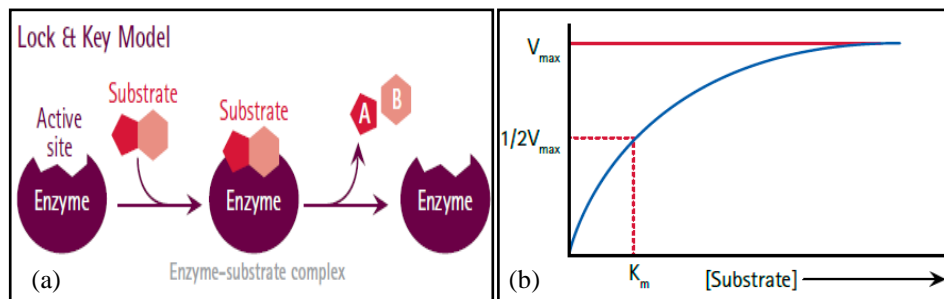


Figure 1.15 (a) lock and key model, (b) Relationship between substrate concentration and maximum velocity of reaction.

- **K_m** : It is the substrate concentration, $[S]$ at which the velocity of the reaction is half-maxima is observed under definite circumstances (Figure 1.15 (b)). This is an inverse measurement of the bond strength between the substrate molecule and the lower enzyme K_m means better affinity and decreases the concentration of the substrate required to achieve maximum reaction speed. K_m values depend on pH, temperature and other reaction conditions.
- **V_{max}** : It is the maximum velocity of reaction under certain conditions (Figure 1.15 (b)). V_{max} is attained when all enzyme sites are saturated with the substrate. This will happen when substrate concentration $[S]$ is greater than K_m so that $[S]/([S]+K_m)$ approaches 1.
- **IC_{50}** : The concentration requisite to produce 50% inhibition (Figure 1.16). The amount of inhibitor required depends on different factors such as substrate concentration, target accessibility, cell permeability, duration of incubation, type of cells used, and so on. It is best to examine the literature to determine initial concentration. If K_i or IC_{50} values are unknown, an extensive variety of inhibitory

concentrations must be tested and kinetic Michaelis-Menten (see below) ought to be noted to evaluate the K_i value. It is not unusual to see any inhibition or even a reverse effect when using high concentrations of inhibitors.

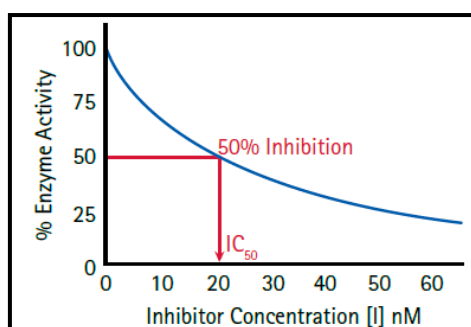


Figure 1.16 IC_{50} value

- **K_i (Inhibition constant):** The inhibitor concentration at which 50% inhibition is observed. Cheng et. al. [112] introduced an equation that used for the determination of K_i by using known IC_{50} .

$$K_i = \frac{IC_{50}}{1 + \frac{[S]}{K_m}}$$

Where $[S]$ is the substrate concentration, and K_m is the substrate concentration (in the absence of inhibitor) at which the rate of the reaction is half-maxima. For a particular substrate the K_i value of an inhibitor (fixed K_m) is constant but for different substrate, K_m is different, and so is the K_i .

1.3.3.4 How to determine K_m and V_{max} : Lineweaver-Burk Plot

K_m and V_{max} can be evaluated experimentally by incubating the enzyme with various substrate concentrations. The results obtained were recorded as a function of rate of reaction or velocity (V) against substrate $[S]$ concentration. This will make a hyperbolic curve. The reaction velocity and K_m have the following relationship.

$$V = \frac{V_{max}}{1 + \frac{K_m}{[S]}}$$

Even under expert hands, it is difficult to fit the best hyperbola through all the experimental values to determine V_{max} exactly. So scientists have introduced a new method, i.e. rearrange the Michaelis-Menten equation to form more accurate fitting to the experimental values and calculate V_{max} and K_m . However, with every method, there are certain advantages and disadvantages.

The Lineweaver-Burk i.e. double reciprocal plot (Figure 1.17) which is the one of the most widespread equation that reorganizes the Michaelis-Menten equation as follows:

$$\frac{1}{V} = \frac{K_m}{V_{max}} \left(\frac{1}{[S]} \right) + \frac{1}{V_{max}}$$

When we plot $1/V$ against $1/[S]$, a straight line is obtained its Y intercept = $1/V_{max}$; gradient = K_m/V_{max} ; and X intercept = $-1/K_m$. Lineweaver-Burk plots are the most extensively used graph for determine more accurately K_m and V_{max} .

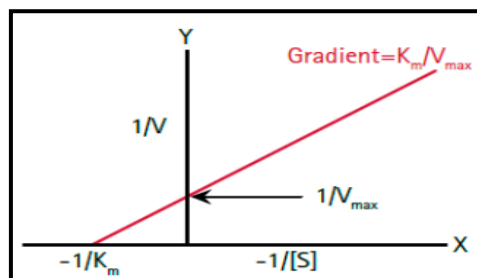


Figure 1.17 The Lineweaver-Burk double reciprocal plot

1.3.3.5 Classification of enzyme inhibitors

By the catalytic activity, enzymes can accelerate the velocity or rate of a reaction without affecting in the reaction. The capacity of an enzyme to catalyze a reaction can be retard by binding different small molecules (inhibitors) to the active site or, sometimes, other than the active site [113-114].

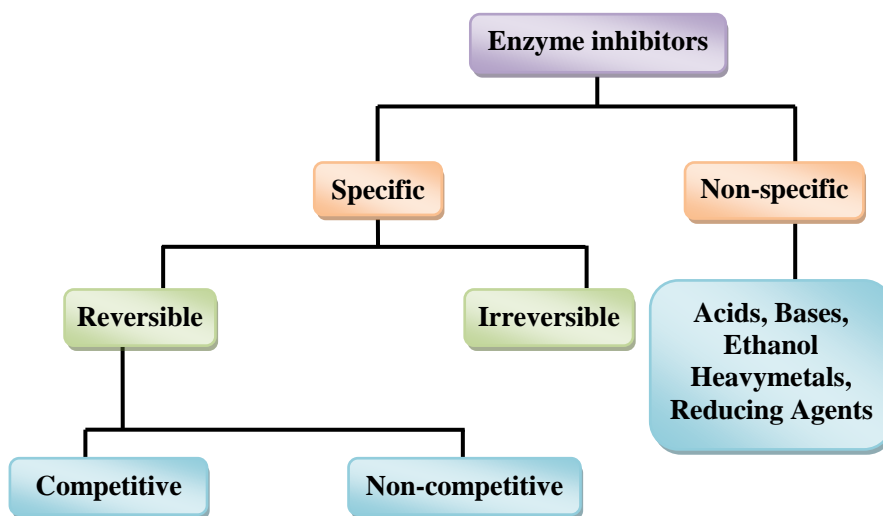


Figure 1.18 The schematic representation of classification of enzyme inhibitors

The most important factors that affect enzymatic activity are: concentration of enzyme, the amount of specific enzyme substrate,

hydrogen ion concentration (pH) of the reaction medium, temperature, and the presence of activators and inhibitors.

Enzyme inhibitors are generally low molecular weight compounds. They interact with the enzymes to form an enzyme-inhibitor complex, either reducing or completely inhibiting the catalytic activity of the enzyme and consequently reducing the rate of reaction. Binding of an inhibitor to the active site of enzyme can block the entry of substrate to the site. Alternatively, some inhibitors can bind to a site other than the active site and induce a conformational change that prevents the entry of substrate to the active site. Based on the nature of interaction of small molecule with the enzyme, inhibitors can be classified as reversible or irreversible (Figure 1.18) inhibitors.

1.3.3.5.1 Reversible inhibitors

Reversible inhibitors are generally two types competitive, non-competitive. They bind to enzyme with noncovalent interactions, such as hydrogen bonds, ionic bonds, and hydrophobic interactions (Figure 1.19). Irreversible inhibitors can react with the enzyme covalently and induce chemical changes to modify key amino acids that are required for enzymatic activity [115].

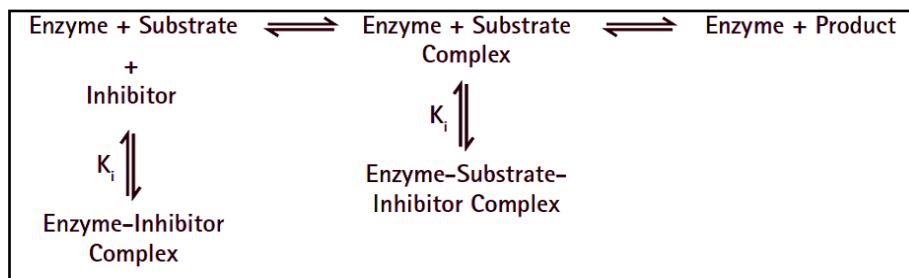


Figure 1.19 Reversible inhibitors

1.3.3.5.1.1 Competitive inhibitors

In competitive inhibition, the inhibitor usually has structural similarity with the natural substrate and competes with the substrate for access to the active site (Figure 1.20). The inhibitor has affinity for the active site, and if it binds more tightly than the substrate, then it is an effective competitive inhibitor. Conversely, if it binds less strongly, it is considered as a poor inhibitor. In competitive inhibition, the inhibitor can bind only to the free enzyme and not with the enzyme-substrate complex [116]. Hence, inhibition can be overcome by increasing the concentration of substrate in the reaction mixture. By competing with substrate, V_{\max} can still be achieved. However, in the presence of inhibitor, substrate concentration has to be increased to achieve V_{\max} . This will increase the K_m value.

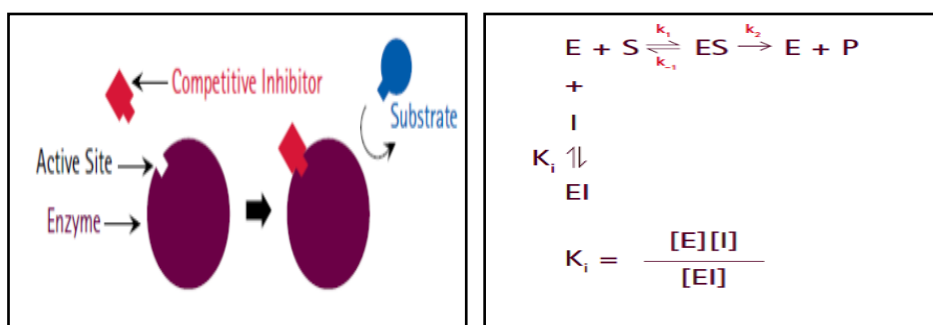


Figure 1.20 Competitive Inhibitor

For competitive inhibition, one can determine K_i , the inhibition constant, which is the dissociation constant for the enzyme-inhibitor complex. The lower the K_i value, the lower is the amount of inhibitor required to reduce the rate of reaction. This relationship can be simplified as:

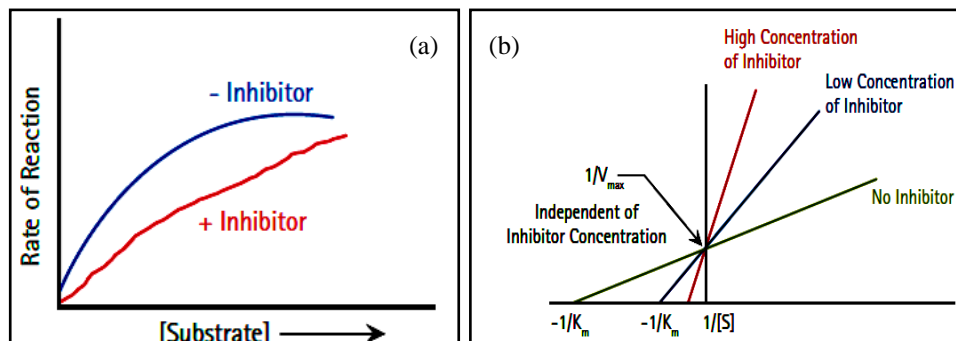


Figure 1.21 (a) Michaelis- Menten (b) Lineweaver-Burk plot for competitive inhibitor

The result of competitive inhibition can be represented in a Lineweaver-Burk plot (Figure 1.21). Because K_m increases as a consequence of competitive inhibition, in the presence of an inhibitor the X-intercept moves closer to the origin. As we increase concentration of inhibitor, K_m will increase more and X-intercept will move very close to the origin. Note that all lines go through the identical Y-intercept, for the reason that a competitive inhibitor does not influence V_{max} .

1.3.3.5.1.2 Noncompetitive inhibitors

In noncompetitive inhibition, the binding of the inhibitor diminishes the activity of enzyme, however does not influence the binding of substrate (Figure 1.22). Therefore, the degree of inhibition is dependent only on the inhibitor concentration. These inhibitors bind noncovalently to sites other than the active (substrate binding) site. Inhibitor binding does not control the accessibility of the binding site for substrate [117]. Hence, the binding of the substrate and the inhibitor are independent of each other and inhibition cannot be overcome by increasing substrate concentration. Noncompetitive inhibitors have same affinities for enzyme

and enzyme-substrate complex; therefore, $K_i = K'_i$. Hence, V_{\max} is reduced, but K_m is unaffected. V_{\max} cannot be obtained in the existence of a noncompetitive inhibitor.

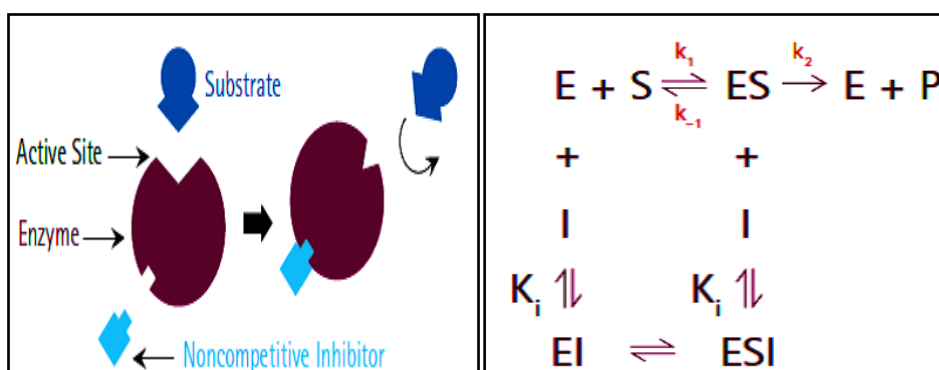


Figure 1.22 Noncompetitive inhibitor

The effect of a noncompetitive inhibitor is presented in Figure 1.22. Since the Y intercept is $1/V_{\max}$, as V_{\max} decreases, $1/V_{\max}$ increases. On other hand, K_m remains the same for all concentration of the noncompetitive inhibitor. Hence, all lines go through the same X-intercept.

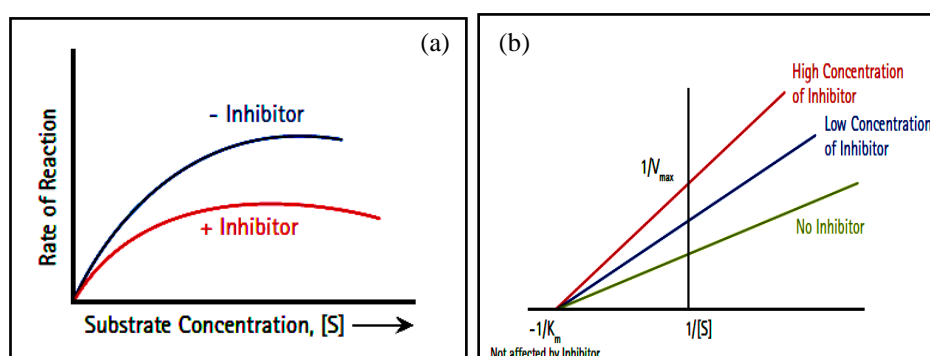


Figure 1.23 (a) Michaelis- Menten (b) Lineweaver-Burk plot for Non-competitive inhibitor

1.4 Scope and objectives of the present study

Research in the field of coordination chemistry is a growing, constantly with the synthesis of organic ligands having a wide variety of donor atoms/groups and significant biological/pharmaceutical importance. Flavonoids are benzopyran derivatives, which are able to suppress the formation of free radicals and have antioxidant activity.

Hydrazones obtained from a hydrazide and aldehydes are the most important group of ligands because they can coordinate to metal ions through azomethine nitrogen and have been studied. First row transition metal complexes have found a huge variety of applications in different research areas, such as probes for biological macromolecules, artificial photosynthesis, oxidation catalysis, photo molecular devices and organic synthesis. Especially nickel, copper and zinc (II) complexes have fascinated important attention due to their catalytic and biological applications such as anti- cancer, anti-HIV, anti-microbial, anti- inflammatory etc.

Binding studies of small molecules/atoms to DNA on a molecular level are extremely significant in the development of new pharmacophores/chemotherapeutics and sensitive diagnostic materials. The interaction of DNA with metal complexes has been an intense, interesting area of both inorganic and biochemists. A lot of transition metal complexes, mainly copper (II) complexes have been used as probes of DNA structure therefore development of tiny complexes can interact/bind with specific sequences of DNA.

A detailed survey of the literature revealed that metal complexes of hydrazones having ONO/ NO donor groups expansively examined,

however those obtained from heterocyclic systems especially those having benzopyran moiety received moderately a lesser amount of consideration.

Hence the author have aimed to report through thesis embodies the study performed to meet the following objectives -

- 1) Synthesis of nickel, copper and zinc (II) metal complexes from various ONO, NO tridentate/bidentate chromone hydrazone systems.
- 2) To study and substantiate the structural variations of tridentate/bidentate complex species on the basis of spectroscopic studies.
- 3) To study the antimicrobial activities of ligands and complexes.
- 4) To assess the DNA binding capacity of metal complexes of chromone hydrazones.
- 5) To study the enzyme inhibition of α -amylase and α -glucosidase of ligands and complexes.
- 6) To study cytotoxicity of chromone hydrazones and metal complexes.

1.5 Physical measurements

The physicochemical methods adopted during the present study are discussed below.

1.5.1 Elemental analysis

Elemental analysis is a process where a sample of a chemical compound is analyzed for its elemental and sometimes isotopic

composition. Elemental analysis can be qualitative (determining what elements are present) and it can be quantitative (determining how much of each is present). This information is important to help to determine the purity of a synthesized compound. Elemental analyses of C, H, N and S present in all the compounds were done on a Vario EL III CHNS elemental analyzer at the Sophisticated Analytical Instrument Facility, Cochin University of Science and Technology, Kochi-22, Kerala, India.

1.5.2 Conductivity measurements

The conductivity (or specific conductance) of an electrolyte solution is a measure of its ability to conduct electricity. The SI unit of conductivity is siemens per meter (S/m). Conductivity measurements are used as a fast, inexpensive and reliable way of measuring the ionic content in a solution. The molar conductivity of the complexes in DMF solutions (10^{-3} M) at room temperature were measured using a Systronic model 303 direct reading conductivity meters at the Department of Applied Chemistry, Cochin University of Science and Technology, Kochi-22, Kerala, India.

1.5.3 Magnetic susceptibility measurements

The magnetic susceptibility is a dimensionless proportionality constant that indicates the degree of magnetization of a material in response to an applied magnetic field. Magnetic susceptibility measurements of the complexes were carried out on powdered samples at 298K using a Sherwood Scientific Magnetic Susceptibility Balance (M.S.B.) MK1 using $\text{Hg}[\text{Co}(\text{SCN})_4]$ as calibrant at the Department of Applied Chemistry, Cochin University of Science and Technology,

Kochi-22, Kerala, India and the diamagnetic contribution to the susceptibility was estimated through Pascal's constants.

1.5.4 Infrared spectroscopy

Different bonds have different vibrational frequencies and therefore the presence of such bonds can be easily identified from its characteristic frequency appearing as an absorption band in the infrared spectrum. In the case of coordination complexes, the ligand based vibrations, metal-ligand vibrations and the formation of new bonds can be easily accessed by this technique. The changes occurring as a result of complexation will affect the vibrational modes of bonds, which are reflected in the nature of the spectrum. Also, the characteristic infrared absorptions associated with each functional group can be used to deduce the presence of such groups in complexes.

Infrared spectra of the compounds were recorded on a JASCO FT-IR-5300 Spectrometer in the 4000-400 cm^{-1} range using KBr pellets at the Department of Applied Chemistry, Cochin University of Science and Technology, Kochi-22, India. The azomethine bond formation and the mode of their coordination (monodentate/bidentate) in complexes are identified from their IR data.

1.5.5 Electronic spectroscopy

This is based on the fact that electronic transitions occur between levels whose energy separations correspond to wavelengths characteristic of visible and ultraviolet region of the spectrum. Factors like geometry of the complex, nature of the bonded ligands and the oxidation state of the

central metal atom can alter the gap between the energy levels, thereby reflecting in the electronic spectra.

The absorption spectra of a complex can be due to any of the following reasons:

- a) Ligand spectra: These are the intraligand transitions that appear even after complexation, with a slight shift in its position and intensity from the free ligand.
- b) Charge-transfer spectra: It can be of either ligand to metal (LMCT) or metal to ligand (MLCT) type and it involves transitions between orbitals that mainly belong to metal and orbitals that belong to ligand. This is an evidence for complexation.
- c) Ligand-field spectra: The *d* orbitals of the metal which are split by the influence of the ligand field produce ligand-field spectra; these are otherwise called *d-d* spectra. The nature and the region of absorption of the *d-d* spectra can be used to identify the metal present in the complex.

The electronic spectra of the compounds were recorded in DMF on a Thermo Scientific Evolution 220 UV-vis Spectrophotometer in the 200-900 nm range at the Department of Applied Chemistry, Cochin University of Science and Technology, Kochi-22, India. For recording the spectra in solution, quartz cuvettes with a path length of 1 cm is used.

1.5.6 NMR spectroscopy

Nuclear magnetic resonance spectroscopy involves the interaction between an oscillating magnetic energy of hydrogen nucleus or some other nucleus when they are placed in an external magnetic field. In ^1H NMR spectroscopy, the nucleus of hydrogen atom behaves as a spinning bar magnet because it possesses both electronic and magnetic spin. This technique consists in exposing the protons in organic molecules to a powerful magnetic field. The proton will precess at different frequencies. Now we irradiate these precessing protons with readily changing frequencies and observe the frequency at which absorption occurs. Usually in NMR spectrum we measure applied field strength for each set of protons and absorption peaks are plotted.

NMR spectra of chromone hydrazones were recorded in DMSO on a Bruker AMX advance III 400MHz FT-NMR spectrometer using TMS as the internal standard at Sophisticated Analytical Instrument Facility, Cochin University of Science and Technology, Kochi-22, India.

1.5.7 Mass spectroscopy

Mass spectroscopy is the most accurate method for determining the molecular mass of a compound and its elemental composition. In this technique molecules are bombarded with highly energetic electrons. The molecules are ionized and broken up into many fragments. Some of which are positive ions. Each kind of ion has a particular mass to charge ratio (m/z). It is used to prove the identity of a compound and establish structure for a new compound. It helps to establish exact molecular mass and molecular formula. It can reveal the presence of certain structural

units present in a molecule. In mass spectrometer the sample is introduced into an inlet chamber and volatilized it is subsequently introduced into the high vacuum chamber where neutral molecules pass through a beam of electrons where ionization occurs.

Mass spectra of the chromone hydrazones were recorded by direct injection on WATERS 3100 Mass Detector using Electron Spray Ionization (ESI) technique designed for routine HPLC-MS analyses at the Department of Applied Chemistry, Cochin University of Science and Technology, Kochi-22, India.

1.5.8 EPR spectroscopy

EPR spectroscopy is the branch of absorption spectroscopy that utilizes microwave frequency so as to probe the electronic structure of paramagnetic molecules. The ESR signature of a complex is used to gain information about the metal ligand bonding, unpaired electron distribution and spatial disposition of ligands around the central metal ion. Several microwave frequencies like S-band (3.5 GHz), X-band (9.25 GHz), K-band (20 GHz), Q-band (35 GHz) and W-band (95 GHz) are available. ESR spectrometer operating in X-band frequency is used.

EPR spectra can be recorded by two modes

- a) CW-EPR spectroscopy (CW- continuous wave)
- b) Pulsed-EPR spectroscopy

The primary coordination sphere (inner sphere) of the complex consists of the central Cu (II) ion and the directly coordinating atoms (like N, O or S). The CW-EPR spectroscopy is sensitive to the identity and the

number of equatorially coordinating atoms and this interaction is reflected as a change in the CW-EPR parameters like g_1 and A_1 . The interaction between the axially coordinating atoms and the central ion is relatively weak [78]. The secondary coordination sphere (outer sphere) includes non-coordinating atoms linked to central metal ion *via* multiple chemical bonds. The interactions between the central metal ion and an atom with non-zero spin in the outer sphere are detected by pulsed-EPR spectroscopy.

The number, type and the electronegativity of the equatorially aligned coordinating atoms will influence the hyperfine interaction parameters. As the number of nitrogen atoms increase, g_1 values tend to decrease and A_1 will increase. The interaction with the nuclear spins of directly coordinating atoms - known as superhyperfine interactions can also be detected in X-band frequency and is an evidence for the delocalization of the electrons.

The EPR spectra of the complexes in the solid state at 298 K and in DMF at 77 K were recorded on a Varian E-112 spectrometer using TCNE as the standard with 100 kHz modulation frequency, 2 G modulation amplitude and 9.1 GHz microwave frequency at the Sophisticated Analytical Instrument Facility, Indian Institute of Technology, Bombay, India. Some of the EPR spectra are simulated using EasySpin [86].

1.5.9 Thermal analysis

Thermal methods of analysis involve those techniques in which changes in physical or chemical properties of a substance are measured as a function of temperature.

Thermogravimetric Analysis (TGA)

Here, the mass of the sample in a controlled atmosphere is recorded continuously as a function of temperature or time as the temperature of the sample is increased. A plot of mass or mass percentage as a function of time is called a thermogram or thermal decomposition curve. TGA gives quantitative information about the mass loss associated with a transition. The changes in mass are as a result of the rupture or formation of chemical bonds at elevated temperatures and loss of some volatile products. TGA is useful in determining the

- Moisture content
- Decomposition, oxidation process
- Physical processes like vaporization, sublimation and desorption.

Here, the first derivative of mass change with respect to time is recorded as a function of time or temperature. The derivative curve is obtained from TG curve either by manual differentiation or the electronic differentiation of the TG signals and the area of the DTG curve at any temperature gives the rate of mass change at that temperature. DTA is a qualitative technique where difference in temperature is measured. It is used to study decomposition temperatures, phase transitions, melting, crystallization points and thermal stability.

TG-DTG analyses of the complexes were carried out in a Perkin Elmer Pyris Diamond TG/DTA analyzer under nitrogen at a heating rate of $10^{\circ}\text{C min}^{-1}$ in the $50\text{-}700^{\circ}\text{C}$ range at the Sophisticated Analytical Instrument Facility, Cochin University of Science and Technology, Kochi-22, India.

References

- [1] A. Werner, A. Miolati, *Z. Anorg.Chem.*, 3 (1893) 267.
- [2] M. M. T. Khan, S. B. Halligudi, S. Shukla, Z. A. Shaikh, *J. Mol. Cata.*, 57 (1990) 301.
- [3] S. Un, P. Dorlet, G. Voyard, L. C. Tabares, N. Cortez, *J. Am. Chem., Soc.* 126 (2004) 2770.
- [4] J. J. R. Frausto da Silva, R. J. P. Williams, *The Biological Chemistry of the Elements*, Clarendon Press, Oxford, 1993. p. 4-5.
- [5] J. Z. Wu, H. Li, J. G. Zhang, H. Xu Ju, *Inorg. Chem. Commun.*, 5(2002) 71.
- [6] M. M. Heravi, L. Ranjbar, F. Derikvand, H. A. Oskooie, F. F. Bamoharram, *J. Mol. Catal. A: Chem.*, 265 (2007) 186.
- [7] R. C. Maurya, S. Rajput, *J. Mol. Struct.*, 833 (2007) 133.
- [8] U. O. Ozmen, G. Olgun, *Spectrochim. Acta Part A*, 70 (2008) 641.
- [9] N. Ozbek, G. Kavak, Y. Ozcan, S. Ide, N. Karacan, *J. Mol. Struct.*, 919 (2009) 154.
- [10] O. Pouralimardan, A. C. Chamayou, C. Janiak, H. H. Monfared, *Inorg. Chim. Acta*, 360 (2007) 1599.
- [11] F. Cariati, U. Caruso, R. Centore, W. Marcolli, A. De Maria, B.: Panunzi, M.A. Tuzi, *Inorg. Chem.*, 41 (2002) 6599.
- [12] E. Ainscough, A. Brodie, J. Ranford, M. Waters, *Inorg. Chim. Acta*, 236 (1995) 83.
- [13] T. R. Rao, M. Sahay, R. C. Aggarwal, *Synth. React. Inorg. Met-Org. Chem.*, 15 (1985) 209.
- [14] A. R. Todeschini, A. L. Miranda, C. M. Silva, S. C. Parrini, E. J. Barreiro, *Eur. J. Med. Chem.*, 33 (1998) 189.
- [15] S. Rollas, S. Guniz kucukguzel, *Molecules*, 12 (2007) 1910.

- [16] S. K. Sridhar, S. N. Pandeyta, J. P. Stables, A. Ramesh, *Eur. J. Pharm. Sci.* 16 (2002) 129.
- [17] M. Carcelli, P. Mazza, C. Pelizzi, G. Pelizzi, F. Zani, *J. Inorg. Biochem.*, 57 (1995) 43.
- [18] Md. A. Affin, S. W. Foo, I. Jusoh, S. Hanapi. E. R. T. Tiekink, *Inorg. Chim. Acta*, 362 (2009) 5031.
- [19] B. Narasimha, P. kumar, D. Sharma, *Act. Pharm. Scien.*, 52 (2010) 169.
- [20] D. K. Johnson, T. B Murphy, N. J. Rose, W. H. Goodwin, L. Pickart, *Inorg. Chim Acta*, 67 (1982) 159.
- [21] H. Yin, *Acta Cryst.*, 64 (2008) 324.
- [22] I. A. Tossidis, C. A. Bolos, *Inorg. Chimi. Acta*, 112 (1986) 93.
- [23] A. A. Abu-Hashem, M. M. Youssef, *Molecules*, 16 (2011) 1956.
- [24] (a) J. D. Hepworth, in: A. J. Boulton, A. McKillop (Edn.), *Comprehensive Heterocyclic Chemistry 3*, Pergamon Press, Oxford, 1984, 835. (b) M. R. Detty, *Organometallics*, 17 (1988) 2188.
- [25] (a) S. V. Jovanovic, S. Steenken, M. Tasic, B. Marjanovic, *M.G. Simic. J. A. C. S.*, 116 (1994) 4846. (b) S. Martens, A. Mithofer, *Phytochemistry*, 66 (2005) 2399.
- [26] M. Kuroda, S. Uchida, K. Watanabe, K. Mimaki, *Phytochemistry* 70 (2009) 288.
- [27] T. Zhou, Q. Shi, K.H. Lee, *Tetrahedron Letters*, 51 (2010) 4382.
- [28] M. Gabor, *Progress in Clinical and Biological Research*, 213 (1986) 471.
- [29] D. C. Pierre, G. Donatien, T. Marguerite, N. T. Bonaventure, P. Pierre, A. A. Ahmed, G. M. Amira, A. I. Godwin, T. Hirata, M. J. Tom, *Natural Product Communications*, 1 (2006) 961.
- [30] M. L. Borges, O. C. Matos, I. M. Pais, J. Seixas, C. P. Ricardo, A. Macanita, R. S. Becker, *Pesticide Science*, 44 (1995) 155.

- [31] A. Kriza, A. Reiss, S. Florea T. Caproiu, *J. Ind. Chem. Soc.*, 77 (2000) 207.
- [32] L. Bravo, *Nutr. Rev.*, 56 (1998) 317.
- [33] S. M. Kuo, *Crit. Rev. Oncog.*, 8 (1997) 47.
- [34] J. Mermur, *J. Mol. Biol.*, 3 (1961) 208.
- [35] J. Alderete, J. Belmar, M. Parra, M. Zarraga, C. Zuniga, *Liq. Cry.*, 35(2) (2008) 157.
- [36] B. A. Jackson, V. Y. Alekseyev, J. K. Barton, *Biochem.*, 38 (1999) 4655.
- [37] R. Zong, R. P. Thummel, *J. Am. Chem. Soc.*, 127 (2005) 12802.
- [38] G. Suss-Fink, A. Meister, G. Meister, *Coord. Chem. Rev.*, 143 (1995) 97.
- [39] T. Miura, A. Hori, H. Mototani, H. Takeuchi, *Biochem.*, 38 (2009) 11560.
- [40] V. Rajendiran, R. Karthik, M. Palaniandavar, H. S. Evans, V. S. Periasamay, M. A. Akbarsha, B. S. Srinag, H. Krishnamurthy, *Inorg. Chem.*, 46 (2007) 8208.
- [41] D. C. Rees, M. Lewis, W. N. Lipscomb, *J. Mol. Biol.*, 168 (1983) 367.
- [42] W. Kaim, B. Schwiderski, *Bioinorganic Chemistry, Inorganic Elements in the Chemistry of Life*, Wiley, New York, 1991.
- [43] D. Bryce-Smith, *Chem. Brit.*, 25 (1989) 783.
- [44] B. C. Cunningham, M. G. Mulkerrin, J. A. Wells, Dimerization of human growth hormone by zinc, *Science*, 253 (1991) 545.
- [45] B. L. Valle, K. H. Falchuk, *Physiol. Rev.*, 73 (1993) 79.
- [46] C. J. Chang, E. M. Nolan, J. Jaworski, S. C. Burdette, M. Sheng, S. J. Lippard, *Chem. Biol.*, 11 (2004) 203.
- [47] A. Ajayaghosh, P. Carol, S. Sreejith, *J. Am. Chem. Soc.*, 127 (2005) 14962.
- [48] Y. Li, Z. Y. Yang, J. C. Wu, *Eur. J. Med. Chem.*, 45 (2010) 5692.

- [49] Y. S. Shim, K. C. Kim, D. Y. Chi, K. H. Lee, H. Cho, *Bioorganic Med. Chem. Lett.*, 13(2013) 2561.
- [50] K. M. Khan, N. Ambreen, U. R. Mughal, S. Jalil, S. Perveen, M. I. Choudhary, *Eur. J. Med. Chem.*, 45 (2010) 4058.
- [51] G. Mhaske, P. Nilkanth, A. Auti, S. Davange, S. Shelke, *IJRSET*, 3 (2014) 8156.
- [52] M. T. Hussain, N. H. Rama, K. M. Khan, *Lett. Org.Chem.*, 7 (2010) 557.
- [53] A. A. Osowole, *Elixir Applied Chem.*, 39 (2011) 4827.
- [54] K. M. Khan, A. Ahmad, N. Ambreen, *Lett. Drug Des. Discov.*, 6 (2009) 363.
- [55] S. Bhatnagar, S. Sahi, P. Kackar, *Bioorganic Med. Chem. Lett.*, 20 (2010) 4945.
- [56] A. Gomes, O. Neuwirth, M. Freitas, *Bioorganic Med.Chem.*, 17 (2009) 7218.
- [57] L. Z. Piao, H. R. Park, Y. K. Park, S. K. Lee, J. H. Park, M. K. Park. *Chem. Pharm. Bull.*, 50 (2002) 309.
- [58] R. M. Mohareb, F Al-Omran, *Steroids*, 77 (2012) 1551.
- [59] S. A. Elsayed, I. S. Butler, B. J. Claude, *Trans. Met Chem.*, 40 (2015) 179.
- [60] N. A. Al-Masoudi, N. M. Aziz, A. T. Mohammed, *Phosphorus Sulfur Silicon Relat. Elem.*, 184 (2009) 2891.
- [61] P. Sathyadevi, P. Krishnamoorthy, M. Alagesan, K. Thanigaimani, P. T. Muthiah, N. Dharmaraj, *Polyhedron*, 31 (2012) 294.
- [62] Y. P. Singh, R. N. Patel, Y. S. Ray, J. B. Pradeep, K. Vishakarma, R. K. B. Singh, *Polyhedron*, 122 (2017) 1.
- [63] H. Q. Chang, L. Jia, J. Xu, *Transition Met. Chem.*, 40 (2015) 485.
- [64] Y. L. Zheng, Y. Y. Ming, F. Wang, *Eur. J. Med. Chem.*, 44 (2009) 4585.

- [65] R. S. Hunoor, B. R. Patil, D. S. Badiger, R. S. Vadavi, K. B. Gudasi, V. M. Chandrashekhar, I. S. Muchchandi, *Spectrochim. Acta Part A*, 77 (2010) 838.
- [66] A. Kajal, S. Bala, N. Sharma, S. Kamboj, V. Saini, *Int J Med Chem.*, doi.org/10.1155/2014/761030.
- [67] R. S. Hoonur,, B. R. Patil,, D. S. Badiger,, R. S. Vadavi, K. B. Gudasi, P. R. Dandawate, M. M. Ghaisas,, S. B. Padhye, M. Nethaji, *Eur. J. Med. Chem.*, 45 (2010) 2277.
- [68] R. S. Hunoor, B. R. Patil, D. S. Badiger, R. S. Vadavi, K. B. Gudasi, V. M. Chandrashekhar, I. S. Muchchandi, *Appl. Organometal. Chem.*, 25 (2011) 476.
- [69] L. V. Tamayo, A. F. Santos, I. P. Ferreira, V. G. Santos, M. T. P. Lopes, H. Beraldo, *Biometals*, 30 (2017) 379.
- [70] M. Shebl, M. A. Ibrahim, S. M. E. Khalil, S. L. Stefan, H. Habib, *Spectrochim. Acta Part A*, 115 (2013) 399.
- [71] M. D. Altintop, A. Ozdemir, G. Turan-Zitouni, S. Ilgin, O. Atli, *Eur. J. Med. Chem.*, 58 (2012) 299.
- [72] F. Chimenti, B. Bizzarri, E. Maccioni, D. Secci, A. Bolasco, *Bioorg. Med. Chem. Lett.*, 17 (2007) 4635.
- [73] (a) S. A. Iqbal, S. Jose, G. Jacob, *Oriental Journal of Chemistry*, 27 (2011) 731. (b) A. Levina, P. A. Lay, *Dalton Trans.*, 40 (2011) 11675.
- [74] S. M. El-Megharbel, *J Microb Biochem Technol.*, 7 (2015) 65.
- [75] B. J. Pages, D. L. Ang, E. P. Wright, J. R. Aldrich-Wright, *Dalton Trans.*, 44 (2015) 3505.
- [76] A. D. Moghaddam, J. D. White, R. M. Cunningham, A.N. Loes, M. M. Haley, V. J. DeRose, *Dalton Trans.*, 44 (2015) 3536.
- [77] M. Sunita, B. Anupama, B. Ushaiah, C. G. Kumari, *Arabian J. Chem.*, 10 (2017) S3367.

- [78] M. Sirajuddin, S. Ali, A. Badshah, J. Photochem. Photobio., 124 (2013) 1.
- [79] A. D. Tiwari, A. K. Mishra, S. B. Mishra, B. B. Mamba, B. Maji, S. Bhattacharya, Spectrochim. Acta Part A, 79 (2011) 1050.
- [80] G. Barone, A. Terenzi, A. Lauria, A. M. Almerico, J. M. Leal, N. Busto, B. Garcia, Coord Chem Rev., 257 (2013) 2848.
- [81] X. Q. Zhou, Y. Li, D. Y. Zhang, Y. Nie, Z. J. Li, W. Gu, X. Liu, J. L. Tian, S. P. Yan, Eur. J. Med. Chem., 114 (2016) 244.
- [82] A. Kosiha, C. Parthiban, K. P. Elang, J. Photochem. Photobio., 168 (2017) 165.
- [83] M. B. Halli, R. B. Sumathi, Arab. J. Chem., 10 (2017) S1748.
- [84] Y. Li, Z. Yang, M. Zhou, J. He, X. Wang, Y. Wu, Z. Wang, J. Mol. Struct., 1130 (2017) 818.
- [85] R. Fekri, M. Salehi, A. Asadi, M. Kubicki, Polyhedron, 128 (2017) 175.
- [86] M. Muralisankar, S. Sujith, N. S. P. Bhuvanesh, A. Sreekanth, Polyhedron, 118 (2016) 103.
- [87] E. Stofer, R. Lavery, Biopolymers, 34 (1994) 337
- [88] J. E. Quin, J. R. Devlin, D. Cameron, K. M. Hannan, R. B. Pearson, R. D. Hannan, Biochim. Biophys. Acta, Mol. Basis Dis., 1842 (2014) 802.
- [89] J. D. Watson and F. H. C. Crick, Nature, 171 (1953) 737.
- [90] N. C. Seeman, H. Wang, X. Yang, F. Liu, C. Mao, W. Sun, L. Wenzler, Z. Shen, R. Sha, H. Yan, M. H. Wong, P. Sa-Ardyen, B. Liu, H. Qiu, X. Li, J. Qi, S. M. Du, Y. Zhang, J. E. Mueller, T.-J. Fu, Y. Wang, J. Chen, Nanotechnology, 9 (1998) 257.
- [91] S. Arnott, Nature, 320 (1986) 313.
- [92] C. Oguey, N. Foloppe and B. Hartmann, PLoS One, 5 (2010) 15931.

- [93] I. Rouzina, V. A. Bloomfield, *J. Phys. Chem.*, 100 (1996) 4305.
- [94] N. Shahabadi, S. Kashanian, F. Darabi, *Eur. J. Med. Chem.*, 45 (2010) 4239.
- [95] R. Palchaudhuri, P. J. Hergenrother, *Curr. Opin. Biotechnol.*, 18, (2007) 497.
- [96] (a) H. Mei, J. Barton, *J. Am. Chem. Soc.*, 108 (1986) 7414 (b) N. Raman, A. Selvan, *J. Enzyme Inhib. Med. Chem.*, 27 (2012) 380.
- [97] R. Sinha, M. M. Islam, B. Kakali, S. K. Gopinatha, A. Banerjee, M. Maiti, *Bioorg. & Medic. Chem.*, 14 (2006) 800.
- [98] K. Fukui, K. Tanaka, *Nucleic Acids Res.*, 24 (1996) 3962.
- [99] C. Moucheron, M. Kirsch-De J. *Phys. Org. Chem.*, 11 (1998) 577.
- [100] M. Sirajuddin, S. Ali, N. A. Shah, M. R. Khan, *Polyhedron*, 40 (2012) 19.
- [101] E. Meggers, *Angew. Chem., Int. Edn.*, 50 (2011) 2442.
- [102] (a) C. M. Che, F. M. Siu, *Curr. Opin. Chem. Biol.*, 14 (2010) 255. (b) P. C. A. Bruijninx, P. J. Sadler, *Curr. Opin. Chem. Biol.*, 12 (2008) 197.
- [103] (a) A. Y. Louie, T. J. Meade, *Chem. Rev.*, 99 (1999) 2711. (b) E. Meggers, *Chem. Commun.*, 0 (2009) 1001.
- [104] (a) G. Gasser, N. Metzler-Nolte, in *Bioinorganic Medicinal Chemistry*, ed E. Alessio, Wiley-VCH Verlag GmbH & Co. KGaA, 2011, p. 351. (b) R. M. F. Bezerra, P. A. Pinto, I. Fraga, A. A. Dias, *Comput. Methods Programs Biomed.*, 125 (2016) 111. (c) B. A. Orsi, K. F. Tipton, *Methods Enzymol.*, 63 (1979) 159.
- [105] R. M. F. Bezerra, I. Fraga, A. A. Dias, *Comput. Methods Programs Biomed.*, 109 (2013) 26.
- [106] J. P. Changeux, *Nat. Rev. Mol. Cell Biol.*, 14 (2013) 819.
- [107] K. Kamata, M. Mitsuya, T. Nishimura, J. Eiki, Y. Nagata, *Structure*, 12 (2004) 429.

- [108] (a) H. Bisswanger, *Enzyme Kinetics: Principles and Methods*. 2nd edn. Weinheim, Germany: Wiley-VCH; 2008. (b) K. Buchholz, V. Kasche, U. T. Bornscheuer, *Biocatalysts and Enzyme Technology*. 2nd edn. Weinheim, Germany: Wiley-VCH; 2012.
- [109] (a) R. A. Copeland In: *Evaluation of Enzyme Inhibitors in Drug Discovery: A Guide for Medicinal Chemists and Pharmacologists*. 2nd edn. N. J. Hoboken, editor. John Wiley & Sons, Inc; 2013. (b) M. J. McGrath, C. N. Scanail, *Sensor Technologies: Healthcare, Wellness and Environmental Applications*. New York: Apress Media, LLC; 2014.
- [110] (a) M. D. Trevan, *Immobilized Enzymes: An Introduction and Applications in Biotechnology*. Chichester: John Wiley & Sons; 1980. (b) R. J. Whitehurst, M. van Oort, *Enzymes in Food Technology*. 2nd edn. Chichester: Wiley-Blackwell; 2009.
- [111] (a) T. M. Devlin, *Biochemistry with Clinical Correlations*. New York: Wiley-Liss (1997). (b) A. Fersht, *Enzyme Structure and Mechanism*, 3rd edn. New York: W. H. Freeman (1999). (c) J. Kyte, *Mechanism in Protein Chemistry*. New York: Garland Publishing (1995).
- [112] Y. Cheng, W. H. Prusoff, *Biochem. Pharmacol.*, 22 (1973) 3099.
- [113] (a) M. Golicnik, *J. Enzyme Inhib. Med. Chem.*, 28 (2013) 879. (b) G. L. Atkins, I. A. Nimmo, *Biochem. J.*, 135 (1973) 779.
- [114] A. Krantz, *Bioorganic Med. Chem. Lett.*, 11 (1992) 1327.
- [115] C. Veeger, D. V. Der Vartanian, W. P. Zeylemaker, *Methods Enzymol.*, 8 (1969) 81.
- [116] M. B. Jeremy, L. T. John, S. Lubert, *Biochemistry*, 7th edn., U.S.A, Kate Ahr Parker. (2012) p.246
- [117] J. Berg, M. Tymoczko, L. John, S. Lubert, *Enzymes Can Be Inhibited by Specific Molecules*. *Biochemistry*. 5th edn., W H Freeman (2002).
- [118] Y. Blat, *Chem. Biol. Drug Des.*, 75 (2010) 535.



Chapter 2

SYNTHESIS AND SPECTRAL CHARACTERIZATION OF ONO/NO DONOR CHROMONE HYDRAZONES

Contents	2.1 Introduction
	2.2 Materials and Methods
	2.3 Result and Discussion
	2.4 Conclusion

Conspectus: Hydrazones are known to be a significant class of nitrogen oxygen donor ligands because of their variable bonding modes towards transition metal ions and their extremely fascinating chemical, biological and medicinal applications. Among this great family of molecules, chromones are of great interest due to their extensive pharmacological activity. The above said facts prompted us to synthesize and characterize some 3-formyl chromone hydrazones. We have synthesized eight hydrazones using benzhydrazide, 4-hydroxybenzoic hydrazide, nicotinic hydrazide, isonicotinic hydrazide, 3-formyl chromone and 6-methyl -3-formyl chromone. The characterization and elucidation of the structure of the prepared compounds were performed by elemental analysis, FT-IR, ESI-MS, electronic, ^1H NMR and ^{13}C NMR spectral methods.

2.1 Introduction

Chromone hydrazones are extremely promising ligands in coordination chemistry and in the biological properties of their metal complexes has been growing in recent years [1-2]. The coordination chemistry of transition metals with ligands from the hydrazone family has been of interest due to different bonding modes shown by these ligands. Generally the possible donor sites in hydrazones are amide oxygen and azomethine nitrogen. However, there remains the possibility of generating complexes with new molecular architectures by suitable substitution in carbonyl and hydrazide part [3]. This is partially due to their capability of acting as NO, ONO, NNO and ONNO donors with the formation of either mono or bi or polynuclear complexes [4-5].

Chromone hydrazones as well as their derivative analogues with potential biological activity are the focus of extensive investigation. Specifically the chromone hydrazones have been screened for their antifungal, antibacterial, antioxidant, antimalarial, anti-inflammatory and DNA binding [6-15].

Keeping in view the above points and by considering the biological potentials of hydrazones we have synthesized eight chromone hydrazones. The two chromones (3-formyl chromone and 6-methyl-3-formyl chromones) selected here are having a keto group which provides further binding site for metal cations and they behave as chelating ligands. The spectroscopic data showed that the ONO/NO donor ligands act as monobasic tri/bidentate chelates. The coordination sites with the metal (II) ion are pyrone oxygen, azomethine nitrogen and hydrazonic oxygen. The ligand systems of our interest and their abbreviations are as follows.

2.2 Materials and Methods

3-Formyl chromone, 6-methyl-3-formyl chromone, benzohydrazide, 4-hydroxybenzhydrazide, nicotinic acid hydrazide, isonicotinic acid hydrazide $\text{Ni}(\text{OCOCH}_3)_2 \cdot 4\text{H}_2\text{O}$, $\text{Cu}(\text{OCOCH}_3)_2 \cdot \text{H}_2\text{O}$ and $\text{Zn}(\text{OCOCH}_3)_2 \cdot 2\text{H}_2\text{O}$ (Sigma-Aldrich), were of Analar grade and were used as received. The solvent methanol, ethanol, acetone, chloroform, ethyl acetate, acetic acid, DMF and DMSO (Merck) was used. All materials used were of the high purity available and used without further purifications. Solvents employed were either of 99% purity or purified by known laboratory procedures [16].

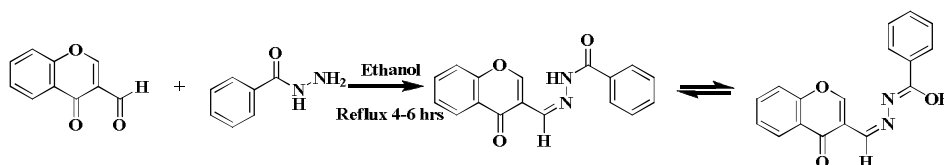
2.2.1 Synthesis of 3-formyl chromone hydrazones

The hydrazones were synthesized by adapting the reported procedure [17], namely *via* condensation between appropriate aldehyde/ketone with the respective hydrazide as described below. There are eight 3-formyl chromone hydrazones were synthesised. The synthesised compounds were analytically pure, crystalline, non-hygroscopic, coloured, insoluble in water, sparingly soluble in methanol, ethanol, acetone, chloroform, and ethyl acetate but soluble in DMF, DMSO

2.2.1.1 Synthesis of hydrazone derived from 3-formyl chromone and benzhydrazide (FB)

Hydrazone (FB) was prepared by the condensation of 3-formyl chromone and benzohydrazide (Scheme 2.1). An ethanol solution containing benzoyl hydrazide (0.136 g, 1 mmol) was added drop wise to ethanolic solution of 3-formyl chromone containing few drops of acetic acid (0.174 g, 1 mmol). The mixture was refluxed for 4-6 h at 60-80 °C yielding a

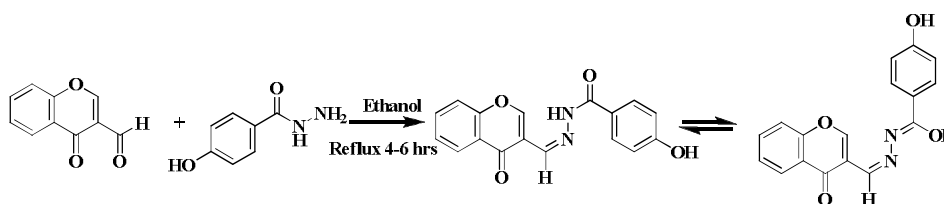
precipitate, which was filtered off, washed with ethanol and dried in a vacuum. The solid was recrystallized from ethanol to yield a yellow solid and then dried. Yield and melting point of the compound was noted.



Scheme 2.1 Synthesis of FB

2.2.1.2 Synthesis of hydrazone derived from 3-formyl chromone and 4-hydroxybenzhydrazone (FBH)

Hydrazone (FBH) was synthesized by the reaction between 3-formyl chromone and 4-hydroxy benzohydrazide (Scheme 2.2). Ethanolic solution 4-hydroxybenzohydrazide (0.152g, 1 mmol) was added drop wise to ethanol solution 3-formyl chromone (0.174g, 1 mmol). The mixture was refluxed for 4-6 h at 60-80°C yielding a precipitate, which was filtered, washed with ethanol and recrystallized from ethanol to yield a yellow solid and then dried. Yield and melting point of the compound was determined.

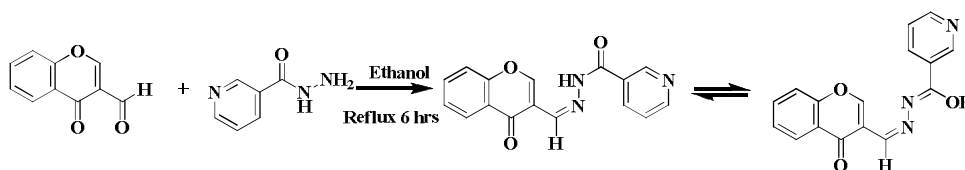


Scheme 2.2 Synthesis of FBH

2.2.1.3 Synthesis of hydrazone derived from 3-formyl chromone and nicotinic hydrazide (FN)

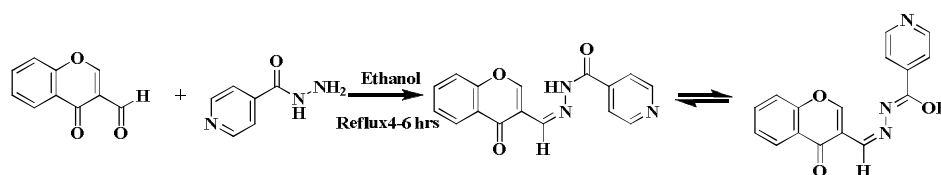
Nicotinic acid hydrazide (0.137 g, 1 mmol) in ethanol (20 mL) was added drop wise to an ethanolic solution containing few drops of acetic

acid and 3-formyl chromone (0.174 g, 1 mmol). The mixture was refluxed for 6 h at 60-80°C. The resulting solution was concentrated and cooled. The precipitate was collected and recrystallized from ethanol. The yellow crystalline compounds were collected. The yield and melting point of the product was noted.



2.2.1.4 Synthesis of hydrazone derived from 3-formyl chromone and isonicotinic hydrazide (FIN)

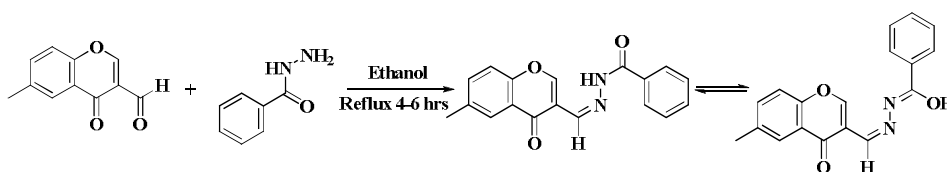
To an ethanolic solution of 3-formyl chromone (0.174 g, 1 mmol) containing few drops of acetic acid, ethanolic solution of isonicotinic acid hydrazide (0.137 g, 1 mmol) was added drop wise. The above mixture was refluxed for 4-6 h at 60-80°C. After completion of reaction, cooled to room temperature and solvent evaporated slowly. The yellow needle like crystalline compound was separated out. It was washed with alcohol and recrystallized from ethanol. The yield and melting point of the compound was determined.



2.2.1.5 Synthesis of hydrazone derived from 6-methyl-3-formyl chromone and benzhydrazide (FMB)

Benzhydrazide (0.136 g, 1 mmol) in ethanol was added drop wise to ethanolic solution of 6-methyl-3-formyl chromone (0.188 g, 1 mmol)

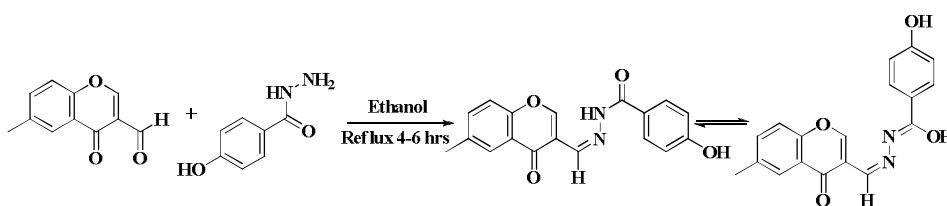
contain two drops of acetic acid were mixed, boiled under reflux for 4-6 h at 60-80°C. The resulting solution was concentrated and allowed to cool room temperature. The precipitate formed was collected and recrystallized from ether by slow evaporation. The yellowish crystalline product was obtained. The yield and melting point of the compound was determined.



Scheme 2.5 Synthesis of FMB

2.2.1.6 Synthesis of hydrazone derived from 6-methyl-3-formyl chromone and 4-hydroxybenzohydrazide (FMBH)

An ethanol solution of 4-hydroxy benzohydrazide (0.152 g, 1 mmol) was added drop wise to ethanolic solution 6-methyl-3-formyl chromone (0.188 g, 1 mmol) contain one or two drops of acetic acid. The mixture was refluxed for 4-6 h at 60-80°C. The solution was evaporated slowly. Crystalline product obtained was filtered, washed with ether and recrystallized from ethanol to form a yellow solid and then dried. Yield and melting point of the compound was determined.

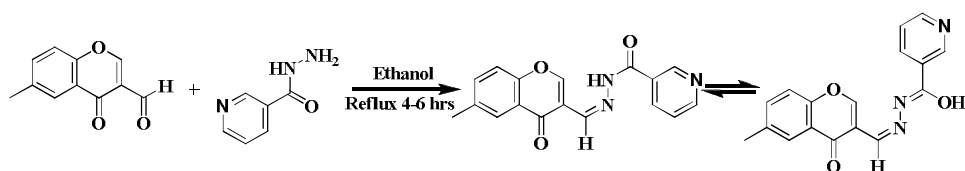


Scheme 2.6 Synthesis of FMBH

2.2.1.7 Synthesis of hydrazone derived from 6-methyl-3-formyl chromone and nicotinic hydrazide (FMN)

Hydrazone (FMN) was obtained by the condensation of 6-methyl-3-formyl chromone and nicotinic acid hydrazide (Scheme 2.7). To a

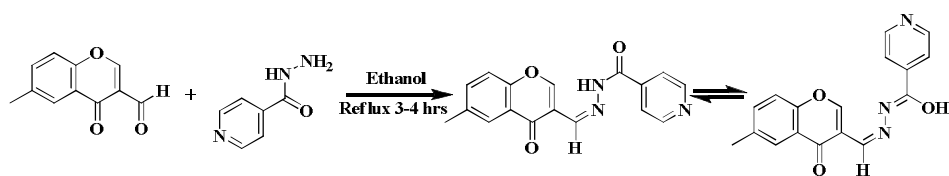
solution of nicotinic acid hydrazide (0.137 g, 1 mmol) in ethanol was added drop wise to ethanolic solution containing 6-methyl-3-formyl chromone (0.188 g, 1mmol) and one or two drops of acetic acid. The above mixture was refluxed at 60-80°C for 4-6 h. After completion of the reaction, cooled to room temperature, solvent evaporate slowly. The crystalline compound was filtered off, washed with ether, recrystallized from ethanol and dried. Yield and melting point of the compound was noted.



Scheme 2.7 Synthesis of FMN

2.2.1.8 Synthesis of hydrazone derived from 6-methyl-3-formyl chromone and isoniazid hydrazide (FMIN)

Isoniazid hydrazide (0.137 g, 1 mmol) in ethanol (15 mL) was added drop wise to ethanolic solution of 6-methyl-3-formyl chromone (0.188 g, 1 mmol) having one drop of acetic acid. The above mixture boiled under reflux at 60-80°C for 4-6 h. the resulting solution is concentrated. The precipitate formed was filtered off, washed with ethanol and dried in a vacuum. The solid was recrystallized from ethanol to yield a yellow solid. Yield and melting point of the product was determined.



Scheme 2.8 Synthesis of FMIN

2.3 Result and Discussion

2.3.1 Characterizations of 3-formyl chromone hydrazones

The synthesised 3-formyl chromone hydrazones were characterized by elemental analysis, ESI-MS, FT-Infrared, Electronic and $^1\text{H}/^{13}\text{C}$ NMR spectra.

2.3.1.1 Elemental analysis

The elemental analysis (C, H, and N) results of 3-formyl chromone hydrazones were given in Table 2.1 which shows that it is analytically pure. The analytical data for FB, FBH, FN, FIN, FMB, FMBH, FMN and FMIN were given in the Table 2.1. They are in good agreement with empirical formula.

Table 2.1: Analytical data of 3-formyl chromone hydrazones

Compound	Empirical formula	Formula weight (g/mol)	m.p °C	Colour (Yield %)	Found (Calculated) %		
					C	H	N
FB	$\text{C}_{17}\text{H}_{12}\text{N}_2\text{O}_3$	292.08	171-173	Yellow (76)	68.40 (69.86)	4.19 (4.14)	9.36 (9.58)
FBH	$\text{C}_{17}\text{H}_{12}\text{N}_2\text{O}_4$	308.18	169-170	Yellow (78)	66.30 (66.23)	3.88 (3.92)	9.13 (9.09)
FN	$\text{C}_{16}\text{H}_{11}\text{N}_3\text{O}_3$	293.08	168	Yellow (66)	65.40 (65.53)	3.70 (3.78)	14.36 (14.33)
FIN	$\text{C}_{16}\text{H}_{11}\text{N}_3\text{O}_3$	293.08	130	Yellow (79)	65.47 (65.53)	3.72 (3.78)	14.39 (14.33)
FMB	$\text{C}_{18}\text{H}_{14}\text{N}_2\text{O}_3$	306.51	171	Yellow (70)	70.50 (70.58)	4.55 (4.61)	9.20 (9.15)
FMBH	$\text{C}_{18}\text{H}_{14}\text{N}_2\text{O}_4$	322.31	169	Yellow (76)	66.98 (67.07)	4.30 (4.38)	8.62 (8.69)
FMN	$\text{C}_{17}\text{H}_{13}\text{N}_3\text{O}_3$	307.09	170	Yellow (75)	66.51 (66.44)	4.21 (4.26)	13.34 (13.67)
FMIN	$\text{C}_{17}\text{H}_{13}\text{N}_3\text{O}_3$	307.09	170	Yellow (71)	66.40 (66.44)	4.19 (4.26)	13.30 (13.67)

2.3.1.2 Mass spectra

The electron spray ionization (ESI) technique was used to measure the mass to charge (m/z) ratio of charged particles. The organic molecules are bombard with high energy electrons and the result is quantitatively recorded as a spectrum of positive ion fragments. The most abundant ion formed in the ionization chamber gives rise to the tallest peak in the spectrum called the base peak. The spectral intensities are normalized by setting the base peak to relative abundance 100 and the rest of the ions are recorded as percentages of the base peak intensity. Mass spectrum is a plot of m/z of positive ion fragments versus their relative abundance. Hydrazones, which are formed from the reaction between carbonyl compounds and hydrazides are stable at room temperature but unstable at higher temperatures and have relatively high boiling points. Therefore GC-MS is not easy to apply for hydrazone analysis due to these physical natures. So, LC-MS has been used to analyze these derivatives [18-19]. In the present study, the molecular ion ($M+1$) peaks at 293.1, 309.2, 294.8, 294.5, 307.1, 323.30, 308.11 and 308.51 amu for the 3-formyl chromone hydrazones FB, FBH, FN, FIN, FMB, FMBH, FMN and FMIN respectively confirms the expected molecular weight of respective 3-formyl chromone hydrazones synthesized (Figures. 2.1-2.8).

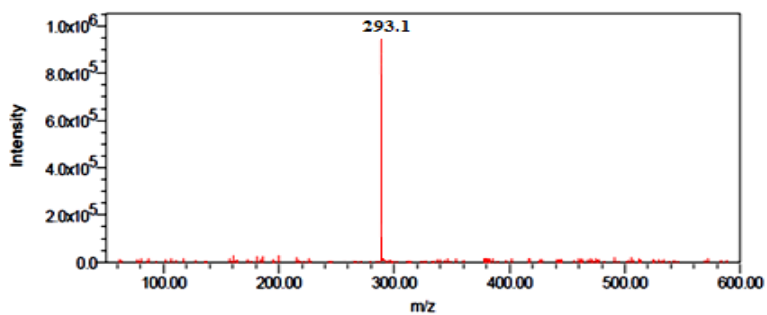


Figure 2.1 ESI-MS spectrum of FB

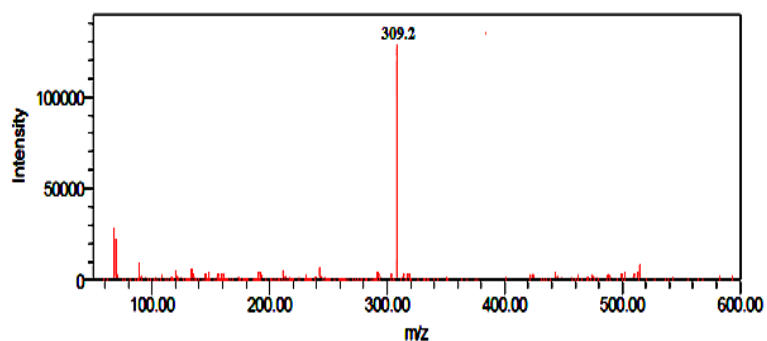


Figure 2.2 ESI-MS spectrum of FBH

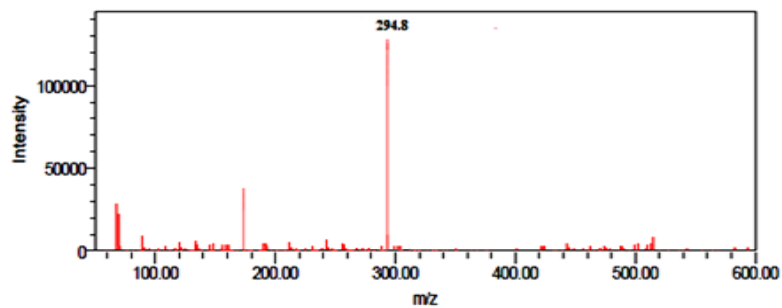


Figure 2.3 ESI-MS spectrum of FN

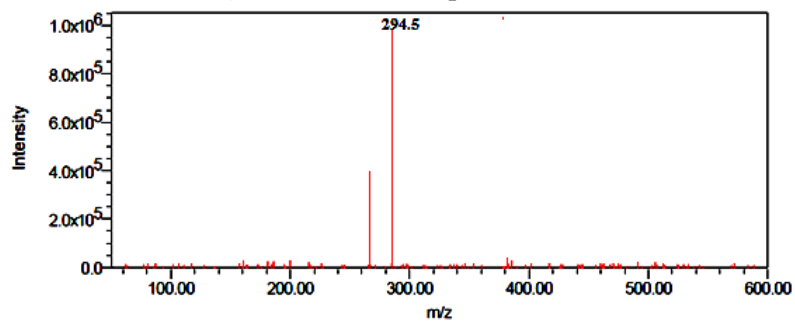


Figure 2.4 ESI-MS spectrum of FIN

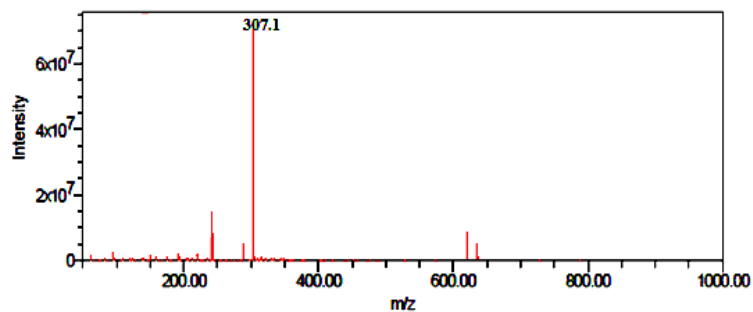


Figure 2.5 ESI-MS spectrum of FMB

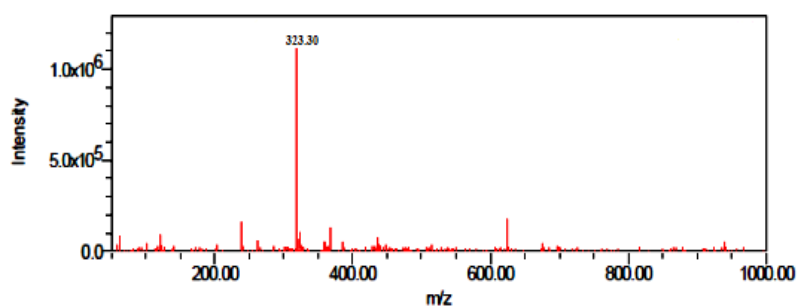


Figure 2.6 ESI-MS spectrum of FMBH

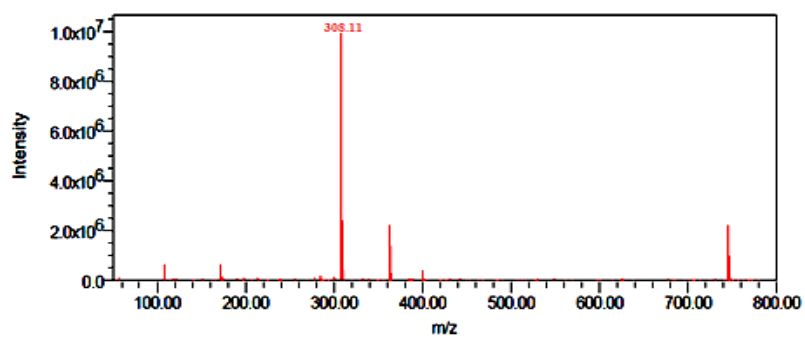


Figure 2.7 ESI- MS spectrum of FMN

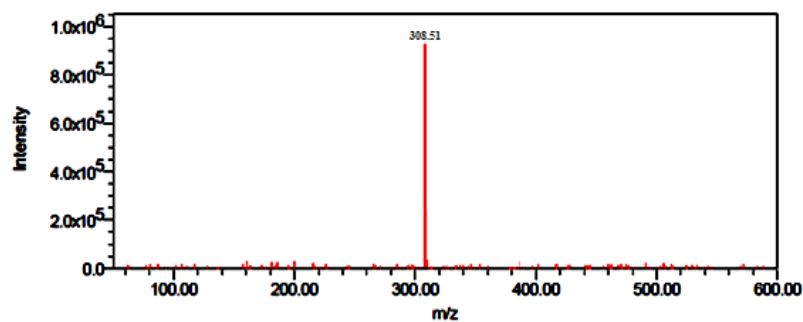


Figure 2.8 ESI-MS spectrum of FMIN

2.3.1.3 FT-Infrared spectra

The characteristic IR bands of the chromone hydrazones give important information about the various functional groups present in it. Strong bands due to the ν (N-H) and ν (C=O) modes at 3206-3100 cm^{-1} and 1658-1641 cm^{-1} are observed in the spectrum of 3-formyl chromone hydrazones (Figures 2.9-2.16) which suggests that the hydrazone exists in the amido form in the solid state [20]. Another band at 1683-1674 cm^{-1} is due to the presence of (C=O, pyrone). A prominent band at 1597-1584 cm^{-1} due to azomethine ν (C=N) linkage is observed in the spectrum indicating that condensation between aldehyde moiety of 3-formyl chromone and that of the aromatic/hetero aromatic hydrazides has taken place resulting into the formation of desired 3-formyl chromone hydrazone ligand. It further confirms the ν (C-O), ν (N-N) bands at 1238-1232, 1035-1027 cm^{-1} [21] respectively.

Table 2.2 FT-IR spectral data of 3-formyl chromone hydrazone ligands (cm^{-1})

No	Compounds	IR spectra (cm^{-1}) ¹					
		ν (OH, NH)	ν (C=O) pyrone	ν (C=O) hydrazoneic	ν (C=N)	ν (C-O)	ν (N-N)
1	FB	-, 3220	1678	1641	1597	1238	1035
2	FBH	3394 (broad)	1675	1650	1590	1232	1028
3	FN	3310, 3126	1677	1651	1596	1237	1029
4	FIN	3500-3000 (broad)	1674	1645	1597	1234	1033
5	FMB	-, 3206	1680	1655	1595	1238	1035
6	FMBH	3346, 3100	1675	1650	1590	1232	1028
7	FMN	-, 3206	1679	1647	1584	1236	1032
8	FMIN	-, 3100	1683	1658	1587	1234	10277

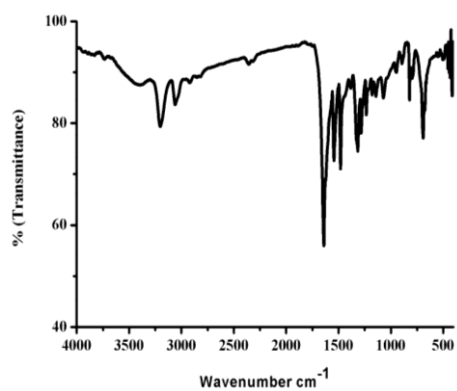


Figure 2.9 FT-IR spectrum of FB

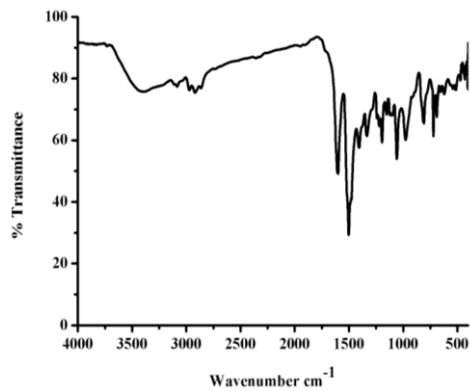


Figure 2.10 FT-IR spectrum of FBH

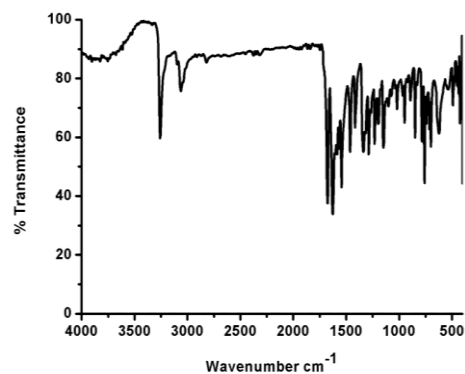


Figure 2.11 FT-IR spectrum of FN

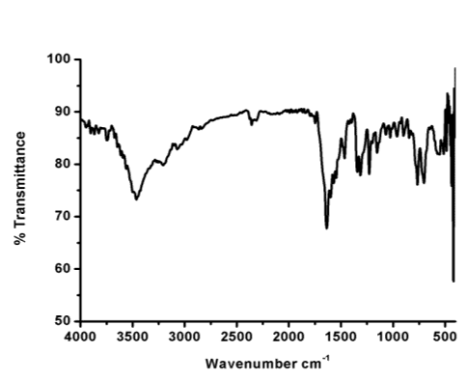


Figure 2.12 FT-IR spectrum of FIN

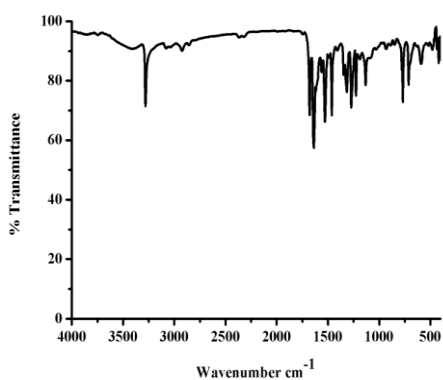


Figure 2.13 FT-IR spectrum of FMB

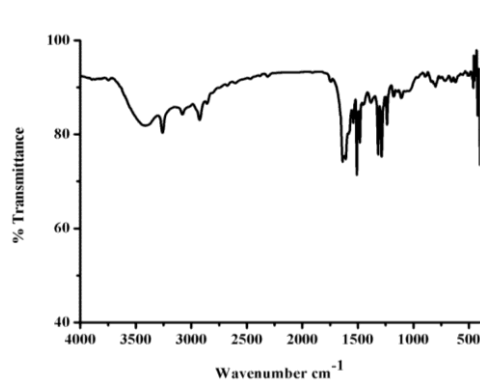


Figure 2.14 FT-IR spectrum of FMBH

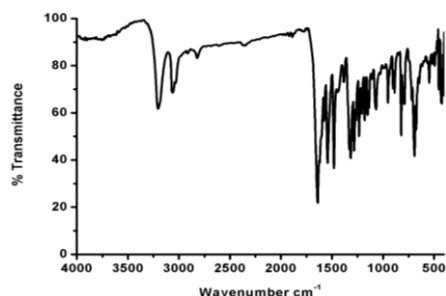


Figure 2.15 FT-IR spectrum of FMN

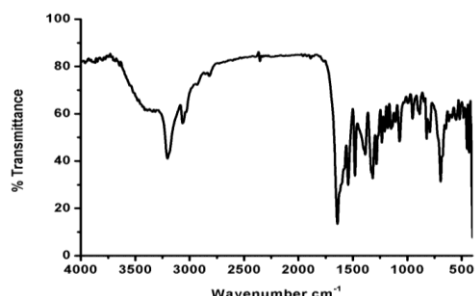


Figure 2.16 FT-IR spectrum of FMIN

2.3.1.4 Electronic spectra

The electronic spectral data of the ligand (3-formyl chromone hydrazone) in DMF (10^{-3} M) (Table 2.3) showed two bands with λ_{\max} (DMF) 307-311 nm (32573 - 32154 cm^{-1}) and 342-361 nm (29239 - 27700 cm^{-1}) for 3-formyl hydrazone ligands. The higher energy band may be assigned to π - π^* transitions of the azomethine linkage and the aromatic rings. The medium energy band may be assigned to n - π^* transitions of the C=O and C=N groups (Figures 2.17- 2.24).

Table 2.3 UV-visible spectral data of 3-formyl chromone hydrazone ligands in DMF (10^{-3} M)

No	Compounds	Electronic spectral bands (nm) λ_{\max} (nm)/($\epsilon_{\max} * 10^3$ L cm^{-1} mol $^{-1}$)
1	FB	307 (1.39) - $\pi \rightarrow \pi^*$ 349 (4.6) - $n \rightarrow \pi^*$
2	FBH	304 (1.48) - $\pi \rightarrow \pi^*$ 342 (7.2) - $n \rightarrow \pi^*$
3	FN	320 (1.32) - $\pi \rightarrow \pi^*$ 356 (4.9) - $n \rightarrow \pi^*$
4	FIN	309 (1.45) - $\pi \rightarrow \pi^*$ 351 (5.9) - $n \rightarrow \pi^*$
5	FMB	310 (1.37) - $\pi \rightarrow \pi^*$ 361 (8.6) - $n \rightarrow \pi^*$
6	FMBH	305 (1.41) - $\pi \rightarrow \pi^*$ 357 (7.9) - $n \rightarrow \pi^*$
7	FMN	313 (1.31) - $\pi \rightarrow \pi^*$ 356 (5.2) - $n \rightarrow \pi^*$
8	FMIN	311 (1.46) - $\pi \rightarrow \pi^*$ 353 (5.7) - $n \rightarrow \pi^*$

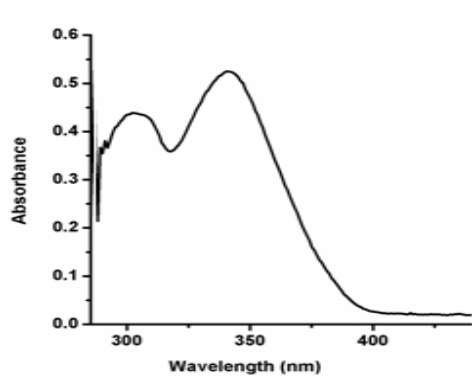


Figure 2.17 UV-visible spectrum of FB

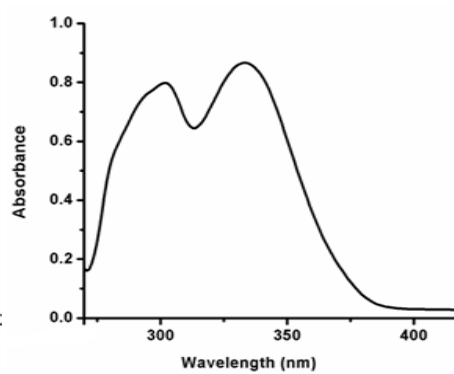


Figure 2.18 UV-visible spectrum of FBH

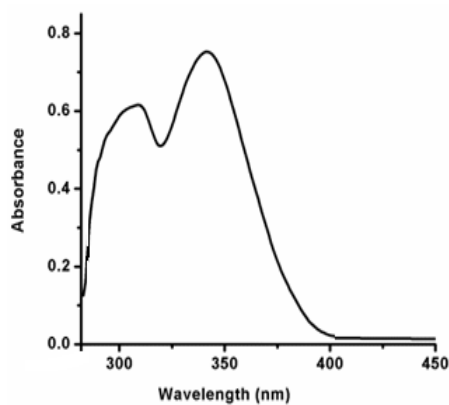


Figure 2.19 UV-visible spectrum of FN

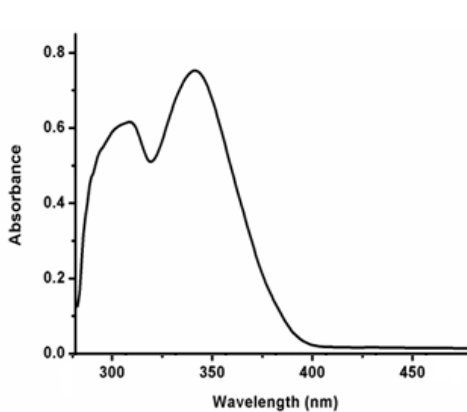


Figure 2.20 UV-visible spectrum of FIN

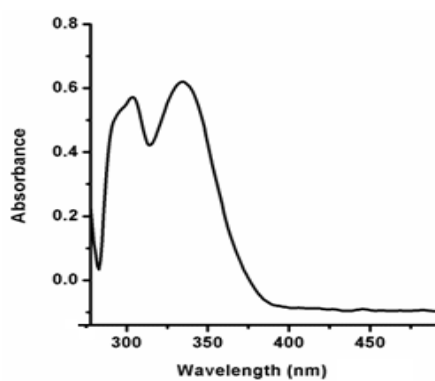


Figure 2.21 UV-visible spectrum of FMB

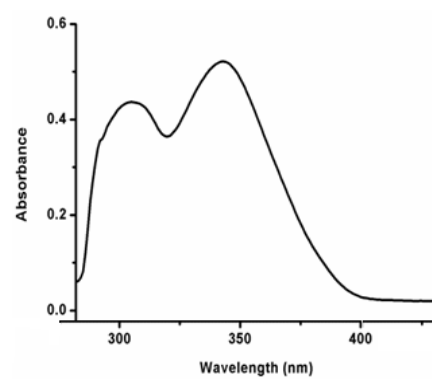


Figure 2.22 UV-visible spectrum of FMBH

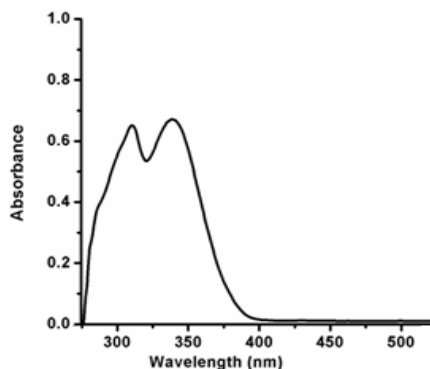


Figure 2.23 UV-visible spectrum of FMN

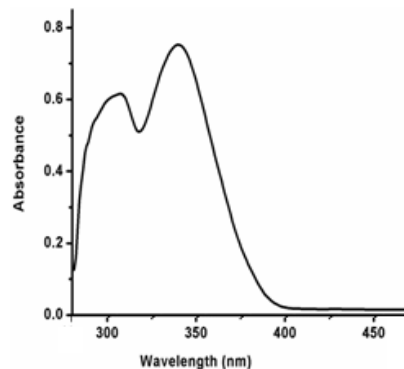


Figure 2.24 UV-visible spectrum of FMIN

2.3.1.5 NMR spectra

The NMR spectral assignments were done on the basis of ^1H NMR and ^{13}C NMR

2.3.1.5.1 ^1H NMR spectra

The ^1H NMR spectra of 3-formyl chromone hydrazone were recorded in DMSO-d_6 using TMS as the internal standard (Figures 2.25-2.32) and assignments were done with that of the respective standard values (Table 2.4). The ^1H NMR spectra of 3-formyl chromone hydrazones the sharp singlet at the range of $\delta 11.72$ - 12.12 ppm in the downfield region of the spectrum which integrates as one hydrogen is due to OH proton the existence of the compound in the iminolic form of the hydrazone. A singlet at the range of $\delta 10.12$ - 10.13 ppm in the spectra is assigned to the phenolic proton (Figures 2.26 & 2.30). Absence of any coupling interactions by protons on neighbouring atoms renders singlet peaks for these iminolic and phenolic protons. A sharp singlet at the region of $\delta 8.78$ - 9.08 ppm is due to $=\text{CH}$ of azomethine group. A sharp singlet at region of $\delta 8.59$ ppm is due to presence of hydrogen at oxo-ring of chromone part.

Table 2.4 ^1H NMR and ^{13}C NMR spectral data of 3-formyl chromone hydrazone ligands

Compounds	Assignments
FB	^1H NMR (DMSO- d_6 δ ppm); 11.72 (1H,s, iminolic -OH), 8.78 (1H,s, -CH=N-), 8.59 (1H,s, H oxo-ring), 7.92-6.84 (m, aromatic ring); ^{13}C NMR (DMSO- d_6 δ ppm) 177.50 (C=O), 163.77 (=N-N=CH-), 162.7 (C8), 157.20 (C9), 152.80 (C5), 135.2 (C11), 131.00 (C1), 129.80 (C4), 128.80 (C2), 128.10 (C3), 125.80 (C13), 123.97 (C14), 123.47 (C12), 116.10 (C10), 102.41 (C7).
FBH	^1H NMR (DMSO- d_6 δ ppm); 11.73 (1H,s, iminolic -OH), 10.12 (1H,s, phenolic -OH), 8.80 (1H,s, -CH=N-), 8.60 (1H,s, H oxo-ring), 8.15-6.87 (m, aromatic ring); ^{13}C NMR (DMSO- d_6 δ ppm) 176.00 (C=O), 163.71 (=N-N=CH-), 162.72 (C9), 160.83 (C1), 157.21 (C10), 152.83 (C5), 135.23 (C12), 130.67 (C3), 125.85 (C14), 123.92 (C15), 123.42 (C13), 122.40 (C4), 116.60 (C11), 116.01 (C2), 102.47(C7).
FN	^1H NMR (DMSO- d_6 δ ppm); 12.08 (1H,s, iminolic -OH), 9.08(1H,s, -CH=N-), 8.83 (1H,s, H oxo-ring), 8.78-7.56 (m, aromatic ring); ^{13}C NMR (DMSO- d_6 δ ppm) 178.02 (C=O), 163.70 (=N-N=CH-), 162.31. (C9), 152.82 (C6), 152.26 (C10), 151.50 (C5).
FIN	^1H NMR (DMSO- d_6 δ ppm); 11.72 (1H,s, iminolic -OH), 8.83 (1H,s, -CH=N-), 8.63 (1H,s, H oxo-ring), 8.78-7.69 (m, aromatic ring); ^{13}C NMR (DMSO- d_6 δ ppm) 178.40 (C=O), 163.71 (=N-N=CH-), 162.50 (C7), 152.82 (C4), 152.21 (C8).
FMB	^1H NMR (DMSO- d_6 δ ppm); 11.72(1H,s, iminolic -OH), 8.78 (1H,s, -CH=N-), 8.59 (1H,s, H oxo-ring), 7.92-7.56 (m, aromatic ring), 2.45 (3H,s, -CH $_3$); ^{13}C NMR (DMSO- d_6 δ ppm) 177.50 (C=O), 163.77 (=N-N=CH-), 162.50 (C8), 154.20 (C9), 152.80 (C5) 138.90 (C11), 133.10 (C12), 131.19 (C1), 129.80 (C4), 128.80 (C2), 128.10 (C3), 124.40 (C3), 123.57 (C14), 113.47 (C10), 102.97 (C7), 21.32 (C16).
FMBH	^1H NMR (DMSO- d_6 δ ppm); 11.72 (1H,s, iminolic -OH), 10.13 (1H,s, phenolic -OH), 8.78 (1H,s, -CH=N-), 8.59 (1H,s, H oxo-ring), 7.92-6.87 (m, aromatic ring), 2.45 (3H,s, -CH $_3$); ^{13}C NMR (DMSO- d_6 δ ppm) 175.00 (C=O), 163.00 (=N-N=CH-), 162.40 (C8), 160.70 (C1), 154.11 (C9) 154.06 (C5), 135.70 (C11), 135.64 (C12), 129.70 (C3) 124.40 (C13), 123.60 (C14), 123.01 (C4), 118.47(C2), 118.32 (C10), 114.99 (C7). 20.43 (C16).
FMN	^1H NMR (DMSO- d_6 δ ppm); 12.08 (1H,s, iminolic -OH), 9.08 (1H,s, -CH=N-), 8.83 (1H,s, H oxo-ring), 8.78-7.56 (m, aromatic ring), 2.45 (3H,s, -CH $_3$); ^{13}C NMR (DMSO- d_6 δ ppm) 174.92 (C=O), 161.50 (=N-N=CH-), 154.52 (C9), 154.05 (C10), 152.31 (C4) 141.23 (C1), 135.78 (C12), 135.69 (C3), 135.40 (C13), 128.89 (C5), 124 40 (C14), 123.57 (C2), 122.99 (C15), 118.47 (C11), 117.97 (C8), 20.42 (C17).
FMIN	^1H NMR (DMSO- d_6 δ ppm); 12.12 (1H,s, iminolic -OH), 8.82 (1H,s, -CH=N-), 8.65 (1H,s, H oxo-ring), 8.79-7.60 (m, aromatic ring), 2.44 (3H,s, -CH $_3$); ^{13}C NMR (DMSO- d_6 δ ppm) 175.40 (C=O), 163.47 (=N-N=CH-), 161.50 (C7), 154.52 (C8), 152.31 (C4), 149.56 (C1), 141.23 (C10), 135.69 (C3), 135.40 (C11), 128.89 (C12), 124.40 (C2), 123.57 (C13), 113.47 (C9), 102.97 (C6),20.42 (C15).

The downfield shifts of these protons are may be assigned to their hydrogen bonding interactions. Hydrogen bonding decreases the electron density around the proton and thus moves the proton absorption to a lower field. Absence of any coupling interactions of these protons due to the lack of availability of protons on neighbouring atoms renders singlet peaks for them. Multiplets around δ 7.92-6.84 ppm are assigned to protons of the chromone ring system and the protons attached to the aromatic ring. The three hydrogen singlet at around δ 2.45 ppm is assigned for $-\text{CH}_3$ protons (Figures 2.29-2.32).

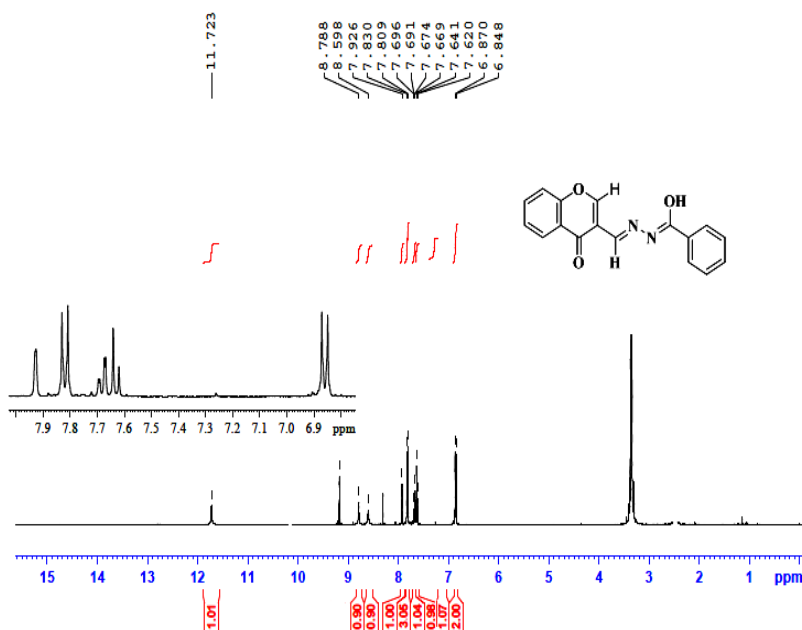


Figure 2.25 ^1H NMR spectrum of FB

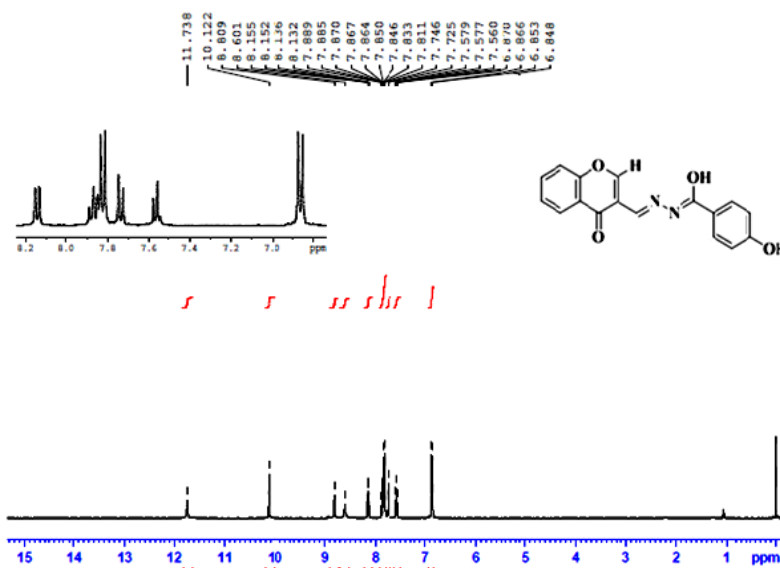


Figure 2.26 ^1H NMR spectrum of FBH

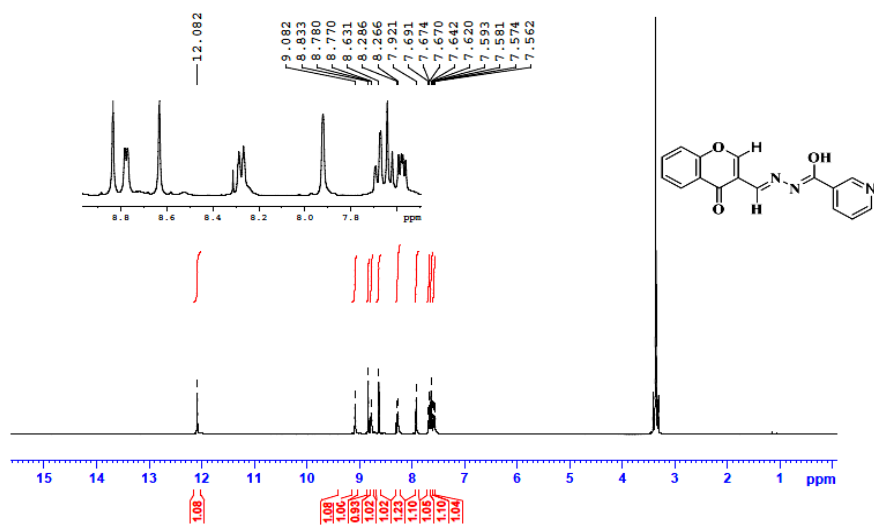


Figure 2.27 ^1H NMR spectrum of FN

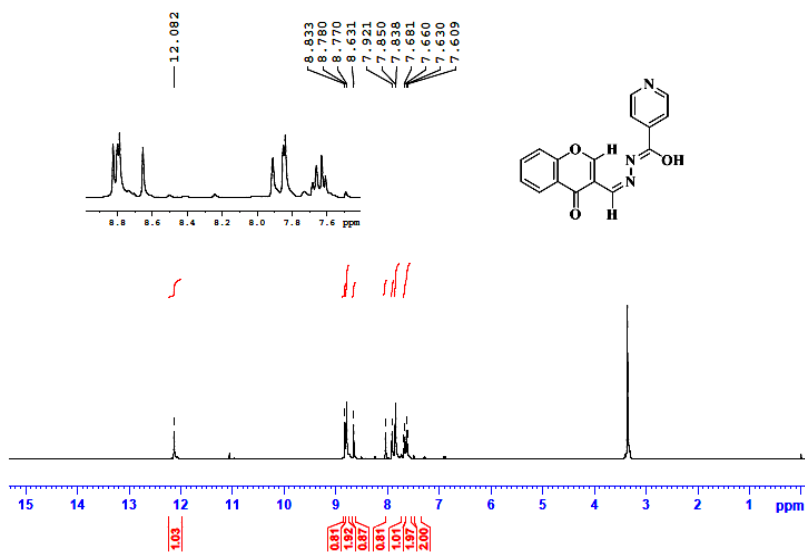


Figure 2.28 ¹H NMR spectrum of FIN

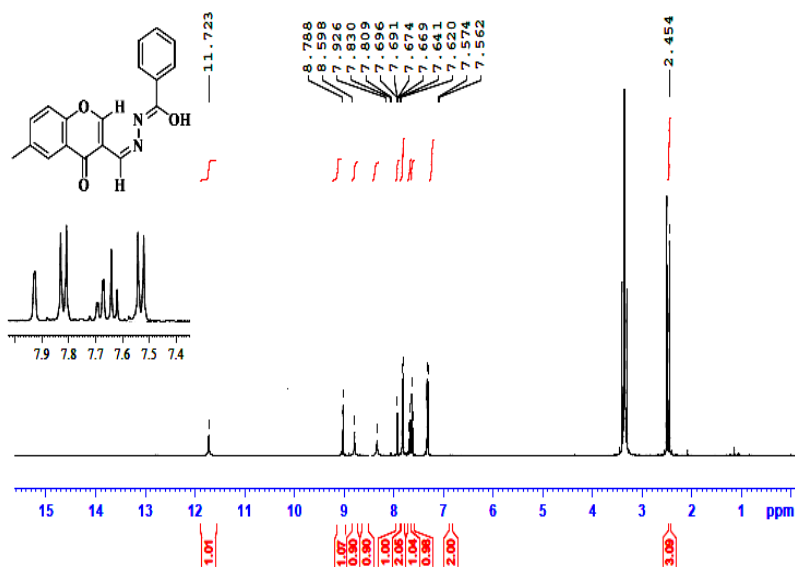


Figure 2.29 ¹H NMR spectrum of FMB

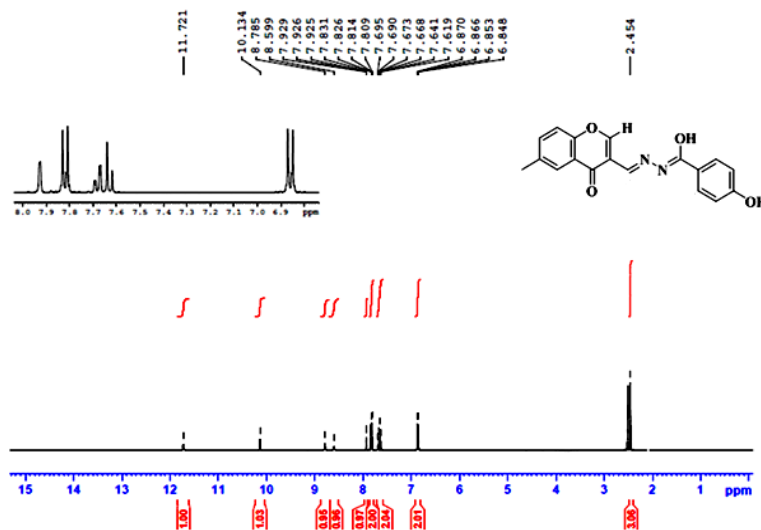


Figure 2.30 ¹H NMR spectrum of FMBH

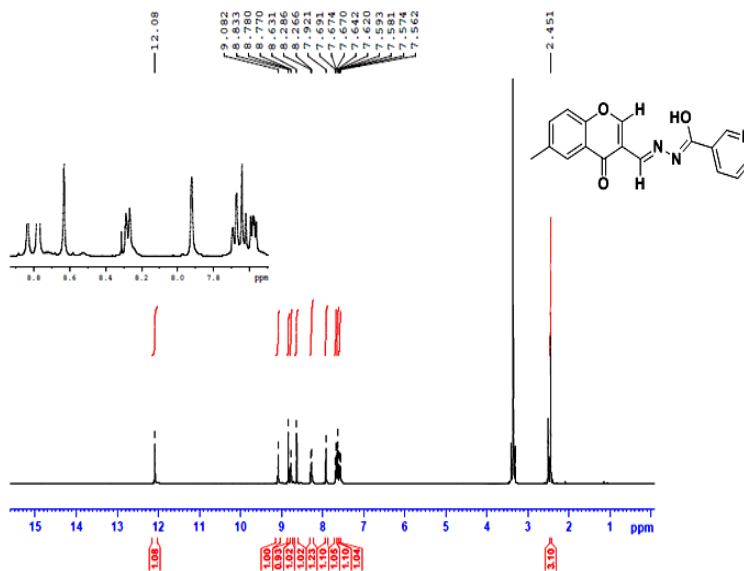


Figure 2.31 ¹H NMR spectrum of FMN

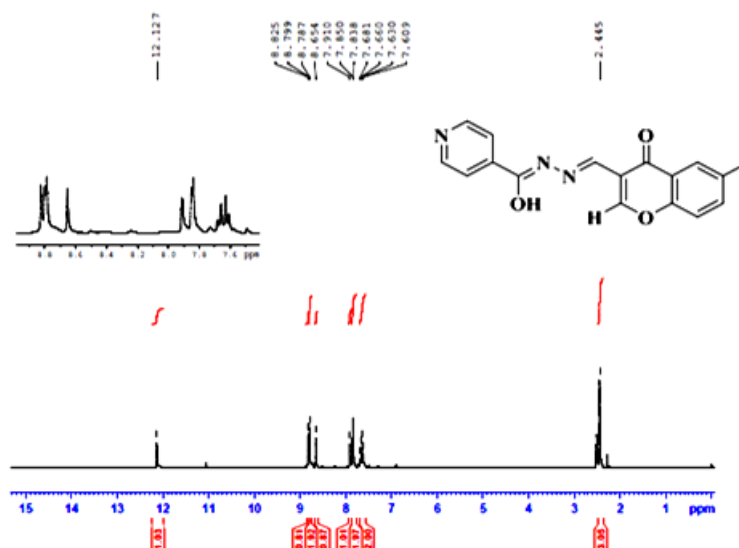


Figure 2.32 ¹H NMR spectrum of FMIN

2.3.1.5.2 ¹³C NMR spectra

The proton decoupled ¹³C NMR spectrum provides direct information about the carbon skeleton of the molecule. The ¹³C NMR spectrum of the compound (Figures 2.33-2.40) shows carbon signals supporting the ¹H NMR assignments. There are unique carbon atoms in the molecule which give different peaks in the spectrum (Table 2.4). The non protonated carbon atom is shifted farthest downfield in the spectra around δ 177.50 ppm are due to the C=O group of chromone ring. A non protonated carbon atom is shifted to downfield in the spectra in the region of δ 163.77 ppm are due to the conjugative effect of the =N-N=CH-hydrazone skeleton.

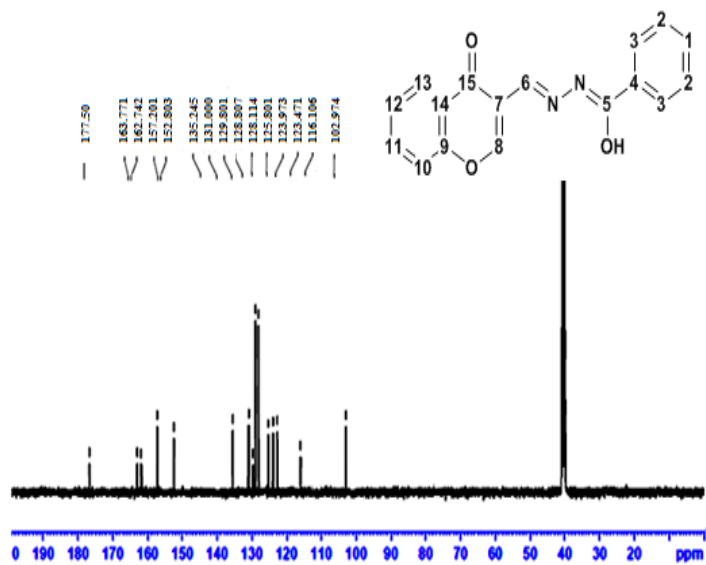


Figure 2.33 ¹³C NMR spectrum of FB

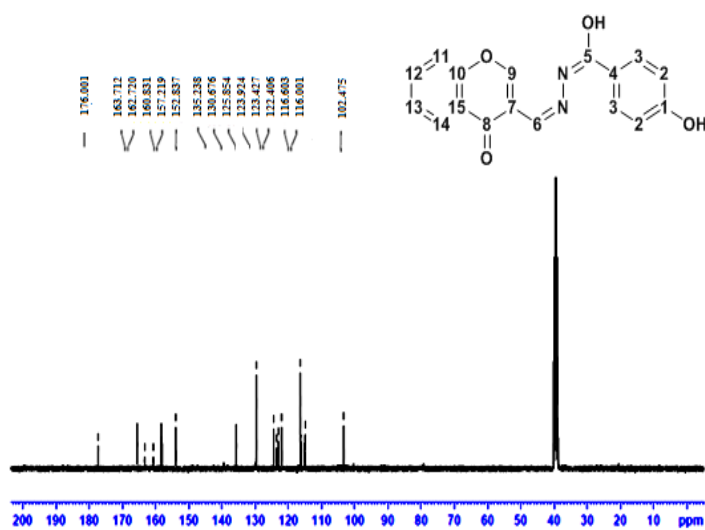


Figure 2.34 ¹³C NMR spectrum of FBH

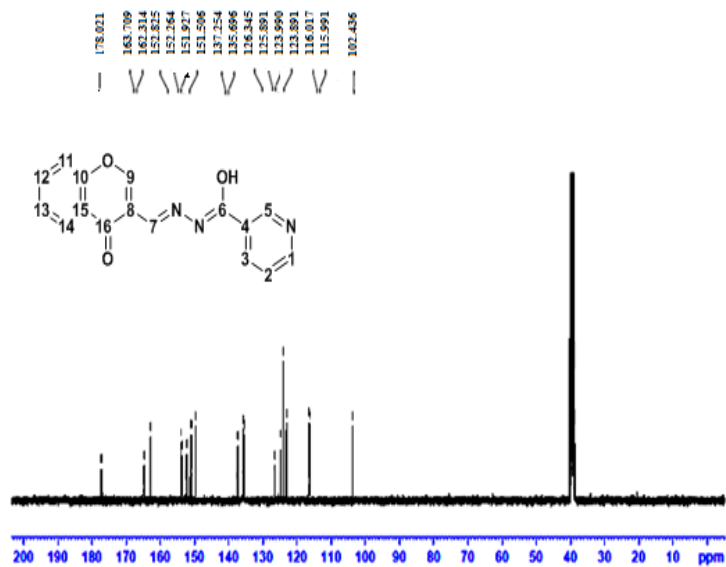


Figure 2.35 ^{13}C NMR spectrum of FN

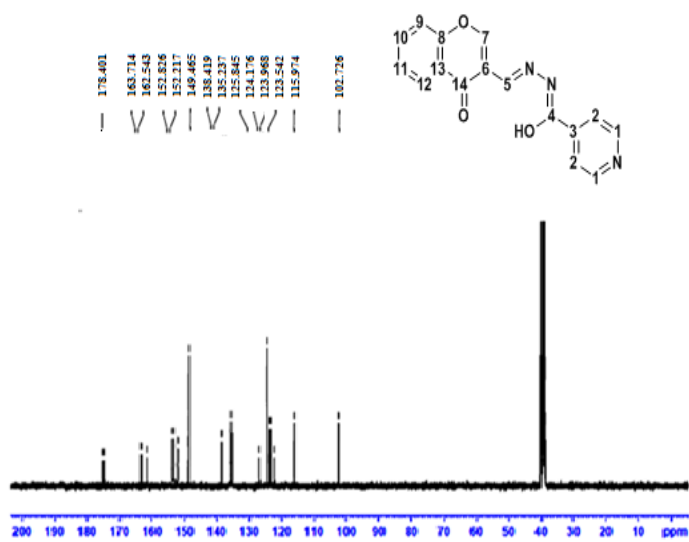


Figure 2.36 ^{13}C NMR spectrum of FIN

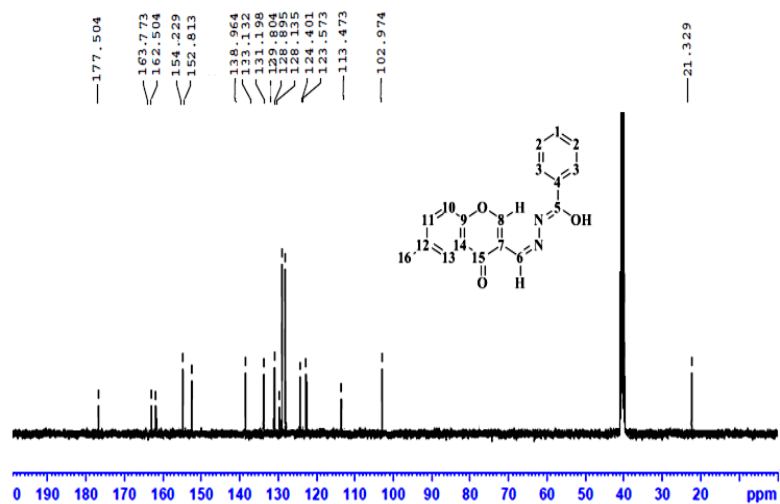


Figure 2.37 ¹³C NMR spectrum of FMB

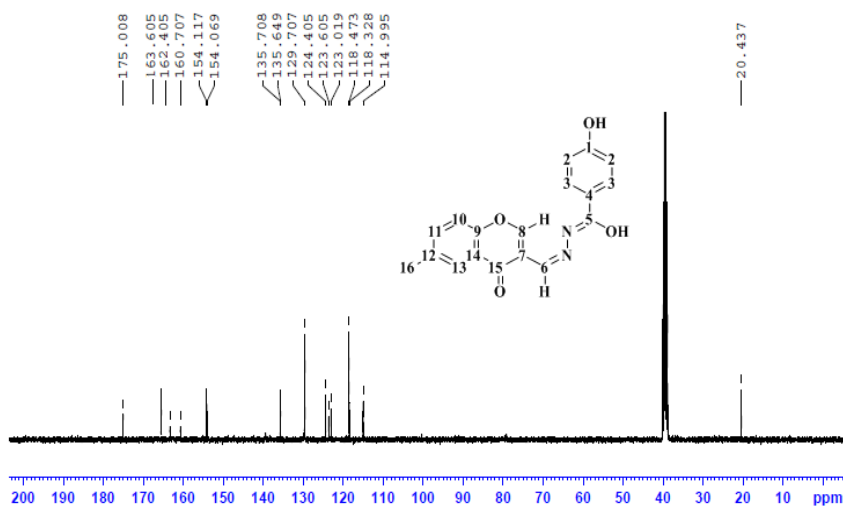


Figure 2.38 ¹³C NMR spectrum of FMBH

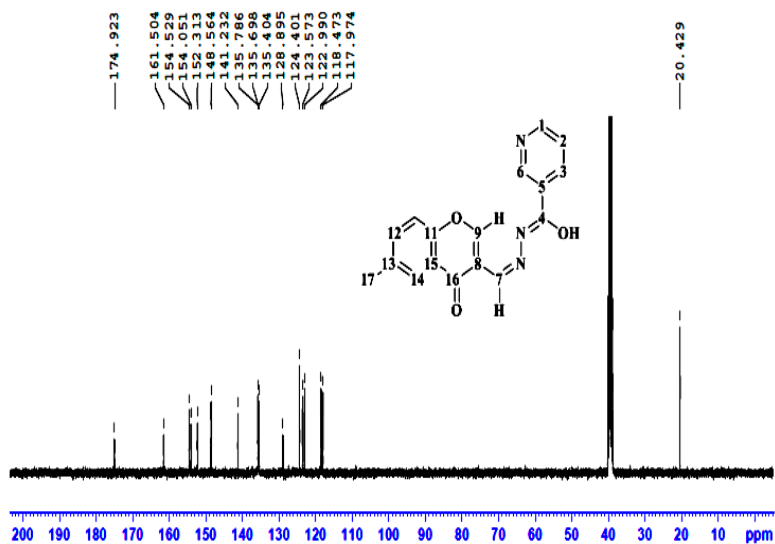


Figure 2.39 ¹³C NMR spectrum of FMN

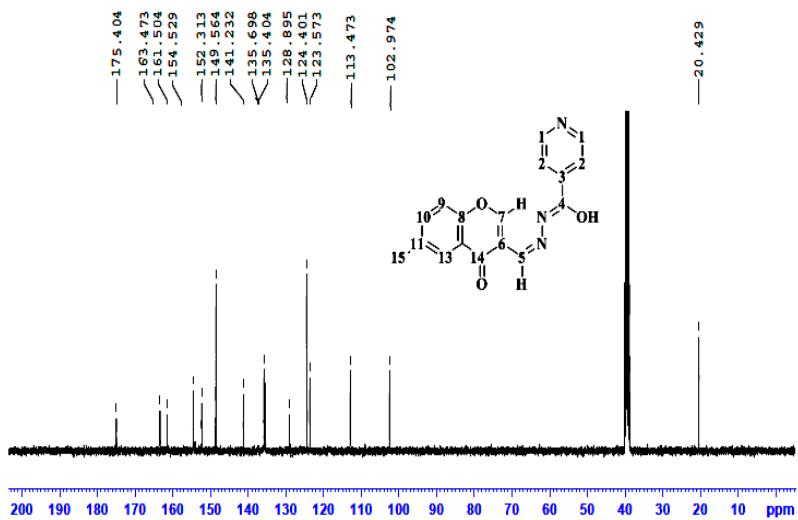


Figure 2.40 ¹³C NMR spectrum of FMIN

2.4 Conclusion

The synthesis of 3-formyl chromone and benzhydrazide (FB), 3-formyl chromone and 4-hydroxybenzhydrazide (FBH), 3-formyl chromone and nicotinic hydrazide (FN), 3-formyl chromone and isonicotinic hydrazide (FIN), 6-methyl-3-formyl chromone and benzhydrazide (FMB), 6-methyl-3-formyl chromone and 4-hydroxybenzhydrazide (FMBH), 6-methyl-3-formyl chromone and nicotinic hydrazide (FMN), 6-methyl-3-formyl chromone and isonicotinic hydrazide (FMIN). All hydrazones were characterized by physicochemical methods such as elemental, FT-IR spectra, UV-Vis., ESI-MS spectra and $^1\text{H}/^{13}\text{C}$ NMR spectra. All these studies give good evidence for the synthesized compounds are crystalline and pure.

References

- [1] D. S. Kalinowski, P. C. Sharpe, P. V. Bernhardt, Des R. Richardson, J. Med Chem., 51 (2008) 331.
- [2] R. C. Maurya, S. Rajput, J. Mol. Struct., 833 (2007) 133.
- [3] C. M. Armstrong, P. V. Bernhardt, P. Chin, Des R. Richardson, Eur. J. Inorg. Chem., 4 (2003) 1145.
- [4] V. M. Leovac, L. S. Jovanovic, V. Divjakovic, A. Pervec, I. Lebnan, T. R. Ambruster, Polyhedron, 26 (2007) 49.
- [5] H. Beraldo, D. Gambino, Mini-Review Med. Chem., 4 (2004) 31.
- [6] R. S. Keri, S. Budagumpi, R. K. Pai, R. G. Balakrishna, Eur. J. Med. Chem., 78 (2014) 340.
- [7] J. Wang, Z. Y. Yang, X. Y. Yi, B. D. Wang, J. Photochem. Photobiol. A: Chem., 201 (2009) 183.

- [8] W. Samee, P. Nunthanavanit, J. Ungwitayatorn, *Int. J. Mol. Sci.*, 9 (2008) 235.
- [9] P. Lerdsirisuk, C. Maicheen, J. Ungwitayatorn, *Bioorg. Chem.*, 57 (2014) 142.
- [10] P. Krishnamoorthy, P. Sathyadevi, P. T. Muthiahb, N. Dharmaraj, *RSC Adv.*, 2 (2012) 12190.
- [11] K. M. Khan, N. Ambreen, U. R. Mughal, S. Jalil, S. Perveen, M. I. Choudhary, *Eur. J. Med. Chem.*, 45 (2010) 4058.
- [12] Z. A. Kaplancikli, M. D. Altintopa, A. Ozdemira, G. T. Zitounia, S. I. Khanb, N. Tabancad, *Lett. Drug Des. Discov.*, 9 (2012) 310.
- [13] P. Krishnamoorthy, P. Sathyadevi, R. R. Butorac, A. H. Cowley, N. S. P. Bhuvaneshc, N. Dharmaraj, *Dalton Trans.*, 41 (2012) 4423.
- [14] M. Kalanithia, D. Kodimunthiric, M. Rajarajan, P. Tharmaraj, *Spectrochim. Acta A*, 82 (2011) 290.
- [15] N. Mathew, M. Kuriakose, E. B. Seena, M. R. P. Kurup, *Acta Cryst. E*, 63 (2007) 2190.
- [16] D. D. Perrin, W. L. F. Armarego, D. R. Perrin, *Purification of Laboratory Chemicals*, Pergamon Press, New York, 1980.
- [17] (a) S. R. Sheeja, N. A. Mangalam, M. R. P. Kurup, Y. S. Mary, K. Raju, H. T. Varghese, C. Y. Panicker, *J. Mol. Struct.*, 973 (2010) 36. (b) J. E. Philip, S. A. Antony, S. E. Jose, M. R. P. Kurup, M. P. Velayudhan, *Inorg. Chim. Acta.*, 469 (2018) 87.(c) A. A. R. Despaigne, J. G. Da Silva, A. C. M. Carmo, O. E. Piro, E. E. Castellano, H. Beraldo, *Inorg. Chim. Acta*, 362 (2009) 2117.
- [18] A. Yasuhara, Y. Tanaka, M. Makishima, S. Suzuki, T. Shibamoto, *J. Chromatograph. Separat. Techniq.*, 2 (2011) 1.
- [19] D. Strazic, T. Benkovic, D. Gembarovski, D. Kontrec, N. Galic, *Int. J. Mass Spectrom.*, 371 (2014) 54.

- [20] (a). N.K . Ngan, K. M. Lo, C. S. R. Wong, *Polyhedron*, 33 (2012) 235.
(b). M. K. Prasanna, K. Pradeepkumar, *Int. J. Pharm. Biomed. Sci.*, 4 (2013) 24.
- [21] (a) O. S. Devi, A. M. Singh, *J. Chem. Pharm. Res.*, 3 (2011) 1055. (b).
P. Krishnamoorthy, P. Sathyadevi, R. R. Butorac, A. H. Cowley, N. S.
P. Bhuvanesh, N. Dharmaraj, *Dalton Trans.*, 41 (2012) 6842.

.....❧.....

Chapter 3

SYNTHESIS AND SPECTRAL CHARACTERIZATION OF Ni (II), Cu (II) & Zn (II) COMPLEXES OF ONO/NO DONOR CHROMONE HYDRAZONES

Contents

- 3.1 Introduction
- 3.2 Materials and Methods
- 3.3 Result and Discussion
- 3.4 Conclusion

Conspectus: In the present investigation, the reactions of the 3-formyl chromone hydrazones with transition metals such as Ni, Cu, and Zn (II) salts of acetate afforded mononuclear metal complexes. Characterization and structure elucidation of the prepared chromone hydrazone metal (II) complexes were done by elemental, IR, electronic, EPR spectra and thermo gravimetric analyses as well as conductivity and magnetic susceptibility measurements. The spectroscopic data showed that the ligand acts as a mono basic bidentate with coordination sites are azomethine nitrogen and hydrazone oxygen and for tridentate the coordination sites are pyrone oxygen, azomethine nitrogen and hydrazone oxygen. Thermal analyses have been performed in order to understand the thermal decomposition pattern of the complexes. Spin Hamiltonian and bonding parameters of Cu (II) have been calculated from EPR analysis. The g values, calculated for the copper complexes in frozen DMF, indicate the presence of an unpaired electron in the $d_{x^2-y^2}$ orbital consistent with a square pyramidal topology whereas that of $[Cu(FMIN)(OAc)(H_2O)].H_2O$ corresponds to a rhombic symmetry.

3.1 Introduction

Hydrazones and their metal complexes have increasing significance like anti-inflammatory, anti-microbial, anti-tubercular, anti-fungal, anti-HIV and anti-cancer activities [1-10]. Numerous researchers have synthesized these compounds as target structures and evaluated their biological properties. In several cases it was reported that metal complexes have superior biological properties than their corresponding ligands [11]. The biological property of hydrazones may be due to the availability of multidentate coordination sites and their capability to form stable complexes with critical metal ions which organisms require in their metabolic activity [12-13]. Hydrazones having an azomethine -NH-N=CH- proton comprise an important class of compounds for development of new therapeutic agents. Pinheiro et al. synthesized a series of hydrazone derivatives with significant antitubercular activity [14]. B. C. Raju et al. synthesized potential anti-mycobacterial and anticancer agents [15].

The first row transition metal play an imperative role in the synthesis of numerous coordination complexes due their variable oxidation states which facilitate their structural, stereo chemical, electrochemical and spectroscopic properties. Among the diverse transition metals, the current study is focused on nickel, copper and zinc metal ions based on their extensive biological applications.

3.1.1 Importance of Ni (II), Cu (II) and Zn (II) complexes

Nickel ion is frequently dispositive in its compounds, but it can also exhibit in the variable oxidation states such as 0, 1⁺, 3⁺, and 4⁺. In addition to the simple nickel compounds or salts, nickel forms a variety of

coordination compounds. At present, the bioinorganic chemistry of nickel is an escalating interesting area because the study of the interactions of Ni ion with hydrazones offers an opening to recognize a variety of properties of Ni (II). Since nickel compounds are in the active sites of urease and are used widely in the design and construction of new magnetic materials, the study of nickel compounds is of enormous interest in diverse aspects of chemistry [16-18].

Copper complexes with physiologically endogenous transition metal element centers show various geometries, coordination numbers, various oxidation states, better solubility, and higher affinity for the nucleobases [19-21]. Copper (II) complexes are considered the most hopeful substitutes to cisplatin as anticancer drugs. The biologically accessible oxidative/reductive potential has made copper complexes a class of the most often studied metallonuclease [22]. The copper complexes with hydrazones have extensive importance in the field of analytical chemistry, food industry, in the dyeing industries, catalysis, antimicrobial, agrochemical, anti-inflammatory and anticancer agents [23-25]. Research in the literature exposed that copper complexes elucidate hopeful perspectives and showed a significantly higher level of antitumor, antimicrobial, antiproliferative and antimitotic activity for tumor metastases and showed a lower overall host toxicity compared to platinum compounds [26-28].

Zinc is a vital metal next to iron and one of the most important transition metal ions for biology (human beings contain an average of about 2-3 g of zinc). The cations of zinc (II), owing to their d^{10} electronic configuration, form complexes with a flexible coordination environment

and the geometries of these complexes can vary from tetrahedral to octahedral and severe distortions of the ideal polyhedra occur easily. Many characteristics of zinc, such as its ability to aid Lewis activation, nucleophile generation, fast exchange of ligands and leaving-group stabilization, make Zn (II) ideal for the catalysis of hydrolytic reactions, including DNA binding and DNA cleavage, which are important properties for use as anticancer agents[29-32].

The transition metal ions (Ni, Cu and Zn) attached to the donor atoms of the hydrazone ligand form stable metal complexes. Metal-based anticancer drugs show superior selectivity and novel modes of DNA interaction, such as non-covalent interactions that impersonate the mode of interaction of biomolecules [33]. In current scenario a number of research articles have been available on transition metal complexes of Ni (II), Cu (II) and Zn (II) with hydrazones [34-38]. The new compounds were investigated for inhibition against human TRK in vitro cytotoxicity for four human tumor cell lines. The Zn (II) complex showed potent inhibition against human TRK in the four cell lines (HepG2, MCF7, A549, HCT116) by the ratio 80, 70, 61 and 64% respectively as compared to the inhibition in the untreated cells in comparison with the reference drug (doxorubicin) [39]

N. Joksimovic et al have developed a facile and efficient synthetic route to novel Cu (II) complexes with ethyl-2-hydroxy-4-aryl-4-oxo-2-butenolate at ambient temperature. Antimicrobial evaluations of the novel complexes were investigated via treatment of a series of bacteria and fungi strains [40]. Cu (II) complexes of salicylaldehyde-N substituted thiosemicarbazones having 5-nitro-substitution in the 2-hydroxy phenyl ring

along with different substituents at N¹ nitrogen using 2,2'-bipyridine and 1,10-phenanthroline as co-ligands have shown significant growth inhibitory activity against *Staphylococcus aureus*, methicillin resistant *Staphylococcus aureus*, *Klebsiella pneumonia*, *Shigella flexneri*, *Salmonella typhimurium* and *Candida albicans*. It is interesting to note that complexes are highly active against *Shigella flexneri* and *Pseudomonas aeruginosa* while only a few complexes with 5-methoxy substitution at 2-hydroxyphenyl ring of thio-ligand are active against these microorganisms [41].

Shikha and coworkers reported antimicrobial activity of mixed-ligand Zn (II) complexes of 5-nitro-salicylaldehyde thiosemicarbazones. These Zn (II) complexes have shown significant antimicrobial activity against *Staphylococcus aureus*, methicillin resistant *Staphylococcus aureus*, *Klebsiella pneumonia*, *Shigella flexneri*, *Salmonella typhimurium* and *Candida albicans*. This work makes a significant contribution to the use of Zn (II) thiosemicarbazone complexes as efficient antimicrobial agents [42].

3.2 Materials and Methods

3.2.1 Materials

The details of materials used for the synthesis of 3-formyl chromone hydrazone ligands and complexes have been given in Chapter 2 (section 2.2).

3.2.2 Synthesis of ligands

Details regarding the preparation and purification of the hydrazone ligands FB, FBH, FN, FIN, FMB, FMBH, FMN and FMIN are described in Chapter 2 (section 2.2.1.1-2.2.1.8).

3.2.3 Synthesis of complexes

About 1 mmol of metal (II) acetate [nickel (II) acetate (0.248g), cupric (II) acetate (0.199g) and zinc (II) acetate (0.219g)] dissolved in 30 mL methanol was added gradually to 1 mmol of the ligand, dissolved in DMF. The reaction mixture was heated under reflux for 8 h at 60°C. The resulting precipitates were filtered, washed with methanol and hexane then diethyl ether and finally air-dried. The complexes were kept in desiccators over anhydrous calcium chloride. The yield was noted. All complexes were prepared similarly.

3.3 Result and Discussion

Twenty four complexes out of which eight nickel, eight copper and eight zinc complexes of the chromone hydrazones were synthesized. The complexes were prepared by the reaction of equimolar mixture of the appropriate chromone hydrazones and metal (II) acetate. The complexes formed are of fairly good stability and are found to be coloured. All the complexes are insoluble in water and common organic solvents but are soluble in DMF and DMSO. In all the complexes, chromone hydrazones exist in the amino-imino form and act as deprotonated tridentate ligands coordinating through pyrone oxygen, azomethine nitrogen and hydrazonic oxygen. They are characterized by the following physico-chemical methods.

3.3.1 Elemental analysis and AAS

The elemental analysis values showed that the found and calculated values are in close agreement with the proposed formula of the complexes. The analytical data indicate that the observed C, H, N values are

consistent with the formulae suggested for the complexes (Table 3.1-3.3). However we could not isolate single crystals of suitable quality for XRD studies for any of these complexes. The metal content % of the complexes was determined by AAS after digestion with conc. HNO₃ and is found to be in good agreement with that of the theoretical results.

Table 3.1 Analytical data of Nickel (II) complexes

Compound	M.W. (g/mol)	Colour (yield)	Element analysis Found (calc.)			% of metal found (calc.)
			C	H	N	Ni
[Ni(FB)(OAc)(H ₂ O)].2H ₂ O (1)	463.06	Brown (70%)	49.33 (49.20)	4.47 (4.35)	6.15 (6.05)	12.53 (12.68)
[Ni(FBH)(H ₂ O)(OAc)].2H ₂ O (2)	479.06	Yellow (75%)	47.58 (47.64)	4.29 (4.21)	5.72 (5.85)	12.07 (12.25)
[Ni(FN)(OAc)].H ₂ O (3)	428.02	Yellow (65%)	50.45 (50.51)	3.36 (3.53)	9.73 (9.82)	13.49 (13.71)
[Ni(FIN)(OAc)(H ₂ O)].H ₂ O (4)	446.03	Green (70%)	48.31 (48.47)	3.46 (3.84)	9.75 (9.42)	13.11 (13.16)
[Ni(FMB) ₂ (H ₂ O) ₂].H ₂ O (5)	723.35	Dark green (73%)	59.44 (59.78)	4.45 (4.46)	7.75 (7.75)	8.01 (8.11)
[Ni(FBH) ₂ (H ₂ O) ₂].2H ₂ O (6)	773.36	Yellow (55%)	56.07 (55.91)	4.04 (4.43)	7.41 (7.24)	7.48 (7.59)
[Ni(FMN)(OAc)].2H ₂ O (7)	460.06	Brown (67%)	49.07 (49.60)	4.29 (4.16)	8.99 (9.13)	12.70 (12.76)
[Ni(FMIN)(OAc)(H ₂ O)].1.5H ₂ O (8)	469.07	Dark Brown (71%)	48.58 (48.65)	4.24 (4.30)	8.90 (8.96)	12.44 (12.51)

Table 3.2 Analytical data of Copper (II) complexes

Compound	M.W. (g/mol)	Colour (yield)	Element analysis Found(calc.)			% of metal found (calc.)
			C	H	N	Cu
[Cu(FB)(OAc)].H ₂ O (9)	431.88	Dark brown (79%)	53.03 (52.84)	3.38 (3.73)	6.40 (6.49)	14.64 (14.71)
[Cu(FBH)(H ₂ O)(OAc)].H ₂ O (10)	465.90	Dark brown (75%)	48.89 (48.98)	3.93 (3.89)	6.12 (6.01)	13.51 (13.64)
[Cu(FN)(OAc)].2H ₂ O (11)	450.88	Dark brown (70%)	47.69 (47.95)	3.54 (3.80)	9.21 (9.32)	14.17 (14.09)
[Cu(FIN)(OAc)(H ₂ O)].2H ₂ O (12)	468.90	Black (64%)	46.33 (46.11)	4.21 (4.08)	8.79 (8.96)	13.47 (13.55)
[Cu(FMB) ₂ (H ₂ O) ₂].H ₂ O (13)	728.20	Black (70%)	59.25 (59.38)	4.38 (4.43)	7.73 (7.69)	8.79 (8.73)
[Cu(FMBH) ₂ (H ₂ O) ₂].2H ₂ O (14)	778.22	Green (68%)	55.60 (55.56)	4.38 (4.40)	7.02 (7.20)	8.32 (8.17)
[Cu(FMN)(OAc)].H ₂ O (15)	446.90	Brown (72%)	51.11 (51.06)	3.89 (3.83)	9.35 (9.40)	14.18 (14.22)
[Cu(FMIN)(OAc)(H ₂ O)].H ₂ O (16)	464.91	Dark green (78%)	49.16 (49.08)	4.06 (4.12)	9.15 (9.04)	13.60 (13.67)

Table 3.3 Analytical data of Zinc (II) complexes

Compound	M.W. (g/mol)	Colour (yield)	Element analysis Found(calc.)			% of metal found (calc.)
			C	H	N	Zn
[Zn(FB)(OAc)].2.5H ₂ O (17)	459.04	Brown (66%)	49.47 (49.53)	4.06 (4.16)	6.13 (6.08)	14.11 (14.20)
[Zn(FBH)(OAc)] (18)	431.73	Orange (75%)	52.79 (52.86)	3.20 (3.27)	6.41 (6.49)	15.09 (15.15)
[Zn(FN)(OAc)].H ₂ O (19)	434.73	Brown (68%)	49.65 (49.73)	3.34 (3.48)	9.58 (9.67)	15.17 (15.05)
[Zn(FIN)(OAc)] (20)	416.72	Yellow (73%)	51.69 (51.88)	3.27 (3.14)	10.15 (10.08)	15.63 (15.70)
[Zn(FMB) ₂].2H ₂ O (21)	712.05	Pale Orange (79%)	60.89 (60.72)	4.23 (4.25)	7.86 (7.87)	9.01 (9.19)
[Zn(FMBH)(OAc)].H ₂ O (22)	463.77	Green (72%)	51.51 (51.80)	3.61 (3.91)	6.95 (6.04)	14.29 (14.10)
[Zn(FMN)(OAc)].H ₂ O (23)	448.76	Pale Yellow (64%)	50.79 (50.85)	3.89 (3.82)	9.40 (9.36)	14.52 (14.58)
[Zn(FMIN)(OAc)].0.5 H ₂ O (24)	439.75	Yellow (60%)	51.82 (51.89)	3.61 (3.67)	9.50 (9.56)	14.79 (14.87)

3.3.2 Molar conductivity and magnetic susceptibility measurements

The molar conductivity measurements have been demonstrated to be a very useful tool in the investigation of geometrical structure of inorganic compounds. The conductivity measurements were made in DMF (10^{-3} M) and it is observed that the values lie in the range 4.00-16.80 $\text{ohm}^{-1}\text{cm}^2\text{mol}^{-1}$ (Table 3.4-3.6), which are well below the range (65-90 $\text{ohm}^{-1}\text{cm}^2\text{mol}^{-1}$) for uni-univalent electrolytes in the same solvent, indicating the non-electrolytic nature of the complexes [43]. These results indicate that the complexes dissociate very slightly in this solvent. Analytical data and molar conductance values for Zn (II) complex sufficiently supports the tetrahedral geometry for Zn (II) complex because it is well known that the Zn (II) generally forms tetrahedral complexes because of its d^{10} electronic configuration.

Table 3.4 Magnetic moment values and molar conductance (DMF 10^{-3} M) data of Ni (II) complexes

Compound	Molar conductance ($\text{ohm}^{-1}\text{cm}^2\text{mol}^{-1}$)	μ_{eff} (B.M.)
[Ni(FB)(OAc)(H ₂ O)].2H ₂ O (1)	12.50	2.45
[Ni(FBH)(H ₂ O)(OAc)].2H ₂ O (2)	15.40	2.32
[Ni(FN)(OAc)].H ₂ O (3)	7.30	3.69
[Ni(FIN)(OAc)(H ₂ O)].H ₂ O (4)	8.60	3.06
[Ni(FMB) ₂ (H ₂ O) ₂].H ₂ O (5)	10.30	2.85
[Ni(FBH) ₂ (H ₂ O) ₂].2H ₂ O (6)	11.90	3.12
[Ni(FMN)(OAc)].2H ₂ O (7)	9.80	3.85
[Ni(FMIN)(OAc)(H ₂ O)].1.5H ₂ O (8)	16.80	2.96

Table 3.5 Magnetic moment values and molar conductance (DMF 10^{-3} M) data of Cu (II) complexes

Compound	Molar conductance ($\text{ohm}^{-1}\text{cm}^2\text{mol}^{-1}$)	μ_{eff} (BM)
[Cu(FB)(OAc)].H ₂ O (9)	9.40	1.65
[Cu(FBH)(H ₂ O)(OAc)].H ₂ O (10)	13.70	1.72
[Cu(FN)(OAc)].2H ₂ O (11)	12.72	1.85
[Cu(FIN)(OAc)(H ₂ O)].2H ₂ O (12)	10.56	1.71
[Cu(FMB) ₂ (H ₂ O) ₂].H ₂ O (13)	8.70	1.65
[Cu(FMBH) ₂ (H ₂ O) ₂].2H ₂ O (14)	12.50	1.71
[Cu(FMN)(OAc)].H ₂ O (15)	10.62	1.89
[Cu(FMIN)(OAc)(H ₂ O)].H ₂ O (16)	11.67	1.86

Table 3.6 Molar conductance (DMF 10^{-3} M) data of Zn (II) complexes

Compound	Molar conductance ($\text{ohm}^{-1}\text{cm}^2\text{mol}^{-1}$)
[Zn(FB)(OAc)].2.5H ₂ O (17)	8.60
[Zn(FBH)(OAc)] (18)	9.50
[Zn(FN)(OAc)].H ₂ O (19)	5.60
[Zn(FIN)(OAc)] (20)	4.00
[Zn(FMB) ₂].2H ₂ O (21)	6.50
[Zn(FMBH)(OAc)].H ₂ O (22)	9.80
[Zn(FMN)(OAc)].H ₂ O (23)	13.28
[Zn(FMIN)(OAc)].0.5 H ₂ O (24)	7.60

For Ni (II), and Cu (II), the magnetic susceptibility measurements were carried out, and data are presented in Table 3.4 and 3.5. From the results they were found to be paramagnetic in nature. In paramagnetic Ni (II) and Cu (II) complexes, often the magnetic moment (μ_{eff}) gives the spin only value ($\mu_{\text{eff}} = \sqrt{n(n+2)} B.M.$) corresponding to the number of unpaired electron. The variation from the spin only value is attributed

to the orbital contribution and it varies with the nature of coordination and consequent delocalization [44].

Ni (II) has the electronic configuration $3d^8$ and should exhibit a magnetic moment higher than that expected for two unpaired electrons in octahedral (2.8-3.2B.M.) and tetrahedral (3.4-4.2B.M.) complexes, whereas its square planar complexes would be diamagnetic. The effective magnetic moments of complexes in the polycrystalline state are shown in Table 3.4 which is consistent with two unpaired electrons. The magnetic moment observed for the complexes $[\text{Ni}(\text{FB})(\text{OAc})(\text{H}_2\text{O})].2\text{H}_2\text{O}$, $[\text{Ni}(\text{FBH})(\text{H}_2\text{O})(\text{OAc})].2\text{H}_2\text{O}$, $[\text{Ni}(\text{FIN})(\text{OAc})(\text{H}_2\text{O})].\text{H}_2\text{O}$, $[\text{Ni}(\text{FMB})_2(\text{H}_2\text{O})_2].\text{H}_2\text{O}$, $[\text{Ni}(\text{FBH})_2(\text{H}_2\text{O})_2].2\text{H}_2\text{O}$ and $[\text{Ni}(\text{FMIN})(\text{OAc})(\text{H}_2\text{O})].1.5\text{H}_2\text{O}$ lies within the region 2.32-3.12 B.M expected for octahedral stereochemistry of the complexes [45]. The magnetic moment of other Ni (II) complexes $[\text{Ni}(\text{FN})(\text{OAc})].\text{H}_2\text{O}$ and $[\text{Ni}(\text{FMN})(\text{OAc})].2\text{H}_2\text{O}$ were 3.69 and 3.85 B.M. which is consistent with the tetrahedral complexes.

Due to the Jahn-Teller distortion of Cu^{II} -ion (d^9) it lower the symmetry, complete interpretations of the spectra and magnetic properties are somewhat difficult [40]. Magnetic moment (μ_{eff}) values of copper (II) complexes in the polycrystalline state fall in the range 1.7-1.9 B.M. (Table 3.5); corresponding to an unpaired electron and this is an indication of monomeric compounds with square pyramidal or square planar geometry [46]. The copper (II) ion (d^9) has one unpaired electron in the 3d shell, therefore its compounds were considered to have magnetic moments close to the spin-only value, 1.73 B.M. but due to spin orbit coupling, higher values are often observed [47].

Due to completely filled 'd' shell as expected for Zn (II) ion, it exhibits diamagnetic nature. The present Zn (II) complexes are found to be diamagnetic in nature for tetrahedral geometry [48].

3.3.3 Infrared spectra

The comparison of the main vibrational bands of the chromone hydrazones with those of the complexes helps to establish their ligating behaviour to the metal center. The IR bands that are considered most useful in ascertaining the mode of coordination of the hydrazones to the metal (II) ion are summarized in Table 3.7-3.9. The IR spectra of hydrazones exhibit bands at around 3300-3100 cm^{-1} due to $\nu(\text{N-H})$ stretching and 1680-1670 cm^{-1} due to $\nu(\text{C=O})$ stretching, which are indicative of their amido nature in the solid-state [49]. These bands disappear on complexation and a new band appearing in the region 1360-1385 cm^{-1} is assigned to $\nu(\text{C-O})$ indicating the involvement of the original carbonyl-oxygen in bonding as an enolate. Each of the chromone hydrazones under discussion display a strong and sharp band in the region 1595-1580 cm^{-1} ascribed to $\nu(\text{C=N})$ of the azomethine group [50]. Figures 3.1-3.24 depict the infrared spectra of the metal (II) complexes of 3-formyl chromone hydrazones.

The comparison of the complexes with respective chromone hydrazone shown that complexes had broad band in the range of 3690-2919 cm^{-1} assigned to $\nu(\text{OH})$ of the coordinated water molecules linked with the complexes [51] and also the OH of the hydrazone moiety which are confirmed by elemental, AAS, and thermal analyses. The band at around 1595 cm^{-1} assigned to $\nu(\text{-C=N-})$, in the chromone hydrazones were

shifted to lower wave number region in all complexes. The entire metal (II) complexes displayed distinct sharp band in 1571-1534 cm^{-1} region corresponds to the characteristic -C=N- group stretching vibration indicating the coordination of azomethine nitrogen to metal (II) centre as observed in the literature [52]. This coordination of azomethine nitrogen is also supported by band at 1029-1013 cm^{-1} corresponding to $\nu(\text{N-N})$ stretching vibration. On comparison with literature reports, $\nu(\text{N-N})$ vibrations was found to be in higher frequencies in the complexes due to the increase in double bond character, off-setting the loss of electron density via donation to the metal [53]. The band at 1655 cm^{-1} assigned to $\nu(\text{C=O})$ hydrazonic in the free ligand was shifted to (1647-1598) cm^{-1} [54] which indicate that the azomethine nitrogen and hydrazonic (C=O) are in chelation. In complexes $[\text{Ni}(\text{FB})(\text{OAc})(\text{H}_2\text{O})].2\text{H}_2\text{O}$, $[\text{Ni}(\text{FBH})(\text{H}_2\text{O})(\text{OAc})].2\text{H}_2\text{O}$, $[\text{Ni}(\text{FIN})(\text{OAc})(\text{H}_2\text{O})].\text{H}_2\text{O}$, $[\text{Ni}(\text{FMIN})(\text{OAc})(\text{H}_2\text{O})].1.5 \text{H}_2\text{O}$ and $[\text{Cu}(\text{FBH})(\text{H}_2\text{O})(\text{OAc})].\text{H}_2\text{O}$ the chelating bidentate acetate (CH_3COO^-) group was present due to the bands around 1457-1414 cm^{-1} and 1337-1325 cm^{-1} . These two bands are due to $\nu_{\text{as}}(\text{COO}^-)$ and $\nu_{\text{s}}(\text{COO}^-)$, respectively. The separation of the two bands, $\Delta\nu = (\nu_{\text{as}} - \nu_{\text{s}}) = 88 \text{ cm}^{-1}$, is comparable to the values cited for the bidentate character of the acetate group $\Delta\nu = 75-90 \text{ cm}^{-1}$ [55]. On the other hand, complexes $[\text{Ni}(\text{FN})(\text{OAc})].\text{H}_2\text{O}$, $[\text{Ni}(\text{FMN})(\text{OAc})].2\text{H}_2\text{O}$, $[\text{Cu}(\text{FB})(\text{OAc})].\text{H}_2\text{O}$, $[\text{Cu}(\text{FN})(\text{OAc})].2\text{H}_2\text{O}$, $[\text{Cu}(\text{FIN})(\text{OAc})(\text{H}_2\text{O})].2\text{H}_2\text{O}$, $[\text{Cu}(\text{FMN})(\text{OAc})].\text{H}_2\text{O}$ and $[\text{Cu}(\text{FMIN})(\text{OAc})(\text{H}_2\text{O})].\text{H}_2\text{O}$ showed new bands characteristic for $\nu_{\text{as}}(\text{COO}^-)$ and $\nu_{\text{s}}(\text{COO}^-)$ of acetate ion in the ranges 1549-1531 cm^{-1} and 1413-1389 cm^{-1} . The higher difference between the two bands indicates the monodentate nature of the acetate group, in which one 'O' atom of acetate was coordinated to the metal center, while the

second was hydrogen bonded to, a geminal H₂O [56]. The appearance of the non-ligand bands at 557-510 cm⁻¹ and 473-403 cm⁻¹ were assigned to ν (M-O) and ν (M-N), respectively.

Table 3.7 IR spectral assignments (cm⁻¹) of hydrazones and their Ni (II) complexes

Compound	ν (OH, NH)	ν (C=O) pyrone	ν (C=O) hydrazonic	ν (C=N)	Mono/Bidentate acetate
FB	-, 3220	1678	1641	1597	-
[Ni(FB)(OAc)(H ₂ O)].2H ₂ O (1)	3666-2919 (b)	1645	1617	1545	ν_{as} 1431, ν_s 1328
FBH	3394 (b)	1675	1650	1590	-
[Ni(FBH)(H ₂ O)(OAc)].2H ₂ O (2)	3690-3043 (b)	1639	1617	1571	ν_{as} 1451, ν_s 1364
FN	-, 3233	1677	1651	1596	-
[Ni(FN)(OAc)].H ₂ O (3)	3500-2987 (b)	1648	1622	1564	ν_{as} 1533, ν_s 1386
FIN	-, 3267	1674	1645	1597	-
[Ni(FIN)(OAc)(H ₂ O)].H ₂ O (4)	3546-3016 (b)	1658	1625	1547	ν_{as} 1457, ν_s 1363
FMB	-, 3206	1680	1655	1595	-
[Ni(FMB) ₂ (H ₂ O) ₂].2H ₂ O (5)	3655-3192 (b)	1652	1620	1570	-
FMBH	3346, 3100	1675	1650	1590	-
[Ni(FBH) ₂ (H ₂ O) ₂].2H ₂ O (6)	3445, 3100 (b)	1649	1627	1562	-
FMN	-, 3206	1679	1647	1584	-
[Ni(FMN)(OAc)].2H ₂ O (7)	3507, 3250	1665	1623	1553	ν_{as} 1531, ν_s 1389
FMIN	-, 3100	1683	1658	1587	-
Ni(FMIN)(OAc)(H ₂ O)].1.5 H ₂ O (8)	3468, 3165	1667	1619	1539	ν_{as} 1414, ν_s 1325

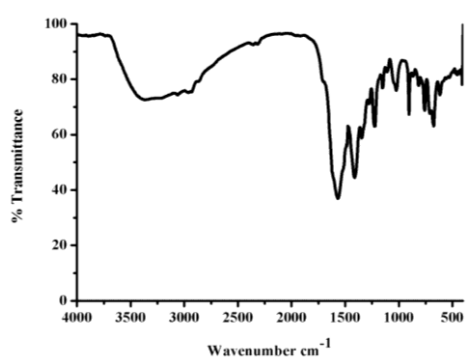


Figure 3.1 FT-IR spectrum of [Ni(FB)(OAc)(H₂O)].2H₂O

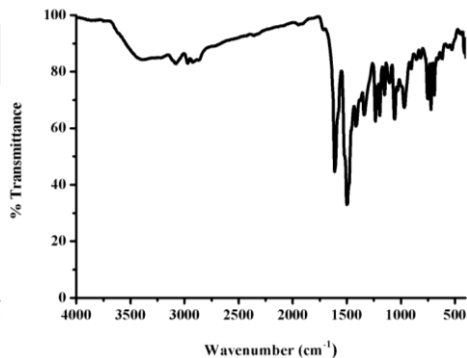


Figure 3.2 FT-IR spectrum of [Ni(FBH)(H₂O)(OAc)].2H₂O

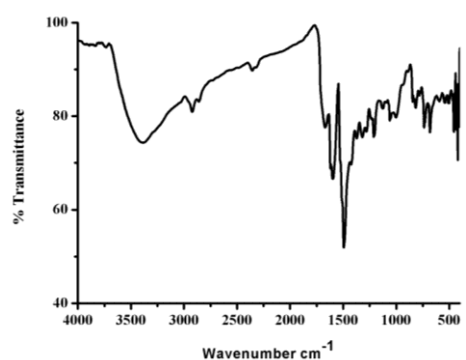


Figure 3.3 FT-IR spectrum of [Ni(FN)(OAc)].H₂O

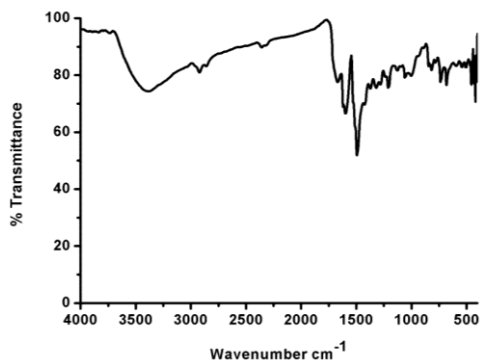


Figure 3.4 FT-IR spectrum of [Ni(FIN)(OAc)(H₂O)].H₂O

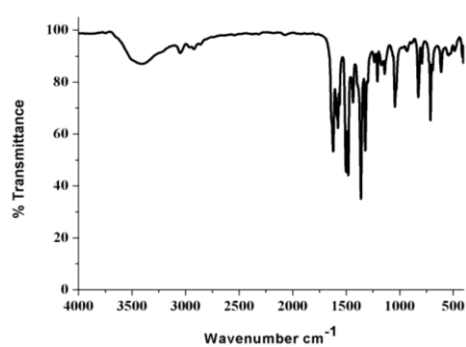


Figure 3.5 FT-IR spectrum of [Ni(FMB)₂(H₂O)₂].2H₂O

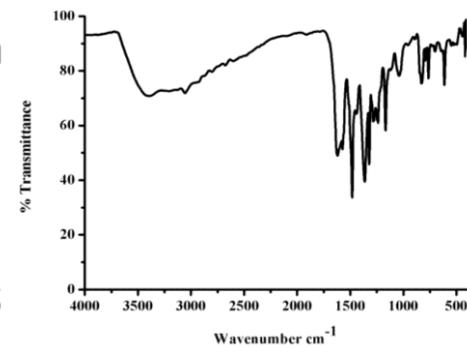


Figure 3.6 FT-IR spectrum of [Ni(FMBH)₂(H₂O)₂].2H₂O

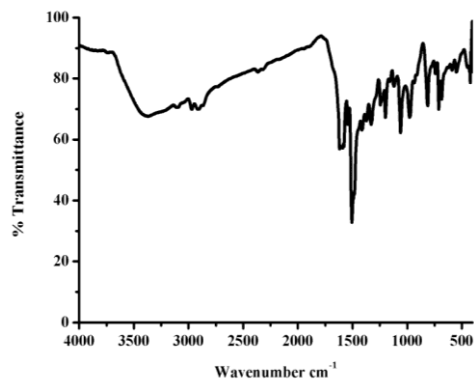


Figure 3.7 FT-IR spectrum of $[\text{Ni}(\text{FMN})(\text{OAc})].2\text{H}_2\text{O}$

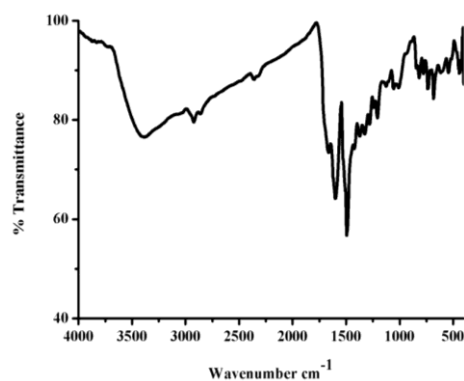


Figure 3.8 FT-IR spectrum of $\text{Ni}(\text{FMIN})(\text{OAc})(\text{H}_2\text{O}).1.5\text{H}_2\text{O}$

Table 3.8 IR spectral assignments (cm^{-1}) of hydrazones and their Cu (II) complexes

Compound	$\nu(\text{OH}, \text{NH})$	$\nu(\text{C}=\text{O})$ pyrone	$\nu(\text{C}=\text{O})$ hydrazoneic	$\nu(\text{C}=\text{N})$	Mono/Bidentate acetate
FB	-, 3220	1678	1641	1597	-
$[\text{Cu}(\text{FB})(\text{OAc})].\text{H}_2\text{O}$ (9)	3445	1656	1605	1551	ν_{as} 1531, ν_{s} 1323
FBH	3394 (b)	1675	1650	1590	-
$[\text{Cu}(\text{FBH})(\text{H}_2\text{O})(\text{OAc})].\text{H}_2\text{O}$ (10)	3416-3025	1634	1598	1555	ν_{as} 1436, ν_{s} 1327
FN	-, 3233	1677	1651	1596	-
$[\text{Cu}(\text{FN})(\text{OAc})].2\text{H}_2\text{O}$ (11)	3619-2898	1658	1617	1546	ν_{as} 1511, ν_{s} 1374
FIN	-, 3267	1674	1645	1597	-
$[\text{Cu}(\text{FIN})(\text{OAc})(\text{H}_2\text{O})].2\text{H}_2\text{O}$ (12)	3627-3048	1659	1621	1541	ν_{as} 1533, ν_{s} 1321
FMB	-, 3206	1680	1655	1595	-
$[\text{Cu}(\text{FMB})_2(\text{H}_2\text{O})_2].\text{H}_2\text{O}$ (13)	3597-3192	1642	1605	1548	-
FMBH	3346, 3100	1675	1650	1590	-
$[\text{Cu}(\text{FMBH})_2(\text{H}_2\text{O})_2].2\text{H}_2\text{O}$ (14)	3416-3025	1647	1612	1555	-
FMN	-, 3206	1679	1647	1584	-
$[\text{Cu}(\text{FMN})(\text{OAc})].\text{H}_2\text{O}$ (15)	3458, 3238	1668	1604	1549	ν_{as} 1524, ν_{s} 1337
FMIN	-, 3100	1683	1658	1587	-
$[\text{Cu}(\text{FMIN})(\text{OAc})(\text{H}_2\text{O})].\text{H}_2\text{O}$ (16)	3412, 3148	1679	1625	1534	ν_{as} 1533, ν_{s} 1363

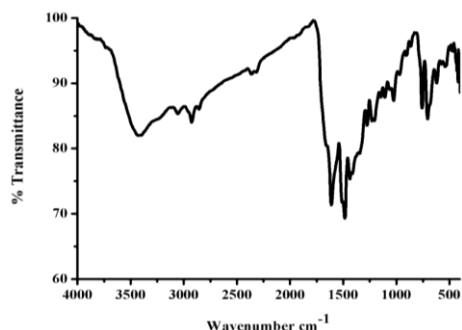


Figure 3.9 FT-IR spectrum of [Cu(FB)(OAc)].H₂O

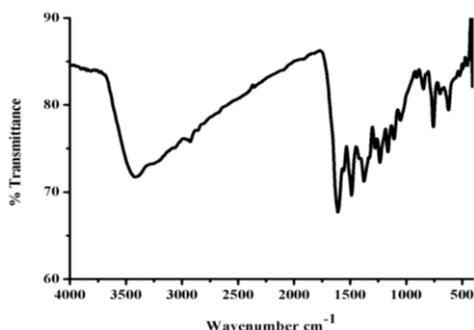


Figure 3.10 FT-IR spectrum of [Cu(FBH)(H₂O)(OAc)].H₂O

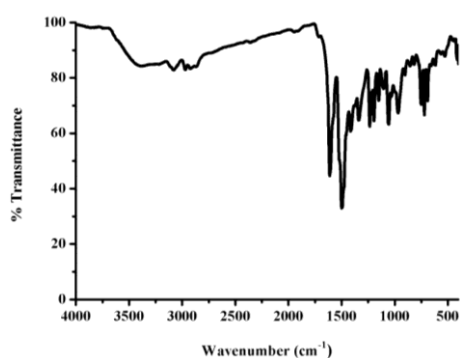


Figure 3.11 FT-IR spectrum of [Cu(FN)(OAc)].2H₂O

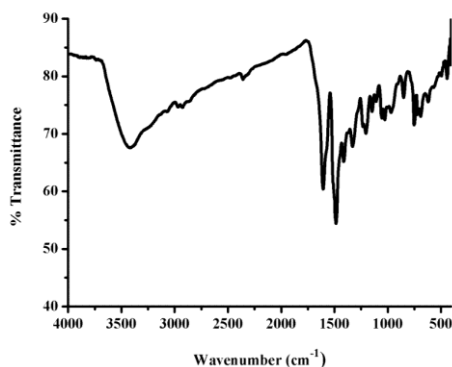


Figure 3.12 FT-IR spectrum of [Cu(FIN)(OAc)(H₂O)].2H₂O

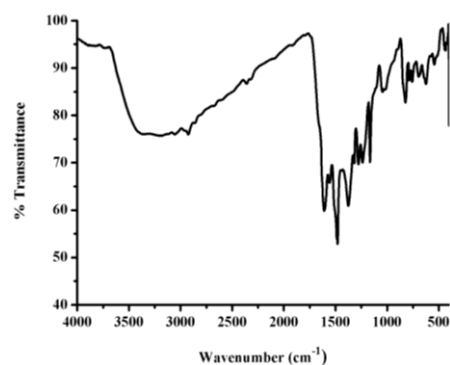


Figure 3.13 FT-IR spectrum of [Cu(FMB)₂(H₂O)₂].H₂O

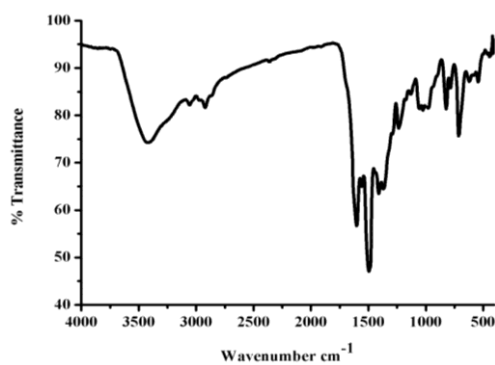


Figure 3.14 FT-IR spectrum of [Cu(FMBH)₂(H₂O)₂].2H₂O

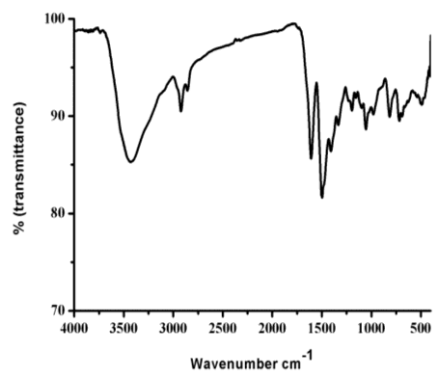


Figure 3.15 FT-IR spectrum of
[Cu(FMN)(OAc)].H₂O

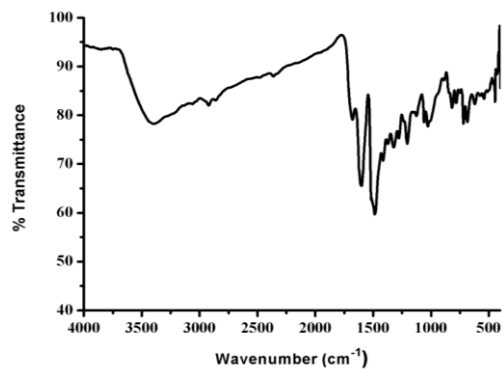


Figure 3.16 FT-IR spectrum of
[Cu(FMIN)(OAc)(H₂O)].H₂O

Table 3.9 IR spectral assignments (cm⁻¹) of hydrazones and their Zn (II) complexes

Compound	$\nu(\text{OH, NH})$	$\nu(\text{C=O})$ pyrone	$\nu(\text{C=O})$ hydrazone	$\nu(\text{C=N})$	Mono/Bidentate acetate
FB	-, 3220	1678	1641	1597	-
[Zn(FB)(OAc)].2.5 H ₂ O (17)	3618-3088	1641	1597	1560	ν_{as} 1529, ν_{s} 1397
FBH	-, 3394 (b)	1675	1650	1590	-
[Zn(FBH)(OAc)] (18)	3630-2997	1654	1593	1550	ν_{as} 1536, ν_{s} 1388
FN	-, 3233	1677	1651	1596	-
[Zn(FN)(OAc)].H ₂ O (19)	3567-3045	1657	1628	1553	ν_{as} 1514, ν_{s} 1376
FIN	-, 3267	1674	1645	1597	-
[Zn(FIN)(OAc)] (20)	-, 3346	1661	1616	1561	ν_{as} 1537, ν_{s} 1383
FMB	-, 3206	1680	1655	1595	-
[Zn(FMB) ₂].2H ₂ O (21)	3568-2996	1663	1621	1568	-
FMBH	3346, 3100	1675	1650	1590	-
[Zn(FMBH)(OAc)].H ₂ O (22)	3435-3032	1668	1598	1577	ν_{as} 1546, ν_{s} 1413
FMN	-, 3206	1679	1647	1584	-
[Zn(FMN)(OAc)].H ₂ O (23)	3312, 3245	1673	1609	1542	ν_{as} 1549, ν_{s} 1418
FMIN	-, 3100	1683	1658	1587	-
[Zn(FMIN)(OAc)].0.5 H ₂ O(24)	3378, 3134	1671	1607	1546	ν_{as} 1546, ν_{s} 1413

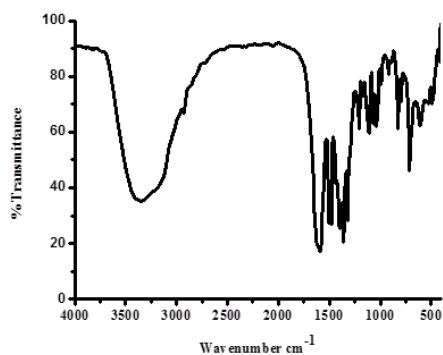


Figure 3.17 FT-IR spectrum of [Zn(FB)(OAc)].2.5H₂O

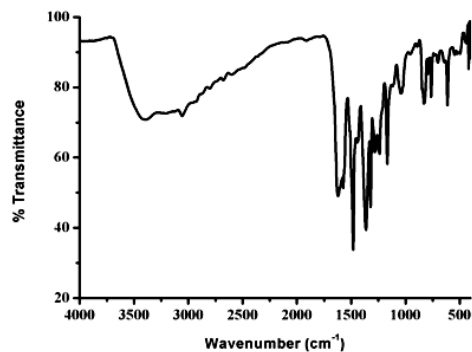


Figure 3.18 FT-IR spectrum of [Zn(FBH)(OAc)]

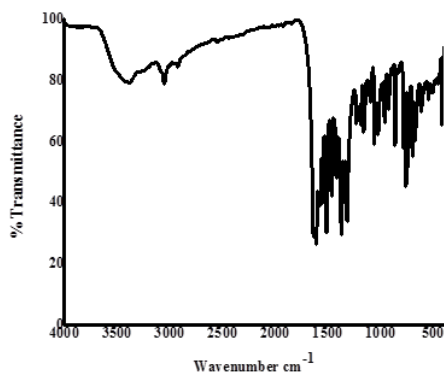


Figure 3.19 FT-IR spectrum of [Zn(FN)(OAc)].H₂O

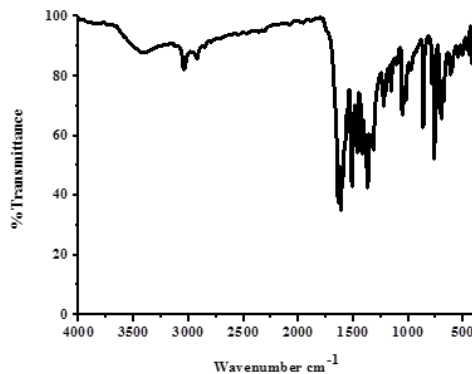


Figure 3.20 FT-IR spectrum of [Zn(FIN)(OAc)]

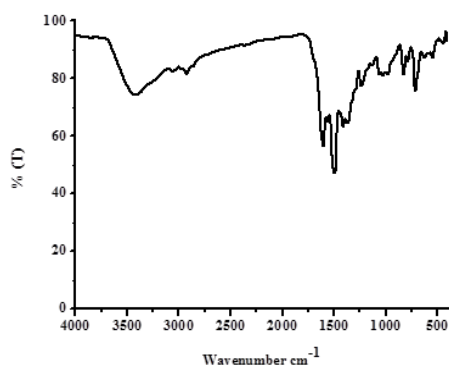


Figure 3.21 FT-IR spectrum of [Zn(FMB)₂].2H₂O

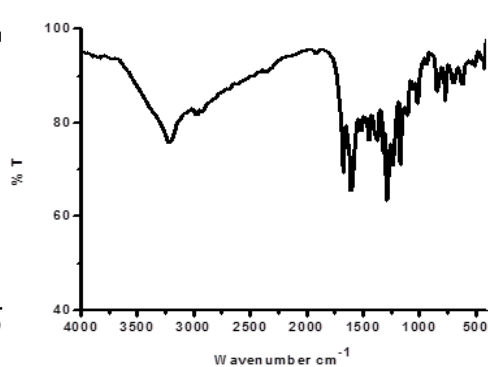


Figure 3.22 FT-IR spectrum of [Zn(FMBH)(OAc)].H₂O

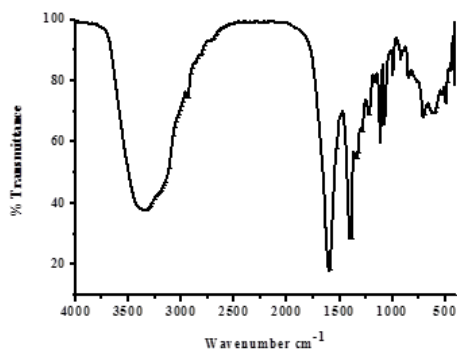


Figure 3.23 FT-IR spectrum of $[\text{Zn}(\text{FMN})(\text{OAc})]\cdot\text{H}_2\text{O}$

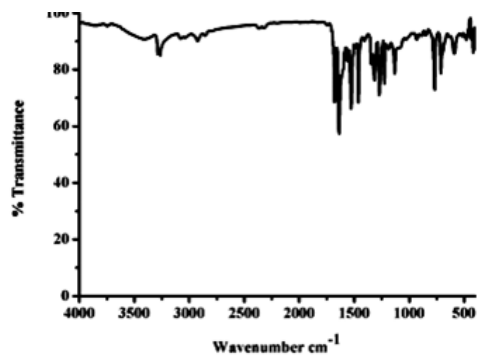


Figure 3.24 FT-IR spectrum of $[\text{Zn}(\text{FMIN})(\text{OAc})]\cdot 0.5 \text{H}_2\text{O}$

3.3.4 Electronic spectra

The electronic spectra of the ligands and metal complexes were recorded in DMF (10^{-3}M) in the range 900-200 nm ($11111-50000 \text{ cm}^{-1}$) and are given in Figures 3.25-3.48. The spectral bands and their assignments are listed in Tables 3.10-3.12. The spectral data of the hydrazones shows two bands in the range 250-350 nm ($40000-28571 \text{ cm}^{-1}$) due to $\pi \rightarrow \pi^*$ and $n \rightarrow \pi^*$ transitions [57]. The higher energy band may be assigned to $\pi \rightarrow \pi^*$ transitions of the azomethine linkage and the aromatic rings. The medium energy band may be assigned to $n \rightarrow \pi^*$ transitions of the C=O and C=N groups.

The spectra of all metal complexes exhibit bands above 400 nm (25000 cm^{-1}) in addition to the $n \rightarrow \pi^*$ transition in the ligands. In absence of X-ray diffraction studies, the electronic spectra can be used in determination of the structure of metal complexes as the number and position of spectral bands provide good insight to the geometry of a metal complex [58]. The metal complexes in DMF solutions present absorption maxima attributable to the hydrazone ligand together with the absorptions, around 419-697 nm ($23866-14347 \text{ cm}^{-1}$), due to ligand to metal charge transfer and d-d transitions of the metals in the complexes [59]. The bands in the electronic

spectra of hydrazones due $\pi \rightarrow \pi^*$ and $n \rightarrow \pi^*$ transitions suffered marginal shifts upon complexation. This may be due to the weakening of the $-C=O-$ bond and the extension of conjugation upon complexation. The shift occurs also due to the coordination of the metal (II) ion are pyrone oxygen, azomethine nitrogen and hydrazone oxygen.

The electronic spectra of nickel (II) complexes the bands in the 345-275 nm ($28985-36363 \text{ cm}^{-1}$) region can be assigned to the intra ligand transitions and the bands observed in the region 445-400 nm ($22471-25000 \text{ cm}^{-1}$) are due to ligand to metal charge transfer transitions.

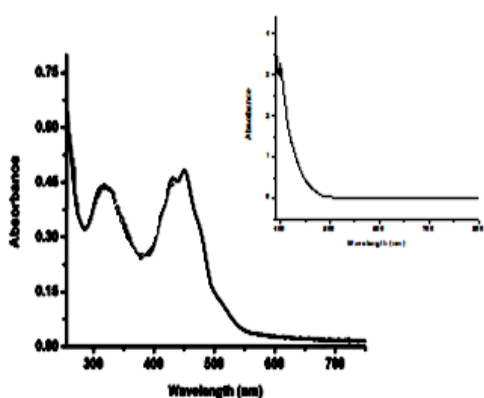


Figure 3.25 UV-vis. spectrum of [Ni(FB)(OAc)(H₂O)].2H₂O

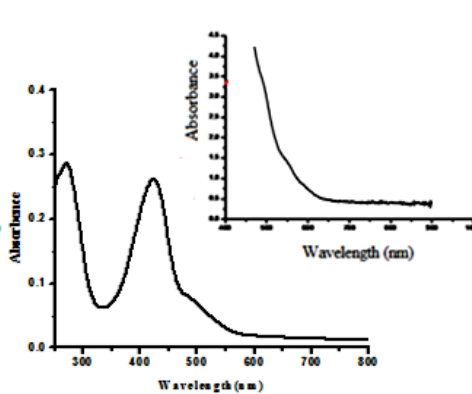


Figure 3.26 UV-vis. spectrum of [Ni(FBH)(H₂O)(OAc)].2H₂O

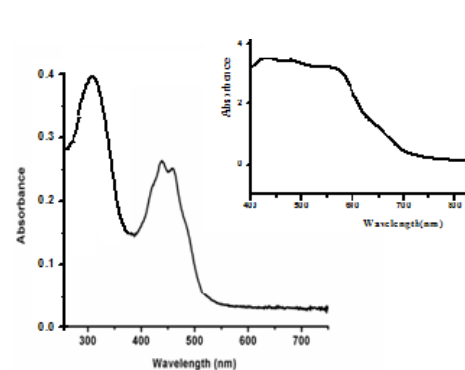


Figure 3.27 UV-visible spectrum of [Ni(FN)(OAc)].H₂O

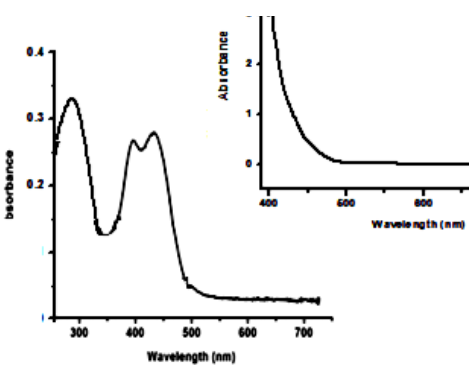


Figure 3.28 UV-visible spectrum of [Ni(FIN)(OAc)(H₂O)].H₂O

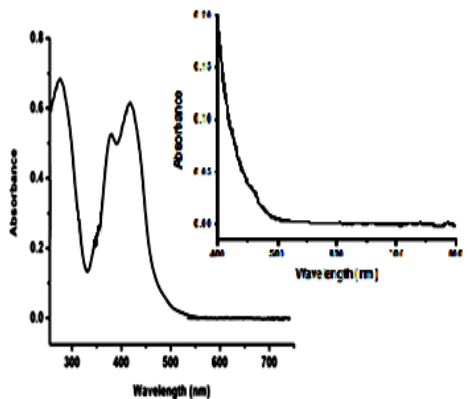


Figure 3.29 UV-visible spectrum of $[\text{Ni}(\text{FMB})_2(\text{H}_2\text{O})_2]\cdot\text{H}_2\text{O}$

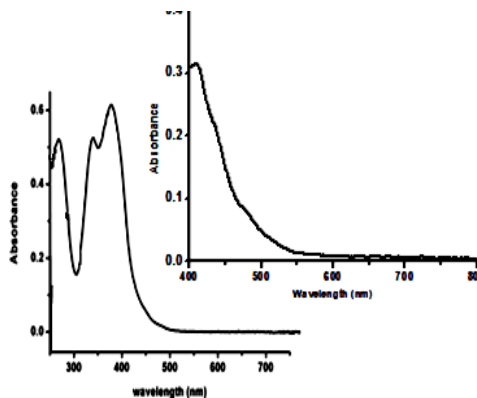


Figure 3.30 UV-visible spectrum of $[\text{Ni}(\text{FMBH})_2(\text{H}_2\text{O})_2]\cdot 2\text{H}_2\text{O}$

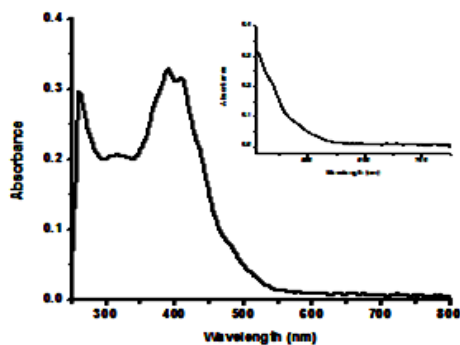


Figure 3.31 UV-visible spectrum of $[\text{Ni}(\text{FMN})(\text{OAc})]\cdot 2\text{H}_2\text{O}$

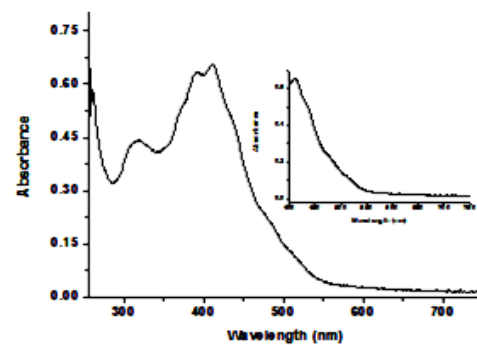


Figure 3.32 UV-visible spectrum of $[\text{Ni}(\text{FMIN})(\text{OAc})(\text{H}_2\text{O})]\cdot 1.5\text{H}_2\text{O}$

Figures 3.25-3.32 depict the electronic spectra of the Ni (II) complexes. All the complexes synthesized except $[\text{Ni}(\text{FN})(\text{OAc})]\cdot\text{H}_2\text{O}$ and $[\text{Ni}(\text{FMIN})(\text{OAc})(\text{H}_2\text{O})]\cdot 1.5\text{H}_2\text{O}$ have octahedral geometry as evidenced from their magnetic moments. In nickel (II) complexes with octahedral geometry, we expect three transitions; ${}^3T_{1g}(\text{P}) \leftarrow {}^3A_{2g}(\text{F}) (v_3)$, ${}^3T_{1g}(\text{F}) \leftarrow {}^3A_{2g}(\text{F}) (v_2)$ and ${}^3T_{2g}(\text{F}) \leftarrow {}^3A_{2g}(\text{F}) (v_1)$ [60-61]. But we could locate only one band due to masking by high intensity charge transfer bands. The ground state of Ni (II) in tetrahedral complex is ${}^3T_1(\text{F})$ and also three spin allowed transitions are expected i.e. ${}^3T_1(\text{P}) \leftarrow {}^3T_1(\text{F})$, ${}^3A_2(\text{F}) \leftarrow {}^3T_1$

(F), 3T_2 (F) \leftarrow 3T_1 (F); but unfortunately these *d-d* bands are masked by the strong charge transfer (CT) absorption bands in these complexes.

Table 3.10 Electronic spectral assignments for Ni (II) complexes

Compound	Electronic spectral bands :nm(cm ⁻¹)	log ϵ (L mol ⁻¹ cm ⁻¹)	Band assignment
[Ni(FB)(OAc)(H ₂ O)].2H ₂ O (1)	284 (35211) 325 (30769) 505 (19801) 510 (19607)	3.77 2.64 1.66 1.65	Intra ligand transition CT ${}^3A_{2g}(F) \rightarrow {}^3T_{1g}(P)$ ${}^3A_{2g}(F) \rightarrow {}^3T_{1g}(F)$
[Ni(FBH)(H ₂ O)(OAc)].2H ₂ O (2)	275 (36363) 450 (22222) 565 (17699) 670 (14925)	3.47 3.44 2.07 1.01	Intra ligand transition CT ${}^3A_{2g}(F) \rightarrow {}^3T_{1g}(P)$ ${}^3A_{2g}(F) \rightarrow {}^3T_{1g}(F)$
[Ni(FN)(OAc)].H ₂ O (3)	298 (33557) 445 (22471) 460 (21734) 645 (15503)	3.60 2.39 1.36 0.50	Intra ligand transition CT ${}^3T_1(F) \rightarrow {}^3A_2(F)$
[Ni(FIN)(OAc)(H ₂ O)].H ₂ O (4)	290 (34482) 420 (23809) 463 (21598) 677 (14771)	3.53 2.43 2.38 1.90	Intra ligand transition CT ${}^3A_{2g}(F) \rightarrow {}^3T_{1g}(P)$ ${}^3A_{2g}(F) \rightarrow {}^3T_{1g}(F)$
[Ni(FMB) ₂ (H ₂ O) ₂].H ₂ O (5)	285 (35087) 400 (25000) 450 (22222) 612 (16339)	3.65 2.56 1.60 1.17	Intra ligand transition CT ${}^3A_{2g}(F) \rightarrow {}^3T_{1g}(P)$
[Ni(FBH) ₂ (H ₂ O) ₂].2H ₂ O (6)	307 (32573) 420 (23810) 465 (21505) 550 (18182)	4.00 3.91 1.48 1.23	Intra ligand transition CT ${}^3A_{2g}(F) \rightarrow {}^3T_{1g}(P)$ ${}^3A_{2g}(F) \rightarrow {}^3T_{1g}(F)$
[Ni(FMN)(OAc)].2H ₂ O (7)	287 (34843) 320 (31250) 410 (24390) 429 (23310) 580 (17241)	3.46 2.32 1.54 1.50 1.32	Intra ligand transition CT ${}^3T_1(F) \rightarrow {}^3A_2(F)$
[Ni(FMIN)(OAc)(H ₂ O)].1.5H ₂ O (8)	296 (33783) 345 (28985) 421 (23752) 458 (21834) 619 (16155)	3.77 2.64 1.82 1.79 1.51	Intra ligand transition CT ${}^3A_{2g}(F) \rightarrow {}^3T_{1g}(P)$ ${}^3A_{2g}(F) \rightarrow {}^3T_{1g}(F)$

In UV-Visible spectra the intra ligand transitions of copper (II) complexes are assigned to bands in the range of 267-400 nm (37453-25000 cm^{-1}). It is due to the $n \rightarrow \pi^*$ and $\pi \rightarrow \pi^*$ transitions of hydrazone ligands suffered a marginal shift up on complexation. The shift of the bands may be caused by intra ligand transitions which weakening of the C=N bond and extension of conjugation upon complexation. The shift is also due to coordination *via* azomethine nitrogen and iminolate oxygen that is an iminolization followed by the deprotonation can be take place during complexation. A band is observed in the range 365-457 nm (27397-21881 cm^{-1}) could be due to Cu (II) \rightarrow ligand charge transfer (MLCT) transitions.

Cu (II) complexes has the spectroscopic ground state term 2D which will be split by an octahedral field into two (2E_g and $^2T_{2g}$) levels. However, Cu (II) complexes in lower symmetry, the energy levels again split into more transitions are observed. The band in the wavelength around in the range 451-675 nm (22172-14814 cm^{-1}) corresponds to d-d transition [62]. $^2B_{1g} \rightarrow ^2A_{1g}$ ($d_x^2 - y^2 - d_z^2$), $^2B_{1g} \rightarrow ^2B_{2g}$ ($d_x^2 - y^2 - d_{xy}$) and $^2B_{1g} \rightarrow ^2E_g$ ($d_x^2 - y^2 - d_{xz}, d_{yz}$) are the three possible spin allowed transitions for square planar or square pyramidal copper complexes with $d_x^2 - y^2$ ground state. The four *d* orbitals lie very close together, so each transition cannot be distinguished by its energy and hence it is very difficult to resolve the three bands into separate components. In the present study, these transitions are observed as shoulders in the range 451-675 nm (22172-14814 cm^{-1}) for all copper complexes [63].

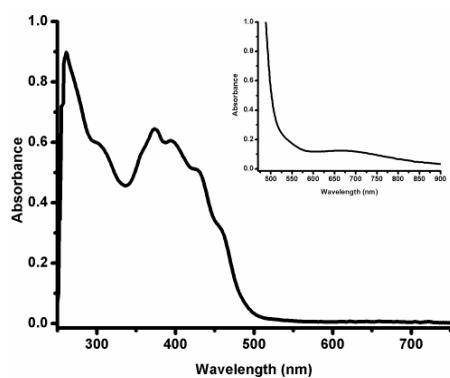


Figure 3.33 UV-visible spectrum of [Cu(FB)(OAc)].H₂O

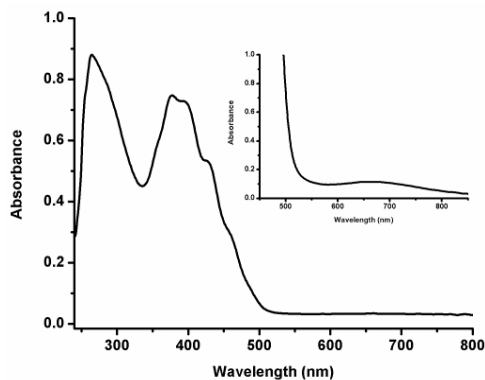


Figure 3.34 UV-visible spectrum of [Cu(FBH)(H₂O)(OAc)].H₂O

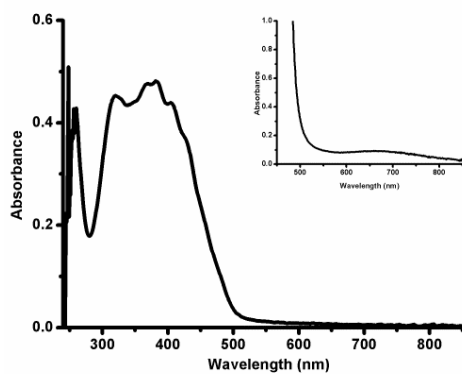


Figure 3.35 UV-visible spectrum of [Cu(FN)(OAc)].2H₂O

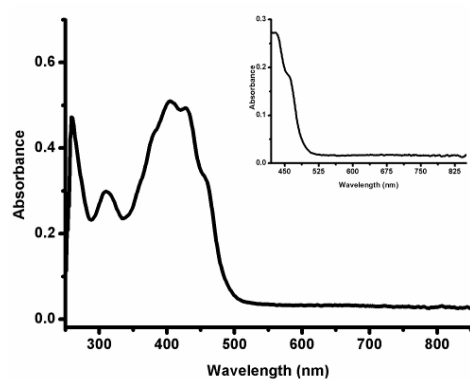


Figure 3.36 UV-visible spectrum of [Cu(FIN)(OAc)(H₂O)].2H₂O

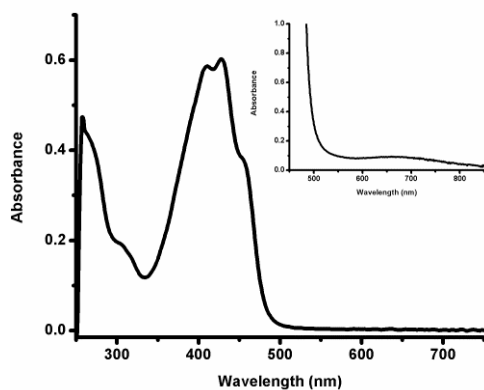


Figure 3.37 UV-visible spectrum of [Cu(FMB)₂(H₂O)₂].H₂O

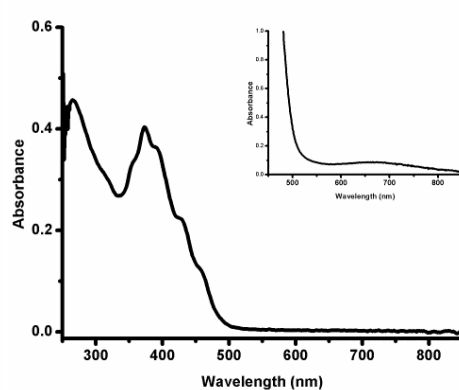


Figure 3.38 UV-visible spectrum of [Cu(FMBH)₂(H₂O)₂].2H₂O

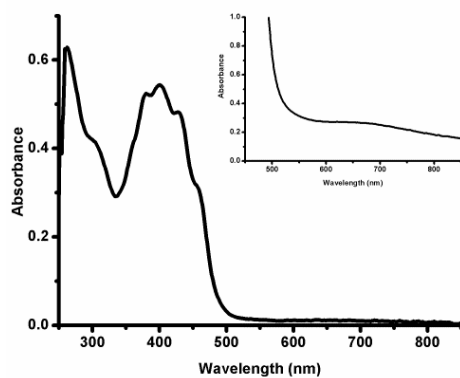


Figure 3.39 UV-visible spectrum of [Cu(FMN)(OAc)].H₂O

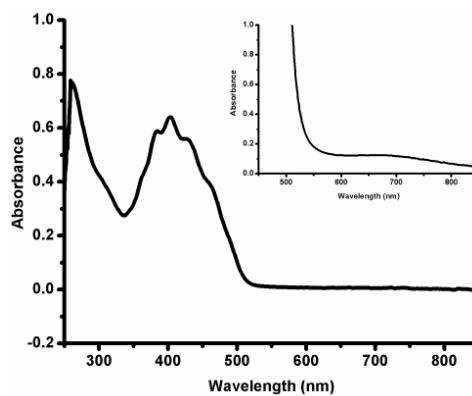


Figure 3.40 UV-visible spectrum of [Cu(FMIN)(OAc)(H₂O)].H₂O

Table 3.11 Electronic spectral assignments for Cu (II) complexes

Compounds	Electronic spectral bands :nm (cm ⁻¹)	log ϵ (L mol ⁻¹ cm ⁻¹)	Band assignment
[Cu(FB)(OAc)].H ₂ O (9)	279 (35842) 365 (27397) 425 (23529) 480 (20833) 648 (15416)	3.95 2.79 1.69 1.54 1.0	Intra ligand transition Intra ligand transition ² B ₁ → ² E(dx ² -y ² → dxz, dyz) ² B ₁ → ² B ₂ (dx ² -y ² → dxy) ² B ₁ → ² A ₁ (dx ² -y ² → dz ₂)
[Cu(FBH)(H ₂ O)(OAc)].H ₂ O (10)	293 (37453) 386 (25906) 451 (22172) 483 (20703) 639 (15627)	3.95 3.85 2.69 2.47 1.20	Intra ligand transition Intra ligand transition ² B ₁ → ² E(dx ² -y ² → dxz, dyz) ² B ₁ → ² B ₂ (dx ² -y ² → dxy) ² B ₁ → ² A ₁ (dx ² -y ² → dz ₂)
[Cu(FN)(OAc)].2H ₂ O (11)	285 (35087) 325 (30769) 410 (24390) 457 (21881) 617 (14814)	3.68 3.6 2.68 2.65 1.07	Intra ligand transition Intra ligand transition Intra ligand transition ² B ₁ → ² E(dx ² -y ² → dxz, dyz) ² B ₁ → ² B ₂ (dx ² -y ² → dxy)
[Cu(FIN)(OAc)(H ₂ O)].2H ₂ O (12)	295 (33898) 337 (29673) 480 (20833) 667 (14973)	3.65 3.47 2.69 1.17	Intra ligand transition Intra ligand transition ² B _{1g} → ² Eg(dx ² -y ² →dxz, dyz) ² B _{1g} → ² B _{2g} (dx ² -y ² → dxy)
[Cu(FMB) ₂ (H ₂ O) ₂].H ₂ O (13)	290 (34482) 312 (32051) 450 (22222) 677 (14771)	3.68 3.32 2.77 1.23	Intra ligand transitions Intra ligand transitions ² B _{1g} → ² Eg(dx ² -y ² →dxz, dyz) ² B _{1g} → ² B _{2g} (dx ² -y ² → dxy)
[Cu(FMBH) ₂ (H ₂ O) ₂].2H ₂ O (14)	287 (34843) 400 (25000) 453 (22075) 489 (20449) 656 (15224)	3.69 3.60 3.43 2.42 1.07	Intra ligand transitions Intra ligand transitions ² B _{1g} → ² Eg(dx ² -y ² →dxz, dyz) ² B _{1g} → ² B _{2g} (dx ² -y ² →dxy) ² B _{1g} → ² A _{1g} (dx ² -y ² →dz ₂)
[Cu(FMN)(OAc)].H ₂ O (15)	293 (34129) 327 (30581) 450 (22222) 497 (20120) 647 (15451)	3.79 3.68 2.69 2.49 1.43	Intra ligand transition Intra ligand transition ² B ₁ → ² E (dx ² -y ² → dxz, dyz) ² B ₁ → ² B ₂ (dx ² -y ² → dxy) ² B ₁ → ² A ₁ (dx ² -y ² → dz ₂)
[Cu(FMIN)(OAc)(H ₂ O)].H ₂ O (16)	292 (34246) 396 (25252) 457 (21881) 489(20533) 610 (16370)	3.89 3.77 3.72 2.61 1.23	Intra ligand transition Intra ligand transition ² B ₁ → ² E(dx ² -y ² →dxz, dyz) ² B ₁ → ² B ₂ (dx ² -y ² → dxy) ² B ₁ → ² A ₁ (dx ² -y ² → dz ₂)

The electronic spectrum of all Zn (II) complexes are presented in Figures 3.41-3.48 and Table 3.12. The absorption bands due to $n \rightarrow \pi^*$ and $\pi \rightarrow \pi^*$ transitions of free hydrazone ligands suffered substantial shift upon complexation. This may be due to the weakening of the C=O bond and the extension of conjugation upon complexation. That is due to the hydrazone oxygen atom and azomethine nitrogen atom in coordination. The new bands observed for complexes in the 457-387 nm (21881-25839 cm^{-1}) region can be assigned to the metal to ligand charge transfer (MLCT) transitions which are compactable with tetrahedral structure for Zn (II) complexes [64-65]. No appreciable absorptions occurred below 500 nm (20000 cm^{-1}) indicating the absence of $d-d$ bands which is in accordance with d^{10} configuration of Zn (II) ions [66-67].

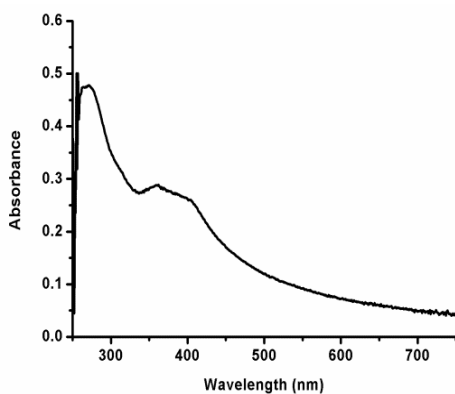


Figure 3.41 UV-visible spectrum of [Zn(FB)(OAc)].2.5 H₂O

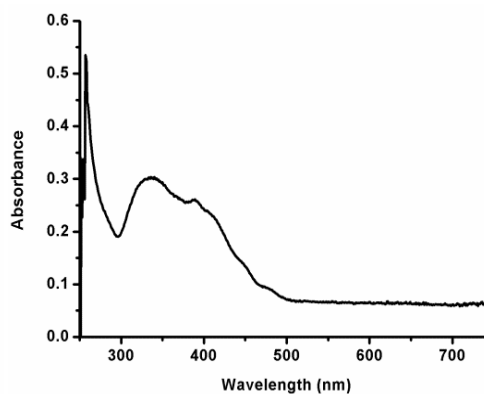


Figure 3.42 UV-visible spectrum of [Zn(FBH)(OAc)]

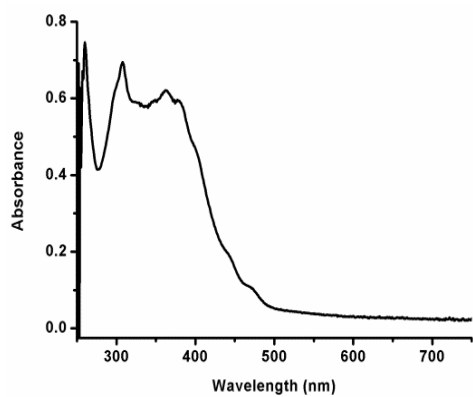


Figure 3.43 UV-visible spectrum of [Zn(FN)(OAc)].H₂O

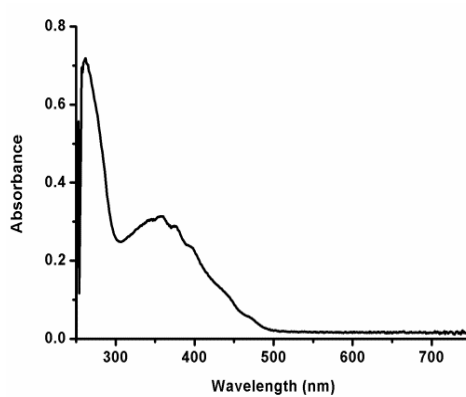


Figure 3.44 UV-visible spectrum of [Zn(FIN)(OAc)]

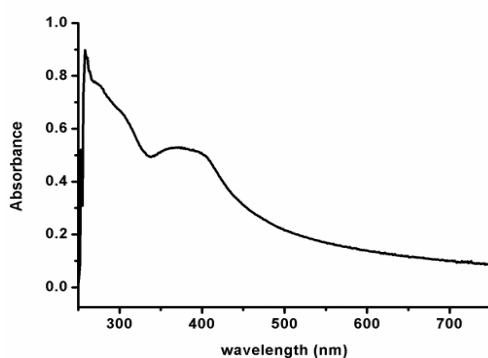


Figure 3.45 UV-visible spectrum of [Zn(FMB)₂].2H₂O

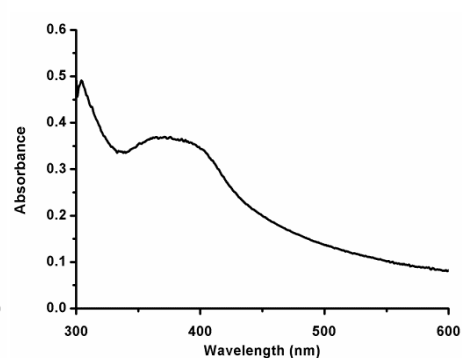


Figure 3.46 UV-visible spectrum of [Zn(FMBH)(OAc)].H₂O

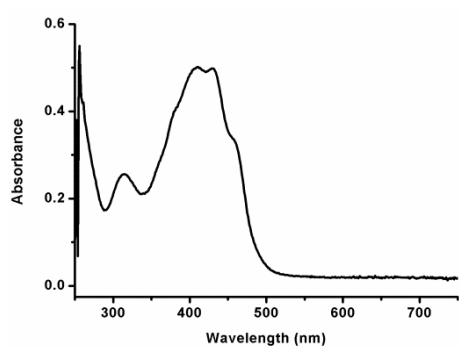


Figure 3.47 UV-visible spectrum of [Zn(FMN)(OAc)].H₂O

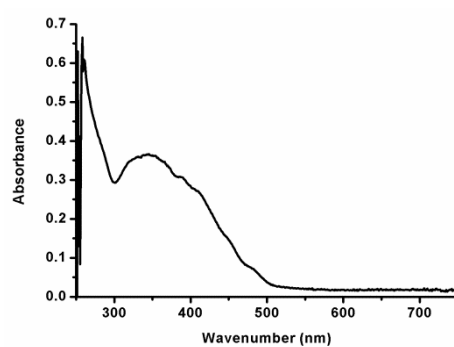


Figure 3.48 UV-visible spectrum of [Zn(FMIN)(OAc)].0.5 H₂O

Table 3.12 Electronic spectral assignments for Zn (II) complexes

Compounds	Electronic spectral bands : nm(cm ⁻¹)	log ϵ (L mol ⁻¹ cm ⁻¹)	Band assignment
[Zn(FB)(OAc)].2.5 H ₂ O	295 (33898) 387 (25839)	3.60 3.47	$\pi \rightarrow \pi^*/n \rightarrow \pi^*$ MLCT
[Zn(FBH)(OAc)]	287 (34843) 368 (27173) 410 (24390)	3.71 3.46 3.41	$\pi \rightarrow \pi^*/n \rightarrow \pi^*$ MLCT MLCT
[Zn(FN)(OAc)].H ₂ O	288 (34722) 327 (30581) 425 (23529)	3.86 3.81 3.77	$\pi \rightarrow \pi^*/n \rightarrow \pi^*$ MLCT MLCT
[Zn(FIN)(OAc)]	293 (34129) 387 (25706)	3.85 3.50	$\pi \rightarrow \pi^*/n \rightarrow \pi^*$ MLCT
[Zn(FMB) ₂].2H ₂ O	299 (33444) 397 (25188)	3.69 3.57	$\pi \rightarrow \pi^*/n \rightarrow \pi^*$ MLCT
[Zn(FMBH)(OAc)].H ₂ O	283 (35335) 394 (25380)	3.96 3.76	$\pi \rightarrow \pi^*/n \rightarrow \pi^*$ MLCT
[Zn(FMN)(OAc)].H ₂ O	287 (34843) 334 (29940) 457 (21881)	3.75 3.70 3.39	$\pi \rightarrow \pi^*/n \rightarrow \pi^*$ MLCT MLCT
[Zn(FMIN)(OAc)].0.5 H ₂ O	295 (33898) 357 (28011)	3.83 3.56	$\pi \rightarrow \pi^*/n \rightarrow \pi^*$ MLCT

3.3.5 Electronic paramagnetic resonance spectra

The EPR spectra of the copper (II) complexes in DMF at 77 K and in a polycrystalline state at 298 K were recorded in the X-band, using 100-kHz modulation frequency and 9.5 GHz microwave frequency. All the EPR spectra are simulated using Easy Spin 5.0.20 package [68] and the experimental (red) and simulated (blue) best fits are included. EPR parameters of the copper (II) complexes are presented in Table 3.13-3.14 and Figures 3.49-3.65

Copper (II) complexes displayed Figures 3.49-3.56 axial spectra in the polycrystalline state at 298 K with g_{\parallel} and g_{\perp} values. The variation in the g_{\parallel} and g_{\perp} values indicates that in the solid state, the geometry of the compounds is affected by the nature of coordinating ligands.

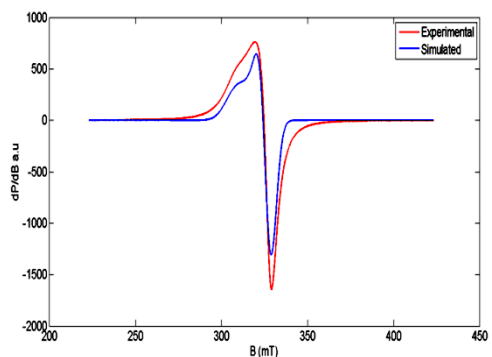


Figure 3.49 EPR spectrum of [Cu(FB)(OAc)].H₂O at 298 K

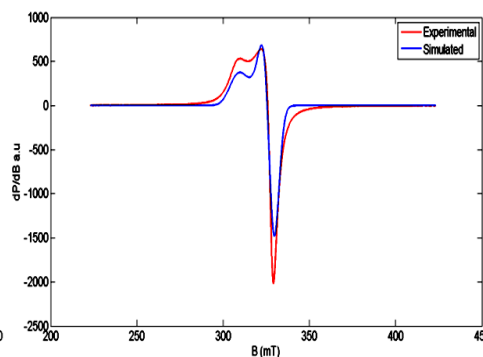


Figure 3.50 EPR spectrum of [Cu(FBH)(H₂O)(OAc)].H₂O at 298 K

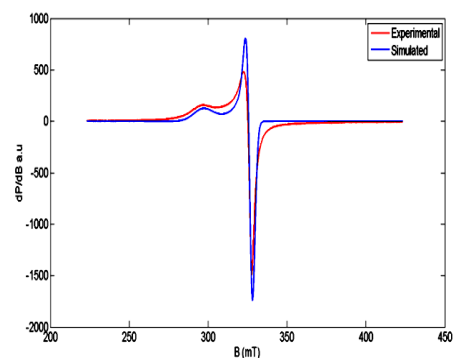


Figure 3.51 EPR spectrum of [Cu(FN)(OAc)].2H₂O at 298 K

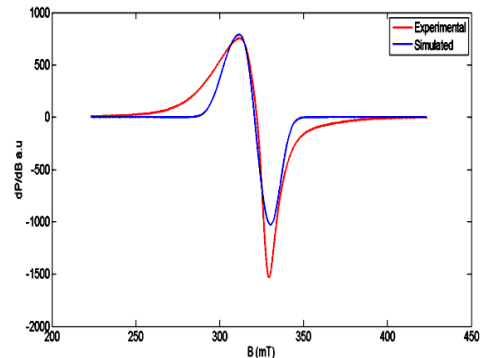


Figure 3.52 EPR spectrum of [Cu(FIN)(OAc)(H₂O)].2H₂O at 298 K

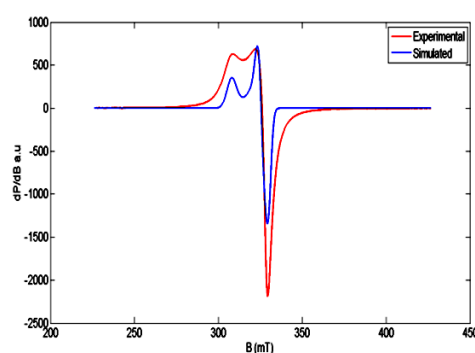


Figure 3.53 EPR spectrum of [Cu(FMB)₂(H₂O)₂].H₂O at 298 K

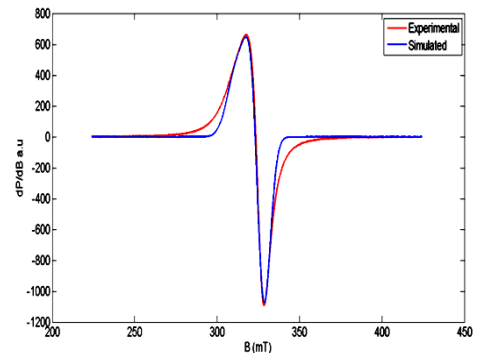


Figure 3.54 EPR spectrum of [Cu(FMBH)₂(H₂O)₂].2H₂O at 298 K

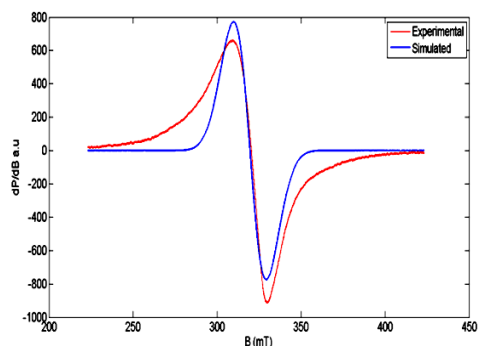


Figure 3.55 EPR spectrum of $[\text{Cu}(\text{FMN})(\text{OAc})]\cdot\text{H}_2\text{O}$ at 298 K

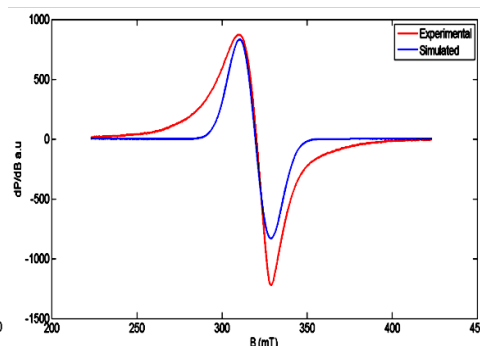


Figure 3.56 EPR spectrum of $[\text{Cu}(\text{FMIN})(\text{OAc})(\text{H}_2\text{O})]\cdot\text{H}_2\text{O}$ at 298 K

Table 3.13 Spin Hamiltonian and bonding parameters of copper (II) complexes at 298 K

Polycrystalline at 298 K					
Compounds	g_{\parallel}/g_x	g_{\perp}/g_y	g_z	$g_{\text{iso}}/g_{\text{av}}$	G
$[\text{Cu}(\text{FB})(\text{OAc})]\cdot\text{H}_2\text{O}$ (9)	2.190	2.066	-	2.1073	2.9466
$[\text{Cu}(\text{FBH})(\text{H}_2\text{O})(\text{OAc})]\cdot\text{H}_2\text{O}$ (10)	2.190	2.059	-	2.1027	3.3104
$[\text{Cu}(\text{FN})(\text{OAc})]\cdot 2\text{H}_2\text{O}$ (11)	2.204	2.070	-	2.1147	2.9793
$[\text{Cu}(\text{FIN})(\text{OAc})(\text{H}_2\text{O})]\cdot 2\text{H}_2\text{O}$ (12)	2.280	2.065	-	2.1367	4.4290
$[\text{Cu}(\text{FMB})_2(\text{H}_2\text{O})_2]\cdot\text{H}_2\text{O}$ (13)	2.192	2.060	-	2.1040	3.2877
$[\text{Cu}(\text{FMBH})_2(\text{H}_2\text{O})_2]\cdot 2\text{H}_2\text{O}$ (14)	2.170	2.070	-	2.1033	2.4771
$[\text{Cu}(\text{FMN})(\text{OAc})]\cdot\text{H}_2\text{O}$ (15)	-	-	-	2.1100	-
$[\text{Cu}(\text{FMIN})(\text{OAc})(\text{H}_2\text{O})]\cdot\text{H}_2\text{O}$ (16)	-	-	-	2.1100	-

The spectra of $[\text{Cu}(\text{FMN})(\text{OAc})]\cdot\text{H}_2\text{O}$ and $[\text{Cu}(\text{FMIN})(\text{OAc})(\text{H}_2\text{O})]\cdot\text{H}_2\text{O}$ complexes shows an isotropic spectrum with $g_{\text{iso}}=2.11$ at room temperature (Figures 3.55-3.56). This spectrum consists of only one broad signal and hence only one g value due to dipolar broadening and enhanced spin lattice relaxation [69]. This type of spectra did not give any information about the electronic ground state of Cu (II) ion present in the complexes. For

complexes, displayed axial features; since it is magnetically concentrated, hyperfine splitting was not clear in both parallel and perpendicular regions. All other copper (II) complexes displayed axial spectra with g_{\parallel} and g_{\perp} values. As $g_{\parallel} > g_{\perp} > 2.0023$, which is consistent with a $d_{x^2-y^2}$ ground state in a square planar or square pyramidal geometry can be assigned to the copper (II) complexes, thereby ruling out the possibility of a trigonal bipyramidal structure (where $g_{\parallel} < g_{\perp}$).

The geometric parameter G , represents the exchange interaction between copper centers in the polycrystalline compound and is calculated for each complexes using the equation, $G = (g_{\parallel} - 2.0023)/(g_{\perp} - 2.0023)$ for axial spectra [70]. If $G > 4.4$, exchange interaction is negligible and if it less than 4.4, considerable exchange interaction is indicated in the solid complex. The calculated G values are greater than 4.4 for complex $[\text{Cu}(\text{FIN})(\text{OAc})(\text{H}_2\text{O})] \cdot 2\text{H}_2\text{O}$ which indicate that there are no copper-copper exchange interaction is present in the polycrystalline state of the complex. G values are less than 4.4 for complexes $[\text{Cu}(\text{FB})(\text{OAc})] \cdot \text{H}_2\text{O}$, $[\text{Cu}(\text{FBH})(\text{H}_2\text{O})(\text{OAc})] \cdot \text{H}_2\text{O}$, $[\text{Cu}(\text{FN})(\text{OAc})] \cdot 2\text{H}_2\text{O}$, $[\text{Cu}(\text{FMB})_2(\text{H}_2\text{O})_2] \cdot \text{H}_2\text{O}$ and $[\text{Cu}(\text{FMBH})_2(\text{H}_2\text{O})_2] \cdot 2\text{H}_2\text{O}$ which indicate that considerable exchange interaction is present

At 77 K in DMF solution, complexes (Table 3.14 and Figures 3.57-3.65) exhibits axial spectrum and this gives more information about the geometry of the complexes [59]. For the copper complexes, $[\text{Cu}(\text{FN})(\text{OAc})] \cdot 2\text{H}_2\text{O}$, $[\text{Cu}(\text{FIN})(\text{OAc})(\text{H}_2\text{O})] \cdot 2\text{H}_2\text{O}$, $[\text{Cu}(\text{FMN})(\text{OAc})] \cdot \text{H}_2\text{O}$ and $[\text{Cu}(\text{FMIN})(\text{OAc})(\text{H}_2\text{O})] \cdot \text{H}_2\text{O}$ four well resolved hyperfine lines are observed in the parallel region due to coupling of the electron spin with the

nuclear spin (^{63}Cu , $I = 3/2$), the splitting are not well differentiable in the perpendicular region. In DMF at 77K, complex $[\text{Cu}(\text{FMIN})(\text{OAc})(\text{H}_2\text{O})]\cdot\text{H}_2\text{O}$ having three sets of resonances at low, mid and high fields corresponding to g_x , g_y and g_z respectively. From the peak positions, the g values evaluated are $g_x = 2.036$, $g_y = 2.080$ and $g_z = 2.450$. Hyperfine structure was not resolved in perpendicular region. The calculated g values provide valuable information on the electronic ground state of the ion. If g values $g_z > g_y > g_x$, and the quantity of R [$R = (g_y - g_x)/(g_z - g_y)$] is greater than unity, the ground state is (d_z^2) and if R is less than unity, the ground state is $(d_x^2 - y^2)$. For $[\text{Cu}(\text{FMIN})(\text{OAc})(\text{H}_2\text{O})]\cdot\text{H}_2\text{O}$ the value of 'R' = 0.118 indicates $d_x^2 - y^2$ as ground state suggesting a rhombic structure. EPR parameters g_{\parallel} and g_{\perp} incorporated with the energies of d-d transition were used to evaluate the bonding parameters.

α^2 , the value of in-plane sigma bonding parameter was estimated by using the expression

$$\alpha^2 = -A_{\parallel}/0.036 + (g_{\parallel} - 2.0023) + 3/7(g_{\perp} - 2.0023) + 0.04 [61]$$

The bonding parameters $K_{\parallel}^2 = \alpha^2\beta^2$ and $K_{\perp}^2 = \alpha^2\gamma^2$ were calculated by using following simplified expression

$$K_{\parallel}^2 = (g_{\parallel} - 2.0023) E_{d-d}/8\lambda_0$$

$$K_{\perp}^2 = (g_{\perp} - 2.0023) E_{d-d}/2\lambda_0$$

Where K_{\parallel} and K_{\perp} are orbital reduction factors and λ_0 represents the one electron spin orbit coupling constant which equals -828 cm^{-1} .

Hathaway [70] has pointed out that for pure sigma bonding $K_{\parallel} \approx K_{\perp} \approx 0.77$, for in plane π -bonding $K_{\parallel} < K_{\perp}$ and for out-of-plane π -bonding,

$K_{\perp} < K_{\parallel}$ For complexes $[\text{Cu}(\text{FB})(\text{OAc})] \cdot \text{H}_2\text{O}$, $[\text{Cu}(\text{FBH})(\text{H}_2\text{O})(\text{OAc})] \cdot \text{H}_2\text{O}$, $[\text{Cu}(\text{FIN})(\text{OAc})(\text{H}_2\text{O})] \cdot 2\text{H}_2\text{O}$, $[\text{Cu}(\text{FMBH})_2(\text{H}_2\text{O})_2] \cdot 2\text{H}_2\text{O}$, $[\text{Cu}(\text{FMIN})(\text{OAc})(\text{H}_2\text{O})] \cdot \text{H}_2\text{O}$ and $[\text{Cu}(\text{FMB})_2(\text{H}_2\text{O})_2] \cdot \text{H}_2\text{O}$ it is observed that $K_{\parallel} < K_{\perp}$ which indicates the presence of significant in-plane π -bonding. In complexes, $[\text{Cu}(\text{FN})(\text{OAc})] \cdot 2\text{H}_2\text{O}$ and $[\text{Cu}(\text{FMN})(\text{OAc})] \cdot \text{H}_2\text{O}$ out-of-plane π -bonding is significant.

The g_{\parallel} values also provide information regarding the nature of metal-ligand bond [71]. The g_{\parallel} value is normally 2.3 or larger for ionic and less than 2.3 for covalent metal-ligand bonds. The g_{\parallel} values obtained for complexes indicate a significant degree of covalency in the metal-ligand bonds [72]. Also the nature of metal-ligand bond is evaluated by comparing the value of in-plane sigma bonding parameter α^2 i.e., if the M-L bond is purely ionic, the value of α^2 is unity and it is completely covalent, if $\alpha^2 = 0.5$. Here for all complexes, the value of $\alpha^2 < 1.0$ which indicate that the metal-ligand bonds in the complexes under investigation are partially ionic and partially covalent nature.

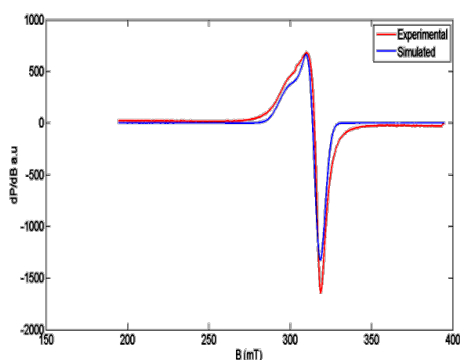


Figure 3.57 EPR spectrum of $[\text{Cu}(\text{FB})(\text{OAc})] \cdot \text{H}_2\text{O}$ in DMF at 77K

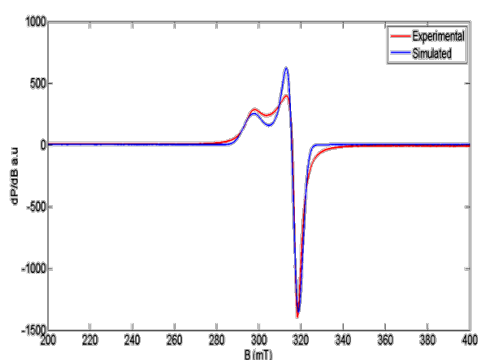


Figure 3.58 EPR spectrum of $[\text{Cu}(\text{FBH})(\text{H}_2\text{O})(\text{OAc})] \cdot \text{H}_2\text{O}$ in DMF at 77K

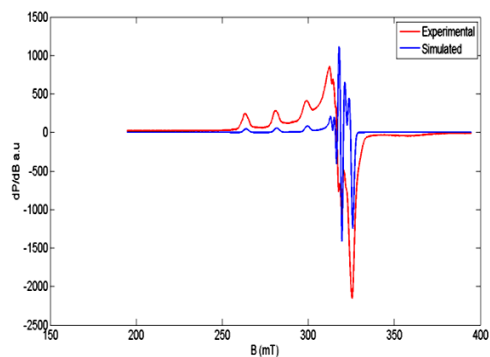


Figure 3.59 EPR spectrum of $[\text{Cu}(\text{FN})(\text{OAc})] \cdot 2\text{H}_2\text{O}$ in DMF at 77K

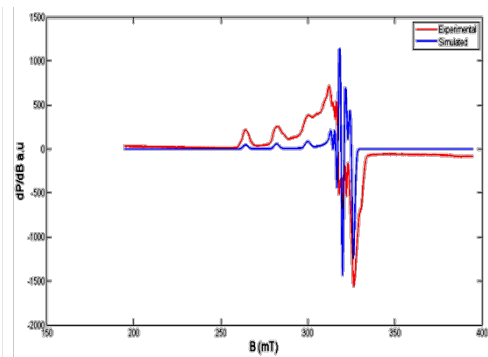


Figure 3.60 EPR spectrum of $[\text{Cu}(\text{FIN})(\text{OAc})(\text{H}_2\text{O})] \cdot 2\text{H}_2\text{O}$ in DMF at 77K

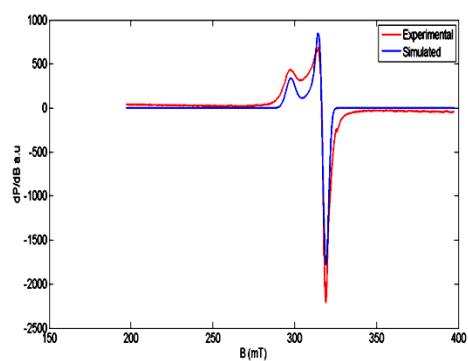


Figure 3.62 EPR spectrum of $[\text{Cu}(\text{FMB})_2(\text{H}_2\text{O})_2] \cdot \text{H}_2\text{O}$ in DMF at 77K

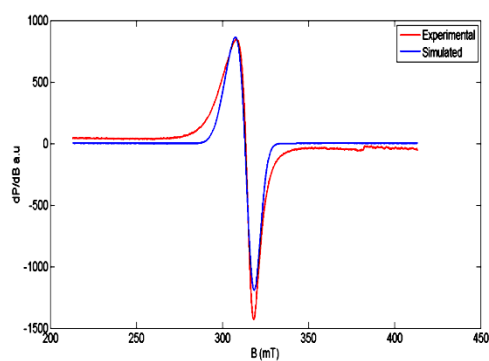


Figure 3.63 EPR spectrum of $[\text{Cu}(\text{FMBH})_2(\text{H}_2\text{O})_2] \cdot 2\text{H}_2\text{O}$ in DMF at 77K

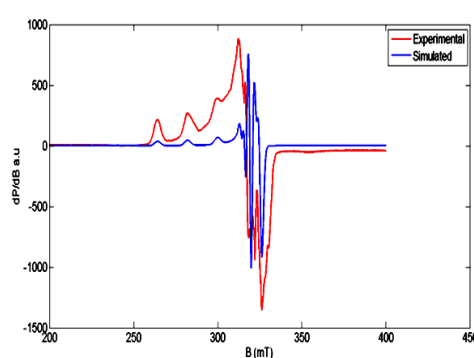


Figure 3.62 EPR spectrum of $[\text{Cu}(\text{FMN})(\text{OAc})] \cdot \text{H}_2\text{O}$ in DMF at 77K

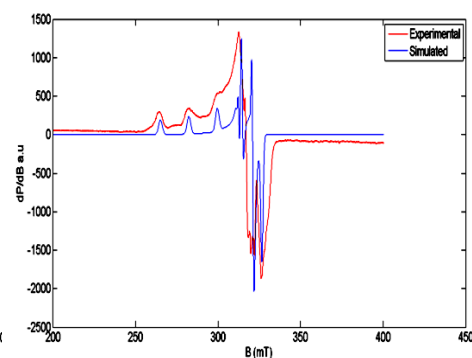


Figure 3.63 EPR spectrum of $[\text{Cu}(\text{FMIN})(\text{OAc})(\text{H}_2\text{O})] \cdot \text{H}_2\text{O}$ in DMF at 77K

Table 3.14 EPR spectral parameters of Copper (II) complexes in DMF solution at 77K

Compounds	Solution at 77 K (DMF)									
	A (mT)	g _x	g _y	g _z	a^2	E_{d-d}	$K_{ }^{Cu^{2+}}$	$K_{\perp}^{Cu^{2+}}$	β^2 (Cu ²⁺)	γ^2 (Cu ²⁺)
[Cu(FB)(OAc)].H ₂ O (9)		2.190	2.066	0		15416	0.6609	0.7700		
[Cu(FBH)(H ₂ O)(OAc)].H ₂ O (10)		2.20	2.057	0		15627	0.6829	0.7185		
[Cu(FN)(OAc)].2H ₂ O (11)	20.0	2.246	2.05	0	0.8860	16188	0.7717	0.6829	0.8710	0.7708
[Cu(FIN)(OAc)(H ₂ O)].2H ₂ O (12)	20.0	2.05	2.245	0	0.7228	14973	0.3284	1.4814	0.4543	2.0495
[Cu(FMB) ₂ (H ₂ O) ₂].H ₂ O (13)		2.197	2.055	0		14990	0.6638	0.6907		
[Cu(FMBH) ₂ (H ₂ O) ₂].2H ₂ O (14)		2.15	2.070	0		15224	0.5826	0.7889		
[Cu(FMN)(OAc)].H ₂ O (15)	20.0	2.245	2.050	0	0.8848	15451	0.7524	0.6671	0.8504	0.754
[Cu(FMIN)(OAc)(H ₂ O)].H ₂ O (16)	19.3	2.036	2.080	2.245	0.8155	16370	0.2886	0.8764	0.3539	1.0747

3.3.6 Thermo gravimetric analysis

To determine the thermal stability and chemical composition of Ni (II), Cu (II) and Zn (II) complexes, thermo gravimetric analysis has been performed in a temperature range of 0-700°C in nitrogen atmosphere at a heating rate of 10°C/min. Thermal analysis was used mainly for the confirmation of the water molecule or solvent associated with being in the sphere of coordination or in the outer sphere of the complex [73] and the information about its properties, the nature of the intermediate products and final thermal decomposition. From the TGA curves, the weight loss was calculated for the different steps and compared with the theoretically calculated weight for the suggested formulas based on the results obtained from the elemental analyzes as well as on the measurements of molar conductance and AAS. TGA indicated the formation of metal oxide as the final product from which the metal content could be calculated and compared with that obtained from the analytical determination.

All the complexes show three main decomposition steps in the TG-DTG curves and the decomposition is not complete in the given temperature range (0-700°C). For the complexes, the removal of water can proceed in one or two steps. Thermograms of metal complexes indicate decompositions around 50-120°C is due to hydrated water and around 200°C is due to coordinated water molecules. The thermal stability data are listed in Table 3.15-3.17. The TGA curves of complexes are shown in Figures 3.64-3.87.

[Ni(FB)(OAc)(H₂O)].2H₂O, decomposed in two steps. First step involved weight loss corresponding to the removal of two lattice water molecules (temperature range 80-105°C). Second step involved weight loss corresponding to removal of coordinated water molecule and acetate moiety of T_{DTG} 350°C (temperature range 297-354°C). In the case of nickel complexes mass loss in the temperature range 30-120°C corresponds to the presence of lattice water molecules. The second mass loss in all complexes except [Ni(FN)(OAc)].H₂O and [Ni(FMN)(OAc)].2H₂O the temperature range 170-250°C corresponds to the loss of coordinated water molecules and third steps are found in the temperature above 250°C corresponding to the loss of organic molecules. But in the case of complexes [Ni(FN)(OAc)].H₂O and [Ni(FMN)(OAc)].2H₂O there is no weight loss around 200°C that means no coordinated water molecules present in it . After this temperature a gradual weight loss occurs due to the thermal degradation of organic moiety present.

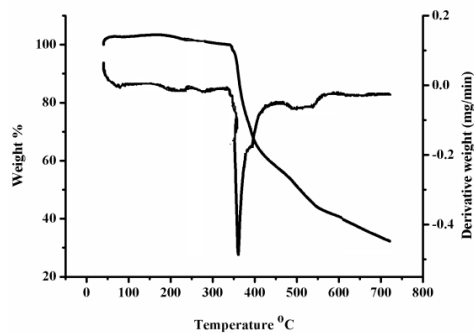


Figure 3.64 TG-DTG curves of $[\text{Ni}(\text{FB})(\text{OAc})(\text{H}_2\text{O})] \cdot 2\text{H}_2\text{O}$

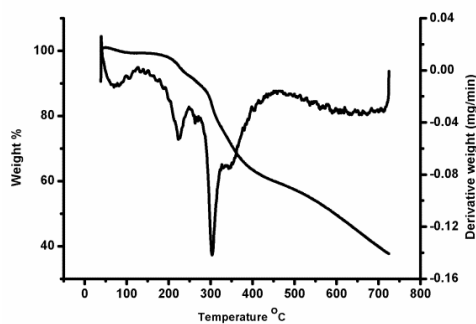


Figure 3.65 TG-DTG curves of $[\text{Ni}(\text{FBH})(\text{H}_2\text{O})(\text{OAc})] \cdot 2\text{H}_2\text{O}$

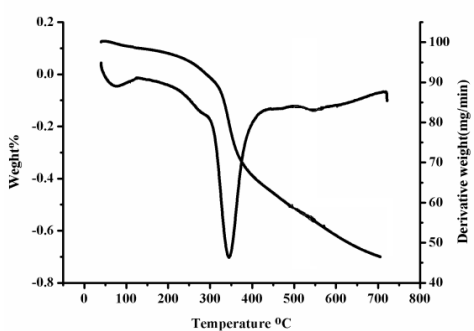


Figure 3.66 TG-DTG curves of $[\text{Ni}(\text{FN})(\text{OAc})] \cdot \text{H}_2\text{O}$

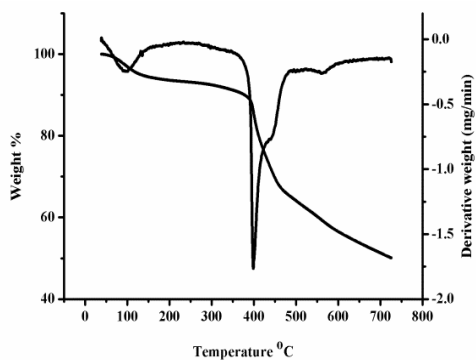


Figure 3.67 TG-DTG curves of $[\text{Ni}(\text{FIN})(\text{OAc})(\text{H}_2\text{O})] \cdot \text{H}_2\text{O}$

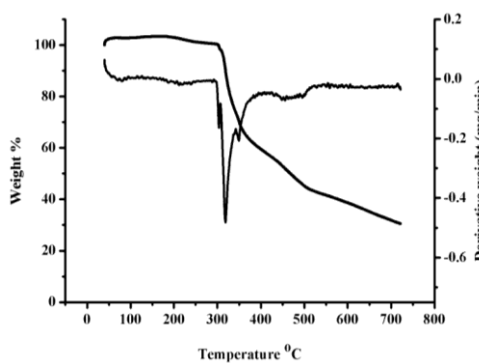


Figure 3.68 TG-DTG curves of $[\text{Ni}(\text{FMB})_2(\text{H}_2\text{O})_2] \cdot \text{H}_2\text{O}$

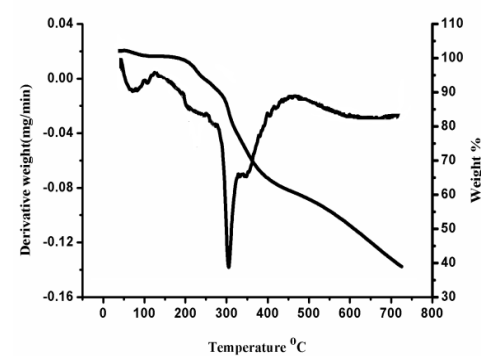


Figure 3.69 TG-DTG curves of $[\text{Ni}(\text{FBH})_2(\text{H}_2\text{O})_2] \cdot 2\text{H}_2\text{O}$

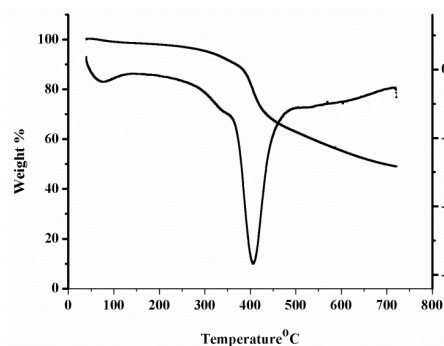


Figure 3.70 TG-DTG curves of $[\text{Ni}(\text{FMN})(\text{OAc})].2\text{H}_2\text{O}$

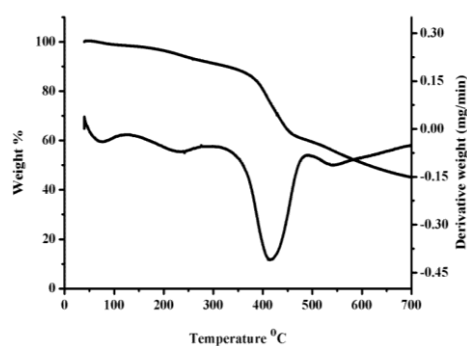


Figure 3.71 TG-DTG curves of $[\text{Ni}(\text{FMIN})(\text{OAc})(\text{H}_2\text{O})].1.5\text{H}_2\text{O}$

Table 3.15 Data of the thermo gravimetric analysis for Ni (II) complexes

Complexes	Temperature Range (°C)	DTG_{max} (°C)	Mass loss (%) Obsd. (Cald.)	Decomposition product
$[\text{Ni}(\text{FB})(\text{OAc})(\text{H}_2\text{O})].2\text{H}_2\text{O}$ (1)	80-105 297-354	97 350	7.62 (7.77) 17.47 (18.03)	Loss of $2\text{H}_2\text{O}$ (hyd) Loss of H_2O (coordinated) & acetate
$[\text{Ni}(\text{FBH})(\text{H}_2\text{O})(\text{OAc})].2\text{H}_2\text{O}$ (2)	50-130 173-248 277-368	98 220 300	7.16 (7.51) 4.33 (4.06) 22.14 (22.05)	Loss of $2\text{H}_2\text{O}$ (hyd) Loss of H_2O (coordinated) $\text{C}_6\text{H}_6\text{O}$
$[\text{Ni}(\text{FN})(\text{OAc})].\text{H}_2\text{O}$ (3)	30-150 270-460	95 345	4.50 (4.20) 14.00 (14.39)	Loss of $2\text{H}_2\text{O}$ (hyd) Loss of acetate
$[\text{Ni}(\text{FIN})(\text{OAc})(\text{H}_2\text{O})].\text{H}_2\text{O}$ (4)	50-150 360-500	96 419	4.60 (4.03) 18.40 (17.98)	Loss of H_2O (hyd) Loss of H_2O (coordinated) & acetate
$[\text{Ni}(\text{FMB})_2(\text{H}_2\text{O})_2].\text{H}_2\text{O}$ (5)	30-110 175-218 280-350	98 210 316	3.00 (2.48) 4.46 (5.10) 19.31 (20.00)	Loss of H_2O (hyd) Loss of $2\text{H}_2\text{O}$ (coordinated) $\text{C}_8\text{H}_{10}\text{N}_2\text{O}$
$[\text{Ni}(\text{FBH})_2(\text{H}_2\text{O})_2].2\text{H}_2\text{O}$ (6)	80-120 150-250 250-350	98 220 305	4.60 (4.65) 4.00 (4.80) 23.67 (24.83)	Loss of $2\text{H}_2\text{O}$ (hyd) Loss of $2\text{H}_2\text{O}$ (coordinated) $\text{C}_{11}\text{H}_{10}\text{O}_2$
$[\text{Ni}(\text{FMN})(\text{OAc})].2\text{H}_2\text{O}$ (7)	75-110 350-500	100 410	8.00 (7.82) 14.50 (14.15)	Loss of $2\text{H}_2\text{O}$ (hyd) Loss of acetate
$[\text{Ni}(\text{FMIN})(\text{OAc})(\text{H}_2\text{O})].1.5\text{H}_2\text{O}$ (8)	50-120 180-300 350-480	100 220 410	5.70 (5.75) 3.50 (4.07) 13.10 (13.91)	Loss of $1.5\text{H}_2\text{O}$ (hyd) Loss of H_2O (coordinated) Loss of acetate

The first step of decomposition in TG curve was found to be in temperature range 30-120°C for Cu (II) complexes (Table 3.16 and

Figures. 3.72-3.79) hence the low temperature range corresponding to this transformation indicates the presence of loss of lattice water and these values are further supported by IR and elemental analysis data. Thermograms of all copper complexes except [Cu(FN)(OAc)].2H₂O and [Cu(FMN)(OAc)].H₂O indicate that decompositions around 200°C due to coordinated water molecules. Above this temperature a gradual weight loss occurs due to decomposition of organic moiety present in it.

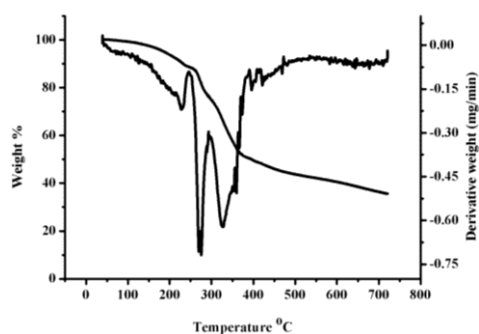


Figure 3.72 TG-DTG curves of [Cu(FB)(OAc)].H₂O

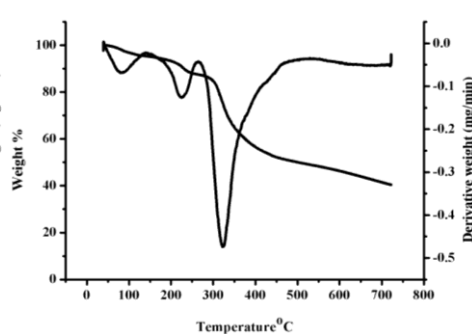


Figure 3.73 TG-DTG curves of [Cu(FBH)(H₂O)(OAc)].H₂O

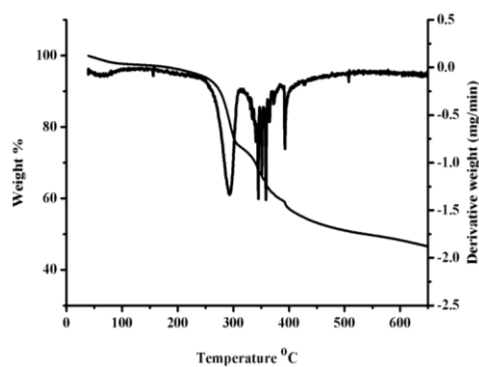


Figure 3.74 TG-DTG curves of [Cu(FN)(OAc)].2H₂O

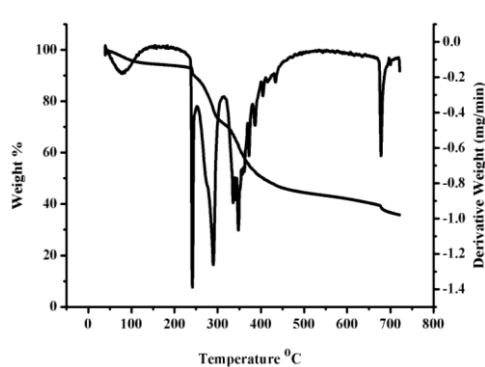


Figure 3.75 TG-DTG curves of [Cu(FIN)(OAc)(H₂O)].2H₂O

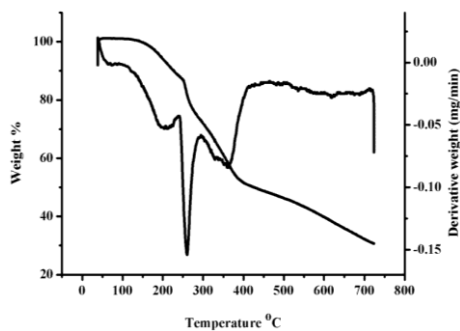


Figure 3.76 TG-DTG curves of $[\text{Cu}(\text{FMB})_2(\text{H}_2\text{O})_2] \cdot \text{H}_2\text{O}$

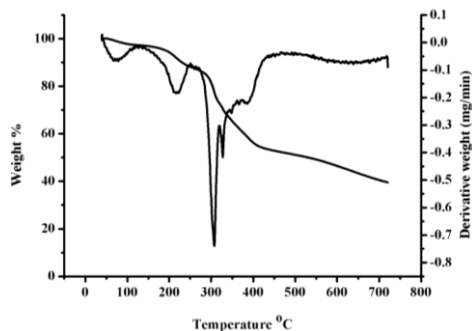


Figure 3.77 TG-DTG curves of $[\text{Cu}(\text{FMBH})_2(\text{H}_2\text{O})_2] \cdot 2\text{H}_2\text{O}$

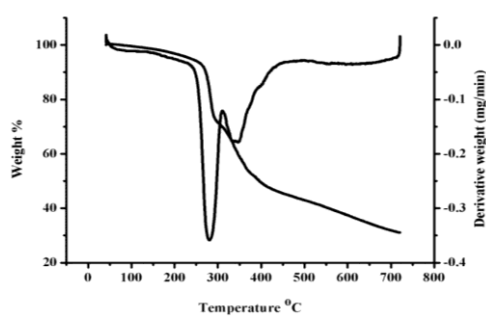


Figure 3.78 TG-DTG curves of $[\text{Cu}(\text{FMN})(\text{OAc})] \cdot \text{H}_2\text{O}$

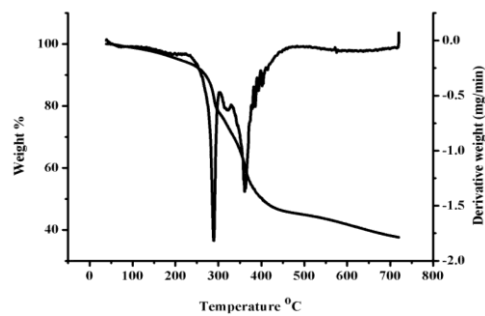


Figure 3.79 TG-DTG curves of $[\text{Cu}(\text{FMIN})(\text{OAc})(\text{H}_2\text{O})] \cdot \text{H}_2\text{O}$

Table 3.16 Data of the thermo gravimetric analysis for Cu (II) complexes

Complexes	Temperature range(°C)	DTG _{max} (°C)	Mass loss (%) Obsd. (Cald.)	Decomposition product
[Cu(FB)(OAc)].H ₂ O (9)	70-120 258-306 307-369	99 270 345	4.55 (4.16) 13.93 (14.25) 22.35(22.07)	Loss of H ₂ O Acetate C ₆ H ₆
[Cu(FBH)(H ₂ O)(OAc)].H ₂ O (10)	60-114 200-248 290-429	98 240 312	4.05 (3.86) 4.26 (4.01) 32.33 (33.08)	Loss of H ₂ O (hyd) Loss of H ₂ O (coordinated) C ₇ H ₉ NO ₂
[Cu(FN)(OAc)].2H ₂ O (11)	50-120 250-350	96 290	7.10(7.98) 15.00(14.22)	Loss of 2H ₂ O (hyd) Loss of acetate
[Cu(FIN)(OAc)(H ₂ O)].2H ₂ O (12)	30-120 230-260	98 247	7.40(7.74) 18.00(17.78)	Loss of H ₂ O (hyd) Loss of H ₂ O (coordinated) & acetate
[Cu(FMB) ₂ (H ₂ O) ₂].H ₂ O (13)	35-115 150-250 250-310	97 202 263	2.21 (2.47) 4.21 (5.06) 24.78 (25.80)	Loss of H ₂ O (hyd) Loss of H ₂ O (coordinated) C ₁₁ H ₁₀ O ₂
[Cu(FMBH) ₂ (H ₂ O) ₂].2H ₂ O (14)	50-120 150-250 250-350	97 210 305	4.50 (4.62) 4.62 (4.85) 45.83 (45.63)	Loss of H ₂ O (hyd) Loss of H ₂ O (coordinated) C ₁₈ H ₁₄ N ₂ O ₄
[Cu(FMN)(OAc)].H ₂ O (15)	50-120 250-350	98 298	4.40(4.02) 13.30 (13.75)	Loss of H ₂ O (hyd) Loss of acetate
[Cu(FMIN)(OAc)(H ₂ O)].H ₂ O (16)	70-110 250-350	99 300	3.90(3.87) 16.70(17.20)	Loss of 1.5 H ₂ O (hyd) Loss of H ₂ O (coordinated) & acetate

For complex [Zn(FB)(OAc)].2.5H₂O the initial step of degradation at 50-120°C with T_{DTG} at 98°C corresponds to 9.96% (Calc. 9.80%) mass loss may be due to the removal of lattice water. The second decomposition at the range of 450-477°C with T_{DTG} at 465°C corresponds to the weight loss of 14.44% (Calc. 14.89%) by the removal of C₂H₄O₂. In the case of zinc complexes [Zn(FBH)(OAc)], [Zn(FN)(OAc)].H₂O, [Zn(FMN)(OAc)].H₂O and [Zn(FMIN)(OAc)].0.5 H₂O mass loss in the

temperature range 30-150°C corresponds to the presence of lattice water molecules (Table 3.17). After this temperature a gradual weight loss occurs due to the thermal degradation of organic moiety in one or two steps. In complexes $[\text{Zn}(\text{FMB})_2] \cdot 2\text{H}_2\text{O}$ and $[\text{Zn}(\text{FMBH})(\text{OAc})] \cdot \text{H}_2\text{O}$ initial step of degradation at 80-120°C with T_{DTG} at 98°C and 100°C, correspond to 5.19% (Calc.5.05%) and 3.01% (Calc. 3.88%) respectively mass loss may be due to the removal of lattice water. Moreover, it was supported by elemental analysis and IR data. But no T_{DTG} peaks were found for coordinated water molecules. The second and third decomposition of $[\text{Zn}(\text{FMB})_2] \cdot 2\text{H}_2\text{O}$ are in the range of 300-450°C and 450-550°C corresponding to the removal of $\text{C}_{11}\text{H}_{10}\text{N}_2\text{O}_2$, C_6H_6 by 29.8% (Calc.28.10%), 15.22% (Calc.16.00%) respectively. For complex $[\text{Zn}(\text{FMBH})(\text{OAc})] \cdot \text{H}_2\text{O}$; 150-300°C and 450-550 °C corresponding to the removal of $\text{C}_{11}\text{H}_{10}\text{N}_2\text{O}_2$, CH_4 by 46.05% (Calc.45.33%), 6.56% (Calc.7.11%) respectively. The TGA curves of complexes are shown in Figures 3.80-3.87.

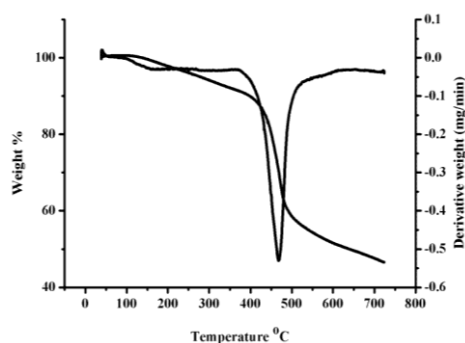


Figure 3.80 TG-DTG curves of $[\text{Zn}(\text{FB})(\text{OAc})] \cdot 2.5\text{H}_2\text{O}$

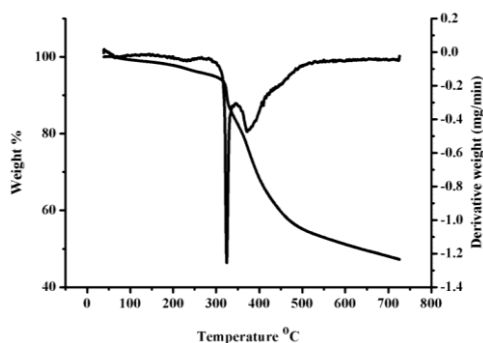


Figure 3.81 TG-DTG curves of $[\text{Zn}(\text{FBH})(\text{OAc})]$

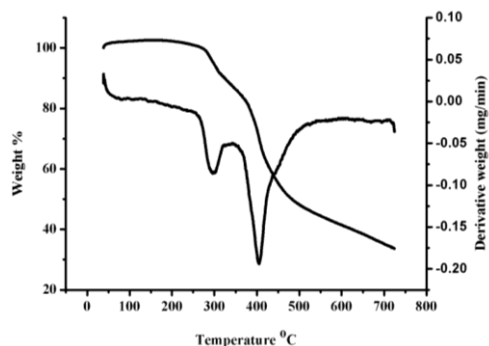


Figure 3.82 TG-DTG curves of $[Zn(FN)(OAc)].H_2O$

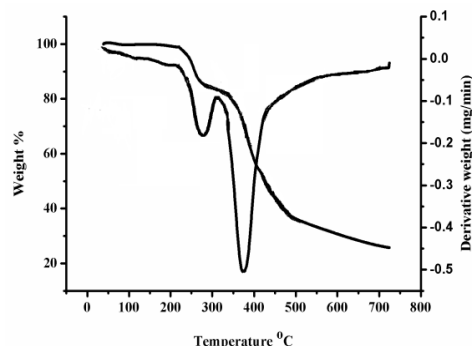


Figure 3.83 TG-DTG curves of $[Zn(FIN)(OAc)]$

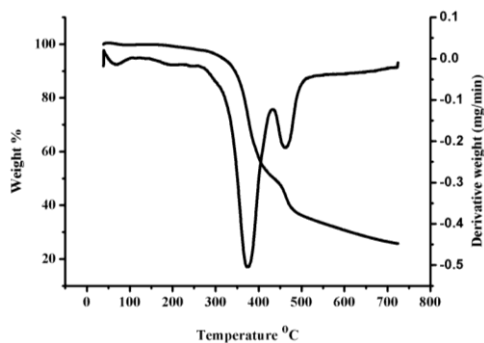


Figure 3.84 TG-DTG curves of $[Zn(FMB)_2].2H_2O$

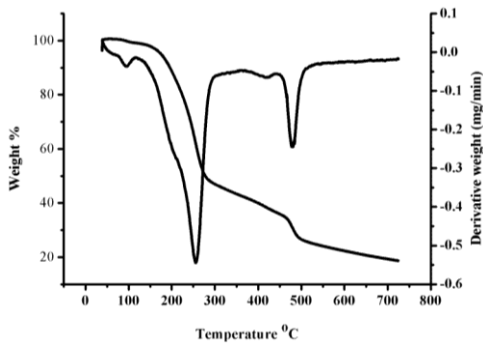


Figure 3.85 TG-DTG curves of $[Zn(FMBH)(OAc)].H_2O$

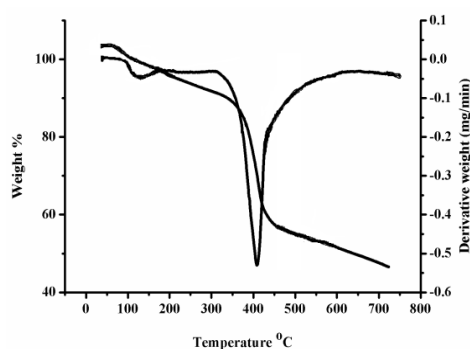


Figure 3.86 TG-DTG curves of $[Zn(FMN)(OAc)].H_2O$

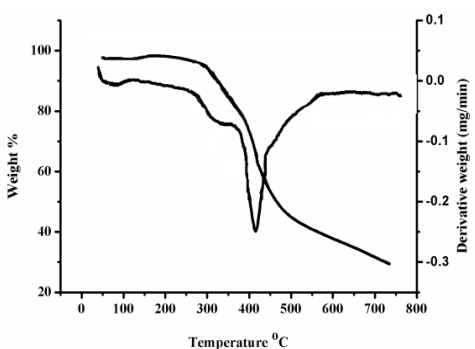


Figure 3.87 TG-DTG curves of $[Zn(FMIN)(OAc)].0.5 H_2O$

Table 3.17 Data of the thermo gravimetric analysis for Zn (II) complexes

Complexes	Temperature range(°C)	DTG _{max} (°C)	Mass loss (%) Obsd. (Cald.)	Decomposition product
[Zn(FB)(OAc)].2.5H ₂ O (17)	50-120 450-477	98 465	9.96 (9.80) 14.44(14.89)	Loss of 2.5 H ₂ O (hyd) C ₂ H ₄ O ₂
[Zn(FBH)(OAc)] (18)	150-280 360-459	335 397	43.66 (43.01) 6.58 (6.97)	C ₁₀ H ₈ N ₂ O ₂ CH ₄
[Zn(FN)(OAc)].H ₂ O (19)	30-120 250-350	97 288	3.70(4.14) 13.50(14.15)	Loss of H ₂ O (hyd) Loss of acetate
[Zn(FIN)(OAc)] (20)	250-300	264	14.80(14.15)	Loss of acetate
[Zn(FMB) ₂].2H ₂ O (21)	80-120 300-450 450-550	98 376 482	5.19 (5.05) 29.8 (28.10) 15.22 (16.00)	Loss of 2 H ₂ O (hyd) C ₁₁ H ₁₀ N ₂ O ₂ C ₆ H ₆
[Zn(FMBH)(OAc)].H ₂ O (22)	80-120 150-300 450-550	100 256 482	3.01 (3.88) 46.05(45.33) 6.56 (7.11)	Loss of H ₂ O (hyd) C ₁₁ H ₁₀ O ₂ CH ₄
[Zn(FMN)(OAc)].H ₂ O (23)	25-150 300-550	100 400	4.60(4.01) 31.00(30.50)	Loss of 2 H ₂ O (hyd) C ₆ H ₇ N ₃ O
[Zn(FMIN)(OAc)].0.5 H ₂ O (24)	80-120 250-350	100 300	2.00(2.01) 14.00(13.69)	Loss of 0.5 H ₂ O (hyd) Loss of acetate

3.3.7 ¹H NMR spectra

Proton Nuclear Magnetic Resonance (¹H NMR) spectroscopy is a powerful tool used for the determination of the structure of compounds. The ¹H NMR spectra of Zn (II) (because of their diamagnetic nature) have been recorded with DMSO as solvent. ¹H NMR spectral data (δ ppm) of the complex relative to TMS (0 ppm) in DMSO-d₆, as shown in Figures 3.88-3.95 give further support of the suggested structure of the complex.

The comparison of the NMR spectra of the complexes with the spectra of ligands (Chapter 2, Section 2.3.1.4.1 & 2.3.1.4.2) gave valuable information regarding the coordination mode of ligands during complexation. The ¹H NMR spectrum obtained for zinc complexes was

not good due to the poor solubility of the compound. In the spectra of the free hydrazones there are sharp singlets in the range of δ 11-12 ppm showing the existence of iminol form in solution. They also gave singlets in the range of δ 10-11 ppm with an area integral of one which is due to phenolic OH protons. Syntheses and characterization of Zn (II) complexes derived from ONO donor chromone hydrazones the intensity of these signals significantly decreases, which suggests that these protons are easily exchangeable and confirm the assignment. Peaks for aromatic protons were found in the region δ 6.8-8 ppm. Peaks in the region δ 11-12 ppm corresponds to iminol protons found in the spectra of free hydrazones were absent in the spectra of complexes indicating the coordination of iminol oxygen to zinc. In the spectrum of complexes, a singlet with an integral area of three is found at δ 2.0-1.9 ppm and it is assigned to the methyl group present in acetate which is coordinated to zinc [74]. Also a singlet with area integral one is appeared at δ 8.27-8.7 ppm may indicate the presence of -CH- proton. For [Zn(FMB)₂].2H₂O, [Zn(FMBH)(OAc)].H₂O, [Zn(FMN)(OAc)].H₂O and [Zn(FMIN)(OAc)].0.5 H₂O complexes a three hydrogen singlet around δ 2.45 ppm region is due to -CH₃ proton. All other peaks observed in the spectra of free hydrazones are slightly shifted.

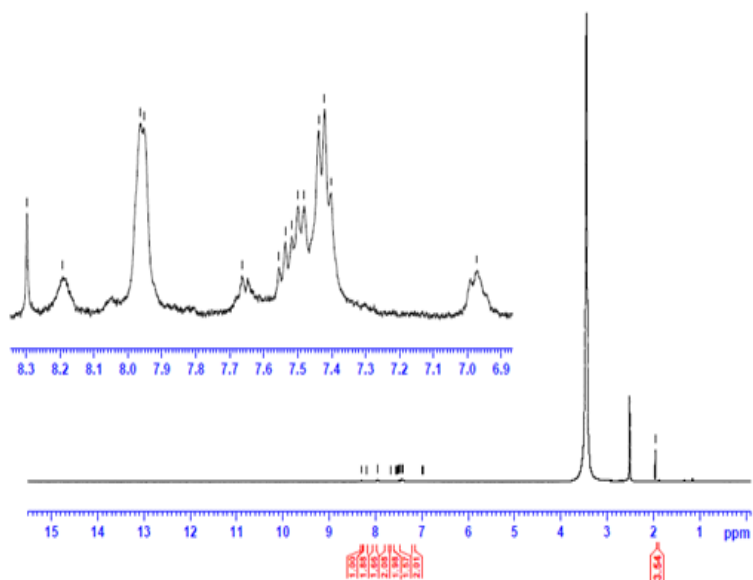


Figure 3.88 ¹H NMR of [Zn(FB)(OAc)].2.5 H₂O

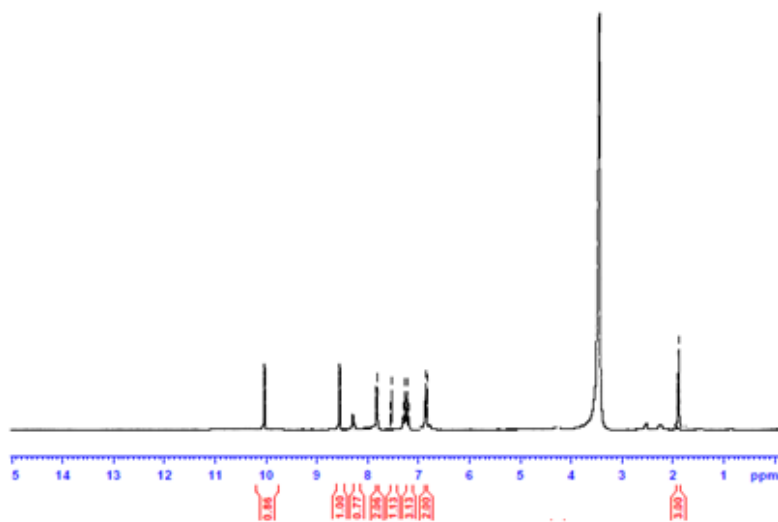


Figure 3.89 ¹H NMR of [Zn(FBH)(OAc)]

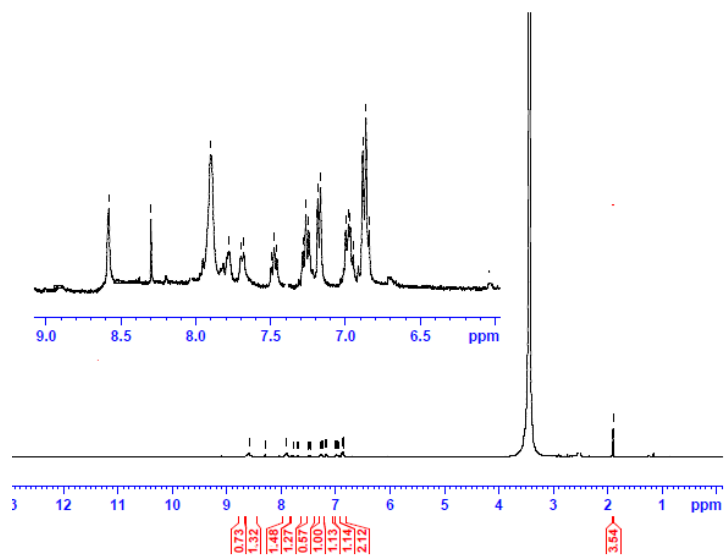


Figure 3.90 ^1H NMR of $[\text{Zn}(\text{FN})(\text{OAc})]\cdot\text{H}_2\text{O}$

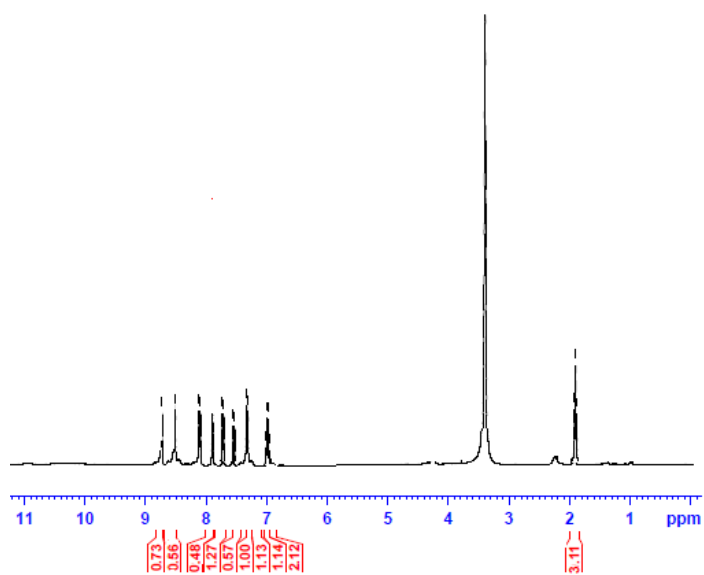


Figure 3.91 ^1H NMR of $[\text{Zn}(\text{FIN})(\text{OAc})]$

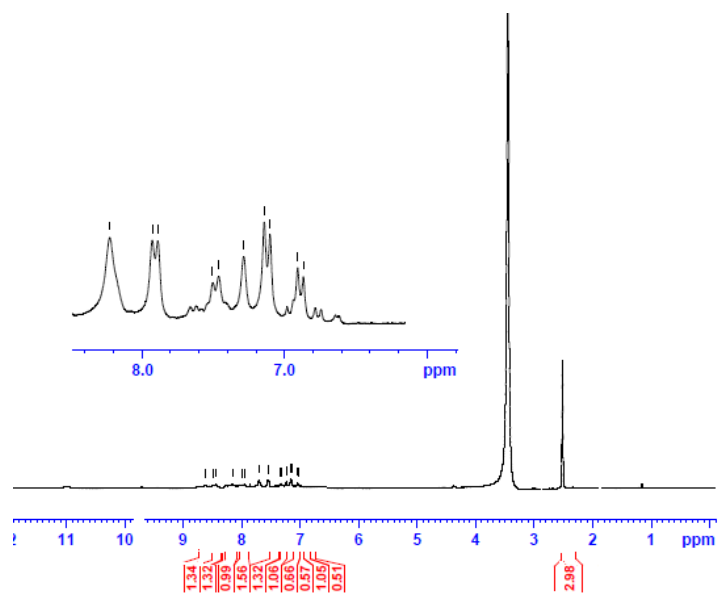


Figure 3.92 ¹H NMR of [Zn(FMB)₂].2H₂O

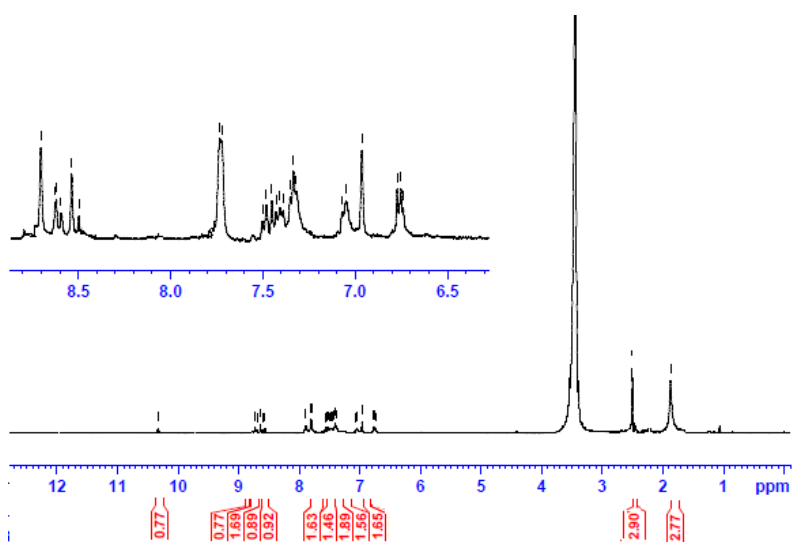


Figure 3.93 ¹H NMR of [Zn(FMBH)(OAc)].H₂O

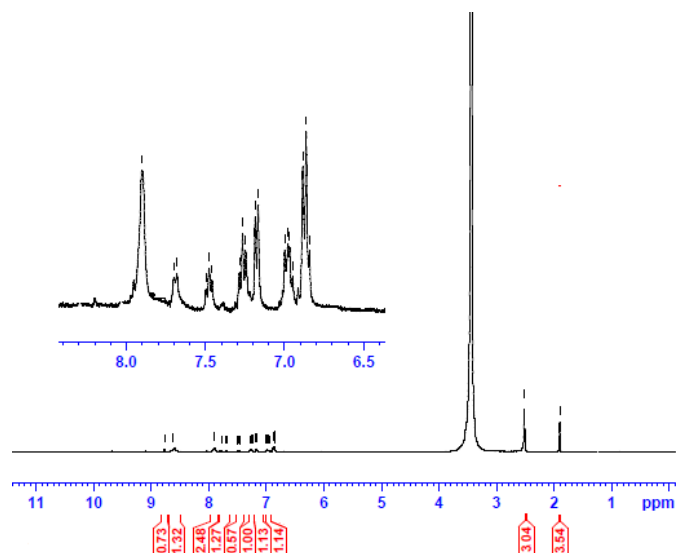


Figure 3.94 ^1H NMR of $[\text{Zn}(\text{FMN})(\text{OAc})]\cdot\text{H}_2\text{O}$

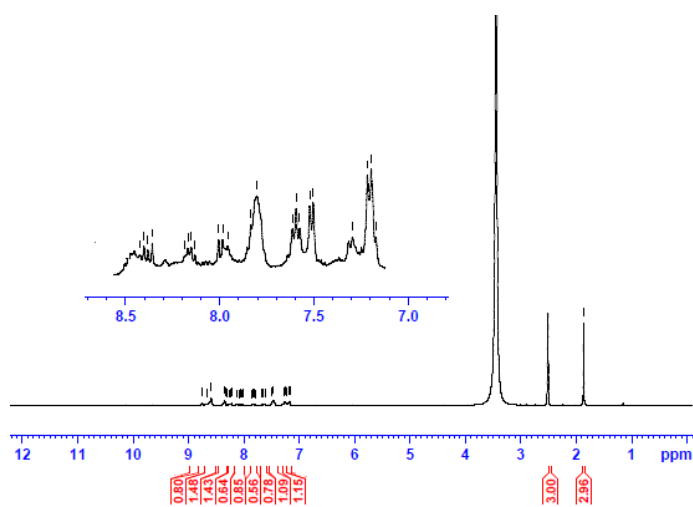


Figure 3.95 ^1H NMR of $[\text{Zn}(\text{FMIN})(\text{OAc})]\cdot 0.5 \text{H}_2\text{O}$

3.3.8 Geometry of the complexes

Based on the above physico-chemical data, the proposed structures for synthesised Ni (II), Cu (II) and Zn (II) complexes of 3-formyl chromone hydrazones are shown in Figures.3.96-3.98.

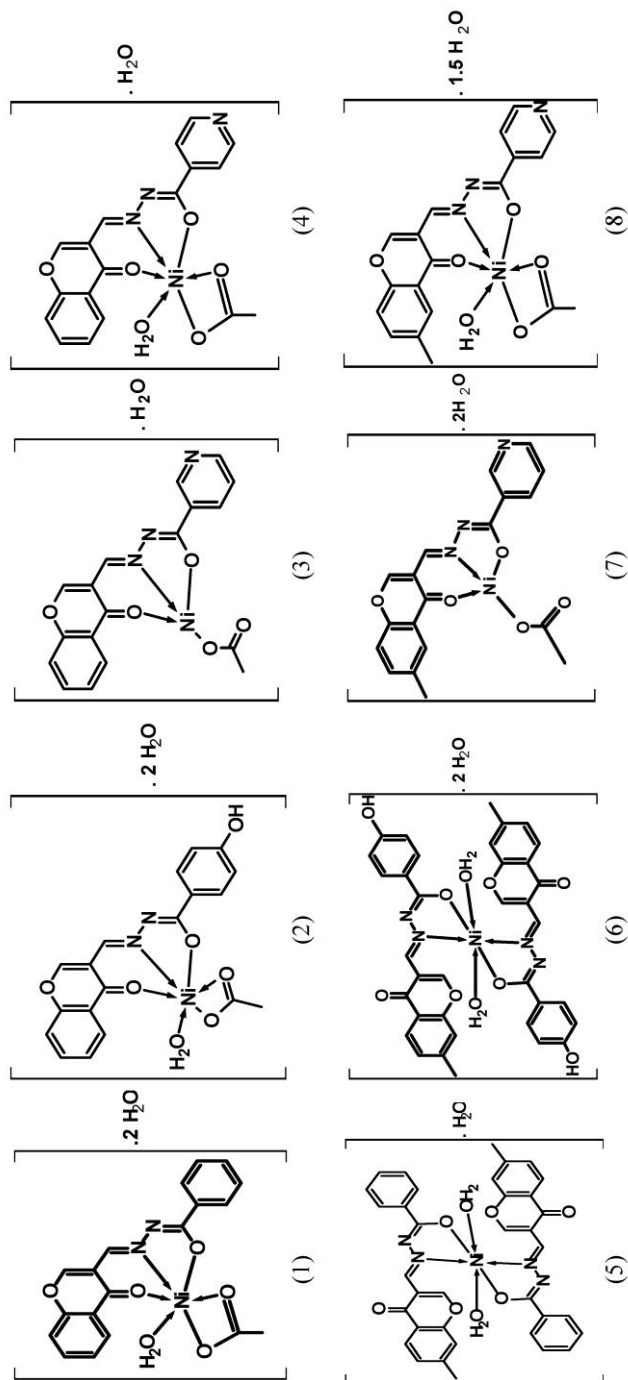


Figure 3.96 proposed structures for synthesized Ni (II) complexes of 3-formyl chromone hydrazones

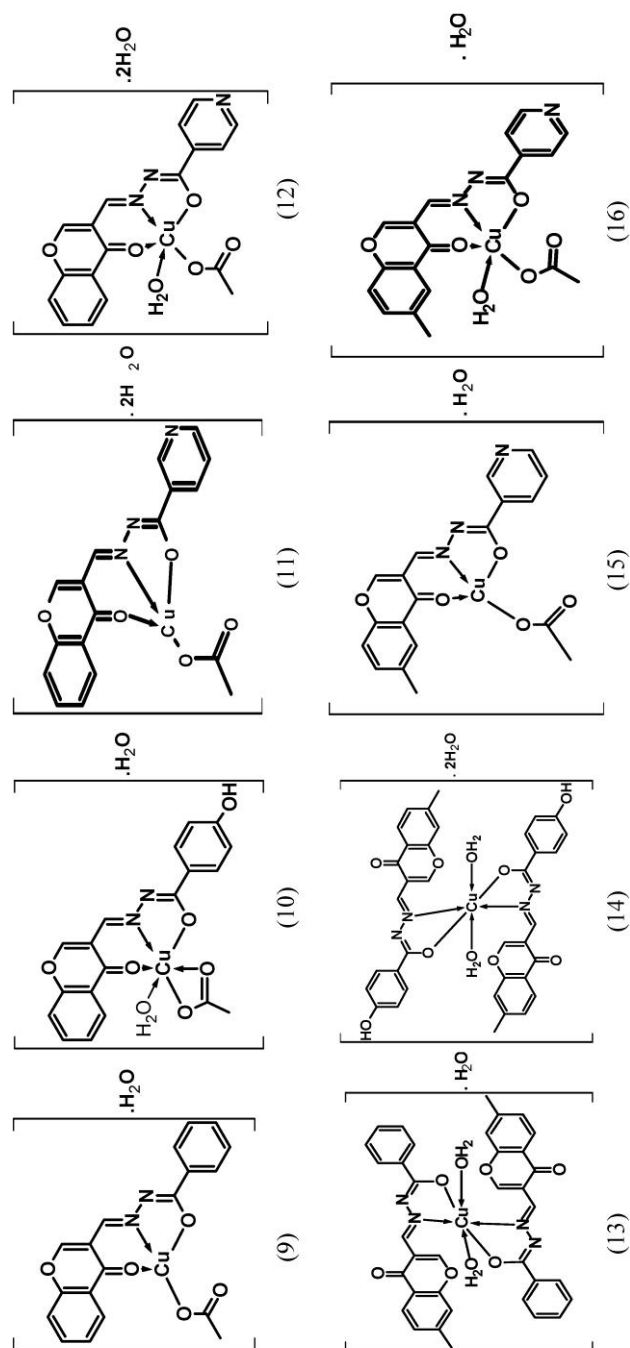
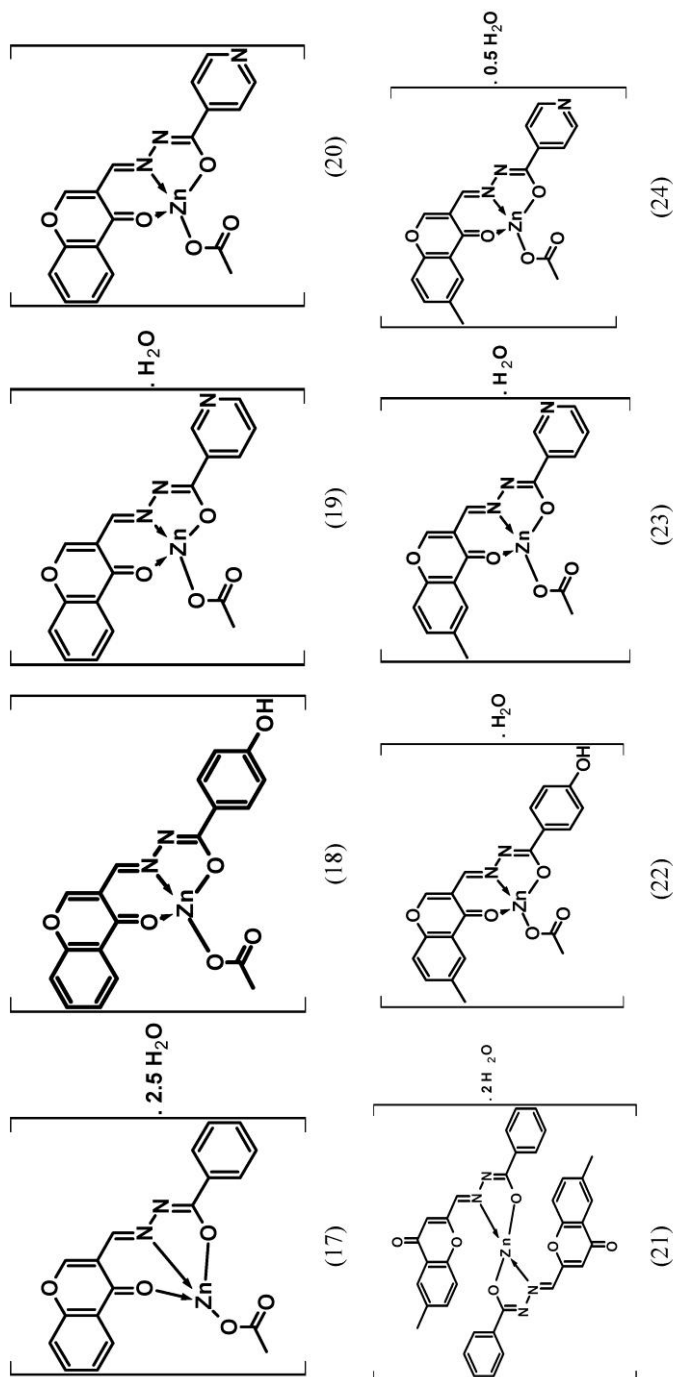


Figure 3.97 proposed structures for synthesized Cu (II) complexes of 3-formyl chromone hydrazones



Figures 3.98 proposed structures for synthesized Zn (II) complexes of 3-formyl chromone hydrazones

3.4 Conclusion

This chapter describes the synthesis and characterization of Ni (II), Cu (II) and Zn (II) complexes of 3-formyl chromone hydrazones. The analytical data suggest that all Ni (II), Cu (II) and Zn (II) complexes are mononuclear. A low molar conductance value indicates that all Ni (II), Cu (II) and Zn (II) complexes are non electrolyte in nature. Thermo gravimetric analysis revealed that all the complexes are found to be thermally stable. Magnetic moment values of nickel complexes $[\text{Ni}(\text{FB})(\text{OAc})(\text{H}_2\text{O})].2\text{H}_2\text{O}$, $[\text{Ni}(\text{FBH})(\text{H}_2\text{O})(\text{OAc})].2\text{H}_2\text{O}$, $[\text{Ni}(\text{FIN})(\text{OAc})(\text{H}_2\text{O})].\text{H}_2\text{O}$, $[\text{Ni}(\text{FMB})_2(\text{H}_2\text{O})_2].\text{H}_2\text{O}$, $[\text{Ni}(\text{FBH})_2(\text{H}_2\text{O})_2].2\text{H}_2\text{O}$ and $[\text{Ni}(\text{FMIN})(\text{OAc})(\text{H}_2\text{O})].1.5\text{H}_2\text{O}$ lies within the region 2.32-3.12 B.M expected for octahedral stereochemistry of the complexes. Ni (II) complexes $[\text{Ni}(\text{FN})(\text{OAc})].\text{H}_2\text{O}$ and $[\text{Ni}(\text{FMN})(\text{OAc})].2\text{H}_2\text{O}$ were 3.69 and 3.85 B.M which is consistent with the tetrahedral complexes. This was also confirmed by electronic and IR spectral studies. Magnetic moment values of all copper complexes gives an indication of distorted octahedral, square pyramidal or square planar structure. The physicochemical and spectral data reveals tetrahedral structure for all Zn (II) complexes. The proposed structures of all Ni (II), Cu (II) and Zn (II) complexes are given in above figures.

References

- [1] C. Selvam, S. M. Jachak, R. Thilagavathi, A. K. Chakraborti, *Bioorganic Med. Chem. Lett.*, 15 (2005) 1793.
- [2] B. Kupcewicz, G. B. Czerniak, M. Małecka, P. Paneth, U. Krajewska, M. Rozalski, *Bioorganic Med. Chem. Lett.*, 23 (2013) 4102.

- [3] E. Venkateswararao, V. K. Sharma, M. Manickam, J. Yun, S. Jung, *Bioorganic Med. Chem. Lett.*, 24 (2014) 5256.
- [4] M. L. Neuhouser, *Nutr. Cancer*, 50 (2004) 1.
- [5] J. P. Cornard, J. C. Merlin, *J. Inorg. Biochem.*, 92 (2002) 19
- [6] B. G. Turner, M. F. Summers, *J. Mol. Biol.*, 285 (1999) 1.
- [7] M. Shebl, *J. Mol. Struct.*, 1128 (2017) 79.
- [8] Y. Sun, G. Liu, H. Huang, P. Yu, *Phytochemistry*, 75 (2012) 169.
- [9] M. S. Masoud, A. A. Soayed, A. F. El-Husseiny, *Spectrochim. Acta A*, 99 (2012) 365.
- [10] K. M. Khan, N. Ambreen, U. R. Mughal, S. Jalil, S. Perveen, M. I. Choudhary, *Eur. J. Med. Chem.*, 45 (2010) 4058.
- [11] S. Y. Ebrahimipour, I. Sheikhshoae, A. Crochet, M. Khaleghi, K. M. Fromm, *J. Mol. Struct.*, 1072 (2014) 267.
- [12] T. Sedaghat, M. Yousefi, G. Bruno, H. A. Rudbari, H. Motamedi, V. Nobakht, *Polyhedron*, 79 (2014) 88.
- [13] I. Babahan, E. P. Coban, H. Biyik, *Int. J. Sci. Technol.*, 7 (2013) 26.
- [14] A. C. Pinheiro, C. R. Kaiser, T. C. Nogueira, S. A. Carvalho, E. F. da Silva, A. L. Candea, M. C. Lourenco, M. V. de Souza, *Med Chem.*, 7 (2011) 611.
- [15] B. C. Raju, R. N. Rao, P. Suman, P. Yogeeswari, D. Sriram, T. B. Shaik, S. V. Kalivendi, *Bioorganic Med. Chem. Lett.*, 21 (2011) 2855.
- [16] N. Kavitha, P. V. Ananthalakshmi, *J. Saudi Chem. Soc.*, 7 (2017) S457.
- [17] S. M. Saadeh, *Arab. J. Chem.*, 6 (2013) 191.
- [18] S. Kumar, A. Hansda, A. Chandra, A. Kumar, M. Kumar, M. Sithambaresan, V. Kumar, R. P. John, *Polyhedron*, 134 (2017) 11.
- [19] M. Sahin, N. Kocak, D. Erdenay, U. Arslan, *Spectrochim. Acta A*, 103 (2013) 400.

- [20] M. Loffler, J. Gregolinski, M. Korabik, T. Lis, J. Lisowski, Dalton Trans., 45 (2016) 15586.
- [21] J. Heinrich, J. Stubbe, N. Kulak, Inorganica Chim. Acta., doi.org/10.1016/j.ica.2017.11.015
- [22] K. Hu, G. Zhou, Z. Zhang, F. Li, J. Li, F. Liang, RSC Adv., 6 (2016) 36077.
- [23] M. V. Angelusiu, S. F. Barbuceanu, C. Draghici, G. L. Almajan, Eur. J. Med. Chem., 45 (2010) 2055.
- [24] G. S. Firmino, M. V. de Souza, C Pessoa, M. C. Lourenco, J. A. Resende, J. A. Lessa, Biometals., 29 (2016) 953.
- [25] S. D. Joshi, D. Kumar, S. R. Dixit, N. Tigadi, U. A. More, C. Lherbet, T. M. Aminabhavi, K. S. Yang, Eur. J. Med. Chem., 4 (2016) 21.
- [26] C. Ustundag, D Satana, G Ozhan, G. Capan, J Enzyme Inhib Med Chem., 31 (2016) 369.
- [27] Q. P. Qin, Y. C. Liu, H. L. Wang, J. L. Qin, F. J. Cheng, S. F. Tang, H. Liang, Metallomics, 7 (2015) 1124.
- [28] Y. Gou, J. Li, B. Fan, B. Xu, M. Zhou, F. Yang, Eur. J. Med. Chem., 7 (2017) 207.
- [29] Y. Li, K. Li, L. Wang, Y. He, J. He, H. Hou, B. Z. Tang, J. Mater. Chem., 5 (2017), 7553.
- [30] (a) A. A. R. Despaigne, J. G. D. Silva, A. C. M. do Carmo, O. E. Piro, E. E. Castellano, H. Beraldo, Inorg. Chim. Acta, 362 (2009) 2117.
(b) E. B. Seena, M. R. P. Kurup, Spectrochim. Acta A, 69 (2008) 726.
- [31] Y. Li, Z. Y. Yang, M. F. Wang, J. Fluoresc., 20 (2010) 891.
- [32] Y. Li, Z. Y. Yang, T. R. Li, Chem Pharm Bull., 56 (2008) 1528.
- [33] M. Ashfaq, T. Najam, S. S. Shah, M. M. Ahmad, S. Shaheen, R. Tabassum, G Rivera, Curr. Med. Chem., 26 (2014) 3081.
- [34] J. Benjamin, L. D. Ang, E. P. Wright, J. R. A. Wright, Dalton Trans., 44 (2015) 3505.

- [35] N. P. Farrell *Chem. Soc. Rev.*, 44 (2015) 8773.
- [36] L. R. Azuara, B. Gomez, *Curr. Med. Chem.*, 17 (2010) 3606.
- [37] Y. L. Zheng, Y. Y. Zhen, C. L. Zi, C. H. Zeng, C. Liu, *Inorg. Chem. Commun.*, 13 (2010) 1213.
- [38] S. Sobha, R. Mahalakshmi, N. Raman, *Spectrochim. Acta A*, 15 (2012) 175.
- [39] (a) M. A. M. Elzaher, A. L. Ammar, A. M. Hanan, A. M. Samia, A. M. Mamdouhand, *J. Basic. Appl. Sci.*, 5 (2016) 85. (b) K. Zahid, T. M. Zahida, A. K. T. Muhammad, M. K. Khalid, L. Mehreen, *J. Basic Appl. Sci. Res.*, 5 (2013) 227.
- [40] N. Joksimovic, D. Baskic, S. Popovic, M. Zaric, M. Kosanic, B. Rankovic, T. Stanojkovic, S. B. Novakovic, G. Davidovic, Z. Bugarcica, N. Jankovic, *Dalton Trans.*, 45 (2016) 15067.
- [41] T. S. Lobana, S. Indoria, H. Kaur, D. S. Arora, A. K. Jassala, J. P. Jasinskic, *RSC Adv.*, 5 (2015) 14916.
- [42] I. Shikha, T. S. Lobana, H. Sood, D. S. Arora, G. Hundal, J. P. Jasinski, *New J. Chem.*, 40 (2016) 3642.
- [43] (a) W. J. Geary, *Coord. Chem. Rev.*, 7 (1971) 81. (b) E. Akila, M. Usharani, R. Rajavel, *Int. J. Inorg. Bioinorg. Chem.*, 2 (2011) 15.
- [44] B. I. Omar, A. M. Mahmoud, S. R. Moamen, *Can. Chem. Trans.*, 2 (2014) 108.
- [45] T. D. Priya, R. K. S. Hemakumar, *J. Chem.*, 3 (2010) 266.
- [46] S. T. Syed, K. Geetha, *Indian J. Adv. Chem. Sci.*, 4 (2016) 40.
- [47] S. N. Madhavan, A. Dasan, S. J. Raphael, *J. Saudi Chem. Soc.*, 16 (2012) 83.
- [48] R. J. Sachin, I. H. Seema, *Orient. J. Chem.*, 3 (2014) 2231.
- [49] (a) T. Ghosh, S. Bhattacharya, A. Das, G. Mukherjee, M. G. B. Drew, *Inorg. Chim. Acta*, 358 (2005) 989. (b) W. Luo, X. G. Meng, G. Z. Cheng, Z. P. Ji, *Inorg. Chim. Acta*, 362 (2009) 551.

- [50] T. Walenzyk, C. Carola, H. Buchholz, B. Konig, *Tetrahedron*, 61 (2005) 7366.
- [51] S. K. Sengupta, S. K. Sahni, R. N. Kapoor, *Polyhedron*, 2 (1983) 317.
- [52] A. Perez-Rebolledo, O. E. Piro, E. E. Castellano, L. R. Teixeira, A. A. Batista, H. Beraldo, *J. Mol. Struct.*, 794 (2006) 18.
- [53] S. A. Khan, M. Yusuf, *Eur. J. Med. Chem.*, 44 (2009) 2270.
- [54] M. Shebl, S. M. E. Khalil, A. Taha, M. A. N. Mahdi, *J. Am. Sci.*, 8 (2012) 183.
- [55] M. Shebl, *J. Coord. Chem.*, 62 (2009) 3217.
- [56] G. S. Groenewold, W. A. de Jong, J. Oomens, M. J. Van Stipdonk, *J. Am. Soc. Mass Spectrom.*, 21 (2010) 719.
- [57] B. Smita, G. Gajendra, D. Babulal, M. R. Kollipara, *J. Organomet. Chem.*, 695 (2010) 2098.
- [58] (a) A. B. Hoda, A. M. A. Alaghaz, S. A. Mutlak, *Int. J. Electrochem. Sci.*, 8 (2013) 9399. (b) M. D. Malik, *J. Pharma. Med. Res.*, 2 (2016) 36.
- [59] A. B. P. Lever, *Inorganic Electronic Spectroscopy*, Elsevier, Amsterdam, 1968.
- [60] N. Chitrapriya, V. Mahalingam, M. Zeller, K. Natarajan, *Inorg. Chim. Acta.*, 363 (2010) 3685.
- [61] M. Calinescu, E. Ion, A. M. Stadler, *Rev. Roum. Chim.*, 53 (2008) 903.
- [62] (a) N. H. Al- Shaalan, *Molecules*, 16 (2011) 8629. (b) B. Subhra, S. Soma, M. Samiran, C. Marschner, W. S. Sheldrick, *Struct. Chem.*, 19 (2008) 115.
- [63] M. K. Abdulla, M. M. Hadi, *Int. j. Electrochem. Sci.*, 7 (2012) 10074.
- [64] M. Y. Ali, *American J. Biosci.*, 2 (2014) 22.
- [65] A. P. Mishra, P. Gupta, *J. Chem. Pharma. Res.*, 3 (2011) 150.

- [66] M. M. Wang, H. Wang, G. Q. Gan, Y. Qu, H. Chen, Z. D. Lin, J. Macromol. Sci., Part A: Pure Appl. Chem., 49 (2012) 355.
- [67] M. M. A. Neaimi, M. M. A. Khuder, Spectrochim. Acta A, 105 (2013) 365.
- [68] I. M. Procter, B. J. Hathaway, P. Nicholls, J. Chem. Soc. A, 0 (1968) 1678.
- [69] J. K. Roji, M. Sithambaresan, A. A. Ambilil, N. Aiswarya, M. R. P. Kurup, Polyhedron, 113 (2016) 73.
- [70] B. J. Hathaway, G. Wilkinson, R. D. Gillard, J. A. Mc Cleverty (Eds.), Vol. 5, Pergamon, Oxford, 1987, p. 533.
- [71] T. D. Smith, J. Pilbrow, Coord. Chem. Rev., 13 (1974) 173.
- [72] D. Kivelson, R. Neiman, J. Chem. Phys., 35 (1961) 149.
- [73] P. K. Singh, D. N. Kumar, Spectrochim. Acta A, 64 (2006) 853.
- [74] B. Anupama, C. G. Kumari, Int. J. Res. Chem. Evt., 3 (2013) 172.

.....✪✪.....

Chapter 4

ANTIMICROBIAL ACTIVITY OF CHROMONE HYDRAZONES AND THEIR Ni (II), Cu (II) AND Zn (II) COMPLEXES

Contents	4.1 Introduction
	4.2 Materials and Methods
	4.3 Result and Discussion
	4.4 Conclusion

Conspectus: The emergence of resistant bacteria or fungus was found to decrease the efficiency of antimicrobial therapies with the existing antibiotics, in that way increasing require for more effective drugs for the treatment of infections. Numerous studies have confirmed an increase in antimicrobial activity subsequent the interaction of some compounds with metal ions. The current study used a methodology adapted for antimicrobial bioassays using 3-formyl chromone hydrazone and its metal (II) complexes, in compliance with the standards of the Laboratory and Clinical Standards Institute against Gram-positive, Gram-negative bacteria and fungus. The results obtained were considered suitable for determining MIC. The bacteria *Bacillus subtilis* showed high sensitivity to the tested compounds, being proficient to evaluate the antibacterial activity. The bioassays with the some Cu (II) complexes of chromone hydrazones exhibited a greater inhibitory activity than that of standard antimicrobial drug chloramphenicol. Metal (II) complexes showed higher inhibition than their individual ligands, thus, the addition indicated an enhancement in the antimicrobial activity after the coordination. Some metal complexes expose high antimicrobial performances, such as low minimum inhibitory concentration ($MIC \leq 250 \mu\text{g/mL}$), bactericidal effect these compounds as appropriate aspirant to the next step of drugs fabrication. Yet, additional studies on the mechanism of growth inhibition and toxicity are essential, in order to evaluate the prospective of therapeutic application.

4.1 Introduction

The science that deals with the study of the deterrence and treatment of diseases caused by microorganisms is known as medical microbiology [1]. They are classified based on the microorganisms - bacteriology (study of bacteria), virology (study of viruses), phycology (study of algae), mycology (study of fungi), and protozoology (study of protozoa) [2]. For the treatment of diseases, the inhibitory compounds or chemicals used to prevent their activity; growth or kill microorganisms are called antimicrobial agents [3]. These are classified according to their application and spectrum of activity, such as germicides that kill microorganisms, while microbiostatic agents inhibit the growth of pathogens and allow leukocytes and other host defense mechanisms to cope with static invaders [4-5]. Germicides may exhibit selective toxicity depending on their spectrum of activity. They can act as bactericides (kill bacteria), algicides (kill algae), fungicides (kill fungi) or viricides (kill viruses) [6].

Antimicrobials are one of the most important weapons in the fight against bacterial infections. Throughout history, there has been a continuous battle between humans and the multitude of microorganisms that cause infection and disease [7-9]. CDC (Centers for Disease Control) study revealed that approximately 19 million new infections happen every year [10]. Bacteria and fungi generally develop drug resistance in three ways: by producing metabolizing enzymes for drug degradation, modifying its objectives to render the drugs ineffective, and expressing a high level of efflux proteins that "pump" the drug to reduce its concentration [11-12]. Growing numerous microbial resistances are of great concern to the

scientific world and have become a threat to human life throughout the world [13-14]. In addition, invasive microbial infections caused by multi-drug-resistant bacteria are difficult to diagnose and treat. They are the main cause of morbidity and mortality, especially in patients immunosuppressed and acquired in the hospital [15]. To overcome these problems, the development of new and safe antimicrobial agents is required with greater effectiveness day by day.

In general, the following five main factors may influence the antimicrobial activity of metal complexes.

- The nature of the ligands
- The chelate effect, i.e. the bidentate ligands, shows greater antimicrobial efficacy against complexes with monodentate ligands
- The total charge of the complex; generally the antimicrobial efficiency decreases in the order cationic > neutral > anionic complex
- The nature of the counter ion in the case of the ionic complexes
- The nuclearity of the metal center in the complex; binuclear centers are more active than mononuclear ones. The antimicrobial activities of metal complexes depended more on the metal center itself than on the geometry around the metal ion [16-17].

To appreciate the mechanisms of resistance, the action of antimicrobial agents is very important. Antimicrobial agents act selectively on vital microbial functions with minimal effects or without affecting host

functions. Several antimicrobial agents act in different ways. Understanding these mechanisms and the chemical nature of antimicrobial agents is crucial in understanding the ways in which resistance develops towards them. The mechanism of action of antimicrobial agents based on the structure or on the function of bacteria that is affected by agents. These generally include the following: [17-19]

- Inhibition of the cell wall synthesis.
- Inhibition of folate metabolism
- Inhibition of nucleic acid synthesis.
- Inhibition of ribosome function
- Inhibition of cell membrane function.

4.1.1 Metal (II) Complexes used for Study - Ni, Cu and Zn

Several biologically important compounds used as drugs possess modified toxicological and pharmacological potentials in the form of metal based compounds [20]. A variety of metal ions efficiently and frequently used are nickel, copper and zinc for the reason that of form low molecular weight complexes and so, prove to be further beneficial against numerous diseases. The antimicrobial activity of metal complexes of N-methylthioformohydroxamic acid against Gram-negative *Escherichia coli* and Gram-positive *Staphylococcus aureus* was evaluated [21].

Neutral thiabendazole (TBZH) ligand is a poor anti-Candida agent and has very small chemotherapeutic activity. Cu (II) complexes of TBZH showed a potent anti-candida agent its activity is comparable to the prescription drug ketoconazole. Copper (II) coordination complexes of TBZH significantly increase its chemotherapeutic potential. Synthesis and

antimicrobial activity of novel metal [Ni (II), Zn (II)] complexes from benzofuran moiety have been reported Reddy et al. in 2013 [22].

Katsarou et al. synthesized and studied its biological activities such as antitumor, antibiotic and antimicrobial property against a novel copper (II) complex of the fluoroquinolone antibacterial drug *N*-propyl-norfloxacin (Hpr-norf) in the presence of 1, 10-phenanthroline (Phen) [23]. The antimicrobial activity of the complex has been evaluated, showing an improved potency in comparison to the free Hpr-norf. (MIC: 4-16 µg/mL).

The 3-formyl chromone hydrazones and its Ni (II), Cu (II) and Zn (II) complexes were evaluated for antimicrobial activity against Gram positive bacteria (*Staphylococcus aureus* and *Bacillus subtilis*), Gram negative bacteria (*Escherichia coli* and *Pseudomonas aeruginosa*) and fungus (*Candida albicans*). The some ligands and most of its complexes were found to be biologically active. Results were revealed that among all the compounds Cu (II) was more effective bactericidal activity against all the microbes. On the other hand ligands are less active than that of metal complexes against selected microbes.

4.1.2 Bacterial and Fungal Species used for Study

4.1.2.1 *Staphylococcus aureus* (also known as *golden staph*) is a Gram-positive, round-shaped bacterium that is a member of the Firmicutes, and it is a member of the normal flora of the body, frequently found in the nose, respiratory tract, and on the skin. It is often positive for catalase and nitrate reduction and is a facultative anaerobe that can grow without the need for oxygen [24]. Although *S. aureus* is not always pathogenic (and

can commonly be found existing as a commensal), it is a common cause of skin infections including abscesses, respiratory infections such as sinusitis, and food poisoning. Pathogenic strains often promote infections by producing virulence factors such as potent protein toxins, and the expression of a cell-surface protein that binds and inactivates antibodies. The emergence of antibiotic-resistant strains of *S. aureus* such as methicillin-resistant *S. aureus* (MRSA) is a worldwide problem in clinical medicine. Despite much research and development there is no approved vaccine for *S. aureus*.

4.1.2.2 *Bacillus subtilis*, known also as the hay bacillus or grass bacillus, is a Gram-positive, catalase-positive bacterium, found in soil and the gastrointestinal tract of ruminants and humans. A member of the genus *Bacillus*, *B. subtilis* is rod-shaped, and can form a tough, protective endospore, allowing it to tolerate extreme environmental conditions. *B. subtilis* has historically been classified as an obligate aerobe, though evidence exists that it is a facultative anaerobe [25]. *B. subtilis* is considered the best studied Gram-positive bacterium and a model organism to study bacterial chromosome replication and cell differentiation.

4.1.2.3 *Pseudomonas aeruginosa* is a common Gram-negative, rod-shaped bacterium that can cause disease in plants and animals, including humans. A species of considerable medical importance, *P. aeruginosa* is a multidrug resistant pathogen recognized for its ubiquity, its intrinsically advanced antibiotic resistance mechanisms, and its association with serious illnesses-hospital-acquired infections such as ventilator-associated pneumonia and various sepsis syndromes [26]. The organism is considered

opportunistic insofar as serious infection often occurs during existing diseases or conditions – most notably cystic fibrosis and traumatic burns. It is also found generally in the immunocompromised but can infect the immunocompetent as in hot tub folliculitis. Treatment of *P. aeruginosa* infections can be difficult due to its natural resistance to antibiotics. When more advanced antibiotic drug regimens are needed adverse effects may result.

4.1.2.4 *Escherichia coli* (also known as *E. coli*) is a Gram-negative, facultatively anaerobic, rod-shaped, coliform bacterium of the genus *Escherichia* that is commonly found in the lower intestine of warm-blooded organisms (endotherms) [27]. Most *E. coli* strains are harmless, but some serotypes can cause serious food poisoning in their hosts, and are occasionally responsible for product recalls due to food contamination. The harmless strains are part of the normal flora of the gut, and can benefit their hosts by producing vitamin K₂, and preventing colonization of the intestine with pathogenic bacteria, having a symbiotic relationship. *E. coli* is expelled into the environment within fecal matter. The bacterium grows massively in fresh fecal matter under aerobic conditions for 3 days, but its numbers decline slowly afterwards. *E. coli* and other facultative anaerobes constitute about 0.1% of gut flora, and fecal-oral transmission is the major route through which pathogenic strains of the bacterium cause disease. Cells are able to survive outside the body for a limited amount of time, which makes them potential indicator organisms to test environmental samples for fecal contamination. A growing body of research, though, has examined environmentally persistent *E. coli* which can survive for extended periods outside a host.

4.1.2.5 *Candida albicans* is an opportunistic pathogenic yeast that is a common member of the human gut flora. It does not proliferate outside the human body. It is detected in the gastrointestinal tract and mouth in 40-60% of healthy adults. It is usually a commensal organism, but can become pathogenic in immunocompromised individuals under a variety of conditions [28]. It is one of the few species of the *Candida* genus that causes the human infection candidiasis, which results from an overgrowth of the fungus. Candidiasis is for example often observed in HIV-infected patients. *C. albicans* is the most common fungal species isolated from biofilms either formed on (permanent) implanted medical devices or on human tissue. It is generally referred to as a dimorphic fungus since it grows both as yeast and filamentous cells. However it has several different morphological phenotypes. *C. albicans* was for a long time considered an obligate diploid organism without a haploid stage.

4.2 Materials and Methods

4.2.1 Bacterial and Fungal Cultures

The synthesized chromone hydrazones and metal complexes were tested for their in vitro antibacterial and antifungal activity against the sensitive organisms *Staphylococcus aureus* (ATCC 25923) and *Bacillus subtilis* (ATCC 6635) as Gram positive bacteria, *Pseudomonas aeruginosa* (ATCC 27853) and *Escherichia coli* (ATCC 25922) as Gram negative bacteria and *Candida albicans* (ATCC 10231) as fungus strain using the disc diffusion method [Kirby-Bauer Test] [29] (for the qualitative determination) and the serial dilutions in liquid broth method for determination of MIC values. All ATCC strains were procured from the American Type Culture

Collection (ATCC, Manassas, VA, USA) and the media used in the study were purchased from Himedia, India.

4.2.2 Maintenance of Cultures

All cultures were preserved in 50% glycerol at -70°C (vol/vol; Himedia, Mumbai india) and maintained on Trypticase Soy Agar (TSA; Difco Laboratories, Detroit, Mich USA) except, *C. albicans* were maintained on Sabouraud Dextrose Agar (SDA; Himedia).

4.2.3 Growth Conditions and Media

Mueller-Hinton Broth (MHB) (Difco laboratories, Becton Dickson) supplemented with calcium (25mg/liter) and magnesium (12.5mg/liter) for all organisms except RPMI 1640 medium (Sigma Chemicals) for fungal strains, was used for all screening, minimum inhibitory concentration (MIC) determination.

4.2.4 In Vitro Antimicrobial Evaluation

4.2.4.1 Agar Diffusion Method

Synthesized Compounds were evaluated for antibacterial activity by agar diffusion method. All the bacterial and fungal suspensions (10 mL) were prepared by suspending 37°C for 18h grown bacterial and 24h fungal culture in sterile normal saline (0.89% NaCl wt/vol). The turbidity of the bacterial suspension was adjusted to 0.5 Mc Farland standard (equivalent to 1.5×10^8 CFU mL⁻¹) and 1.0 Mc Farland standard (equivalent to 1.5×10^8 CFU mL⁻¹) for fungal strains. The plates were dried for 15 minutes and then used for the sensitivity test. The discs which had been impregnated with (10µL) the compounds and were placed

on the Mueller-Hinton agar surface. After incubation for 36 h at 37°C in the case of bacteria and for 48 h at 28°C in the case of fungi, inhibition of the organisms was measured and used to calculate mean of inhibition zones and all experiments were carried out in parallel sets of triplicate for those compounds that showed activity of more than 6.5 mm and their activity was recorded as average zone of inhibition [30]. Data were analyzed by the analysis of variance (ANOVA) using the Origin pro 8.5 statistical software and the mean differences were separated using Tukey's studentized test at the 1% level of probability. Chloramphenicol, nystatin and dimethylsulphoxide (DMSO) were used as standard antibacterial, antifungal drugs and control solvent respectively.

4.2.4.2 Time Kill Kinetic Studies

Time kill kinetic studies were conducted for the compounds against one Gram positive, one Gram negative bacteria and against fungus. In the experiment, an overnight culture of the isolates was used up 1 mL of 10^6 CFU mL⁻¹ of each culture was inoculated in sterilized nutrient broth media containing 25 mgmL⁻¹ of the compounds. The experiment was conducted for 13 h in a shaker at 30 °C. Likewise, control was prepared for each microorganism without having the test compound. The CFU count was taken at regular 1 h interval. For that, 1 mL of each culture was spread on nutrient agar plates from 0 h to 13 h and each plate was incubated for 24 h at 30°C. The CFU (colony forming unit) was calculated and plotted in graph [31].

4.2.4.3 Minimum Inhibitory Concentration (MIC)-Resazurin based Microtiter Dilution Assay (RMDA)

The quantitative antimicrobial activity of the test compounds was evaluated using Resazurin based Microtiter Dilution Assay (RMDA). Under aseptic conditions, 96 well microtitre plates (Himedia) were used for Resazurin based Microtitre Dilution Assay. The first row of microtiter plate was filled with 100 μL of test materials dissolved in sterile water. All the wells of microtitre plates were filled with 50 μL of Luria broth. Two fold serial dilution (throughout the column) was achieved by starting transferring 50 μL test material from first row to the subsequent wells in the next row of the same column and so that each well has 50 μL of test material in serially descending concentrations. 2 μL of resazurin solution as indicator was added in each well. Finally, a volume of 10 μL was taken from bacterial suspension and then added to each well to achieve a final concentration of 5×10^6 CFU mL^{-1} . To avoid the dehydration of bacterial culture, each plate was wrapped loosely with cling film to ensure that bacteria did not become dehydrated. Each microtitre plate had a set of 3 controls: (a) a column with Chloramphenicol, nystatin (antimicrobial drugs) as positive control, (b) a column with all solutions with the exception of the test material and (c) a column with all solutions except bacterial solution replaced by 10 μL of Luria broth. All the plates were incubated at 37°C for 24 h whereas plates of *C.albicans* at 28°C for 48 h. The color change in the well was then observed visually. Any color change observed from purple to pink or colorless was taken as positive. The pink color is due to the formation of resorufin (Figure 4.1). The lowest concentration of the sample at which no color change occurred was recorded as the MIC value. All the experiments were performed in

triplicates. The average values were calculated for the MIC of test material [32].

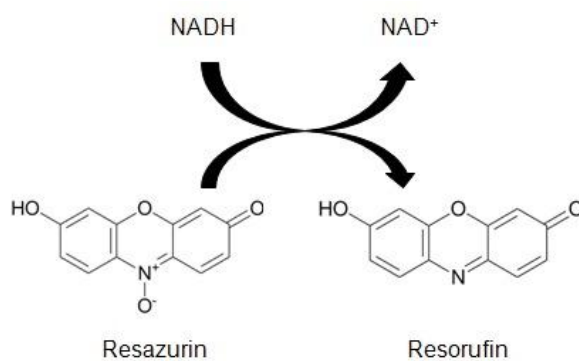


Figure 4.1 Structure of resazurin substrate and the product pink fluorescent resorufin

4.3 Result and Discussion

The antibacterial activity of all compounds against *Mycobacterium* were plotted in a bar diagram. Figures 4.2-4.5 represents the zone of inhibition for bacteria and fungi at three different concentrations (1, 0.5 and 0.25 mgmL⁻¹) with a standard deviation of the triplicate values (Table 4.1-4.2). Figures 4.6 & 4.7 and Table 4.3 & 4.4 represent the MIC of the compounds synthesized against the microorganisms. Chloramphenicol was used as a reference in the case of bacteria and nystatin in the case of fungi were tested at a concentration of 10mgmL⁻¹. Most of the compounds showed good microbial inhibition for all tested microorganisms such as *S. aureus* and *B.subtilis* (Gram positive), two Gram negative bacteria *P. aeruginosa* and *E. coli* and the pathogenic fungus *C. albicans* in the disc diffusion method.

The hydrazones FB and FBH shows activity against all selected microorganisms *Staphylococcus aureus*, *Bacillus subtilis*, *Pseudomonas aeruginosa*, *Escherichia coli* and *Candida albicans* among them good activity against *Bacillus subtilis*. But the hydrazones FN, FIN and FMB are active against only *Bacillus subtilis* that means these ligands did not exhibit any significant effect against other microorganisms. The ligand FMBH shows good or fairly good activity against *Bacillus subtilis*, *Escherichia coli* and did not show activity against *Staphylococcus aureus*, *Pseudomonas aeruginosa* and *Candida albicans*. The compounds FMN and FMIN show activity only against *Bacillus subtilis* and *Candida albicans*. That means all the ligands are active against *Bacillus subtilis* and some of them are also active against *Escherichia coli* and *Candida albicans*. Chromone hydrazones of this series are good antimicrobial agent against *Bacillus subtilis*.

[Ni(FB)(OAc)(H₂O)].2H₂O shows active against all microorganism among them good activity against *Bacillus subtilis* and moderate activity against *Staphylococcus aureus* and *Pseudomonas aeruginosa*. In the case of complex [Ni(FBH)(H₂O)(OAc)].2H₂O active against all the selected microbes but more active against *Bacillus subtilis* and mild active against *Pseudomonas aeruginosa* and *Staphylococcus aureus*. For the complex [Ni(FN)(OAc)].H₂O active against *Staphylococcus aureus*, *Bacillus subtilis*, *Pseudomonas aeruginosa* and *Candida albicans* and shows very good activity against *Bacillus subtilis*. [Ni(FIN)(OAc)(H₂O)].H₂O shows activity against all microorganism except *Candida albicans*. This complex show very low activity against *Staphylococcus aureus* and good active for *Bacillus subtilis* and *Pseudomonas aeruginosa*. [Ni(FMB)₂(H₂O)₂].H₂O exhibited

activity against all tested organism. Complex $[\text{Ni}(\text{FMBH})_2(\text{H}_2\text{O})_2] \cdot 2\text{H}_2\text{O}$ shows good activity against *Pseudomonas aeruginosa* and *Staphylococcus aureus* and inactive against *Bacillus subtilis* and *Escherichia coli*. $[\text{Ni}(\text{FMN})(\text{OAc})] \cdot 2\text{H}_2\text{O}$ exhibited moderate activity against *Staphylococcus aureus*, *Pseudomonas aeruginosa* and strong active against *Bacillus subtilis*. $[\text{Ni}(\text{FMIN})(\text{OAc})(\text{H}_2\text{O})] \cdot 1.5 \text{H}_2\text{O}$ shows good activity against *Bacillus subtilis* and moderate activity against *Staphylococcus aureus*, *Pseudomonas aeruginosa* and *Escherichia coli*.

$[\text{Cu}(\text{FB})(\text{OAc})] \cdot \text{H}_2\text{O}$ shows strong activity against microbes like *Staphylococcus aureus*, *Pseudomonas aeruginosa*, *Bacillus subtilis* and moderate active against *Candida albicans*, *Escherichia coli*. Copper complex $[\text{Cu}(\text{FBH})(\text{H}_2\text{O})(\text{OAc})] \cdot \text{H}_2\text{O}$ displayed very good activity against *Pseudomonas aeruginosa* and *Bacillus subtilis* which is higher than standard antimicrobial drug Chloramphenicol. In the case of *Bacillus subtilis* complex $[\text{Cu}(\text{FN})(\text{OAc})] \cdot 2\text{H}_2\text{O}$ shows higher activity than standard antimicrobial drug but very low activity against *Candida albicans* and *Escherichia coli*. $[\text{Cu}(\text{FIN})(\text{OAc})(\text{H}_2\text{O})] \cdot 2\text{H}_2\text{O}$ shows fairly good activity against *Staphylococcus aureus*, *Pseudomonas aeruginosa*, *Bacillus subtilis* and moderate active against *Escherichia coli*. For complex $[\text{Cu}(\text{FMB})_2(\text{H}_2\text{O})_2] \cdot \text{H}_2\text{O}$ possessed good activity when comparable to Chloramphenicol. $[\text{Cu}(\text{FMBH})_2(\text{H}_2\text{O})_2] \cdot 2\text{H}_2\text{O}$ and $[\text{Cu}(\text{FMN})(\text{OAc})] \cdot \text{H}_2\text{O}$ shows higher activity against *Bacillus subtilis* than that of antimicrobial drug Chloramphenicol and poor activity against *Escherichia coli*, *Candida albicans*. $[\text{Cu}(\text{FMIN})(\text{OAc})(\text{H}_2\text{O})] \cdot \text{H}_2\text{O}$ complex possessed higher activity than that of antimicrobial drug against *Staphylococcus aureus* and *Bacillus subtilis*.

[Zn(FB)(OAc)].2.5H₂O showed higher activity against *Bacillus subtilis*, moderate activity against *Staphylococcus aureus*, *Pseudomonas aeruginosa*, *Candida albicans* and *Escherichia coli*. [Zn(FBH)(OAc)] complex exhibited strong activity against *Pseudomonas aeruginosa*, *Bacillus subtilis* and medium activity against other tested microorganisms. For the complex [Zn(FN)(OAc)].H₂O possesses comparable activity against *Bacillus subtilis* and mild activity against *Staphylococcus aureus*, *Pseudomonas aeruginosa* and *Escherichia coli*. [Zn(FIN)(OAc)] exhibited good activity against *Bacillus subtilis* and inactive against *Escherichia coli*. [Zn(FMB)₂].2H₂O showed higher activity against *Staphylococcus aureus*, *Bacillus subtilis*; poor activity against *Escherichia coli* and inactive against *Pseudomonas aeruginosa*, *Candida albicans*. [Zn(FMBH)(OAc)].H₂O strongly active against *Bacillus subtilis*, *Pseudomonas aeruginosa* and moderate active against other tested microbes. [Zn(FMN)(OAc)].H₂O shows very low activity against *Escherichia coli*, *Candida albicans* and highly active against *Bacillus subtilis*, *Staphylococcus aureus*. [Zn(FMIN)(OAc)].0.5 H₂O shows fairly good activity against *Pseudomonas aeruginosa*, *Bacillus subtilis* and moderate activity against *Staphylococcus aureus*, *Escherichia coli* and *Candida albicans*.

Table 4.1 Antimicrobial activity of 3-formyl Chromone Hydrazones and their Ni (II), Cu (II) and Zn (II) complexes Zone inhibition (mm)^a.

Organism	Mean of zone diameter, nearest whole ^a (mm)				
	Gram-positive bacteria		Gram-negative bacteria		Fungus
	<i>S. aureus</i> (ATCC 25923)	<i>B. subtilis</i> (ATCC 6635)	<i>P.aeruginosa</i> (ATCC 27853)	<i>E. coli</i> (ATCC 25922)	<i>C. albicans</i> (ATCC 10231)
FB	22.4 ± 0.2	26.4 ± 0.3	21.2 ± 0.2	22.1 ± 0.3	21.2 ± 0.2
[Ni(FB)(OAc)(H ₂ O)].2H ₂ O (1)	27.3 ± 0.4	30.5 ± 0.1	27.6 ± 0.1	23.5 ± 0.1	22.5 ± 0.1
[Cu(FB)(OAc)].H ₂ O (9)	31.7 ± 0.2	34.9 ± 0.2	31.0 ± 0.3	28.8 ± 0.2	28.7 ± 0.2
[Zn(FB)(OAc)].2.5H ₂ O (17)	29.5 ± 0.1	33.6 ± 0.2	28.2 ± 0.2	24.3 ± 0.2	24.8 ± 0.1
FBH	23.5 ± 0.2	25.3 ± 0.3	22.4 ± 0.2	22.3 ± 0.1	20.8 ± 0.3
[Ni(FBH)(H ₂ O)(OAc)].2H ₂ O (2)	28.2 ± 0.4	31.5 ± 0.4	29.3 ± 0.1	24.3 ± 0.2	25.6 ± 0.2
[Cu(FBH)(H ₂ O)(OAc)].H ₂ O (10)	31.2 ± 0.1	36.2 ± 0.1	35.7 ± 0.4	30.4 ± 0.2	30.7 ± 0.2
[Zn(FBH)(OAc)] (18)	29.4 ± 0.3	32.6 ± 0.3	31.3 ± 0.1	26.8 ± 0.2	26.3 ± 0.4
FN	-	25.4 ± 0.2	-	-	-
[Ni(FN)(OAc)].H ₂ O (3)	11.4 ± 0.3	31.5 ± 0.1	22.2 ± 0.2	-	19.4 ± 0.1
[Cu(FN)(OAc)].2H ₂ O (11)	30.7 ± 0.1	35.7 ± 0.2	32.0 ± 0.3	21.1 ± 0.3	20.2 ± 0.2
[Zn(FN)(OAc)].H ₂ O (19)	20.3 ± 0.2	32.4 ± 0.4	20.2 ± 0.1	22.6 ± 0.1	-
FIN	-	24.7 ± 0.3	-	-	-
[Ni(FIN)(OAc)(H ₂ O)].H ₂ O (4)	12.5 ± 0.2	32.5 ± 0.2	30.3 ± 0.1	20.3 ± 0.1	-
[Cu(FIN)(OAc)(H ₂ O)].2H ₂ O (12)	31.4 ± 0.3	34.2 ± 0.1	34.7 ± 0.4	27.8 ± 0.1	20.8 ± 0.3
[Zn(FIN)(OAc)] (20)	18.4 ± 0.1	31.3 ± 0.3	23.4 ± 0.2	-	24.6 ± 0.2
Control	00	00	00	00	00
Chloramphenicol	34.0 ± 0.1	35.1 ± 0.2	35.8 ± 0.1	32.1 ± 0.3	-
Nystatin	-	-	-	-	31.5 ± 0.1

Each value represents a mean ± standard deviation (SD) of three replications. Values followed by the same letter(s) in each column are not statistically different according to Tukey's test (P < 0.01).

^aThe zone diameters have been calculated in mm by digital vernier caliper.

–: not detected inhibition.

Control- Dimethylsulfoxide.

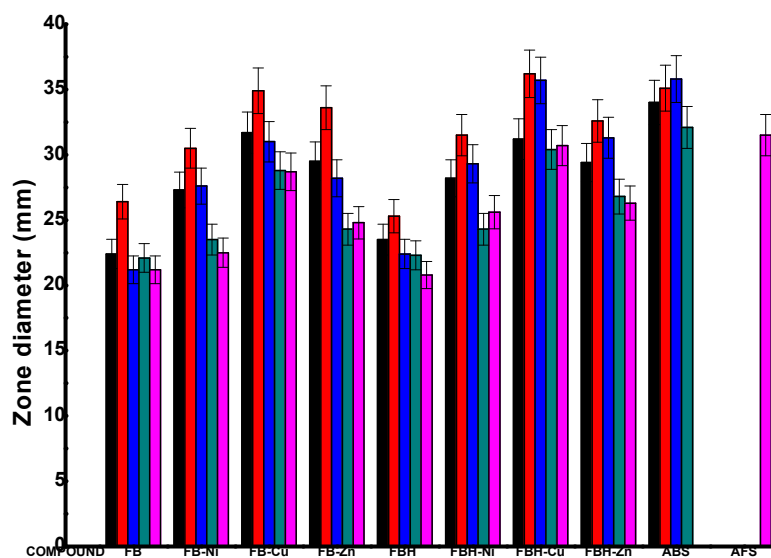


Figure 4.2 Antimicrobial activity of ligands FB, FBH and their Ni (II), Cu (II) and Zn (II) complexes Zone inhibition (mm)

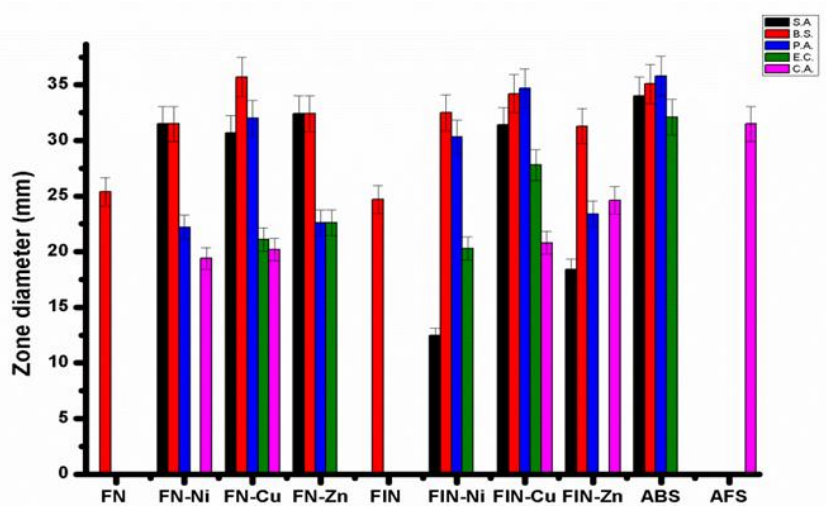


Figure 4.3 Antimicrobial activity of ligands FN, FIN and their Ni (II), Cu (II) and Zn (II) complexes Zone inhibition (mm)

Table 4.2 Antimicrobial activity of 6-methyl-3-formyl Chromone Hydrazones and Ni (II), Cu(II) and Zn(II) complexes Zone inhibition (mm)^a

Organism	Mean of zone diameter, nearest whole ^a (mm)				
	Gram-positive bacteria		Gram-negative bacteria		Fungus
	<i>S. aureus</i> (ATCC 25923)	<i>B. subtilis</i> (ATCC 6635)	<i>P. aeruginosa</i> (ATCC 27853)	<i>E. coli</i> (ATCC 25922)	<i>C. albicans</i> (ATCC 10231)
FMB	-	25.4 ± 0.2	-	-	-
[Ni(FMB) ₂ (H ₂ O) ₂].H ₂ O (5)	28.3 ± 0.1	31.5 ± 0.1	29.6 ± 0.2	21.4 ± 0.1	20.2 ± 0.2
[Cu(FMB) ₂ (H ₂ O) ₂].H ₂ O (13)	32.7 ± 0.2	33.7 ± 0.2	33.0 ± 0.4	26.1 ± 0.3	27.3 ± 0.2
[Zn(FMB) ₂].2H ₂ O (21)	30.6 ± 0.1	32.6 ± 0.4	-	22.3 ± 0.1	-
FMBH	-	26.1 ± 0.2	-	20.0 ± 0.3	-
[Ni(FMBH) ₂ (H ₂ O) ₂].2H ₂ O (6)	29.3 ± 0.4	-	30.3 ± 0.1	-	20.8 ± 0.1
[Cu(FMBH) ₂ (H ₂ O) ₂].2H ₂ O (14)	32.7 ± 0.2	35.2 ± 0.1	34.2 ± 0.3	29.4 ± 0.4	29.7 ± 0.2
[Zn(FMBH)(OAc)].H ₂ O (22)	27.2 ± 0.1	30.1 ± 0.4	30.1 ± 0.4	24.7 ± 0.2	26.3 ± 0.4
FMN	-	24.2 ± 0.2	-	-	19.0 ± 0.2
[Ni(FMN)(OAc)].2H ₂ O (7)	25.7 ± 0.3	30.5 ± 0.1	25.6 ± 0.1	-	-
[Cu(FMN)(OAc)].H ₂ O (15)	32.3 ± 0.2	36.1 ± 0.3	30.0 ± 0.2	21.8 ± 0.3	23.2 ± 0.3
[Zn(FMN)(OAc)].H ₂ O (23)	30.3 ± 0.4	31.2 ± 0.4	27.3 ± 0.1	22.4 ± 0.2	23.5 ± 0.1
FMIN	-	26.7 ± 0.2	-	-	20.8 ± 0.3
[Ni(FMIN)(OAc)(H ₂ O)].1.5 H ₂ O (8)	28.1 ± 0.2	33.6 ± 0.3	28.4 ± 0.1	27.9 ± 0.4	23.7 ± 0.2
[Cu(FMIN)(OAc)(H ₂ O)].H ₂ O (16)	37.3 ± 0.1	35.7 ± 0.1	33.7 ± 0.4	32.4 ± 0.3	26.5 ± 0.3
[Zn(FMIN)(OAc)].0.5 H ₂ O (24)	29.6 ± 0.4	33.3 ± 0.3	30.3 ± 0.3	29.8 ± 0.1	25.1 ± 0.4
Control	00	00	00	00	00
Chloramphenicol	34.0 ± 0.1	35.1 ± 0.2	35.8 ± 0.1	32.1 ± 0.3	-
Nystatin	-	-	-	-	31.5 ± 0.1

Each value represents a mean ± standard deviation (SD) of three replications. Values followed by the same letter(s) in each column are not statistically different according to Tukey's test ($P < 0.01$).

^aThe zone diameters have been calculated in mm by digital vernier caliper.

–: not detected inhibition.

Control-Dimethylsulfoxide.

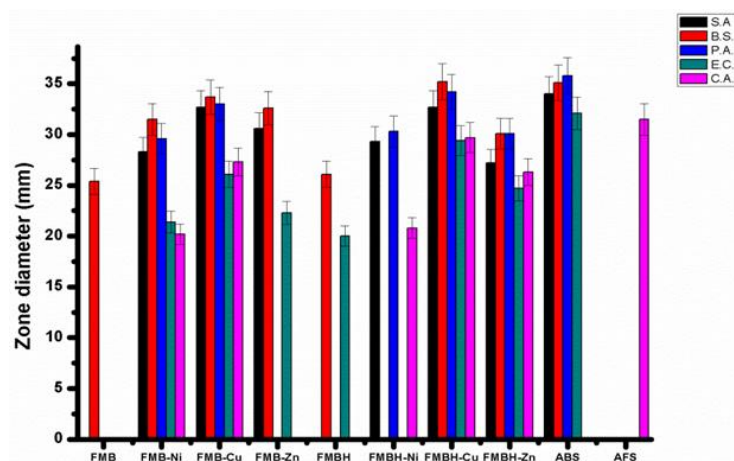


Figure 4.4 Antimicrobial activity of ligands FMB, FMBH and their Ni (II), Cu (II) and Zn (II) complexes Zone inhibition (mm)

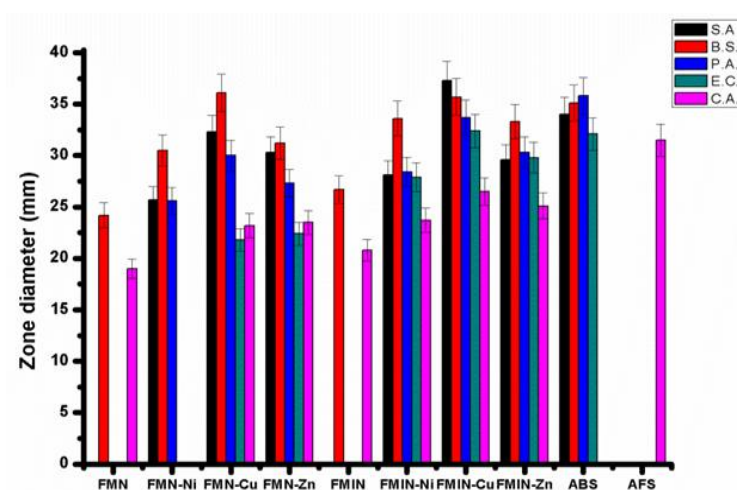


Figure 4.5 Antimicrobial activity of ligands FMN, FMIN and their Ni (II), Cu (II) and Zn (II) complexes Zone inhibition (mm)

Most of the complexes have shown a significant inhibition against Gram-positive bacteria- *Bacillus subtilis*. Among all compounds, copper (II) complex has shown that the best inhibition against all tested microorganisms. The compounds showed greater inhibition of bacteria and less for fungi indicating that the compound may be a better

antibacterial than antifungal activity. This indicates that the synthesized compounds are biologically active as antibacterial. *Bacillus subtilis* was inhibited to the maximum extent by most compounds.

Table 4.3 MIC values ($\mu\text{g/mL}$) for the 3-formyl Chromone Hydrazones and their metal complexes

Microorganism	Gram-positive bacteria		Gram-negative bacteria		Fungus
	<i>S. aureus</i>	<i>B. subtilis</i>	<i>P.aeruginosa</i>	<i>E. coli</i>	<i>C. albicans</i>
	(ATCC 25923)	(ATCC 6635)	(ATCC 27853)	(ATCC 25922)	(ATCC 10231)
FB	125.00	62.50	125.0	250.0	125.0
[Ni(FB)(OAc)(H ₂ O)].2H ₂ O (1)	31.25	15.60	31.25	62.50	62.50
[Cu(FB)(OAc)].H ₂ O (9)	15.60	15.60	15.06	31.25	31.25
[Zn(FB)(OAc)].2.5H ₂ O (17)	31.25	31.25	31.25	62.50	62.50
FBH	62.50	62.50	62.50	125.0	62.50
[Ni(FBH)(H ₂ O)(OAc)].2H ₂ O (2)	31.25	31.25	31.25	62.50	31.25
[Cu(FBH)(H ₂ O)(OAc)].H ₂ O (10)	15.60	15.60	15.60	15.60	15.60
[Zn(FBH)(OAc)] (18)	31.25	15.60	15.60	31.25	31.25
FN	-	125.0	-	-	-
[Ni(FN)(OAc)].H ₂ O (3)	31.25	31.25	31.25	-	15.60
[Cu(FN)(OAc)].2H ₂ O (11)	15.60	15.60	15.60	15.60	15.60
[Zn(FN)(OAc)].H ₂ O (19)	31.25	15.60	15.60	31.25	-
FIN	-	125.0	-	-	-
[Ni(FIN)(OAc)(H ₂ O)].H ₂ O (4)	62.50	31.25	31.25	15.60	-
[Cu(FIN)(OAc)(H ₂ O)].2H ₂ O (12)	31.25	15.60	15.60	15.60	15.60
[Zn(FIN)(OAc)] (20)	62.60	31.25	15.60	-	31.25
Chloramphenicol	12.00	12.00	12.00	12.00	-
Nystatin	-	-	-	-	15.00

(-: not detected inhibition; control; dimethylsulfoxide.)

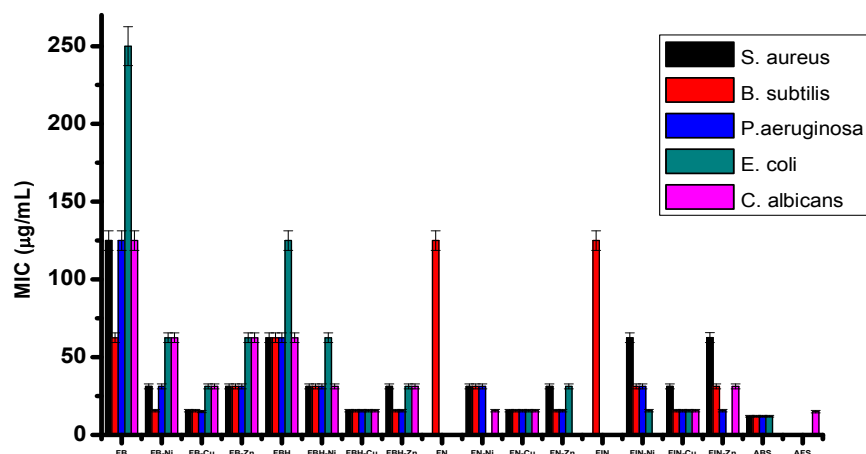


Figure 4.6 MIC values ($\mu\text{g/mL}$) for the 3-formyl Chromone Hydrazones and their metal complexes

Table 4.4 MIC values ($\mu\text{g/mL}$) for the 6-methyl-3-formyl Chromone Hydrazones and their metal complexes.

Microorganisms	Gram-positive bacteria		Gram-negative bacteria		Fungus
	<i>S. aureus</i> (ATCC 25923)	<i>B. subtilis</i> (ATCC 6635)	<i>P. aeruginosa</i> (ATCC 27853)	<i>S. aureus</i> (ATCC 25923)	<i>B. subtilis</i> (ATCC 6635)
FMB	-	125.0	-	-	-
[Ni(FMB) ₂ (H ₂ O) ₂].H ₂ O (5)	62.50	15.60	31.25	62.50	62.50
[Cu(FMB) ₂ (H ₂ O) ₂].H ₂ O (13)	15.60	15.60	15.06	31.25	31.25
[Zn(FMB) ₂].2H ₂ O (21)	31.25	31.25	-	62.50	-
FMBH	-	-	-	-	-
[Ni(FMBH) ₂ (H ₂ O) ₂].2H ₂ O (6)	62.50	62.50	31.25	-	31.25
[Cu(FMBH) ₂ (H ₂ O) ₂].2H ₂ O (14)	15.60	31.25	15.60	15.60	15.60
[Zn(FMBH)(OAc)].H ₂ O (22)	31.25	15.60	15.60	31.25	31.25
FMN	-	62.50	-	-	31.25
[Ni(FMN)(OAc)].2H ₂ O (7)	31.25	31.25	125.0	-	-
[Cu(FMN)(OAc)].H ₂ O (15)	15.60	15.60	15.60	15.60	15.60
[Zn(FMN)(OAc)].H ₂ O (23)	31.25	15.60	15.60	31.25	15.60
FMIN	-	62.50	-	-	62.50
[Ni(FMIN)(OAc)(H ₂ O)].1.5 H ₂ O (8)	31.25	31.25	31.25	15.60	31.25
[Cu(FMIN)(OAc)(H ₂ O)].H ₂ O (16)	15.60	15.60	15.60	15.60	15.60
[Zn(FMIN)(OAc)].0.5 H ₂ O (24)	31.25	31.25	15.60	31.25	31.25
Chloramphenicol	12.00	12.00	12.00	12.00	-
Nystatin	-	-	-	-	15.00

(-: not detected inhibition; control; dimethylsulfoxide.)

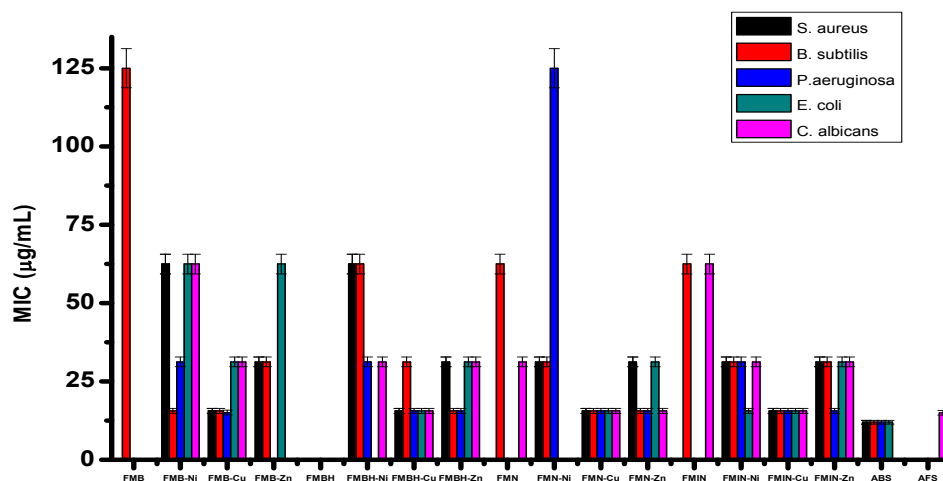


Figure 4.7 MIC values ($\mu\text{g/mL}$) for the 6-methyl-3-formyl Chromone Hydrazones and their metal complexes

Further, to understand the time for actual inhibition of test microorganisms with the application of the compounds, time-kill kinetic study was performed. Time-kill kinetic study exhibits basic pharmacodynamic information on the relationship between the synthesized compound and the growth of microorganisms. This test thereby contributes to a better understanding of current and future application of the compound against the diseases caused by the respective bacteria or fungi. Time kill kinetics study for $[\text{Cu}(\text{FBH})(\text{H}_2\text{O})(\text{OAc})] \cdot \text{H}_2\text{O}$ against one Gram positive, one Gram negative bacteria and on one fungus is shown in Figures 4.7-4.9. As shown in Figures 4.7-4.9, the untreated controls in each case represented the normal growth curve of *Pseudomonas aeruginosa*, *Staphylococcus aureus* and *Candida albicans* where lag period remained for 1 h. After that, the exponential growth or the log phase occurred followed by a stationary phase. Whereas, in case of complex $[\text{Cu}(\text{FBH})(\text{H}_2\text{O})(\text{OAc})] \cdot \text{H}_2\text{O}$ for both the microorganisms, a very

short exponential growth phase was observed in compare to the untreated control. The growth inhibition of *Pseudomonas sp.* and *Staphylococcus sp.* was observed at 3-4 h of incubation period in case of complex [Cu(FBH)(H₂O)(OAc)].H₂O. At 4th hour of incubation the bacterial CFU enters in the declining phase i.e. death phase. When compound complex [Cu(FBH)(H₂O)(OAc)].H₂O was applied to the *Candida sp.* a negligible growth phase was seen to occur. Consequently, the growth inhibition was found at 2nd hour of incubation. After an hour of growth inhibition, the cells entered in the death phase. Thus this observation revealed that the complexes show promising bactericidal and fungicidal activities respectively.

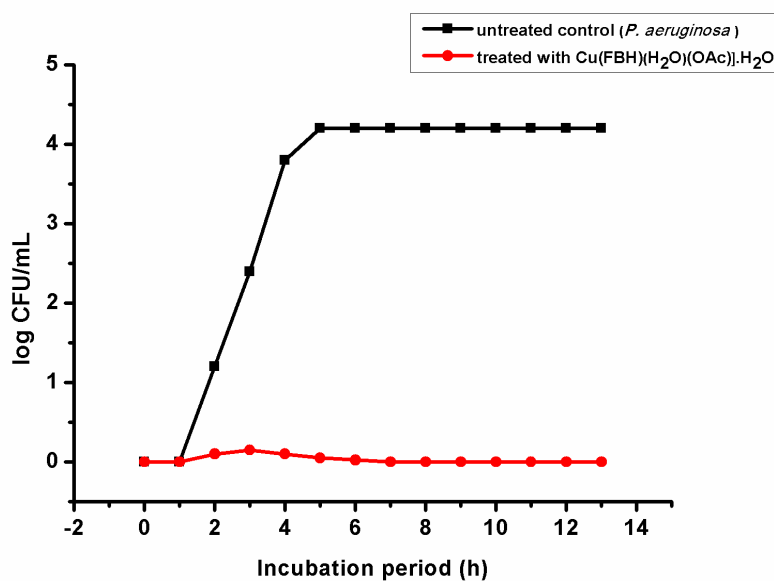


Figure 4.7 Time kill kinetics study for [Cu(FBH)(H₂O)(OAc)].H₂O *Pseudomonas sp.* (Gram negative bacteria).

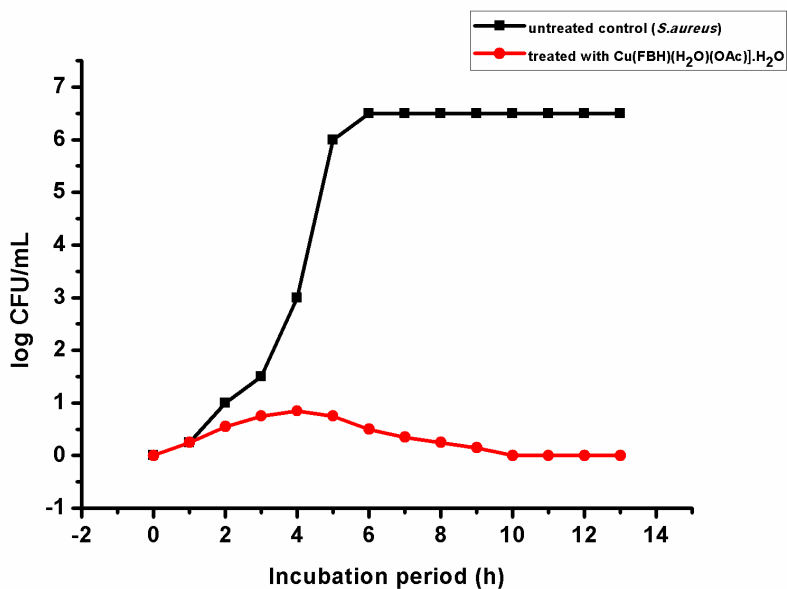


Figure 4.8 Time kill kinetics study for $[\text{Cu}(\text{FBH})(\text{H}_2\text{O})(\text{OAc})]\cdot\text{H}_2\text{O}$ against *Staphylococcus* sp. (Gram positive bacteria)

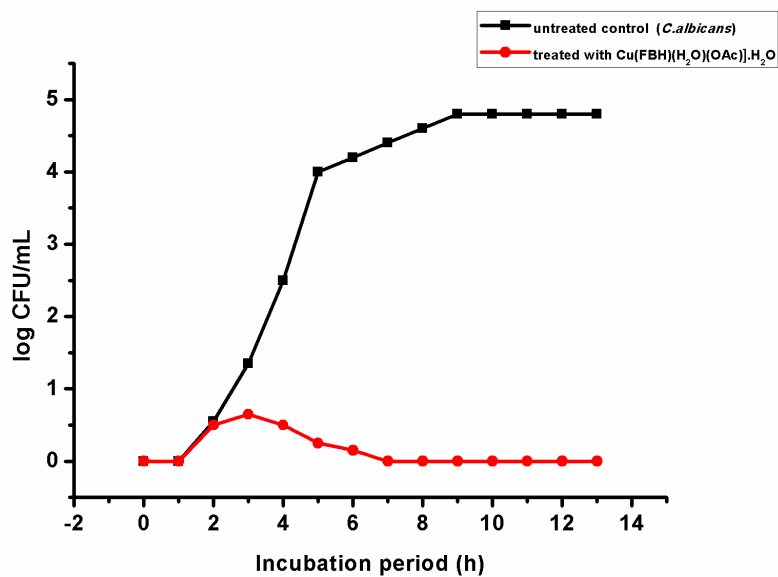


Figure 4.9 Time kill kinetics study for $[\text{Cu}(\text{FBH})(\text{H}_2\text{O})(\text{OAc})]\cdot\text{H}_2\text{O}$ against *Candida* sp. (fungus).

The antibacterial studies shows that Ni (II), Cu (II), Zn (II) metal complexes are more active than the free ligands. The higher activity of the metal complexes may be due to the effect of metal ions on the normal cell membrane and also due to the lipophilic nature of the metal ions in complexes [34]. It also suggests that the complexes possess antibacterial activity inhibiting multiplication process of the microbes by blocking their active sites.

The variation in the activity of different metal complexes against tested micro organisms depends on either the impermeability of cells of the microbes or difference in ribosomes of microbial cells [35]. The higher biological activity of metal complexes than that of the ligands can be explained on the basis of Tweedy's chelation theory and Overtone's concept [36]. Overtone's concept of cell permeability, the lipid membrane that surrounds cell favors the passage of only lipid soluble materials so that liposolubility is an important factor which controls bactericidal activity. This increased lipophilicity enhances the penetration of the complexes into lipid membranes and blocks the metal binding sites in bacterial enzymes. On chelation, metal ion polarity is reduced to a greater extent due to the overlapping of the ligand orbital and partial sharing of positive charge of metal ion with donor groups [37]. Further, the delocalization of the electrons is increased over the whole chelate sphere and enhances the lipophilicity of the complex. The lipophilic nature of the central metal atom is also increased upon chelation, which subsequently favors the permeation through the lipid layer of cell membrane [38]. The normal cell process may be affected by the formation of hydrogen bond through the azomethine nitrogen atom with the active centres of cell

constituents leading to interference with the cell wall synthesis [39]. There are other factors which also increase the activity is solubility, conductivity and bond length between the metal and ligand [40]. The difference in antimicrobial activity is due to the nature of metal ions and also the cell membrane of the microorganisms. It may be concluded that antibacterial activity of the compounds is related to cell wall structure of the bacteria. It is possible because the cell wall is essential to the survival of many bacteria and some antibiotics are able to kill bacteria by inhibiting a step in the synthesis of peptidoglycan [34].

3-formyl chromone hydrazones and its metal complexes showed moderate activity against the Gram negative bacteria compared to that of Gram positive bacteria. This can be explained by considering the effect on lipopolysaccharide (LPS), a major component of the surface of Gram negative bacteria [39]. LPS is an important entity in determining the outer membrane barrier function and the virulence of Gram negative pathogens. The compounds can penetrate the bacterial cell membrane by coordination of metal ion through oxygen or nitrogen donor atom to LPS which leads to the damage of outer cell membrane and consequently inhibits growth of the bacteria [40].

The minimum inhibitory concentration (MIC) of several biochemically active complexes has been determined and the data are placed in Table 4.3 - 4.4. The antimicrobial activity of all compounds against selected five microorganisms MIC is in the range of 15-125 $\mu\text{g mL}^{-1}$. The MIC of complexes active against *Staphylococcus aureus* falls in the wide range, 15.6-125 $\mu\text{g mL}^{-1}$, depending on the nature of the substituent. The most

active complexes [Cu(FB)(OAc)].H₂O, [Cu(FBH)(H₂O)(OAc)].H₂O, [Cu(FN)(OAc)].2H₂O, [Cu(FMB)₂(H₂O)₂].H₂O, [Cu(FMBH)₂(H₂O)₂].2H₂O, [Cu(FMN)(OAc)].H₂O and [Cu(FMIN)(OAc)(H₂O)].H₂O showed the lowest MIC of 15.60 µg mL⁻¹. In respect of microorganism, *Bacillus subtilis*, the MIC falls in the range 15.6-125 µg mL⁻¹ and interestingly each of most active complexes, [Ni(FB)(OAc)(H₂O)].2H₂O, [Cu(FB)(OAc)].H₂O, [Cu(FBH)(H₂O)(OAc)].H₂O, [Zn(FBH)(OAc)], [Cu(FN)(OAc)].2H₂O, [Zn(FN)(OAc)].H₂O, [Cu(FIN)(OAc)(H₂O)].2H₂O, [Ni(FB)(OAc)(H₂O)].2H₂O, [Cu(FB)(OAc)].H₂O, [Cu(FBH)(H₂O)(OAc)].H₂O, [Zn(FBH)(OAc)], [Cu(FN)(OAc)].2H₂O, [Zn(FN)(OAc)].H₂O, [Cu(FIN)(OAc)(H₂O)].2H₂O, [Ni(FMB)₂(H₂O)₂].H₂O, [Cu(FMB)₂(H₂O)₂].H₂O, [Zn(FMBH)(OAc)].H₂O, [Cu(FMN)(OAc)].H₂O, [Zn(FMN)(OAc)].H₂O and [Cu(FMIN)(OAc)(H₂O)].H₂O showed the lowest MIC of 15.6 µg mL⁻¹.

The MIC of compounds against *Escherichia coli* is in the range of 15.6-250 µg mL⁻¹, most active compounds against *E. coli* are [Cu(FBH)(H₂O)(OAc)].H₂O, [Cu(FN)(OAc)].2H₂O, [Ni(FIN)(OAc)(H₂O)].H₂O, [Cu(FIN)(OAc)(H₂O)].2H₂O, [Cu(FMBH)₂(H₂O)₂].2H₂O, [Cu(FMN)(OAc)].H₂O, [Ni(FMIN)(OAc)(H₂O)].1.5 H₂O and [Cu(FMIN)(OAc)(H₂O)].H₂O. In the case of microorganism *Pseudomonas aeruginosa* MIC values are in the range of 15.6-125 µg mL⁻¹, [Cu(FB)(OAc)].H₂O, [Cu(FBH)(H₂O)(OAc)].H₂O, [Zn(FBH)(OAc)], [Cu(FN)(OAc)].2H₂O, [Zn(FN)(OAc)].H₂O, [Cu(FIN)(OAc)(H₂O)].2H₂O, [Zn(FIN)(OAc)], [Cu(FMB)₂(H₂O)₂].H₂O, [Cu(FMBH)₂(H₂O)₂].2H₂O, [Zn(FMBH)(OAc)].H₂O, [Cu(FMN)(OAc)].H₂O, [Zn(FMN)(OAc)].H₂O, [Cu(FMIN)(OAc)(H₂O)].H₂O and [Zn(FMIN)(OAc)].0.5 H₂O. In line with the general behaviour of *Candida albicans*, MIC of complexes lies in the range, 15.6-

125 $\mu\text{g mL}^{-1}$. Most active compounds are $[\text{Cu}(\text{FBH})(\text{H}_2\text{O})(\text{OAc})]\cdot\text{H}_2\text{O}$, $[\text{Ni}(\text{FN})(\text{OAc})]\cdot\text{H}_2\text{O}$, $[\text{Cu}(\text{FN})(\text{OAc})]\cdot 2\text{H}_2\text{O}$, $[\text{Cu}(\text{FIN})(\text{OAc})(\text{H}_2\text{O})]\cdot 2\text{H}_2\text{O}$, $[\text{Cu}(\text{FMBH})_2(\text{H}_2\text{O})_2]\cdot 2\text{H}_2\text{O}$, $[\text{Cu}(\text{FMN})(\text{OAc})]\cdot\text{H}_2\text{O}$, $[\text{Zn}(\text{FMN})(\text{OAc})]\cdot\text{H}_2\text{O}$ and $[\text{Cu}(\text{FMIN})(\text{OAc})(\text{H}_2\text{O})]\cdot\text{H}_2\text{O}$. The MIC of all these new antimicrobial agents, however, is higher than that of the standard chloramphenicol and nystatin as given in Table 4.3-4.4.

4.4 Conclusion

The antibacterial activity of synthesized 3-formyl chromone hydrazone as well as their Ni (II), Cu (II) and Zn (II) metal complexes was tested against Gram positive, Gram negative bacteria and fungus using disc diffusion method. The quantitative antimicrobial activity of the test compounds was evaluated using resazurin based microtiter dilution assay. Chloramphenicol and nystatin were used as standard antibiotics against bacteria and fungus respectively. Compounds individually exhibited varying degrees of inhibitory effects on the growth of the tested bacterial species. Metal complexes exhibited higher antimicrobial activity than the free ligands. Antibacterial activity difference is due to the nature of metal ions and also the cell membrane of the microorganisms.

References

- [1] J. K. Aulakh, T. S. Lobana, H. Sood, D. S. Arora, I. G. Santos, G. Hundal, M. Kaur, V. A. Smolenski, J. P. Jasinski, Dalton Trans., 46 (2017) 1324.
- [2] F. Li, J. G. Collins, F. R. Keene, Chem. Soc. Rev., 44 (2015) 2529.
- [3] J. R. Anaconda, M. Rincones, Spectrochim. Acta A, 141 (2015) 169.

- [4] G. W. Karpin, D. M. Morris, M. T. Ngo, J. S. Merola, J. O. Falkinham, *Med. Chem. Commun.*, 6 (2015) 1471.
- [5] S. Pasa, S. Aydın, S. Kalaycı, M. Boga, M. Atlan, M. Bingul, F. Sahin, H. Temel, *J. Pharma. Analysis*, 6 (2016) 39.
- [6] M. L. Sundararajan, T. Jeyakumar, J. Anandakumaran, B. K. Selvan, *Spectrochim. Acta A*, 131 (2014) 82.
- [7] J. Ramesh, S. Sujatha, C. Arunkumar, *RSC Adv.*, 6 (2016) 63271.
- [8] E. Budzisz, R. Bobka, A. Hauss, J. N. Roedel, S. Wirth, I. P. Lorenz, B. Rozalska, M. W. Szakiel, U. Krajewskad, M. Rozalskid, *Dalton Trans.*, 41 (2012) 5925.
- [9] S. Indoria, T. S. Lobana, H. Sood, D. S. Arora, G. Hundal, J. P. Jasinski, *New J. Chem.*, 40 (2016) 3642.
- [10] Z. A. Siddiqi, M. Khalid, S. Kumar, M. Shahid, S. Noor, *Eur. J. Med. Chem.*, 45 (2010) 264.
- [11] M. Shebl, M. A. Ibrahim, S. M. E. Khalil, S. L. Stefan, H. Habib, *Spectrochim. Acta A.*, 115 (2013) 399.
- [12] J. V. Holtje, *Microbiol. Mol. Biol.*, 62 (1998) 181.
- [13] O. Espeli, K. J. Marians, *Mol. Microbiol.*, 52 (2004) 925.
- [14] K. Drlicaand, M. Snyder, *J. Mol. Biol.*, 120 (1978) 145.
- [15] A. S. Said, A. E. Amr, H. A. El-Sayed, *Int. J. Pharm.*, 11 (2015) 502.
- [16] G. G. Mohamed, M. M. Omar, A. M. M. Hindy, *Spectrochim. Acta A*, 62 (2005) 1140.
- [17] M. Shebl, M. A. El-ghamry, S. M. E. Khalil, M. A. A. Kishk, *Spectrochim. Acta A*, 126 (2014) 232.
- [18] L. D. Gebbharadt, J. G. Bachtold, *Proc. Soc. Exptl. Biol. Med.*, 88 (1955) 103.
- [19] N. Joksimovic, D. Baskic, S. Popovic, M. Zaric, M. Kosanic, B. Rankovic, T. Stanojkovic, S. B. Novakovic, G. Davidovic, Z. Bugarcica, N. Jankovic, *Dalton Trans.*, 45 (2016) 15067.

- [20] R. P. Saini, V. Kumar, A. K. Gupta, G. K. Gupta, *Med. Chem. Res.*, 23 (2014) 690.
- [21] S. J. Bell, S. A. Friedman, J. LEONG, *Antimicrobial Agents and Chemotherapy*, 15 (1979) 38
- [22] N. S. Reddy, B. S. Shankara, P. M. Krishana, C. Basavaraj, B. Mahesh *Int. J. Inorg. Chem.*, 2013 (2013)1.
- [23] M. E. Katsarou, E. K. Efthimiadou, G. Psomas, A. Karaliota, D. Vourloumis, *J Med Chem.*, 51 (2008) 470.
- [24] C. Rayner, W. J. Munckhof, *Intern Med J.*, 35 (2005) 3.
- [25] A. C. Yu, J. F. Loo, S. Yu, S. K. Kong, T. F. Chan, *Appl. Microbiol. Biotechnol.*, 98 (2014) 855.
- [26] A. Balcht, R. Smith, *Infections and Treatment. Informa Health Care.* 1994. p 83.
- [27] A. U. Rahman, M. I. Choudhary, W. J. Thomsen, *Bioassay Techniques for Drug Development*, Harwood Academic Publishers, The Netherlands, 2001.
- [28] A. Juan, P. Yaricruz, B. Alina, C. Juan, *Med Chem.*, 6 (2016) 467.
- [29] J. E. Philip, S. A. Antony, S. Jose, M. R. P. Kurup, M. P. Velayudhan, *Inorganica Chimica Acta*, 469 (2018) 87.
- [30] C. Sridevi, *J. Med. Biol. Eng.*, 4 (2015) 363.
- [31] S. S. Tajudeen, K. Geetha, *I. J. A. C. S.*, 4 (2016) 40.
- [32] P. Ejidike, P. A. Ajibade, *Molecules*, 20 (2015) 9788.
- [33] A. M. Abu-Dief, M. A. Ibrahim, *J. Basic Appl.Sci.*, 4 (2015) 119.
- [34] M. Shoaib, G. Rahman, S. W. Ali Shah, *J. Pharmacol.*, 10 (2015) 332.
- [35] M. Alias, H. Kassum, C. Shakir, *J. Assn. Arab.Univ. Basic Appl. Scien.*, 15 (2014) 28.

- [36] G. G. Mohamed, M. A. Zayeed, S. M. Abdallah, J. Mol. Struct., 979 (2010) 62.
- [37] W. M. Al Momani, Z. A. Thaha, Asian Pac. J. Trop. Biomed., 3 (2013) 367.
- [38] Z. A. Thaha, Asian Pac. J. Trop. Biomed., 3 (2013) 367.

.....✂.....

Chapter 5

DNA INTERACTION STUDIES BY ABSORPTION TITRATION AND VISCOSITY MEASUREMENTS

Contents

- 5.1 Introduction
- 5.2 Materials and Methods
- 5.3 Result and Discussion
- 5.4 Conclusion

Conspectus: The molecules that interact with DNA are classified as having antitumor properties because they may inhibit further DNA replication. Among this great family of molecules, chromones are of great interest due to their extensive pharmacological activity. In fact, they are better known for their antioxidant properties and can act in vitro as reducing agents, hydrogen donors, free radical quenchers and metal ions chelators and this may represent anticancer activity of chromones. In this study, we evaluated the effect of Ni (II), Cu (II) and Zn (II) complexes of chromone hydrazones on DNA binding. The interaction between some new derivatives of chromones and double stranded CT-DNA is monitored by spectroscopic analysis since the electronic absorption spectrum of the complexes are altered upon binding. Based on the variation of spectral characters, we suggested an intercalative mode of binding between DNA and complexes. The interactive mode between DNA and the compounds are complimented by viscometric studies.

5.1 Introduction

In current scenario, several researchers have persisted on the studies of interaction of small molecules with DNA [1-5]. DNA is usually the primary intracellular target of anticancer drugs, so the interaction between DNA and small molecules can cause DNA damage in cancer cells, blocking the division of cancer cells and causing cell death [6-7]. Studies on the interaction of transition metal complexes with DNA continue to attract the researcher's attention due to their importance in the design and development of chemotherapeutic drugs, DNA cleavage agents, synthetic restriction enzymes, DNA printing agents and DNA "molecular light switch" [8-10]. The attention in the mode of union of the metal complex to DNA has been motivated not only by the desire to understand the basic concepts of these modes of interaction but also by the development of metal complexes in antibacterial, antifungal, anticancer reagents or anti-inflammatory. [11].

The hydrazone compounds comprise a vital class of ligands which have been broadly considered in coordination chemistry. The nature of the effect of one ligand and its transcription to another ligand through the central metal ion is extremely significant in coordination chemistry. These interactions can be observed in the kinetic and the thermodynamic aspects of the chemical reactivity [12-15].

The interaction of transition metal complexes with DNA has been broadly considered in the past decades. Due to the unusual binding properties these coordination compounds were appropriate candidates as DNA secondary structure probes, antitumor drugs and photocleavers [16-18]. Tiny metal complexes can be able to interact with DNA through non-

covalent way that means by intercalative mode. Typically the intercalative type binding complex must have an extended aromatic ligand, as its stacking between DNA base pairs (π - π stacking interaction between DNA base pairs and aromatic ligands) is considered to be a most important driving force that leads to binding. The strength and binding mode are sensitively dependent on the size, planarity, shape and electron density of the aromatic ligands. So that systematic study in the influence of varying parameters on the interaction of metal complexes with DNA would be important for the design and synthesis of new therapeutic agents and drugs targeted to DNA. And it is potential to scientifically vary parameters of interest by changing the properties of the intercalating groups [19-21].

On the other hand, nickel, copper and zinc metal ions showed good biological activity. Recently, we found that, the large number of metal (II) complexes exhibited interesting DNA binding properties [22-23]. In addition, several hydrazones and their complexes with metals often have various pharmaceutical and biological actions [24-30]. Our group has incessantly been fascinated in DNA interactions of metal complexes and has reported the synthesis and DNA binding of various metal (II) complexes [22-24]. Nevertheless, up to now the biological activity and interactions of metal complexes of chromone hydrazone with DNA have not been reported. This awakens our attention in the synthesis of chromone hydrazone and its Ni(II), Cu(II) and Zn(II) complexes in view of evaluating their DNA-binding properties.

In order to more clearly evaluate and understand DNA binding properties of metal (II) complexes of chromone hydrazones (synthesis and characterization were given in chapter 2 & 3). Their binding properties to

calf thymus DNA were studied using absorption spectroscopy and viscosity measurements.

Absorption spectroscopy is one of the most imperative techniques to find out the interaction of metal complexes with DNA. This method is frequently employed to find out the mode of binding and binding strength of the metal complex with DNA. The degree of the binding strength of the metal complexes is quantitatively determined by calculating the intrinsic binding (K_b) constants of the complexes. DNA affords an extensive choice of binding modes and binding sites for covalent and non-covalent interactions (Figure 5.1). The non-covalent interactions include intercalation, partial intercalation, groove bindings and electrostatic binding with metal complexes, in which the later two are the non-classical intercalative binding modes.

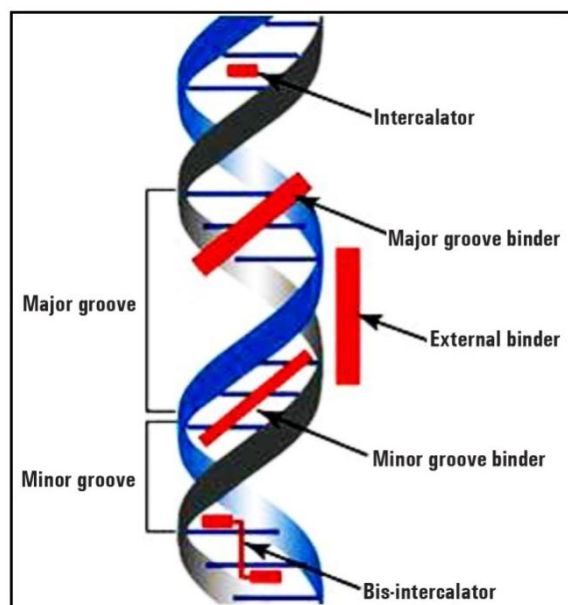


Figure 5.1: Various possibility of binding to DNA

The experimental results give you an idea about that the interactions between the complexes and DNA most probably via an intercalation mechanism. Information from this study will be helpful in the understanding of the mechanism of metal complexes reacting with nucleic acids, as well as laying the foundation for the rational design of new useful DNA probes and effective inorganic complex nucleases.

5.2 Materials and Methods

Preparation and characterization of chromone hydrazones and their Ni (II), Cu (II) and Zn (II) complexes are discussed in Chapter 2 and Chapter 3. These, were serially diluted to get a required concentration to perform DNA binding assays.

- Deoxyribonucleic Acid (DNA)-stored at 0-4°C-SRL Fine Chemicals.
- Tris (Hydroxymethyl)aminomethane (Tris HCl buffer pH 7.1)-stored at 0-4°C- SRL Fine Chemicals.

5.2.1 Preparation of DNA stock solution

The stock solution was prepared by dissolving Calf-Thymus DNA (CT-DNA) in 50mM Tris-HCl buffer (pH=7.1). The DNA concentration was determined by UV spectrophotometer using the molar absorption coefficient $6600 \text{ M}^{-1}\text{cm}^{-1}$ at 260 nm [31]. The stock solution was stored below 4 °C and used for 4 days.

5.2.2 DNA binding experiments

5.2.2.1 Electronic absorption spectral titration

The DNA binding of the metal complexes were studied by UV-Visible Absorption spectra through the changes observed in the

absorbance and shift in the wavelength [31-33]. A solution of CT-DNA in the buffer (5 mM Tris-HCl/50 mM NaCl buffer (pH 7.1)) gave a UV absorbance ratio at 260 and 280 nm of about 1.8-1.9:1, indicating that CT-DNA was free from protein contamination.

Electronic absorption titrations were performed in Tris-HCl buffer using DMF (10%) solution of compounds at room temperature. Absorption titration experiments were made using different concentrations of CT-DNA, keeping the compound concentration constant and maintaining the total volume constant (3mL). Metal complex-DNA solutions were allowed to incubate for 5 minutes at room temperature before the absorption spectra were recorded. Correction was made for absorbance of the CT-DNA itself. The intrinsic binding constant (K_b) was determined by monitoring the changes of absorption in the MLCT band with increasing concentration of DNA using the following equation [31]. The magnitude of spectral perturbation is an evidence for extent of binding.

$$[\text{DNA}]/(\varepsilon_a - \varepsilon_f) = [\text{DNA}]/(\varepsilon_b - \varepsilon_f) + 1/K_b(\varepsilon_b - \varepsilon_f) \quad (1)$$

Where,

[DNA] = Concentration of DNA in base pairs

ε_a = Apparent molar extinction coefficient obtained by calculating

$A_{obs.}/[\text{complex}]$

ε_f = Molar extinction coefficient of the free metal complex

ε_b = Molar extinction coefficient CT-DNA bound metal complex

A plot of $[\text{DNA}]/(\epsilon_a - \epsilon_f)$ versus $[\text{DNA}]$, gave a slope of $1/(\epsilon_a - \epsilon_f)$ and a y-intercept equal to $K_b/(\epsilon_b - \epsilon_f)$, The intrinsic binding constant K_b is the ratio of the slope to the y-intercept.

5.2.2.2 Viscosity measurement

Viscosity measurements were carried out at 25 ± 1 °C using Ostwald viscometer at room temperature. Measurement of DNA viscosity is regarded as the least ambiguous and the most critical test of a DNA binding model in solution and affords stronger arguments for an interactive DNA binding mode. The DNA viscosity is enhanced significantly due to complete or partial intercalation of drugs in to DNA base stacking but it is slightly disturbed by electrostatic or covalent binding of molecules. To understand the nature of DNA binding of the metal complexes, the viscosity measurements were carried out on CT-DNA by varying the concentration of the added complexes. In viscosity measurement, DNA samples approximately 200 base pairs in length were prepared by sonication in order to minimize complexities arising from DNA flexibility [30-31]. Flow times were measured with a digital stopwatch. Each sample was measured three times and an average flow time was calculated. Relative viscosities for DNA in the presence and absence of the complexes were calculated from the relation: $\eta \propto (t - t_0)$ where, t is the observed flow time of DNA-containing solution and t_0 is that of phosphate buffer alone; i.e. relative specific viscosity was calculated according to Cohen and Eisenberg Plots of $(\eta/\eta_0)^{1/3}$ (η and η_0 are the relative specific viscosities of DNA in the presence and absence of the compounds) versus $[\text{compounds}]/[\text{DNA}]$ were constructed.

5.3 Result and Discussion

DNA is an essential drug target and it controls numerous biochemical processes that take place in the cellular system. Transition metal complexes bind to DNA by both non-covalent and covalent interactions [34]. In recent times, there has been incredible attention in studies associated to the interaction of transition metal ions with nucleic acid because of their significance in the development of new reagents for medicine and biotechnology [35].

5.3.1 Electronic Absorption Studies

Electronic absorption spectroscopy is an efficient method to study the binding mode and extent of binding of metal complexes with DNA [36]. “Hypochromic” and “hyperchromic” effects are the spectral characteristics of DNA concerning its double helix structure [37]. The hyperchromic effect might be attributed to external contact (electrostatic binding) or to partial uncoiling of the helical structure of DNA [38]. Hypochromism is usually observed when a complex binds to DNA through intercalation as a consequence of strong stacking interaction between an aromatic chromophore and DNA base pair. The extent of the hypochromism frequently reflects the intercalative binding mode [39]. Upon increasing the concentration of CT-DNA change in absorbance, resulting in hyperchromism with slight blue-shift (2-4nm) (hypsochromism) indicating groove binding between DNA duplex and complexes.

The DNA binding studies of the ligands and metal complexes were carried out by absorption spectral titration experiment with CT-DNA through the changes observed in the absorbance and shift in the

wavelength. The absorption spectra of ligands, Ni, Cu and Zn (II) complexes ($1 \times 10^{-5} \text{M}$) in Tris-HCl buffer pH 7.1 in the absence ($R=0$) and presence of increasing amount of DNA are illustrated in Figures 5.2-5.9, (A plot of $[\text{DNA}] / (\epsilon_b - \epsilon_f)$ versus $[\text{DNA}]$ are represented in site).

In the case of complexes shows hypochromism and a red shift (bathochromism) of the absorption band. Hypochromism is observed due to the presence of aromatic chromophore which might facilitate the interaction of the complexes with the DNA bases through noncovalent π - π^* stacking interactions [40]. When the complexes intercalate to the base pairs of DNA, the π^* orbital of the intercalated ligand in the complexes can couple with π orbital of the DNA base pairs, and then decreasing the π - π^* transition energies. The coupling π orbital was partially filled by electrons, thus decreasing the transition probabilities and concurrently resulting in hypochromism. Complexes containing aromatic heterocyclic ligands could stack among the DNA base pairs.

In order to elucidate the binding strengths of these complexes, the intrinsic binding constant K_b were calculated by monitoring the changes of absorbance in the ligand transfer bands with increasing amounts of DNA. The binding constant values obtained for ligands and its Ni (II), Cu (II), Zn (II) complexes are represented in Table 5.1-5.2. The order of K_b values obtained for the synthesized complexes are as follows:

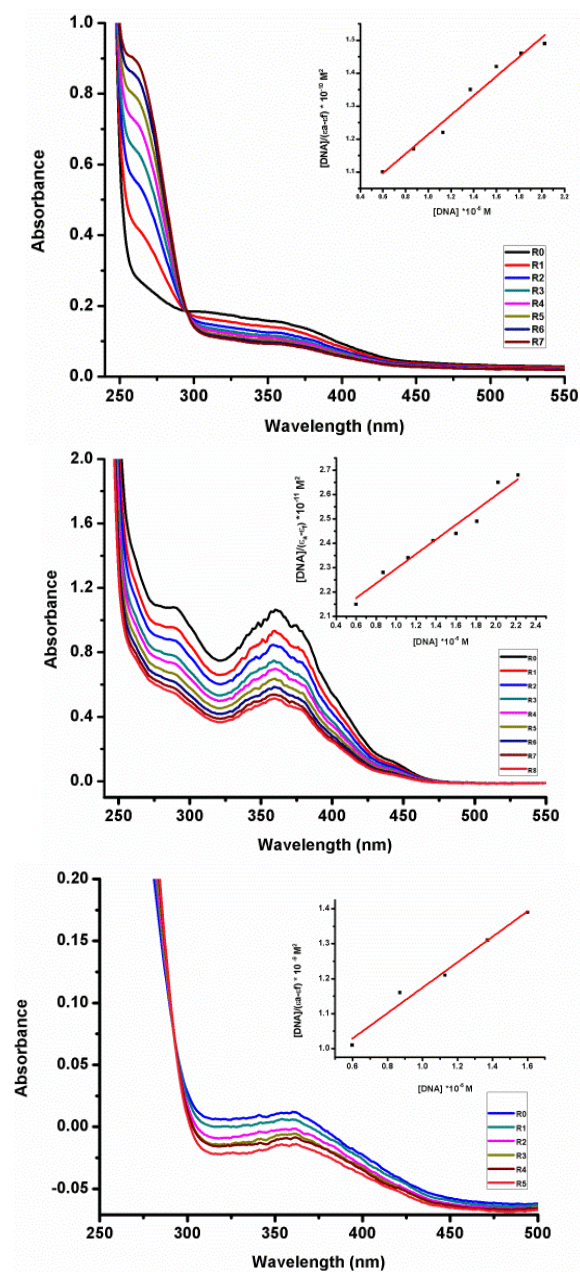


Figure 5.2 Absorption spectra for $[\text{Ni}(\text{FB})(\text{OAc})(\text{H}_2\text{O})].2\text{H}_2\text{O}$ (1), $[\text{Cu}(\text{FB})(\text{OAc})].\text{H}_2\text{O}$ (9) & $[\text{Zn}(\text{FB})(\text{OAc})].2.5\text{H}_2\text{O}$ (17) in *Tris*-HCl buffer upon addition of DNA. $R_0, R_1, R_2, R_3, R_4, R_5, R_6$ & $R_7 = 0.0, 0.2, 0.4, 0.6, 0.8, 1.0, 1.2$ & 1.4 ; $R = [\text{DNA}]/[\text{complex}]$. Inset graph of $[\text{DNA}]/(\epsilon a - \epsilon f)$ vs. $[\text{DNA}]$ for titration of DNA with compounds.

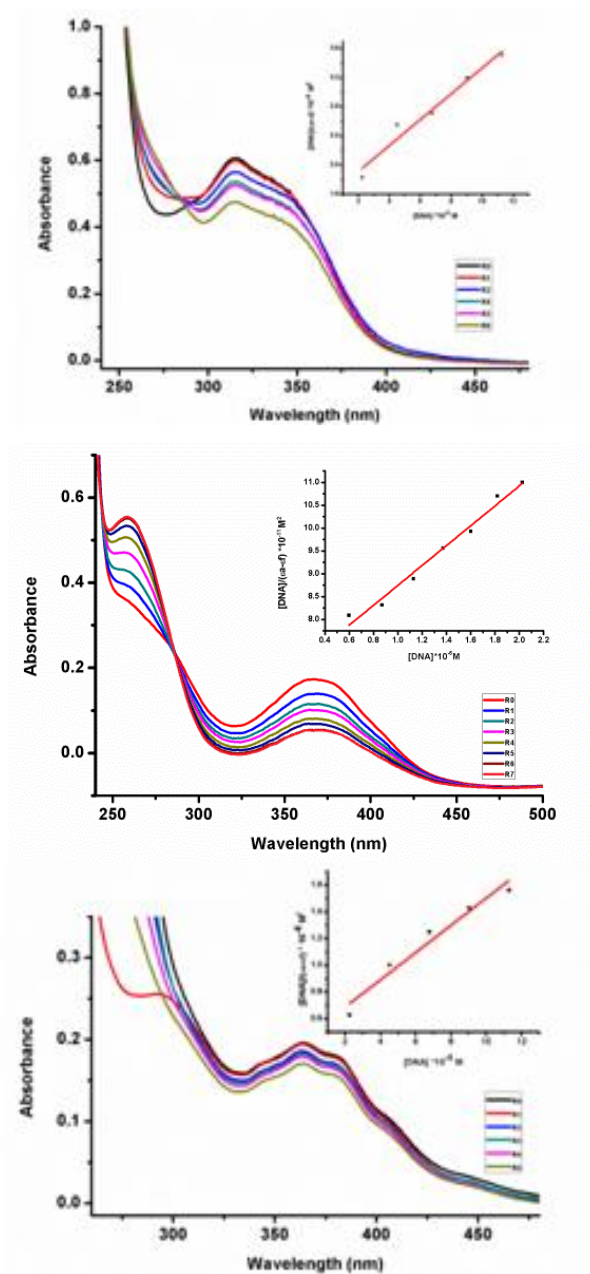


Figure 5.3 Absorption spectra for $[\text{Ni}(\text{FBH})(\text{H}_2\text{O})(\text{OAc})] \cdot 2\text{H}_2\text{O}$ (2), $\text{Cu}(\text{FBH})(\text{H}_2\text{O})(\text{OAc}) \cdot \text{H}_2\text{O}$ (10) & $[\text{Zn}(\text{FBH})(\text{OAc})]$ (18) in *Tris*-HCl buffer upon addition of DNA. $R_0, R_1, R_2, R_3, R_4, R_5, R_6$ & $R_7 = 0.0, 0.2, 0.4, 0.6, 0.8, 1.0, 1.2$ & 1.4 ; $R = [\text{DNA}]/[\text{complex}]$. Inset graph of $[\text{DNA}]/(\epsilon a - \epsilon f)$ vs. $[\text{DNA}]$ for titration of DNA with compounds.

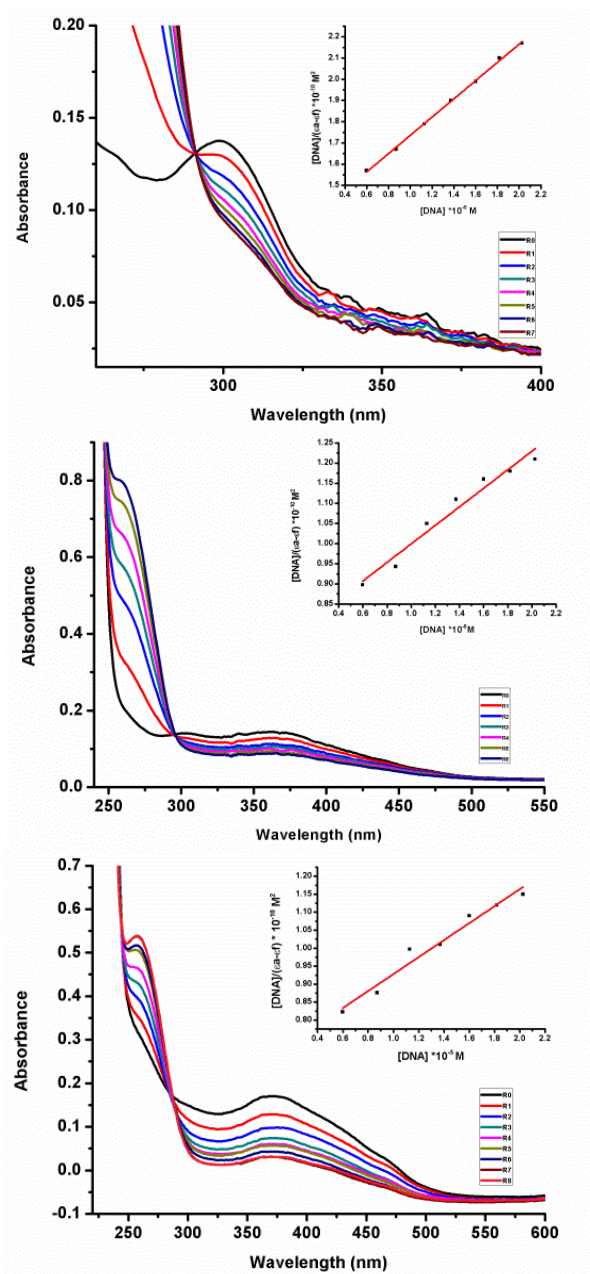


Figure 5.4 Absorption spectra for $[\text{Ni}(\text{FN})(\text{OAc})].\text{H}_2\text{O}(3)$, $[\text{Cu}(\text{FN})(\text{OAc})].2\text{H}_2\text{O}(11)$ & $[\text{Zn}(\text{FN})(\text{OAc})].\text{H}_2\text{O}(19)$ in *Tris*-HCl buffer upon addition of DNA. $R_0, R_1, R_2, R_3, R_4, R_5, R_6$ & $R_7 = 0.0, 0.2, 0.4, 0.6, 0.8, 1.0, 1.2$ & 1.4 ; $R = [\text{DNA}] / [\text{complex}]$. Inset graph of $[\text{DNA}] / (\epsilon a - \epsilon f) \text{ vs. } [\text{DNA}]$ for titration of DNA with compounds.

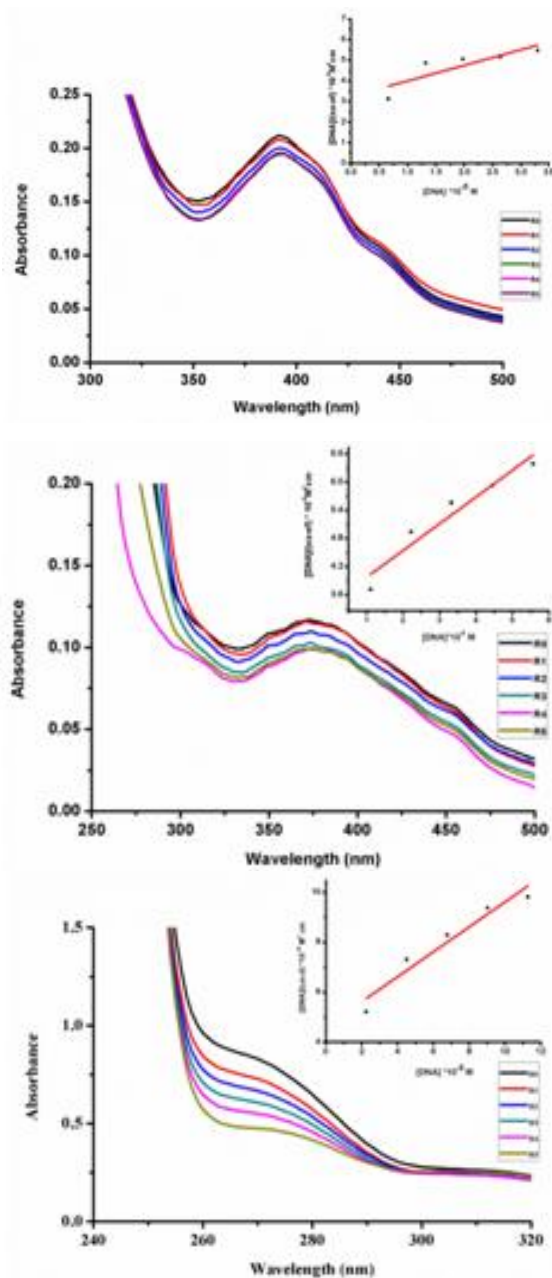


Figure 5.5 Absorption spectra for $[\text{Ni}(\text{FIN})(\text{OAc})(\text{H}_2\text{O})] \cdot \text{H}_2\text{O}$ (4), $[\text{Cu}(\text{FIN})(\text{OAc})(\text{H}_2\text{O})] \cdot 2\text{H}_2\text{O}$ (12) & $[\text{Zn}(\text{FIN})(\text{OAc})]$ (20) in *Tris*-HCl buffer upon addition of DNA. $R_0, R_1, R_2, R_3, R_4, R_5, R_6$ & $R_7 = 0.0, 0.2, 0.4, 0.6, 0.8, 1.0, 1.2$ & 1.4 ; $R = [\text{DNA}]/[\text{complex}]$. Inset graph of $[\text{DNA}]/(\epsilon a - \epsilon f)$ vs. $[\text{DNA}]$ for titration of DNA with compounds.

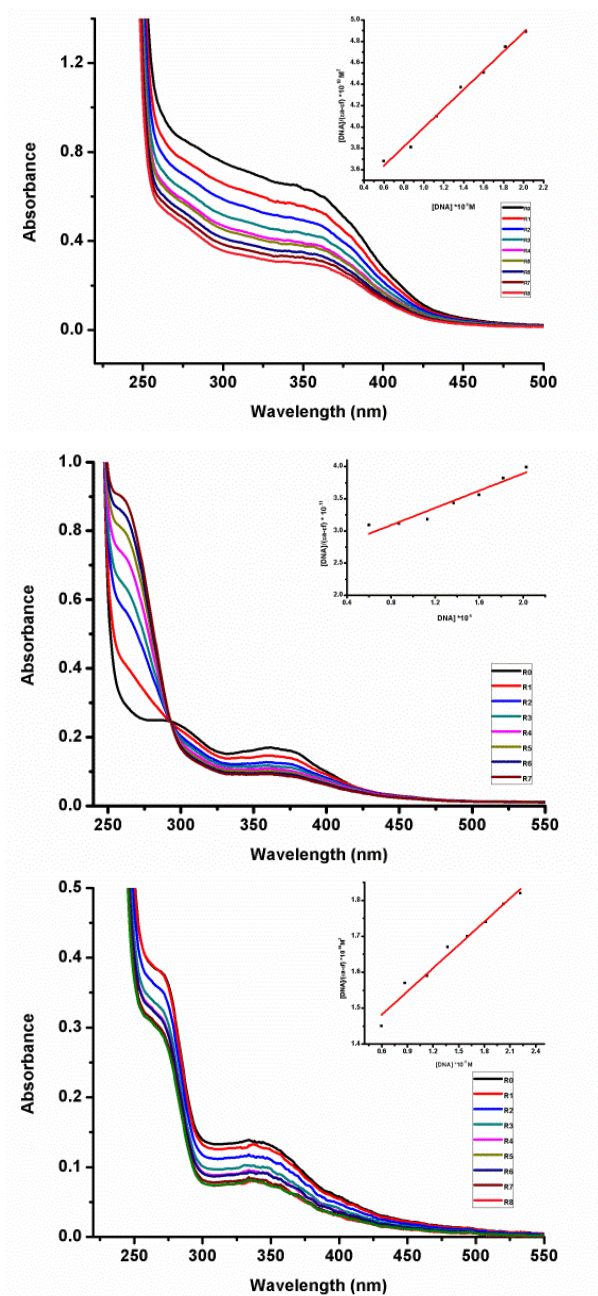


Figure 5.6 Absorption spectra for $[\text{Ni}(\text{FMB})_2(\text{H}_2\text{O})_2] \cdot \text{H}_2\text{O}$ (5), $[\text{Cu}(\text{FMB})_2(\text{H}_2\text{O})_2] \cdot \text{H}_2\text{O}$ (13) & $\text{Zn}(\text{FMB})_2 \cdot 2\text{H}_2\text{O}$ (21) in *Tris*-HCl buffer upon addition of DNA. $R_0, R_1, R_2, R_3, R_4, R_5, R_6$ & $R_7 = 0.0, 0.2, 0.4, 0.6, 0.8, 1.0, 1.2$ & 1.4 ; $R = [\text{DNA}]/[\text{complex}]$. Inset graph of $[\text{DNA}]/(\epsilon a - \epsilon f)$ vs. $[\text{DNA}]$ for titration of DNA with compounds.

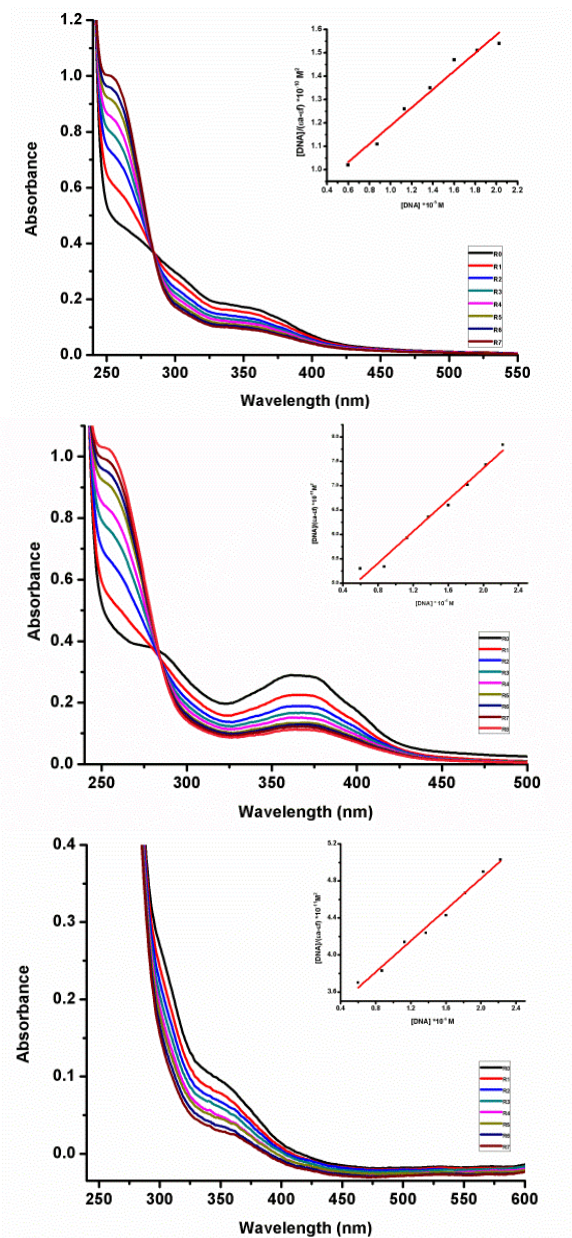


Figure 5.7 Absorption spectra for $[\text{Ni}(\text{FMBH})_2(\text{H}_2\text{O})_2] \cdot 2\text{H}_2\text{O}$ (6), $[\text{Cu}(\text{FMBH})_2(\text{H}_2\text{O})_2] \cdot 2\text{H}_2\text{O}$ (14) & $\text{Zn}(\text{FMBH})(\text{OAc})$ (22) in *Tris*-HCl buffer upon addition of DNA. $R_0, R_1, R_2, R_3, R_4, R_5, R_6$ & $R_7 = 0.0, 0.2, 0.4, 0.6, 0.8, 1.0, 1.2$ & 1.4 ; $R = [\text{DNA}]/[\text{complex}]$. Inset graph of $[\text{DNA}]/(\epsilon a - \epsilon f)$ vs. $[\text{DNA}]$ for titration of DNA with compounds.

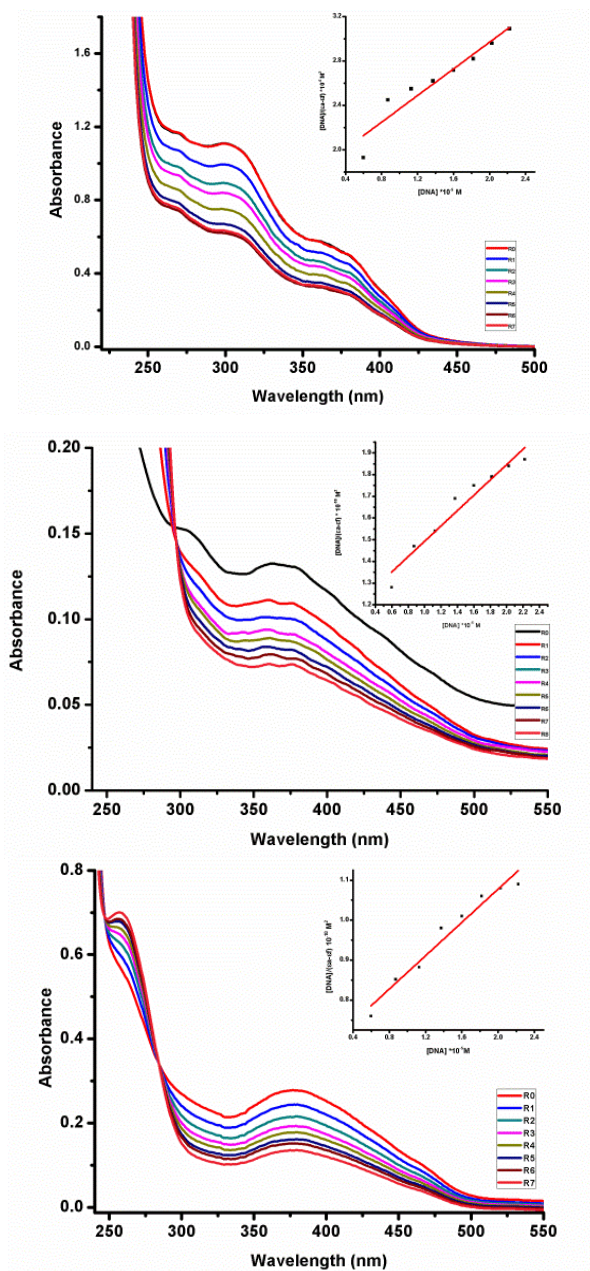


Figure 5.8 Absorption spectra for $[\text{Ni}(\text{FMN})(\text{OAc})] \cdot 2\text{H}_2\text{O}$ (7), $[\text{Cu}(\text{FMN})(\text{OAc})] \cdot \text{H}_2\text{O}$ (15) & $[\text{Zn}(\text{FMN})(\text{OAc})] \cdot \text{H}_2\text{O}$ (23) in *Tris*-HCl buffer upon addition of DNA. $R_0, R_1, R_2, R_3, R_4, R_5, R_6$ & $R_7 = 0.0, 0.2, 0.4, 0.6, 0.8, 1.0, 1.2$ & 1.4 ; $R = [\text{DNA}]/[\text{complex}]$. Inset graph of $[\text{DNA}]/(\epsilon a - \epsilon_f)$ vs. $[\text{DNA}]$ for titration of DNA with compounds.

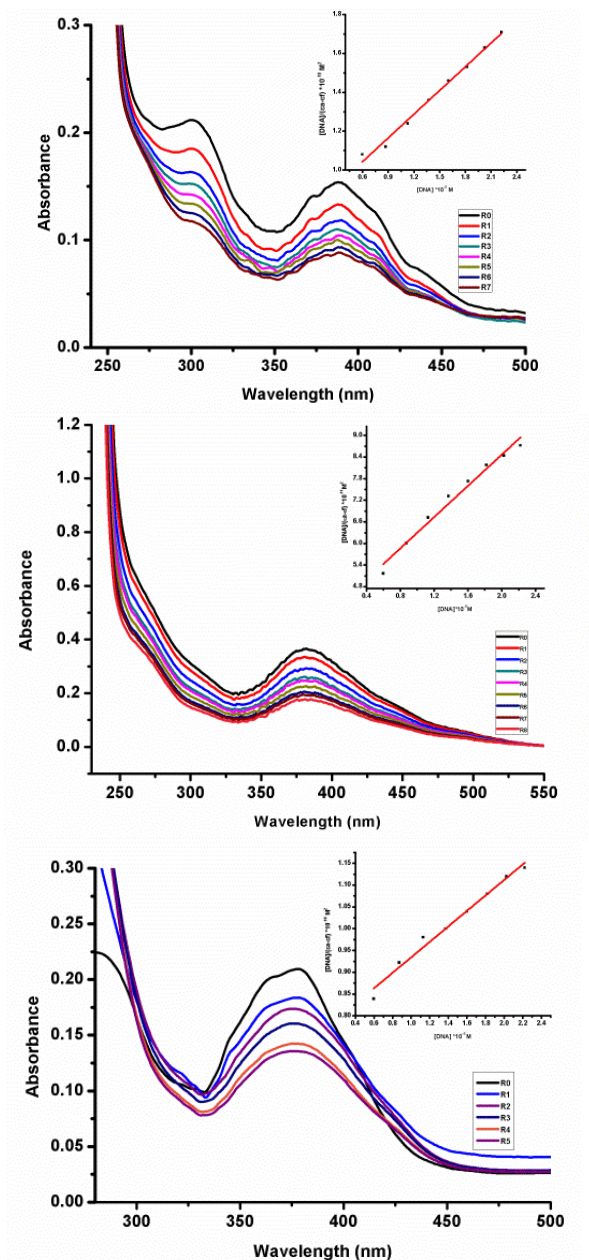


Figure 5.9 Absorption spectra for $[\text{Ni}(\text{FMIN})(\text{OAc})(\text{H}_2\text{O})].1.5 \text{ H}_2\text{O}$ (8), $[\text{Cu}(\text{FMIN})(\text{OAc})(\text{H}_2\text{O})].\text{H}_2\text{O}$ (16) & $[\text{Zn}(\text{FMIN})(\text{OAc})].0.5 \text{ H}_2\text{O}$ (24) in *Tris*-HCl buffer upon addition of DNA. $R_0, R_1, R_2, R_3, R_4, R_5, R_6$ & $R_7 = 0.0, 0.2, 0.4, 0.6, 0.8, 1.0, 1.2$ & 1.4 ; $R = [\text{DNA}]/[\text{complex}]$. Inset graph of $[\text{DNA}]/(\epsilon a - \epsilon f)$ vs. $[\text{DNA}]$ for titration of DNA with compounds.

These results indicate that all the synthesized complexes were strongly interact with DNA by intercalative mode that is metal complexes having high affinity towards DNA.

Table 5.1 Binding constant (K_b) M^{-1}

Complexes	λ_{max}		$\Delta\lambda$	H%*	Binding constant (K_b) $\times 10^4 M^{-1}$
	Free	Bound			
[Ni(FB)(OAc)(H ₂ O)].2H ₂ O (1)	351.2	352.3	1.1	15	4.44
[Cu(FB)(OAc)].H ₂ O (9)	375.4	376.2	0.8	60	2.46
[Zn(FB)(OAc)].2.5H ₂ O (17)	367.8	368.4	1.1	10	2.70
[Ni(FBH)(H ₂ O)(OAc)].2H ₂ O (2)	321.5	322.7	1.2	28	1.52
[Cu(FBH)(H ₂ O)(OAc)].H ₂ O (10)	377.3	378.9	1.6	68	3.30
[Zn(FBH)(OAc)] (18)	368.1	369.5	1.4	15	2.71
[Ni(FN)(OAc)].H ₂ O (3)	315.7	316.3	1.0	7	4.41
[Cu(FN)(OAc)].2H ₂ O (11)	381.2	382.8	1.6	41	2.99
[Zn(FN)(OAc)].H ₂ O (19)	369.7	370.3	0.9	15	3.38
[Ni(FIN)(OAc)(H ₂ O)].H ₂ O (4)	383.5	384.7	1.2	27	3.50
[Cu(FIN)(OAc)(H ₂ O)].2H ₂ O (12)	368.2	369.5	1.3	39	3.19
[Zn(FIN)(OAc)] (20)	278.5	279.9	1.4	44	2.96

Table 5.2 Binding constant (K_b) M^{-1}

Complex	λ_{max}		$\Delta\lambda$	H%*	Binding constant (K_b) $\times 10^4 M^{-1}$
	Free	Bound			
[Ni(FMB) ₂ (H ₂ O) ₂].H ₂ O (5)	371.4	372.7	1.3	25	4.41
[Cu(FMB) ₂ (H ₂ O) ₂].H ₂ O (13)	368.5	369.2	0.7	46	33.8
[Zn(FMB) ₂].2H ₂ O (21)	357.7	358.5	0.8	23	1.58
[Ni(FBH) ₂ (H ₂ O) ₂].2H ₂ O (6)	364.8	365.9	1.1	12	4.85
[Cu(FMBH) ₂ (H ₂ O) ₂].2H ₂ O (14)	373.3	374.2	0.9	35	3.94
[Zn(FMBH)(OAc)]. H ₂ O (22)	361.3	362.7	1.4	42	4.85
[Ni(FMN)(OAc)].2H ₂ O (7)	312.3	313.7	1.4	16	1.2
[Cu(FMN)(OAc)].H ₂ O (15)	374.5	375.2	0.7	22	5.24
[Zn(FMN)(OAc)].H ₂ O (23)	389.7	390.6	0.9	34	3.14
[Ni(FMIN)(OAc)(H ₂ O)].1.5 H ₂ O (8)	394.2	395.1	0.9	17	5.14
[Cu(FMIN)(OAc)(H ₂ O)].H ₂ O (16)	397.1	398.2	1.1	21	30.8
[Zn(FMIN)(OAc)].0.5 H ₂ O (24)	386.5	387.2	0.7	25	2.33

$$*H\% = \frac{A_{free} - A_{bound}}{A_{free}} * 100$$

5.3.2 Viscosity measurement

To clarify the interaction mode of the mononuclear metal (II) complexes with CT-DNA, viscosity measurements were carried out. In classical intercalation, the DNA helix lengthens as base pairs are separated to accommodate the bound ligand leading to increase in DNA viscosity, whereas a partial, non-classical ligand intercalation causes a bend in DNA helix reducing its effective length and thereby its viscosity. Therefore viscosity measurement is regarded as the least ambiguous and the most critical means studying the binding mode of metal complexes with DNA in solution and provides stronger arguments for intercalative binding mode [31]. The effects of the metal (II) complexes on the viscosity of CT-DNA are shown in Figures 5.10-5.13 and Tables 5.3-5.6. As illustrated in this figures, on increasing the amount of the metal (II) complexes, the relative viscosity of CT-DNA increasing steadily, which is proved that the metal (II) complexes bound to CT-DNA by intercalation. This phenomenon may be explained by the insertion of the complexes in between the DNA base pairs, leading to an increase in the separation of base pairs at intercalation sites and, thus, an increase in overall DNA length. It is clear from the figures that all these complexes show increase in the relative viscosity of CT-DNA but less compare to that of ethidium bromide except for copper complexes [Cu(FN)(OAc)].2H₂O (11), [Cu(FMB)₂(H₂O)₂].H₂O (13) & [Cu(FMIN)(OAc)(H₂O)].H₂O (16). The viscosity results may reflect the tendency of each complex to intercalate into DNA base pairs. The increase in DNA viscosity observed in the complexes, suggests a classical intercalative mode.

Table 5.3 Viscosity data of the Ni(II), Cu(II), Zn(II) complexes of FB & FBH

[complex]/ [DNA]	$(\eta/\eta_0)^{1/3}$						
	(1)	(9)	(17)	(2)	(10)	(18)	EB
0.00	1.0000	1.0000	1.0000	1.0000	1.0000	1.0000	1.0000
0.04	1.6228	1.2888	1.4731	1.4369	1.5757	1.2665	1.7856
0.08	1.9309	1.5036	1.722	1.6081	1.9024	1.4102	2.0021
0.12	2.0578	1.6239	1.855	1.6719	2.0782	1.4633	2.2345
0.16	2.1617	1.7467	1.9574	1.8119	2.1742	1.5874	2.3456
0.20	2.2088	1.914	2.0238	1.8526	2.2389	1.6267	2.4697

Table 5.4 Viscosity data of the Ni(II), Cu(II), Zn(II) complexes of FN & FIN

[complex]/ [DNA]	$(\eta/\eta_0)^{1/3}$						
	(3)	(11)	(19)	(4)	(12)	(20)	EB
0.00	1.0000	1.0000	1.0000	1.0000	1.0000	1.0000	1.0000
0.04	1.4152	1.9400	1.5354	1.5112	1.7235	1.2605	1.7856
0.08	1.8944	2.2632	1.6515	1.7404	2.0712	1.4658	2.0021
0.12	1.9608	2.3893	1.8344	1.864	2.2536	1.5928	2.2345
0.16	2.1894	2.4341	2.0591	1.9918	2.3708	1.7379	2.3456
0.20	2.2055	2.4943	2.1192	2.1238	2.3826	1.8556	2.4697

Table 5.5 Viscosity data of the Ni(II), Cu(II), Zn(II) complexes of FMB & FMBH

[complex]/ [DNA]	$(\eta/\eta_0)^{1/3}$						
	(5)	(13)	(21)	(6)	(14)	(22)	EB
0.00	1.0000	1.0000	1.0000	1.0000	1.0000	1.0000	1.0000
0.04	1.2736	1.8311	1.2554	1.2698	1.6649	1.1822	1.7856
0.08	1.4252	2.2725	1.4084	1.4517	2.0561	1.3141	2.0021
0.12	1.5463	2.3608	1.5281	1.6463	2.0964	1.4187	2.2345
0.16	1.6687	2.4121	1.6325	1.6934	2.1802	1.5181	2.3456
0.20	1.7734	2.4991	1.7249	1.7331	2.2405	1.5995	2.4697

Table 5.6 Viscosity data of the Ni(II), Cu(II), Zn(II) complexes of FMN & FMIN

[complex]/ [DNA]	$(\eta/\eta_0)^{1/3}$						
	(7)	(15)	(23)	(8)	(16)	(24)	EB
0.00	1.0000	1.0000	1.0000	1.0000	1.0000	1.0000	1.0000
0.04	1.5445	1.6621	1.2702	1.6509	2.057	1.0572	1.7856
0.08	1.7116	1.9165	1.4023	2.0232	2.524	1.2721	2.0021
0.12	1.8372	2.0394	1.5057	2.1627	2.5893	1.4039	2.2345
0.16	1.9576	2.1119	1.6015	2.2663	2.6781	1.4973	2.3456
0.20	2.0884	2.1386	1.6923	2.2948	2.8067	1.5225	2.4697

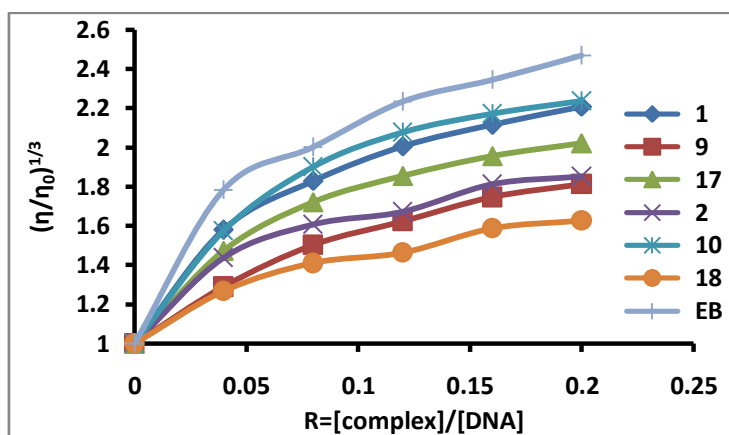


Figure 5.10 Plot of $[\eta/\eta_0]^{1/3}$ versus [Complex]/[DNA] for Ni(II), Cu(II), Zn(II) complexes of FB & FBH

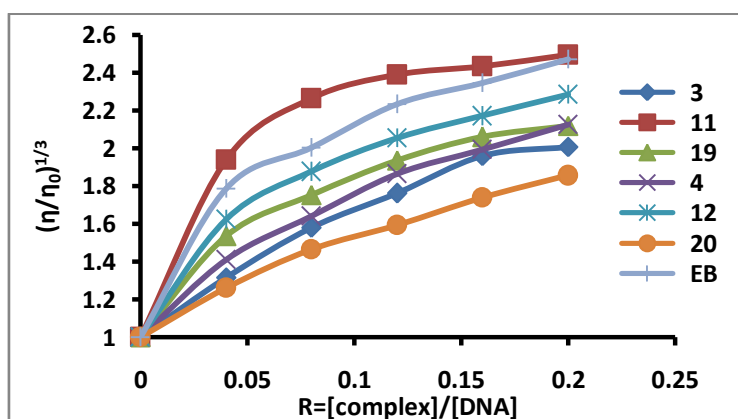


Figure 5.11 Plot of $[\eta/\eta_0]^{1/3}$ versus [Complex]/[DNA] for Ni(II), Cu(II), Zn(II) complexes of FN & FIN

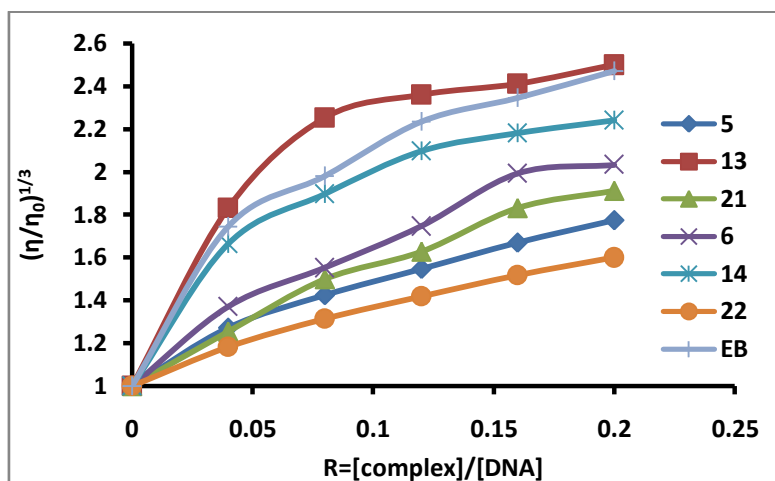


Figure 5.12 Plot of $[\eta/\eta_0]^{1/3}$ versus $[\text{Complex}]/[\text{DNA}]$ for Ni(II), Cu(II), Zn(II) complexes of FMB & FMBH

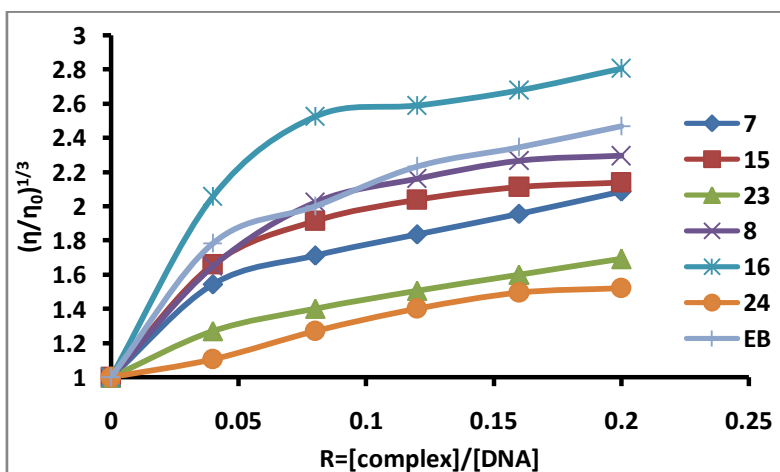


Figure 5.13 Plot of $[\eta/\eta_0]^{1/3}$ versus $[\text{Complex}]/[\text{DNA}]$ for Ni(II), Cu(II), Zn(II) complexes of FMN & FMIN

5.4 Conclusion

The present investigations was consider the binding behavior of different chromone hydrazones and their Ni (II), Cu (II) and Zn (II) complexes towards CT-DNA. Upon electronic absorption spectral titrations, all the synthesized metal complexes showed hypochromism. DNA-binding studies with CT-DNA indicate that metal complexes bind to DNA by intercalation mode. Observed intrinsic binding constant (ranging from 10^4 - 10^5 M⁻¹) is comparable to other intecalaters. Result from viscosity measurments clearly reveals that binding of DNA with metal (II) complexes is through intercalation. Results also showed that copper (II) complexes [Cu(FN)(OAc)].2H₂O (11), [Cu(FMB)₂(H₂O)₂].H₂O (13) & [Cu(FMIN)(OAc)(H₂O)].H₂O (16) have higher relative viscosity values than standard intercalators ethidium bromide.

References

- [1] U. Schatzschneider, J. Niesel, I. Ott, R. Gust, H. Alborzina, S. Wolf, *Chem. Med. Chem.*, 3 (2008) 1104.
- [2] L. F. Tan, J. L. Shen, X. J. Chen, X. L. Liang, *DNA Cell Biol.*, 28 (2009) 461.
- [3] Y. J. Liu, C. H. Zeng, Z. H. Liang, J. H. Yao, H. L. Huang, Z. Z. Li, F. H. Wu, *Eur. J. Med. Chem.*, 45 (2010) 3087.
- [4] S. Shi, X. T. Geng, J. Zhao, T. M. Yao, C. R. Wang, D. J. Yang, L. F. Zheng, L. N. Ji, *Biochimie.*, 92 (2010) 370.
- [5] J. Tan, B. C. Wang, L. C. Zhu, *Bioorg. Med. Chem.*, 17 (2009) 614.
- [6] G. Zuber, J. C. Quada, S. M. Hecht Jr., *J. Am. Soc. Chem.*, 120 (1998) 9368.

- [7] (a) S. M. Hecht, *J. Nat. Prod.* 63 (2000) 158. (b) H. Sigel (Edn.), vol. 33, Marcel Dekker, New York, 1996, p. 177.
- [8] V. G. Vaidyanathan, B. H. Nair, *Dalton Trans.*, 0 (2005) 2842.
- [9] P. U. Maheswari, M. Palaniandavar, *Inorg. Chim. Acta*, 357 (2004) 901.
- [10] J. R. J. Sorenson, in: G. Berthon (Ed.), *Handbook on Metal-Ligand Interactions in Biological Fluids: Bioinorganic Medicine*, vol. 2, Marcel Dekker, New York, 1995, pp. 1128.
- [11] C. W. Jiang, H. Chao, H. Li, L. N. Ji, *J. Inorg. Biochem.*, 93 (2003) 247.
- [12] M. Shebl, *J. Mol. Struct.*, 1128 (2017) 79.
- [13] J. Wang, Z. Y. Yang, X. Y. Yi, B. D. Wang, *J. Photochem. Photobiol.*, 201 (2009) 183.
- [14] N. Raman, R. Mahalakshmi, L. Mitu, *Spectrochim. Acta A*, 115 (2013) 399.
- [15] Y. Iwasaki, M. Kimura, A. Yamada, Y. Mutoh, M. Tateishi, H. Arii, Y. Kitamura, M. Chikira, *Inorg. Chem. Commun.*, 114 (2011) 1569.
- [16] Y. Ni, D. Lin, S. Kokot, *Anal. Biochem.*, 352 (2006) 231.
- [17] C.Y. Zhou, J. Zhao, Y. B. Wu, C. X. Yin, Y. Pin, *J. inorg.biochem.*, 101 (2007) 10.
- [18] H. Farrokhpour, H. Hadadzadeh, F. Darabi, F. Abyar, H. A. Rudbari, T. A. Bagheri *RSC adv.*, 4 (2014) 35390.
- [19] F. Darabi, H. Hadadzadeh, J. Simpson, A. Shahpir, *New J. Chem.*, 40 (2016) 9081.
- [20] R. E. Panah, H. Hadadzadeh, H. Farrokhpour, M. Mortazavi, Z. Amirghofran, *Inorganica Chim. Acta*, 454 (2017) 184.
- [21] Z. S. pour, H. Chiniforoshan, A. A. Momtazi-borojeni, B. Notash, *J. Photochem. Photobiol.*, 162 (2016) 34.

- [22] M. Manjunath, A. D. Kulkarni, G. B. Bagihalli, S. Malladi, S. A. Patil, *J. Mol. Struct.*, 1127 (2017) 314.
- [23] N. Raman, R. Mahalakshmi, L. Mitu, *Spectrochim. Acta A*, 131 (2014) 355.
- [24] Y. Iwasaki, M. Kimura, A. Yamada, Y. Mutoh, M. Tateishi, H. Ariei, Y. Kitamura, M. Chikira *Inorg. Chem. Commun.*, 14 (2011) 1461.
- [25] P. Krishnamoorthy, P. Sathyadevi, K. Senthilkumar, P. T. Muthiah, R. Ramesh, N. Dharmaraj, *Inorg. Chem. Commun.*, 14 (2011) 1318.
- [26] A. K. Asatkar, M. Tripathi, S. Panda, R. Pande, S. S. Zade, *Spectrochim. Acta A*, 171 (2017) 18.
- [27] N. Nanjundan, R. Narayanasamy, S. Geib, K. Velmurugan, R. Nandhakumar, M. D. Balakumaran, P. T. Kalaichelvan, *Polyhedron*, 110 (2016) 203.
- [28] R. Paulpandiyam, N. Raman, *J. Mol. Struct.*, 1125 (2016) 374.
- [29] Q. Wei, J. Dong, P. Zhao, M. Li, F. Cheng, J. Kong, L. Li, J. *Photochem. Photobiol.*, 161 (2016) 355.
- [30] N. Deepika, C. S. Devi, Y. P. Kumar, K. L. Reddy, P. V. Reddy, D. A. Kumar, S. S. Singh, S. Satyanarayana, *J. Photochem. Photobiol.*, 160 (2016) 142.
- [31] J. E. Philip, M. Shahid, M. R. P. Kurup, M. P. Velayudhan, *J. Photochem. Photobiol.*, 175 (2017) 178.
- [32] J. Marmu, *J. Mol. Biol.*, 3 (1961) 208.
- [33] M. E. Reichmann, S. A. Rice, C. A. Thomas, P. Doty, *J. Am. Chem. Soc.*, 76 (1954) 3047.
- [34] N. Arshad, S. I. Farooqi, M. H. Bhatti, S. Saleem, B. Mirza, *J. Photochem. Photobiol.*, 125 (2013) 70.
- [35] P. Krishnamoorthy, P. Sathyadevi, A. H. Cowley, R.R. Butorac, N. Dharmaraj, *Eur. J. Med. Chem.*, 46 (2011) 3376.

- [36] A. M. Pyle, T. Morii, J. K. Barton, *J. Am. Chem. Soc.*, 112 (1990) 9432.
- [37] J. K. Barton, J. M. Goldberg, C.V. Kumar, N. J. Turro, *J. Am. Chem. Soc.*, 108 (1986) 2081.
- [38] T.Ghosh, B. Mondal, T. Ghosh, M. Sutradhar, G. Mukherjee, *Inorg. Chim Acta.*, 360. (2007) 1753.
- [39] M. A. Affan, S. W.Foo, I. Jusoh, S. Hanapi, E. Tiekink, *Inorg. Chim Acta*, 362. (2009) 5031

.....❧.....

Chapter 6

STUDY OF *IN VITRO* INHIBITION OF α -AMYLASE AND α -GLUCOSIDASE BY CHROMONE HYDRAZONES AND THEIR Ni (II), Cu (II) AND Zn (II) COMPLEXES

Contents

- 6.1 Introduction
- 6.2 Materials and Methods
- 6.3 Result and Discussion
- 6.4 Conclusion

Conspectus: Various flavonoids have shown efficacy in the treatment of diabetes. Although it is often assumed that dietary flavonoids exert biological antioxidant effects, it is possible that the observed effects work on carbohydrate metabolism. In this study, we evaluated the effect of chromone hydrazones and their Ni (II), Cu (II) and Zn (II) complexes on α -amylase and α -glucosidase activity, enzymes of great importance in carbohydrate metabolism and diabetes mellitus. In all tests, acarbose, a pharmacological inhibitor of α -amylase and α -glycosidase was included as a positive control. For each compound, the concentration required for 50% inhibition of enzyme activity was determined to compare the potency. For α -amylase, metal complexes demonstrated a similar α -amylase inhibitory activity to acarbose and hydrazones showed a weaker inhibition. In α -glucosidase experiments, copper complexes inhibited enzymatic activity much more strongly than acarbose. The inhibitory activities of individual compounds were also reported. Also determined their kinetic parameters by Michaelis-Menten plot and mode of action against enzymes (α -amylase and α -glucosidase) were determined by using Lineweaver–Burk plot. With this information, it is possible that chromone hydrazones and their Ni (II), Cu (II) and Zn (II) complexes play a role in the prevention or treatment of type II diabetes mellitus.

6.1 Introduction

More than 190 million people worldwide suffer from diabetes [1] a disease characterized by elevated levels of fasting blood glucose as a result of the body's inability to produce or use insulin. The World Health Organization expects the incidence of diabetes to double by 2025. There are two classifications of diabetes mellitus. Type I, characterized by autoimmune destruction of the insulin-producing beta cells of the pancreas, results in an inability to process glucose from the bloodstream. The second classification of this disease is called type II and is characterized by abnormalities in both insulin secretion and action resulting from lifestyle choices and some genetic influence [2]. As with most lifestyle-related diseases, diabetes is a chronic and progressive disease [3]. Type II is especially common among aging populations, and those with unhealthy diets, obesity, and sedentary lifestyles [4].

Overall, diabetes spending in the United States in 2007 is estimated at \$ 174 billion, or \$ 116 billion in surplus health spending and \$ 58 billion in lower production of goods and services in the US economy. In particular, these expenses included 27 billion for direct diabetes treatment and 58 billion for the treatment of diabetes complications, both acute and chronic, and account for 11% of all health care costs in 2007 [5]. Complications include microvascular diseases such as diabetic retinopathy, nephropathy and neuropathy, and macrovascular complications such as atherosclerosis, coronary heart disease and cerebrovascular disease. Spend the most common implications and long-term diabetes, such as glaucoma, cataracts, and foot health and death problems, worth \$ 31 billion [6]. A diabetic patient in 2007 had health costs of about 2.3 times higher than

patients without diabetes [5]. Diabetes and its complications have a negative impact on the quality of life in a patient's health as symptoms progress to these micro and macrovascular complications [2].

Debilitating symptoms, expensive treatments and diabetes complications can be prevented or delayed by a tight glycemic control [7]. However, it is well known that maintenance of blood glucose levels below 110 mgdL^{-1} [8] in fasting diabetic patients is often very difficult. Many current research and alternative therapies focus on various ways to control hyperglycaemia, addressing various organs involved in glucose metabolism as a solution to the symptoms and the treatment of diabetes. One of the treatment options currently available for glycemic control is meglitinide and sulphonylureas. This reduces glucose levels in the blood, increasing the preprandial insulin secretion, but presents serious risks of hypoglycemia compared with other treatments [9-10]. Another therapy uses thiazolidinediones to increase the sensitivity of adipose and muscular cells to insulin by activating signals that activate the synthesis of receptor proteins activated by peroxisome proliferators [11]. Greater sensitivity helps to reduce blood sugar levels, but unfortunately at increased risk of congestive heart failure and bone fractures [9]. Metformin is recognized as a first-line agent for the treatment of type II diabetes [9] and is part of a class of therapeutic drugs called biguanide. This class of drugs triggers a cascade of events that eventually blocks liver glucose release and maintains a fasting blood sugar. Once again, this treatment is associated with an increased risk of gastrointestinal side effects and requires insulin [9-10].

Another type of treatment for type II diabetes is to limit the amount of glucose that reaches the bloodstream. Digestion of starch to glucose requires multiple reactions involving two primary enzymes, α -amylase and α -glucosidase. These enzymes, collectively known as glucosidases, play an essential role in carbohydrate metabolism [12]. α -Amylase is both a component of saliva and pancreas as an endohydrolase that cleaves the internal α -(1,4) bonds of starch into shorter, linear and branched dextrin chains. The resulting dextrin mixture is hydrolyzed into glucose by α -glucosidase, located at the intestinal brush microvilli [13]. The complementary activities of these two enzymes allow for digestion of a spectrum of food starches from more than 400 plants that comprise two-thirds of most human diets [14]. α -Glucosidase inhibitors are drugs that inhibit glucosidases in the intestine and suppress the postprandial elevation of plasma glucose by delaying the digestion and absorption of carbohydrates [8,10]. The overall effect of inhibiting glucosidase also reduces the onset of insulin resistance, preventing other insulin-dependent disorders [14]. Inhibition of pancreatic α -amylase, in particular is an important therapeutic goal of type II diabetes [15]. Currently, there are two pharmaceutical glucosidase inhibitors that have demonstrated their value in the fight against high blood glucose: acarbose and miglitol (Figure 6.1) [14]. These compounds show a higher inhibitory activity for α -glucosidase compared to α -amylase, and competitively as well as noncompetitively and reversibly inhibit both enzymes [14-15]. However, acarbose has a greater affinity for α -glucosidase and α -amylase inhibition due to the ability of analogue tetrascaccharides to occupy extensive C-terminal catalytic subunit sites against the occupation of N-terminal

domains of enzyme [14]. In addition, these drugs are often used in combination with other oral hypoglycemic agents with different mechanisms of action, such as those mentioned above or with insulin [8].

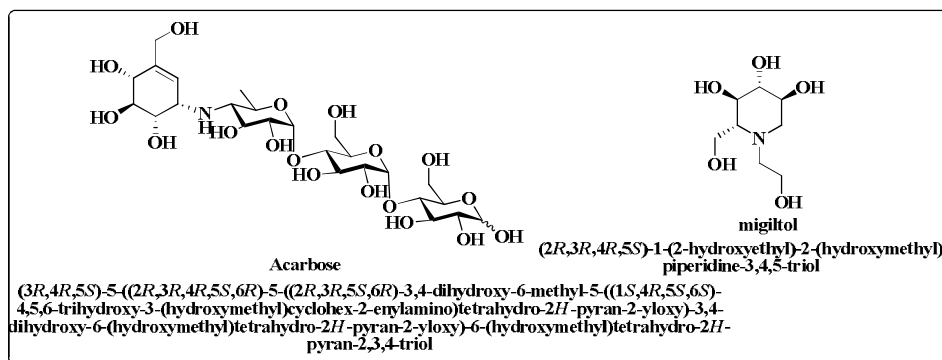


Figure 6.1 Structures of Acarbose and Miglitol

The tetrasaccharide structure of acarbose provides a distinguishing characteristic and an ability to occupy extended binding site of the C-terminal catalytic subunits of glucosidases.

Unfortunately, gastrointestinal side effects such as abdominal pain, flatulence and diarrhea from undigested starches are among the disadvantages of drugs that inhibit α -glucosidase due to relatively high doses to be prescribed [14,17]. In addition, a higher risk of fatal hypoglycaemia to metabolize too little glucose due to the potent drug effect outweighs the benefits of pharmaceutical intervention [18].

Bioflavonoids are a large family of polyphenolic compounds having a common chemical structure and are found in vegetable food. These polyphenols (polyhydroxylated aromatic phytochemicals) are separated into classes of flavonoids and phenolic acids. Flavonoids can be subdivided

into structural classes of flavones, flavanones, flavonols, flavan-3-ol (or catechins) and anthocyanidins. Flavonoids are particularly interesting for their antioxidant and anti-inflammatory action reported [19]. In addition, flavan-3-ols were specifically considered to inhibit the digestion of oligosaccharide by α -amylase and α -glucosidase [20]. As explained above, the inhibition of these digestive enzymes in carbohydrates may be beneficial for patients with type II diabetes as well as for the pre-diabetic population growth in the United States and around the world [10, 21-22]. Included in the structural family of flava-3-ols and commonly known as catechins are the flavan-3-ol monomers and their oxidative coupling products, theaflavins.

Therefore, it is conceivable that natural and dietary glucosidase inhibitors, which probably have fewer side effects than drugs, may be useful in the prevention or treatment of type II diabetes and pre-diabetes.

It is well known that control of postprandial glycaemia is very essential in controlling long term deleterious effect of hyperglycemia. In the present chapter, we propose to investigate the effect of compounds in the following enzyme inhibition assay.

- Alpha-amylase inhibition assay
- Alpha-glucosidase inhibition assay.

6.1.1 Importance Alpha-amylase enzyme in the body

In humans, the digestion of starch involves several stages. Initially, partial digestion by the salivary amylase results in the degradation of polymeric substrates into shorter oligomers. Later on in the gut these are further hydrolyzed by pancreatic amylases into maltose, maltotriose and small malto-oligosaccharides. The digestive enzyme (α -amylase) is

responsible for hydrolyzing dietary starch (maltose), which breaks down into glucose prior to absorption. Inhibition of α -amylase can lead to a reduction in postprandial hyperglycemia in diabetic condition [23].

6.1.2 Importance of Alpha-glucosidase enzyme in the body

Alpha-glucosidase is a membrane bound enzyme located in the epithelium of the small intestine, catalyzing the cleavage of starch and disaccharides to form glucose. Inhibitors can retard the uptake of dietary carbohydrates and suppress post-prandial hyperglycemia. Therefore, inhibition of α -glucosidase could be one of the most effective approaches to control diabetes [24]. Glucosidases are not only essential to carbohydrate digestion, but also vital for the processing of glycoprotein and glycolipids. This enzyme is a target for antiviral agents that interfere with the formation of essential glycoproteins required in viral assembly, secretion and infection [25]. Glucosidases are also involved in a variety of metabolic disorders and carcinogenesis [26].

6.1.3 α -Amylase inhibitors

Alpha Amylase is an endo-acting enzyme that catalyzes the hydrolysis of α -1,4-D-glycosidic linkages of starch, amylose, amylopectin, glycogen, and various maltodextrins. α -Amylases are produced by a variety of organisms, including bacteria, fungi, plants, and animals. α -Amylase inhibitors have many medical applications, such as controlling blood glucose and serum insulin levels, and starch loading tests in animals and humans[27].

6.1.4 α -Glucosidase inhibitors

Alpha Glucosidase inhibitors are used to treat type II diabetes and obesity by suppressing the absorption of glucose and reducing postprandial

hyperglycemia. Current interest in these compounds has been extended to a diverse range of diseases including lysosomal storage disorders, cancer and AIDS [28].

6.2 Materials and Methods

The chromone hydrazones and their Ni (II), Cu (II) and Zn (II) complexes were synthesized as described in Chapter 2 and Chapter 3. These, were serially diluted to get a required concentration to perform both α -amylase and α -glucosidase enzyme inhibition assays.

- α -Amylase [15.8 U/mg solid at pH 6.9]-stored at 0-4°C (Himedia).
- α -Glucosidase [15 U/mL at pH 6.9]-stored at 0-4°C (Sigma Aldrich).
- 3, 5-Dinitrosalicylic acid (DNSA)-stored at RT (Sigma Aldrich).
- Starch 1%.
- p-Nitrophenyl- β -D-glucopyranoside (p-NPG 5mM)-stored at 0-4°C (Sigma Aldrich).
- Sodium carbonate (0.1 M Na₂CO₃)-stored at RT (Sigma Aldrich).
- Positive Control: Acarbose-stored at RT (Bayer Pharmaceuticals, Leverkusen, Germany).
- Sodium dihydrogen orthophosphate (NaH₂PO₄.2H₂O)-stored at RT (Sigma Aldrich).
- Disodium hydrogen phosphate (Na₂HPO₄.2H₂O)-stored at RT (Sigma Aldrich).

6.2.1 Determination of enzyme activity

6.2.1.1 Alpha-amylase inhibition assay

6.2.1.1.1 *Alpha-amylase enzyme solution*

α -Amylase was purchased from Himedia Company. According to the manufacture product description, one α -amylase unit was defined as the amount of enzyme required to release 1 mM maltose/min at 37°C from substrate (starch) under the given experimental conditions. The enzyme concentration used in the assay was 0.083 mg mL⁻¹ [29]. Enzyme powder was dissolved in pre-chilled 0.02 M sodium phosphate buffer, pH 6.9 with 0.006 M sodium chloride, yielding a clear to hazy solution. This is due to the presence of enzyme carriers, lactose, which are partially soluble in the chilled buffer. The enzyme solution was prepared freshly and stored at temperature below 4°C prior to assay.

6.2.1.1.2 *Sodium phosphate buffer (0.02 M), pH 6.90 with 0.006 M sodium chloride*

The following three solutions were prepared separately. 200 mL dH₂O was added to 1.582 g of Na₂HPO₄, 200 mL dH₂O was added to 1.062 g of Na₂PO₄, and 100 mL dH₂O was added to 0.3506 g of NaCl. All three solutions were then mixed well followed by the addition of 400 mL dH₂O as to obtain the desirable pH of 6.90. If the pH deviated from 6.90, the pH was adjusted by adding either Na₂HPO₄ as a base or NaH₂PO₄ as acid. Finally the solution was brought up to the final volume of 1000 mL in standard bottle. The buffer prepared was stored at 25°C and used within 2 weeks [29].

6.2.1.1.3 Dinitrosalicylic acid (DNSA) reagent

The original DNSA reagent developed by Miller, G. L. (1959) [30]. Contained 0.63% DNSA, 18% tartrate, 0.5% phenol, 0.5% sodium bisulfite, and 14% NaOH. A modified DNSA reagent used in this study it was prepared by dissolving (constantly stirring) 2% (w/v) of DNSA with 1% NaOH. The other component of the modified DNSA reagent, the 18.2 % (w/v) potassium sodium tartrate, also known as Rochelle salts, was prepared separately using dH₂O. The reagent was prepared freshly prior to assay. In addition, this colour reagent should be protected from all light sources.

6.2.1.1.4 Starch solution (1%)

Soluble starch (1g) was dissolved in 100 mL of sodium phosphate buffer. Constant stirring at 90°C helped the dissolution of starch in the buffer. The starch solution was then cooled and stored at 4°C. The starch solution was incubated at 25°C for 5 minutes prior to assay.

6.2.1.1.5 Determination of alpha-amylase inhibitory activity

The inhibitory capability for α -amylase was conducted based on the procedure of Shetty et al. [31]. An aliquot of varying concentrations (0.033-0.167 mM) of the sample were prepared and 500 μ L of each was mixed with 500 μ L of 0.02 M sodium phosphate buffer (pH 6.90) containing 0.083mg mL⁻¹ of α -amylase solution and incubated in test tubes at 37°C for 10 min. After pre-incubation, 500 μ L of 1% starch solution in 0.02 M sodium phosphate buffer (pH 6.90) was added to each tube at time intervals. The reaction mixtures were incubated at 37°C for 15 min and stopped with 1.0 mL of dinitrosalicylic acid colour reagent.

The tubes were then incubated in a boiling water bath for 5 min and subsequently cooled to room temperature. The reaction mixtures were then diluted with distilled water (10mL), and the absorbance were measured at 540 nm using a spectrophotometer and the values compared with a blank which contained 500 μ L of the buffer instead of the sample. Acarbose was prepared in DMSO at the same concentrations of the sample and used as control. The experiments were conducted in triplicate, and the α -amylase inhibitory activity was expressed as % inhibition. One α -amylase unit was defined as the amount of enzyme required to release 1 mM maltose/min at 37°C from substrate (starch) under the given assay conditions. The concentration of the compounds and acarbose causing 50% inhibition (IC_{50}) of α -amylase activity was estimated by the equation.

$$\% \text{ Inhibition} = \frac{Abs_{control} - Abs_{sample}}{Abs_{control}} * 100$$

6.2.1.1.6 Determination of kinetic parameters

For the determination of the kinetic parameters, the sample was taken at its IC_{50} value and incubated with α -amylase, while varying the starch (substrate) concentration from 0.3 to 5 mg mL⁻¹ and the reaction was allowed as mentioned above. The amount of maltose (reducing sugar) released was determined spectrophotometrically using a standard curve of maltose. The lineweaver-Burk double-reciprocal frame (1/[V] versus 1/[S]) was constructed and the kinetics of the inhibition of α -amylase by the sample were determined [17].

6.2.1.2 Alpha-glucosidase inhibition Assay

6.2.1.2.1 Alpha-glucosidase enzyme solution

The α -glucosidase solution (eg, extra-pure yeast) (15 U/mL) was prepared in 0.02 M phosphate buffer (pH 6.90) and stored at -20°C . One α -glucosidase unit activity was defined as the amount of enzyme required (at 37°C and pH 6.90) to the substrate (p-NPG) hydrolysis to produce 1 μM p-nitrophenol per minute [29].

6.2.1.2.2 0.02M sodium phosphate buffer (pH 6.90)

Method of preparation of 0.02M sodium phosphate buffer (pH 6.90) as described in Chapter 6 (6.2.1.1.b).

6.2.1.2.3 5mM p-nitrophenyl- β -D-glucopyranoside substrate solution

Sodium phosphate buffer (0.02M, pH 6.90) was slowly added into 5mM p-nitrophenyl- β -D-glucopyranoside until it fully dissolved. This solution was freshly prepared prior to running α -glucosidase assay.

6.2.1.2.4 Determination of alpha-glucosidase inhibitory activity

The α -glucosidase inhibitory activity was measured by modifying Kwon et al. The α -glucosidase solution was prepared in 0.02 M phosphate buffer (pH 6.90). Variable concentrations (0.033-0.167 mM) of the sample and 500 μL of each concentration were mixed with 500 μL of 0.02 M sodium phosphate buffer (pH 6.90) containing 0.1 mgmL^{-1} of solution of α -glucosidase and incubated in test specimens. After incubation for 15 minutes at 37°C , 20 mM of p-nitrophenyl- β -D-glucopyranoside (500 μL) was added. The reaction mixture was further incubated at 37°C for

20 minutes. The enzymatic reaction was stopped by adding a 0.1M Na_2CO_3 solution (1 mL). Blank set contain buffer instead of enzymatic solution and the control set consist of milliQ water in its place of sample. The absorbance of the yellow colour due to the formation of p-nitro phenol was monitored at 405 nm by spectrophotometrically. The control contains all reagents and the enzyme, except the test sample; acarbose used as a standard drug. One α -glucosidase unit was defined the quantity of enzyme required (at 37°C and pH 6.90) to the substrate (p-NPG) hydrolysis to produce 1 μM p-nitrophenol per minute. The concentration of compounds and acarbose causing 50% inhibition (IC_{50}) of α -glucosidase was determined by equation.

$$\% \text{ Inhibition} = \frac{\text{Abs}_{\text{control}} - \text{Abs}_{\text{sample}}}{\text{Abs}_{\text{control}}} * 100$$

6.2.1.2.5 Determination of kinetic parameters

For the determination of the kinetic parameters, the sample was taken at its IC_{50} value and incubated with α -glucosidase, while varying the p-NPG (substrate) concentration from 0.3-5 mg mL^{-1} and the reaction was allowed as mentioned above. The amount of p-nitrophenol released was determined spectrophotometrically using a standard curve of p-nitrophenol. The Lineweaver-Burk double-reciprocal frame ($1/[\text{V}]$ versus $1/[\text{S}]$) was constructed and the kinetics of the inhibition of α -glucosidase by the sample were determined [17].

6.3 Result and Discussion

6.3.1 Antidiabetic activity-(Enzyme Inhibition of α -amylase & α -glucosidase)

Diabetes mellitus, one of the oldest common metabolic disorders continue to be a leading cause of morbidity and mortality for the future. The inhibition of α -amylase activity, together with that of α -glucosidase is considered to be an effective strategy for management of diabetes by controlling the blood glucose level by delaying the digestion of carbohydrate after meal.

Alpha-amylase is an enzyme that causes hydrolysis of α -1,4-glycosidic bonds in starch and other polysaccharides and leads to the number of small sugar molecules such as maltose and glucose. When the amount of these small sugar molecules obtained as a result of the hydrolysis of α -amylase catalyzed polysaccharides exceeds, it is found in diabetes. Therefore, it is necessary to maintain the activity of α -amylase under control to avoid postprandial hyperglycemia (PPHG).

In this experiment, the coordination metal Ni, Cu and Zn (II) complex containing a biological important imine group (C=N) was chosen against the function of the enzymes. It was tested at different concentrations against the action of enzymes. Table 6.1 (α -amylase) and 6.2 (α -glucosidase) gives concentration of the sample for giving 50% inhibition for enzyme activity (IC_{50}). Inhibition activity of acarbose was also studied in the same concentrations for comparison. All the ligands and complexes inhibited α -amylase mildly and α -glucosidase strongly in concentration dependent manner.

Table 6.1 Enzyme inhibition study: α -amylase inhibitory activity and kinetic parameters. (The kinetics study for the tentative mode of inhibition revealed that a characteristic non-competitive (N) and competitive (C) inhibition for α -amylase. The double reciprocal plot revealed that the respective V_{max} values for the ligands, complexes and the control were shown in Table and Figures, while the K_m was 1.65 mM).

Compound	IC ₅₀ (mM)	V _{max} (μmolmin^{-1})	K _m	K _i	Mode of Inhibition
Acarbose (standard)	0.230 \pm 0.2	-	-	-	-
Control	-	0.617	1.65	-	-
FB	0.404 \pm 0.1	0.401	1.649	0.310	N
[Ni(FB)(OAc)(H ₂ O)].2H ₂ O (1)	0.321 \pm 0.2	0.409	1.65	0.329	N
[Cu(FB)(OAc)].H ₂ O (9)	0.267 \pm 0.1	0.425	1.65	0.369	N
[Zn(FB)(OAc)]. 2.5 H ₂ O (17)	0.299 \pm 0.3	0.414	1.65	0.341	N
FBH	0.438 \pm 0.1	0.487	1.65	0.628	N
[Ni(FBH)(H ₂ O)(OAc)].2H ₂ O (2)	0.372 \pm 0.2	0.421	1.65	0.360	N
Cu(FBH)(H ₂ O)(OAc)].H ₂ O (10)	0.231 \pm 0.1	0.347	1.65	0.210	N
[Zn(FBH)(OAc)] (18)	0.288 \pm 0.1	0.406	1.65	0.321	N
FN	0.455 \pm 0.1	0.475	1.65	0.587	N
[Ni(FN)(OAc)].H ₂ O (3)	0.371 \pm 0.2	0.408	1.65	0.325	N
[Cu(FN)(OAc)].2H ₂ O (11)	0.266 \pm 0.1	0.358	1.65	0.230	N
[Zn(FN)(OAc)].H ₂ O (19)	0.288 \pm 0.3	0.373	1.649	0.254	N
FIN	0.440 \pm 0.1	0.380	1.65	0.267	N
[Ni(FIN)(OAc)(H ₂ O)].H ₂ O (4)	0.344 \pm 0.2	0.413	1.65	0.337	N
[Cu(FIN)(OAc)(H ₂ O)].2H ₂ O (12)	0.265 \pm 0.1	0.365	1.65	0.245	N
[Zn(FIN)(OAc)] (20)	0.260 \pm 0.2	0.417	1.65	0.348	N
FMB	0.390 \pm 0.1	0.617	2.56	0.302	C
[Ni(FMB) ₂ (H ₂ O) ₂].H ₂ O (5)	0.328 \pm 0.2	0.617	2.49	0.327	C
[Cu(FMB) ₂ (H ₂ O) ₂].H ₂ O (13)	0.234 \pm 0.3	0.617	3.99	0.117	C
Zn(FMB) ₂].2H ₂ O (21)	0.297 \pm 0.1	0.617	2.23	0.471	C
FMBH	0.375 \pm 0.1	0.617	4.80	0.087	C
[Ni(FBH) ₂ (H ₂ O) ₂].2H ₂ O (6)	0.354 \pm 0.2	0.617	5.09	0.079	C
[Cu(FMBH) ₂ (H ₂ O) ₂].2H ₂ O (14)	0.211 \pm 0.1	0.617	5.11	0.081	C
Zn(FMBH)(OAc)] (22)	0.299 \pm 0.3	0.617	3.92	0.120	C
FMN	0.461 \pm 0.1	0.485	1.65	0.613	N
[Ni(FMN)(OAc)].2H ₂ O (7)	0.371 \pm 0.2	0.408	1.65	0.325	N
[Cu(FMN)(OAc)].H ₂ O (15)	0.263 \pm 0.2	0.485	1.65	0.613	N
[Zn(FMN)(OAc)].H ₂ O (23)	0.321 \pm 0.1	0.349	1.65	0.217	N
FMIN	0.454 \pm 0.1	0.380	1.65	0.267	N
Ni(FMIN)(OAc)(H ₂ O)].1.5 H ₂ O (8)	0.307 \pm 0.3	0.381	1.65	0.270	N
[Cu(FMIN)(OAc)(H ₂ O)].H ₂ O (16)	0.249 \pm 0.2	0.353	1.65	0.223	N
[Zn(FMIN)(OAc)].0.5 H ₂ O (24)	0.294 \pm 0.1	0.400	1.65	0.317	N

Table 6.2 Enzyme inhibition study: α -glucosidase inhibitory activity and kinetic parameters. (The kinetics study for the tentative mode of inhibition revealed that a characteristic non-competitive (N) and competitive (C) inhibition for α -glucosidase. The double reciprocal plot revealed that the respective V_{\max} values for the ligands, complexes and the control were shown in Table and Figures, while the K_m was 1.71mM)

Compound	IC ₅₀ (mM)	V _{max} (μmolmin^{-1})	K _m	K _i	Mode of Inhibition
Acarbose (standard)	0.170 \pm 0.1	-	-	-	-
Control	-	0.342	1.71	-	-
FB	0.268 \pm 0.1	0.210	1.71	0.267	N
[Ni(FB)(OAc)(H ₂ O)].2H ₂ O (1)	0.205 \pm 0.2	0.220	1.71	0.300	N
[Cu(FB)(OAc)].H ₂ O (9)	0.169 \pm 0.1	0.181	1.71	0.187	N
[Zn(FB)(OAc)].2.5H ₂ O (17)	0.194 \pm 0.2	0.184	1.71	0.195	N
FBH	0.279 \pm 0.1	0.255	1.71	0.486	N
[Ni(FBH)(H ₂ O)(OAc)].2H ₂ O (2)	0.238 \pm 0.3	0.223	1.71	0.312	N
[Cu(FBH)(H ₂ O)(OAc)].H ₂ O (10)	0.151 \pm 0.1	0.215	1.71	0.281	N
[Zn(FBH)(OAc)] (18)	0.183 \pm 0.1	0.184	1.71	0.195	N
FN	0.286 \pm 0.2	0.342	5.78	0.070	C
[Ni(FN)(OAc)].H ₂ O (3)	0.237 \pm 0.1	0.342	3.25	0.186	C
[Cu(FN)(OAc)].2H ₂ O (11)	0.159 \pm 0.3	0.342	4.25	0.112	C
[Zn(FN)(OAc)].H ₂ O (19)	0.182 \pm 0.1	0.342	5.58	0.074	C
FIN	0.280 \pm 0.1	0.202	1.71	0.240	N
[Ni(FIN)(OAc)(H ₂ O)].H ₂ O (4)	0.218 \pm 0.2	0.217	1.71	0.289	N
[Cu(FIN)(OAc)(H ₂ O)].2H ₂ O (12)	0.168 \pm 0.1	0.178	1.71	0.182	N
[Zn(FIN)(OAc)] (20)	0.178 \pm 0.3	0.220	1.71	0.302	N
FMB	0.246 \pm 0.1	0.342	2.46	0.383	C
[Ni(FN)(OAc)].H ₂ O (3)	0.209 \pm 0.2	0.342	3.01	0.221	C
[Cu(FN)(OAc)].2H ₂ O (11)	0.147 \pm 0.1	0.342	4.37	0.108	C
[Zn(FN)(OAc)].H ₂ O (19)	0.180 \pm 0.2	0.342	2.48	0.372	C
FMBH	0.239 \pm 0.3	0.253	1.71	0.477	N
[Ni(FBH) ₂ (H ₂ O) ₂].2H ₂ O (6)	0.232 \pm 0.1	0.193	1.71	0.217	N
[Cu(FMBH) ₂ (H ₂ O) ₂].2H ₂ O (14)	0.130 \pm 0.3	0.197	1.71	0.226	N
Zn(FMBH)(OAc) (22)	0.188 \pm 0.1	0.215	1.71	0.281	N
FMN	0.292 \pm 0.2	0.258	1.71	0.510	N
[Ni(FMN)(OAc)].2H ₂ O (7)	0.238 \pm 0.1	0.210	1.71	0.265	N
[Cu(FMN)(OAc)].H ₂ O (15)	0.162 \pm 0.3	0.255	1.71	0.491	N
[Zn(FMN)(OAc)].H ₂ O (23)	0.194 \pm 0.1	0.182	1.71	0.190	N
FMIN	0.287 \pm 0.3	0.234	1.71	0.345	N
Ni(FMIN)(OAc)(H ₂ O)].1.5 H ₂ O (8)	0.193 \pm 0.1	0.205	1.71	0.249	N
[Cu(FMIN)(OAc)(H ₂ O)].H ₂ O (16)	0.159 \pm 0.2	0.186	1.71	0.200	N
[Zn(FMIN)(OAc)].0.5 H ₂ O (24)	0.188 \pm 0.1	0.199	1.71	0.232	N

From the kinetic study (Michael-Menton plots) we determine the V_{\max} and K_m values for the sample and the control were shown in Table 6.1-6.2 and Figures 6.2-6.5 and also the tentative mode of inhibition (LB-Plots) revealed that compounds exhibited a characteristic competitive and non-competitive inhibition for α -amylase and α -glucosidase.

Furthermore, as shown by the IC_{50} values, in α -amylase inhibition ligand FMBH is inhibiting more than the other ligands. Among complexes, $[Cu(FB)(OAc)].H_2O$ (9), $[Cu(FBH)(H_2O)(OAc)].H_2O$ (10), $[Cu(FN)(OAc)].2H_2O$ (11), $[Cu(FIN)(OAc)(H_2O)].2H_2O$ (12), $[Cu(FMB)_2(H_2O)_2].H_2O$ (13), $[Cu(FMBH)_2(H_2O)_2].2H_2O$ (14), $[Cu(FMN)(OAc)].H_2O$ (15), $[Cu(FMIN)(OAc)(H_2O)].H_2O$ (16), $[Zn(FB)(OAc)].2.5H_2O$ (17), $[Zn(FBH)(OAc)]$ (18), $[Zn(FN)(OAc)].H_2O$ (19), $[Zn(FIN)(OAc)]$ (20), $[Zn(FMB)_2].2H_2O$ (21), $[Zn(FMBH)(OAc)]$ (22) and $[Zn(FMIN)(OAc)].0.5 H_2O$ (24) having the most α -amylase inhibition potential with IC_{50} in the range of 0.23-0.30mM. Complexation has increased the inhibitory potential of the compounds. Even though the inhibitory potential of ligands and complexes except $[Cu(FMBH)_2(H_2O)_2].2H_2O$ (14) are still below the therapeutic drug acarbose, from the data it is clear that these compounds can potentially take part in α -amylase inhibition.

Compounds have much less IC_{50} values for the inhibition of α -glucosidase pointing to the stronger inhibition ability. Among ligands, FMBH is the strongest inhibitor. In complexes $[Cu(FB)(OAc)].H_2O$ (9), $[Cu(FBH)(H_2O)(OAc)].H_2O$ (10), $[Cu(FN)(OAc)].2H_2O$ (11), $[Cu(FIN)(OAc)(H_2O)].2H_2O$ (12), $[Cu(FMB)_2(H_2O)_2].H_2O$ (13), $[Cu(FMBH)_2(H_2O)_2].2H_2O$ (14), $[Cu(FMN)(OAc)].H_2O$ (15), $[Cu(FMIN)(OAc)(H_2O)].H_2O$ (16), were having IC_{50} value less than that of acarbose. And complexes

[Zn(FB)(OAc)].2.5H₂O (17), [Zn(FBH)(OAc)] (18), [Zn(FN)(OAc)].H₂O (19), [Zn(FIN)(OAc)] (20), [Zn(FMB)₂].2H₂O (21), [Zn(FMBH)(OAc)] (22), [Zn(FMN)(OAc)].H₂O (23) and [Zn(FMIN)(OAc)].0.5 H₂O (24) values are comparable with that of acarbose. Enhanced activity of FMBH may be due to the presence of electron withdrawing hydroxy group [60]. While comparing the activity of complexes, it is clear that Cu (II) complexes possess more antidiabetic activity than Zn (II) and Ni (II) complexes. Oxidative stress, which is one of the major causative agents of diabetes, can be more tolerated by pancreatic β -cells in the presence of copper. It has been reported, that copper treats hyperglycemia by activating the phosphoinositide 3'kinase (PI3-K/Akt) pathway leading to GLUT 4 translocation [61].

The present study exposed a promising inhibitory activity on ligand and metal complex on α -amylase and α -glucosidase. It was clear that the complexes had significant potential than ligands and moderate inhibitory activity with IC₅₀, for α -amylase as well as for glucosidase compared to control of acarbose. As excessive inhibitory activity will results in the irregular bacterial fermentation of undigested carbohydrates in the intestine [62]. The least inhibitory activity of Ni (II) complexes compared to that of other complexes may be due to the difference in salvation behaviour in the action media. The reason for the activity of inhibition of the complexes may be due to its binding with the oxygen atoms of the enzymes. Therefore, the complex can find greater relevance than the ligand in the development of new oral antidiabetic drugs.

6.3.2 Mode of enzyme inhibition

The mechanism of the inhibition of the enzyme activity by the synthesized compounds was studied using Lineweaver Burk plot by plotting reaction rates with different concentrations of the substrates. Figure 6.2 shows Michael-Menton plots and Figure 6.3 show LB plots in the presence and absence of the α -amylase inhibitors. Figure 6.4 show Michael-Menton plots and Figure 6.5 show LB plots in the presence and absence of the α -glucosidase inhibitors. Table 6.1 & 6.2 gives the kinetic constants, K_m , V_{max} and the mode of inhibition by the compounds. All the compounds except ligands FMB, FMBH, complexes $[\text{Ni}(\text{FMB})_2(\text{H}_2\text{O})_2] \cdot \text{H}_2\text{O}$ (5), $[\text{Cu}(\text{FMB})_2(\text{H}_2\text{O})_2] \cdot \text{H}_2\text{O}$ (13), $\text{Zn}(\text{FMB})_2 \cdot 2\text{H}_2\text{O}$ (21), $[\text{Ni}(\text{FBH})_2(\text{H}_2\text{O})_2] \cdot 2\text{H}_2\text{O}$ (6), $[\text{Cu}(\text{FMBH})_2(\text{H}_2\text{O})_2] \cdot 2\text{H}_2\text{O}$ (14) and $\text{Zn}(\text{FMBH})(\text{OAc})$ (22) inhibit α -amylase noncompetitively. But in the case of α -glucosidase ligands FN, FMB and their complexes $[\text{Ni}(\text{FN})(\text{OAc})] \cdot \text{H}_2\text{O}$ (3), $[\text{Cu}(\text{FN})(\text{OAc})] \cdot 2\text{H}_2\text{O}$ (11), $[\text{Zn}(\text{FN})(\text{OAc})] \cdot \text{H}_2\text{O}$ (19), $[\text{Ni}(\text{FMB})_2(\text{H}_2\text{O})_2] \cdot \text{H}_2\text{O}$ (5), $[\text{Cu}(\text{FMB})_2(\text{H}_2\text{O})_2] \cdot \text{H}_2\text{O}$ (13) and $\text{Zn}(\text{FMB})_2 \cdot 2\text{H}_2\text{O}$ (21) are competitive inhibitors. All other ligands and complexes are inhibiting non-competitively. Non-competitive enzyme inhibition modes by the compounds, revealed by the LB-plot, suggest that the ligand and complex do not compete with the substrate for binding to the active site of the enzymes.

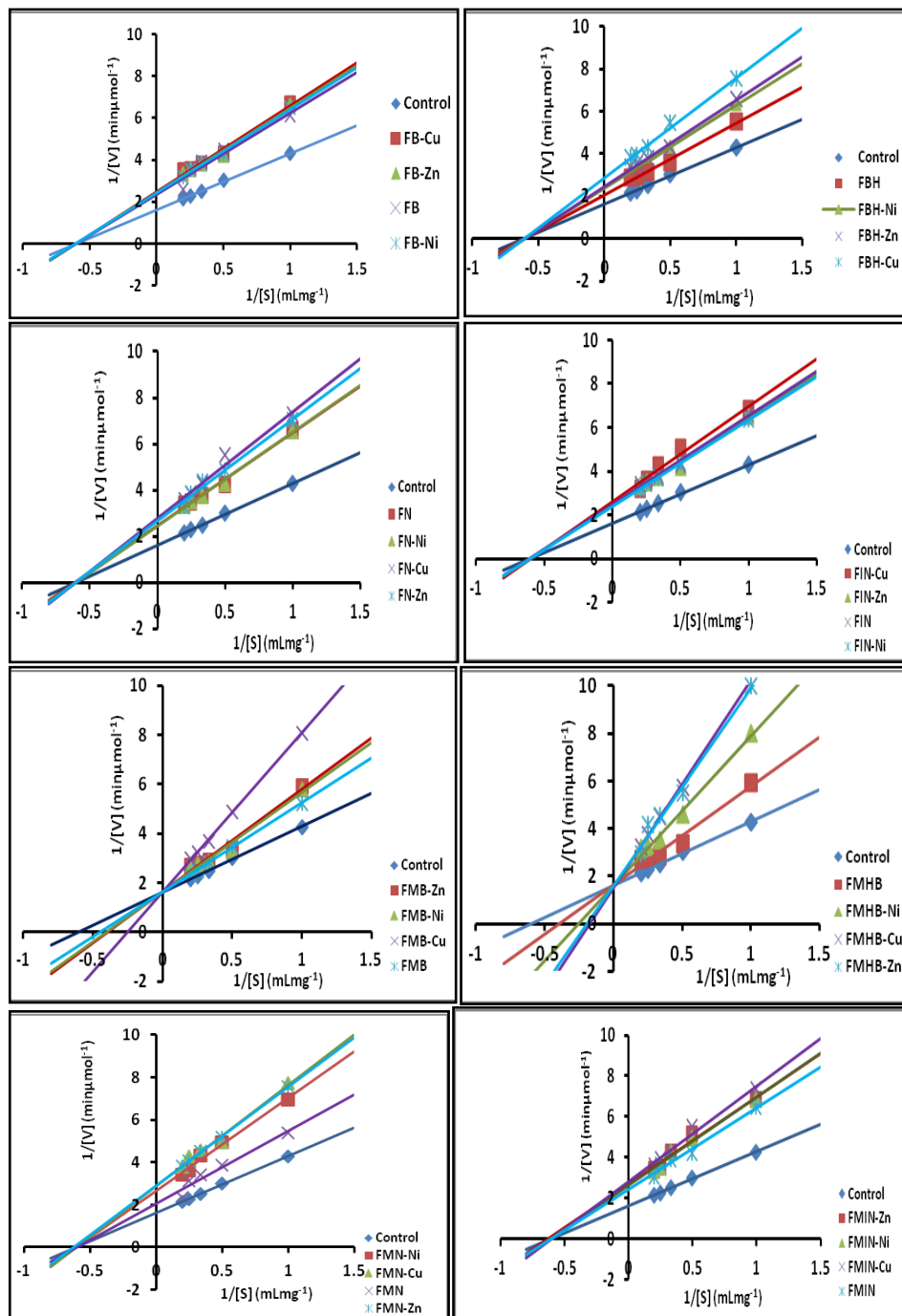


Figure 6.2 Lineweaver-Burk plots for native α -amylase and the enzyme pre-incubated with ligands and metal complexes.

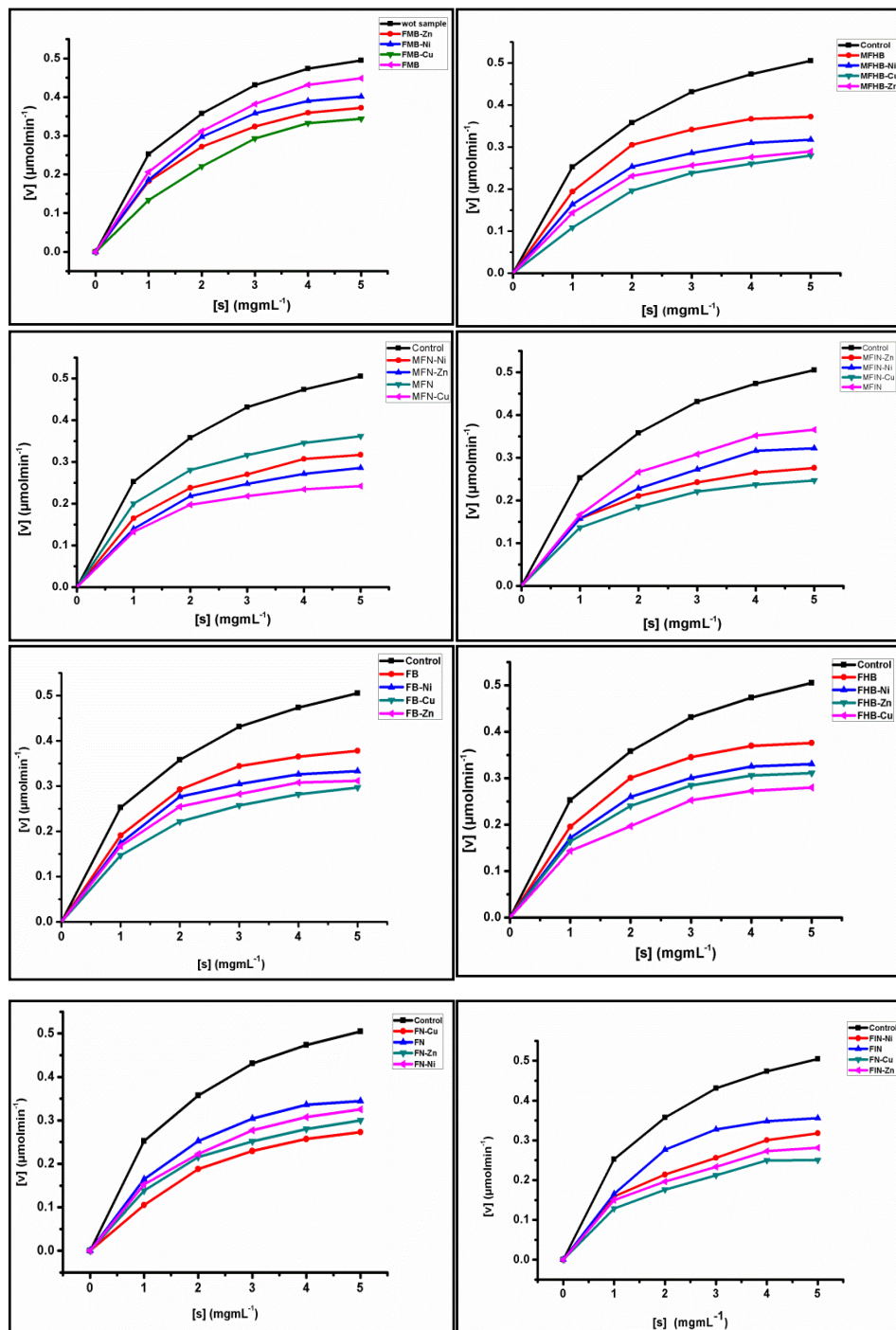


Figure 6.3 Michaelis-Menten graph for ligands and complexes (α -amylase).

This means that they bind to a separate site on the free enzyme or on the enzyme-substrate complex, controlling the conversion rate of the substrate to product and causing conformational changes of the active site which results in the inhibition of activity. The non-competitive type inhibitor does not have structural similarity to the substrate but it binds both of the free enzyme and the enzyme-substrate complex. Thus, its binding manner is not mutually exclusive with the substrate and the presence of a substrate has no influence on the ability of a non-competitive inhibitor to bind an enzyme and vice versa. However, its binding-although away from the active site-alters the conformation of the enzyme and reduces its catalytic activity due to changes in the nature of the catalytic groups at the active site. EI and ESI complexes are nonproductive and increasing substrate to a saturating concentration does not reverse the inhibition leading to unaltered K_m but reduced V_{max} .

The competitive inhibitor is structurally related to the substrate and binds reversibly at the active site of enzyme and occupies it in a mutually exclusive manner with the substrate. Therefore, the competitive inhibitor competes with the substrate for the active site. The binding is mutually exclusive because of their free competition. Kinetically, the inhibitor (I) binds the free enzyme reversibly to form enzyme inhibitor complex (EI) that is catalytically inactive and cannot bind the substrate. The competitive inhibitor reduces the availability of free enzyme for the substrate binding. Thus, the K_m of the normal reaction is increased. Where the substrate concentration at $V_o = \frac{1}{2}V_{max}$ is equal to a K_m . Therefore, competitive inhibitors do not affect the turnover number (active site catalysis per unit time) or the efficiency of the enzyme because once enzyme is free, enzyme behaves normally.

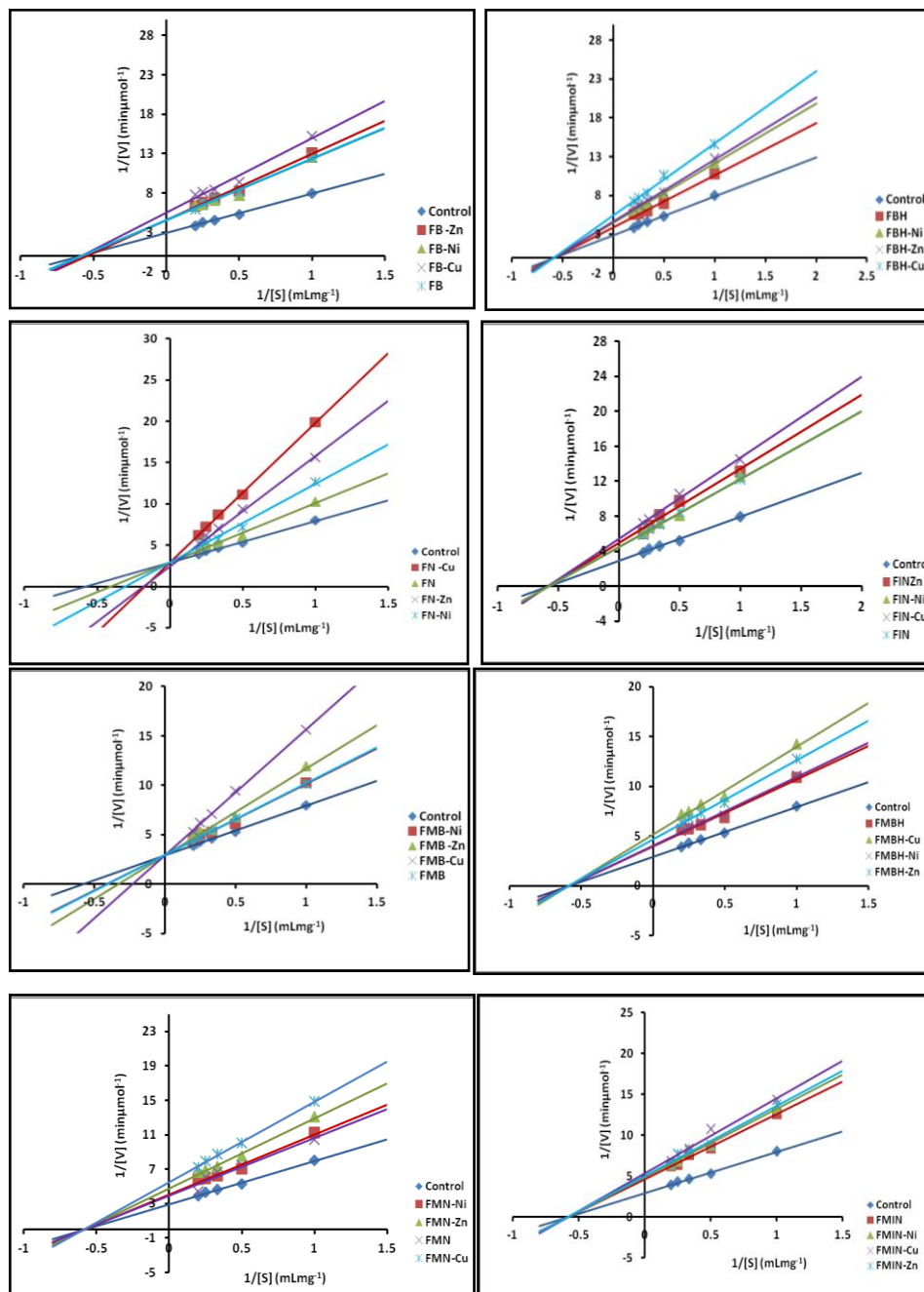


Figure 6.4 Lineweaver–Burk plots for native α -glucosidase and the enzyme pre-incubated with ligands and metal complexes.

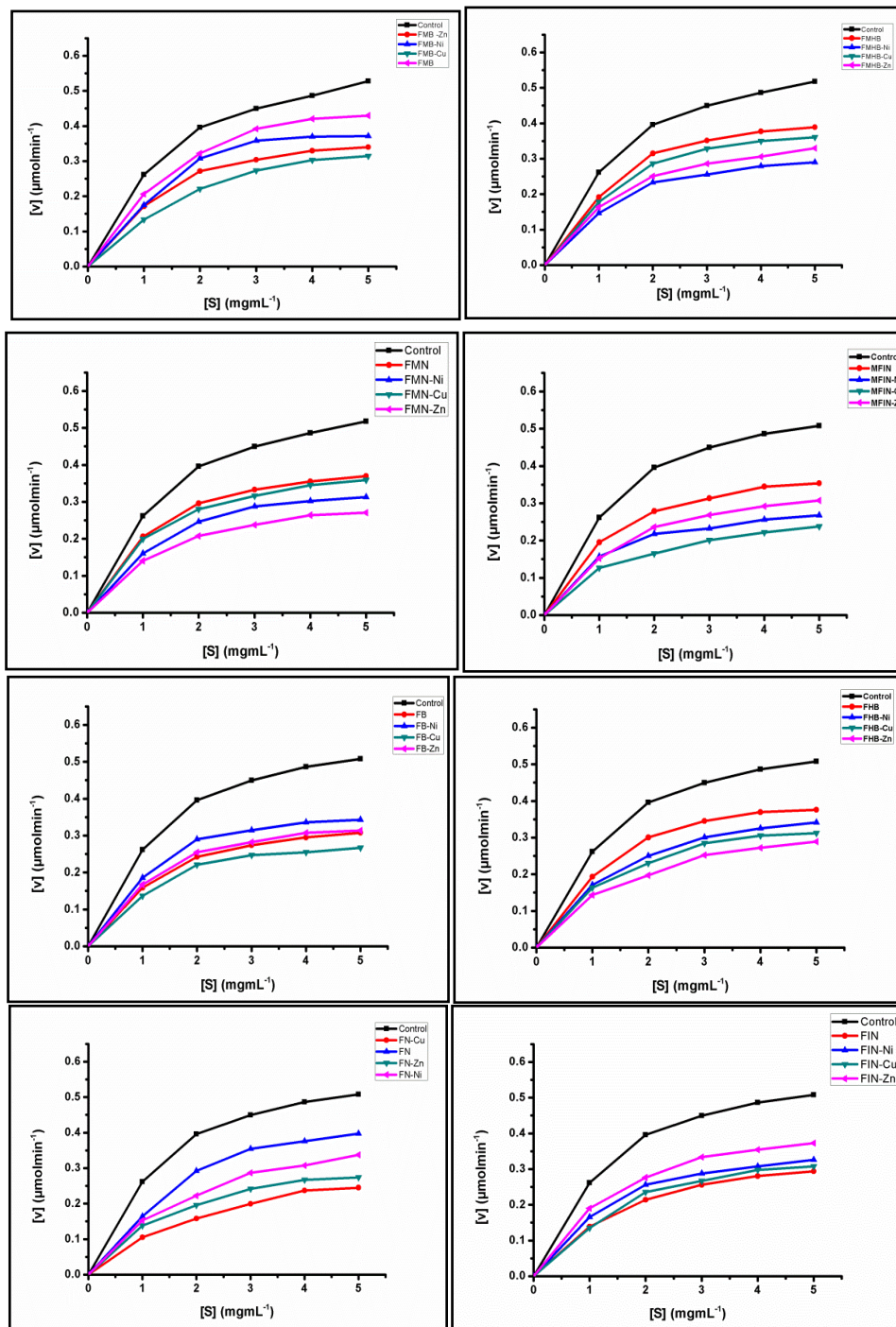


Figure 6.5 Michaelis-Menten graph for ligands and complexes (α -glucosidase).

6.4 Conclusion

The present investigations was undertaken to screen different chromone hydrazones and their Ni (II), Cu (II) and Zn (II) complexes for α -amylase and α -glucosidase inhibitor activity. All the synthesized compounds were screened for α -amylase and α -glucosidase inhibitor activity, α -glucosidase inhibitory activity was found in copper complexes are higher than that of drug acarbose (standard). Nature of inhibition was found to be competitive for ligands FMB, FMBH and their Ni (II), Cu (II) & Zn (II) against α -amylase. In the case of α -glucosidase ligands FN, FMB and their Ni (II), Cu (II), Zn (II) complexes inhibit by competitively. All other ligands and their complexes are inhibiting non-competitively. Inhibitory activity of α -amylase and α -glucosidase suggested its potential in prevention and therapy of obesity. It can also be used as drug designing targets for treatment of diabetes. So, there is a need for the identification of effective α -amylase and α -glucosidase inhibitors with desirable characteristics from new sources.

References

- [1] (a) T. Kawai, I. Takei, A. Shimada, T. Hirata, K. Tanaka, Y. Saisho, J. Ire, C. Horimai, H. Matsumoto, H. Itoh Clin. Drug Investig. 31 (2011) 237.
(b) W. Benalla, S. Bellahcen, M. Bnouham, Curr. Diabetes Rev., 6 (2010) 247.
- [2] D. J. O'Reilly, F. Xie, E. Pullenayegum, H. C. Gerstein, J. Greb, G. K. Blackhouse, J. Tarride, J. Bowen, R. A. Goeree, Qual. Life Res., 20 (2011) 939.
- [3] A. Selea, M. Sumarac-Dumanovic, M. Pesic, D. Suluburic D. Stamenkovic-Pejokovic, G. Cvijovic, D. Mcić Vojnosanitetski Review, 68 (2011) 676.

- [4] T. Matsui, I. A. Ogunwande, K. J. M. Abesundara, K. Matsumoto, *Mini-Rev. Med. Chem.*, 6 (2006) 349.
- [5] K. Bolin, C. Gips, A. C Morks, B. Lindgren, *Diabet. Med.*, 26 (2009) 928.
- [6] T. K Mattila, A. de Boer, *Drugs*, 70 (2010) 2229.
- [7] C. Voulgari, M. Psallas, A. Kokkinos, V. Argiana, N. Katsilambros, N. J. Tentolouris, *Diabet. Compli.*, 25 (2010) 159.
- [8] M. Nemoto, N. Tajima, R. Kawamori, *Acta. Diabetol.*, 48 (2011) 15.
- [9] W. L. Bennett, N. M. Maruthur, S. Singh, J. B. Segal, L. M. Wilson, R. Chatterjee, S. S. Marinopoulous, M. A. Puhan, P. Ranasinghe, L. Block, W. K. Nicholson, S. Hutfless, E. B. Bass, S. Bolen, *Ann. Intern. Med.*, 154 (2011) 602.
- [10] A. J. Krentz, C. J. Bailey *Drugs*, 65 (2005) 385.
- [11] C. Taylor, R. Hobbs, *Br J. Gen. Prac.*, 59 (2009) 520.
- [12] S. Bolen, L. Feldman, J. Vassy, L. Wilson, H. C. Yeh, S. Marinopoulos, C. Wiley, E. Selvin, R. Wilson, E. B. Bass, F. L. Brancati, *Ann. Int. Med.*, 147.6 (2007) 386.
- [13] L. Ren, X. Cao, P. Geng, F. Bai, G. Bai, *Carbohydr. Res.*, 346 (2011) 2688.
- [14] K. Jones, L. Sim, S. Mohan, J. Kumarasamy, H. Liu, S. Avery, H. Y. Naim, R. Quezada-Calvillo, B. L. Nichols, B. M. Pinto, D. R. Rose, *Bio. & Med. Chem.*, 19 (2011) 3929.
- [15] X. Qin, L. Renb, X. Yanga, F. Baib, L. Wanga, P. Gengc, G. Baib, Y. J. Shena, *J. Struct. Bio.*, 174 (2011) 196.
- [16] G. J. Mc Dougall, D. Stewart, *BioFactors*, 23 (2005) 189.
- [17] (a) M. Bhat, S. S. Zinjarde, S. Y. Bhargava, A. R. Kumar, B. N. Joshi, *Evid based Complement Alternat Med.*, (doi:10.1093/ecam/nen040).
(b) G. Vandana, G. Pankaj, H. H. Ian, A. P. Enzo, *BMC Complement. Altern. Med.*, 15 (2015) 1.(doi: 10.1186/s12906-015-0524-8)

- [18] B. Hirshberg, K. I. Rother, B. J. Digon, J. Lee, J. L. Gaglia, K. Hines, E. J. Read, R. Chang, B. J. Wood, D. M. Harlan, *Diabetes Care*, 26 (2003) 3288.
- [19] S. B. Lotito, B. Frei, *Free Radic. Biol. Med.*, 41 (2006) 1727.
- [20] H. W. Ryu, B. W. Lee, M. J. Curtis-Long, S. Jung, Y. B. Ryu, W. S. Lee, K. H. J. Park, *Agric. Food Chem.*, 58 (2010) 202.
- [21] O. Kamiyama, F. Sanae, K. Ikeda, Y. Higashi, Y. Minami, N. Asano, I. Adachi, A. Kato, *Food Chem.*, 122 (2010) 1061.
- [22] Y. Q. Li, F. C. Zhou, F. Gao, J. S. Bian, F. J. Shan, *Agric. Food Chem.*, 57 (2009) 11463.
- [23] A. V. Diez-Roux, C. I. Kiefe, D. R. Jacobs, M. Haan, S. A. Jackson, F. J. Nieto, C. C. Paton, R. Schulz, *Ann Epidemiol.*, 11(2001) 395.
- [24] J. H. Sheikh, T. Iyo, T. Mikako, I. Ashabul, S. B. Rajat, A. Hitoshi, *Food Sci Technol Res.*, 14 (2008) 261.
- [25] A. G. Rob, J. N. Jacques, T. Matthijs, E. Y. Ruud, T. Abraham, G. H. Han, M. Frank, L. P. Hidde, *Nature*, 330 (1987) 74.
- [26] N. Toshio, D. Umeyuki, O. J. Toshihiko, *J. Agric. Food Chem.*, 51 (2003) 90.
- [27] S. H. Yoon, J. F. Robyt, *Carbohydr. Res.*, 338 (2003) 1969.
- [28] B. M. Eduardo, S. G. Adriane, C. Ivone, *Tetrahedron*, 62 (2006) 10277.
- [29] E. Apostolidis, Y. L. Kwon, K. Shetty, *Innov. Food sci. & emerg. technol.*, 8 (2007) 46.
- [30] G. L. Miller *Anal. Chem.*, 31 (1959) 426.
- [31] S. Shetty, K. Secnik, A. Oglesby, *J. Manag. Care Pharm.*, 11 (2005) 559.

.....✂.....

Chapter 7

CYTOTOXICITY STUDIES OF CHROMONE HYDRAZONES AND THEIR Ni (II), Cu (II) AND Zn (II) COMPLEXES

Contents	7.1	Introduction
	7.2	Materials and Methods
	7.3	Result and Discussion
	7.4	Conclusion

Conspectus: Medicinal inorganic chemistry can exploit the unique properties of metal ions for the design of new drugs. This has, for instance, led to the clinical application of chemotherapeutic agents for cancer treatment, such as cisplatin. The use of cisplatin is, however, severely limited by its toxic side-effects. This has spurred chemists to employ different strategies in the development of new metal-based anticancer agents with different mechanisms of action. In fact, they are better known for their antioxidant properties and can act in vitro as reducing agents, hydrogen donors, free radical quenchers and metal ions chelators and this may represent anticancer activity of chromones. In this study, we evaluated the cytotoxicity of Ni (II), Cu (II) and Zn (II) complexes of chromone hydrazones. The interaction between some new derivatives of chromones and 3T3-L1 normal cell is monitored by MTT Assay.

7.1 Introduction

Heterocyclic moieties create huge number of compounds; play a significant function in numerous biological processes. The biological activity of these compounds is primarily dependent upon their molecular structures [1-3]. The azomethine group in hydrazones (-NH-N=CH-) is an important characteristic that makes them significant compounds owing to their wide range of biological activities [4-7]. Hydrazones are capable of reduce/inhibit the growth of large number of animal tumors which can be altered depending upon the kind of substituent present on the aromatic rings. Copper act as an important role in the human organs and the function of copper in the human body is complex and not fully understood [8-11]. The role of copper is a biocatalyst in the redox reactions. The Cu(II) complexes have a wide range of coordination geometries with NN, NO, ONO, ONS and NNO donor ligands and the structure of complex depending on the number, type, and arrangement of ligands around the copper centre. The ligands form stable five- or six-membered rings after complexation with the metal ion [12-15]. A wide range of hydrazones with their reactive azomethine linkage show fascinating inhibitory activity against tumor cells. Hydrazones could be hydrolyzed selectively by the tumor cells to act as alkylating agents [16]. Studies show that the metal complexes of hydrazones have better antimicrobial and anticancer activities as compared to hydrazone [17].

The cytotoxicity test is one of the significant biological evaluations and screening method, using tissue cells *in vitro* to examine the cell growth, reproduction and morphological effects [18]. According to the international organization for standardisation (ISO) and national

standards, medical devices must undergo rigorous testing to determine their biocompatibility when they have contact with the body, regardless of their mechanical, physical and chemical properties [19-20].

V. K. Chityala et al. have synthesized novel mixed ligand bivalent copper complexes [CuLAClO₄] and [CuLA] where L is 2-((3,4-dimethylisoxazol-5-ylimino)methyl)-4-bromophenol (DMIIMBP)/2-((3,4-dimethylisoxazol-5-ylimino)methyl)-4-chlorophenol (DMIIMCP), and A is 1,10-phenanthroline (phen)/2,2'-bipyridyl (bipy)/8-hydroxyquinoline (oxine)/5-chloro-8-hydroxyquinoline (5-Cl-oxine). The cytotoxicity of all the Cu(II) complexes was assayed and it was found that the cytotoxicity of the [Cu(DMIIMBP)(bipy)ClO₄] complex at 10 µg/mL concentration shows 57.51% toxicity suggesting good antitumor agent on human cervical carcinoma cell lines [21]. A new Schiff base of 2-aminobenzimidazole with 2,4-dihydroxybenzaldehyde (H₃L), and its Cu(II), Ni(II) and Co(II) complexes have been synthesized by N. El-wakiel et al. The anticancer activity of the ligand and its metal complexes is evaluated against human liver Carcinoma (HEPG2) cell. These compounds exhibited a moderate and weak activity against the tested HEPG2 cell lines with IC₅₀ of 9.08, 18.2 and 19.7 µgmL⁻¹ for ligand, Cu (II), Ni (II) and Co (II) complexes, respectively [22].

B. Anupama et al. were synthesized ternary Cu(II) complexes [Cu(II)(L)(bpy)Cl], [Cu(II)(L)(Phen)Cl] [L=2,3-dimethyl-1-phenyl-4(2-hydroxy-5-methyl benzylideneamino)-pyrazol-5-one, bpy = 2,2' bipyridine, phen =1,10 phenanthroline). The cytotoxic activity of the Cu(II) complexes was probed in HeLa (human breast adenocarcinoma cell line),

B16F10 (Murine melanoma cell line) and HEPA1-6 cell lines, complex has good cytotoxic activity which is comparable with the doxorubicin drug, with IC_{50} values ranging from 3-12.6 μM [23]. Binary complexes of Cu(II), Ni(II), and Zn(II) ions have been synthesized by K. S. Kumar et al., reacting metal salts with a Schiff base, 2-((E)-(5-methylisoxazol-3-ylimino)methyl)-4-methoxyphenol (MIIMMP) in an alcoholic medium. The cytotoxicity of all the metal complexes was studied, and it is found that the cytotoxic activity of the $[\text{Cu}(\text{MIIMMP})_2(\text{H}_2\text{O})_2]$ complex at 10 $\mu\text{g mL}^{-1}$ concentration shows 64.65% toxicity suggesting good antitumor agent on human cervical carcinoma cell lines [24].

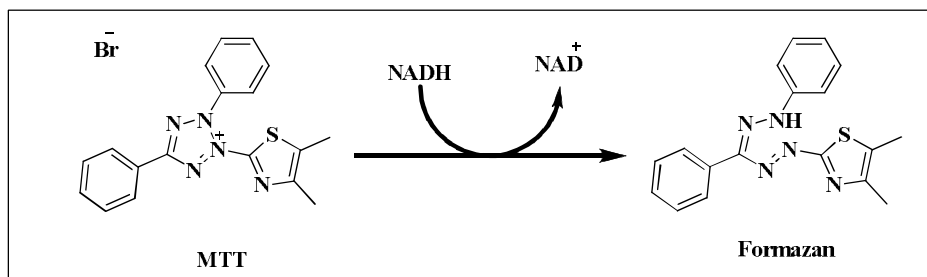
Divalent Co, Ni and Cu hydrazone complexes containing [N'-(phenyl(pyridine-2-yl)methylidene) benzohydrazide] ligand were synthesised and cytotoxicity of the above complexes against HeLa tumor cells and NIH 3T3-L1 normal cells revealed that the complexes are toxic only against tumor cells but not to normal cells [25]. Novel 2-oxo-1,2-dihydroquinoline-3-carbaldehyde (4'-methylbenzoyl) hydrazone and its two copper(II) complexes have been synthesized. Cytotoxic activities of the ligand and copper (II) complexes showed that the complexes exhibited more effective cytotoxic activity against HeLa and HEP-2 cells than the corresponding ligand [26].

Cell viability and cytotoxicity assays are used for drug screening and cytotoxicity tests of chemicals. These are usually used for measuring receptor binding and a mixture of signal transduction events that may involve the expression of genetic reporters, trafficking of cellular components, or monitoring organelle function [27]. They are based on

various cell functions such as enzyme activity, cell membrane permeability, cell adherence, ATP production, co-enzyme production, and nucleotide uptake activity. To measure cell viability, researchers typically use an MTT assay, Cell Titer Blue, Trypan blue exclusion, ATP, Colony Formation method or Crystal Violet method [28-29]. The MTT assay is most commonly used method to test cell growth rate and toxicity of the culture.

7.1.1 Importance of MTT assay

The MTT (3-(4,5-dimethylthiazol-2-yl)-2,5-diphenyltetrazolium bromide) tetrazolium reduction assay was the first homogeneous cell viability assay developed for a 96-well format that was suitable for high throughput screening. It is a sensitive, quantitative and reliable colorimetric assay. MTT assay, which uses tetrazolium salt known as [3-(4,5-dimethyl-2-thiazolyl)-2,5-diphenyl-2H-tetrazolium bromide)], has been a powerful biological tool to measure cell proliferation and cytotoxicity [30-31]. The assay is based on the capacity of mitochondrial dehydrogenase enzymes in living cells to convert the yellow water-soluble substrate 3-(4,5-dimethylthiazol-2-yl)-2,5-diphenyl tetrazolium bromide (MTT) into a dark blue formazan product that is insoluble in water. Viable cells are able to reduce the yellow MTT under tetrazolium ring cleavage to a water-insoluble purple-blue formation which precipitates in the cellular cytosol and can be dissolved after cell lysis, whereas cells being dead following a toxic damage, cannot transform MTT. This formation production is proportionate to the viable cell number and inversely proportional to the degree of cytotoxicity. The reaction is mediated by dehydrogenases enzymes (Scheme 7.1) associated with the endoplasmic reticulum and the mitochondria [32].



Scheme 7.1 Formation formazan

The predispose cell line 3T3-L1 was originally developed by clonal expansion from murine Swiss 3T3 cells. Because of its potential to differentiate from fibroblasts to adipocytes, the cell line has widely been used in more than 5000 published articles on adipogenesis and the biochemistry of adipocytes [33].

7.2 Materials and Methods

7.2.1 Materials

MICE 3T3-L1 preadipocytes from American Type Culture Collection, USA, were grown in Dulbecco's modified eagle's medium (DMEM) supplemented with 10% FCS and antibiotics (100 U/mL of penicillin and 100 µg/mL of streptomycin) under a humidified atmosphere with 5% CO₂ at 37°C. [3-(4, 5-dimethyl-2-thia-zolyl)-2, 5-diphenyl-2H-tetrazolium bromide] (MTT), and dimethyl sulfoxide (DMSO) were purchased from Sigma, St. Louis, MO, USA.

7.2.2 MTT Assay

3T3-L1 cells were grown in Dulbecco's Modified Eagle's Medium (DME) and spread in 96 well plates at a density of 5x10³ cells/well and incubated at 37°C, 5% CO₂ for 24 h prior to addition of complexes. The

cells were then treated with different concentrations (10, 50, 100, 150 μM) of compounds dissolved in DMSO and incubated at 37°C, 5% CO₂ for 24 h. Triplicate was maintained. After 24 h, MTT was added (after removal of media from the wells) at a concentration of 50 $\mu\text{g}/\text{well}$ and incubated CO₂ incubator. The working solution of MTT was prepared in Hank's balanced salt solution (HBSS) without phenol red. After 2.5-3 hrs, the formazan crystals formed were viewed under the phase contrast microscope (Figure 7.1) The crystals were then solubilised by adding DMSO (after removal of MTT) and further incubated for 20 min at 37 °C in the dark. After solubilisation, the plate was read at an absorbance of 570 nm. Control samples were cells without any treatment. The percentage cell viability of control cells were kept as 100%. The relative cell toxicity in percent was calculated as:

$$\% \text{ Toxicity} = 100 - \frac{\text{Absorbance of treated}}{\text{Absorbance of control}} * 100$$

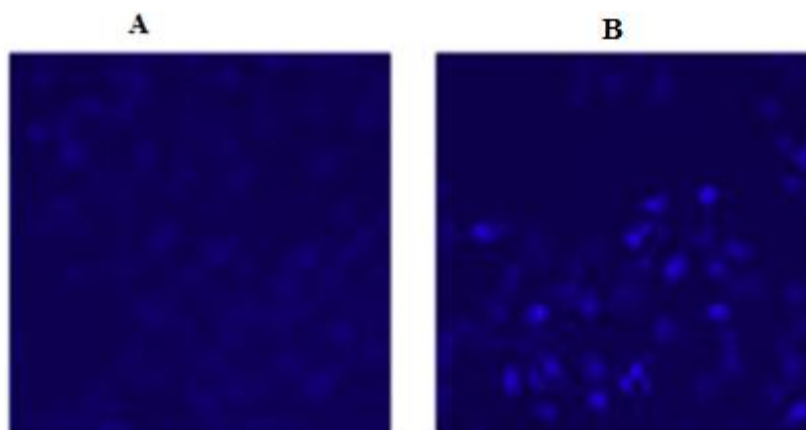


Figure 7.1 (A) shows a field of 3T3-L1 cells photographed immediately after addition of the MTT solution. (B) Shows a change in cell morphology and the appearance of formazan crystals after 3 hours of exposure to MTT

7.3 Result and Discussion

Cytotoxicity is a common limitation in terms of the introduction of new compounds into the pharmaceutical industry. The *in vitro* cytotoxicity of 3-formyl chromone hydrazones and their Ni (II), Cu (II), Zn (II) was evaluated by MTT assay against normal 3T3-L1 cells. The inhibitory effects of the compounds on the growth of cells were determined after 3T3-L1 cells being incubated with different concentrations (10, 50, 100, 150 μ M) of compounds. The results were analyzed by means of cell viability. Viable cells with active metabolism convert MTT into a purple colored formazan product with an absorbance maximum near 570 nm. When cells die, they lose the ability to convert MTT into formazan, thus color formation serves as a useful and convenient marker of only the viable cells.

The cytotoxicity of ligands and their metal complexes have been evaluated by MTT assay against normal 3T3-L1 cells. All ligands FB, FBH, FN, FIN, FMB, FMBH, FMN and FMIN exhibited 100% cell viability (10, 50, 100, 150 μ M) against normal 3T3-L1 cells (Table 7.1).

Table 7.1 The percentage cell viability of hydrazones against 3T3-L1 cells by MTT assay

Compounds	Cells	10 μ M	50 μ M	100 μ M	150 μ M
FB	3T3-L1	100	100	100	100
FBH	3T3-L1	100	100	100	100
FN	3T3-L1	100	100	100	100
FIN	3T3-L1	100	100	100	100
FMB	3T3-L1	100	100	100	100
FMBH	3T3-L1	100	100	100	100
FMN	3T3-L1	100	100	100	100
FMIN	3T3-L1	100	100	100	100

Cell viability results of nickel(II) complexes (Table 7.2) indicates that [Ni(FBH)(H₂O)(OAc)].2H₂O and [Ni(FN)(OAc)].H₂O are non toxic in 10, 50,100,150 μM. [Ni(FMB)₂(H₂O)₂].H₂O and [Ni(FMIN)(OAc)(H₂O)].1.5H₂O shows toxicity at higher concentration (150μM). [Ni(FB)(OAc)(H₂O)].2H₂O, [Ni(FIN)(OAc)(H₂O)].H₂O, [Ni(FMBH)₂(H₂O)₂].2H₂O and [Ni(FMN)(OAc)].2H₂O shows very low toxicity at higher concentrations.

Table 7.2 The percentage cell viability of Ni (II) complexes against 3T3-L1 cells by MTT assay.

Compounds	Cells	10μM	50μM	100μM	150μM
[Ni(FB)(OAc)(H ₂ O)].2H ₂ O (1)	3T3-L1	98	92	79	70
[Ni(FBH)(H ₂ O)(OAc)].2H ₂ O (2)	3T3-L1	100	100	100	100
[Ni(FN)(OAc)].H ₂ O (3)	3T3-L1	100	100	100	100
[Ni(FIN)(OAc)(H ₂ O)].H ₂ O (4)	3T3-L1	96	87	76	62
[Ni(FMB) ₂ (H ₂ O) ₂].H ₂ O (5)	3T3-L1	98	77	53	21
[Ni(FMBH) ₂ (H ₂ O) ₂].2H ₂ O (6)	3T3-L1	87	73	66	51
[Ni(FMN)(OAc)].2H ₂ O (7)	3T3-L1	96	88	79	70
[Ni(FMIN)(OAc)(H ₂ O)].1.5 H ₂ O (8)	3T3-L1	82	58	40	30

Cytotoxicity results of Cu (II) complexes indicates that [Cu(FB)(OAc)].H₂O, [Cu(FN)(OAc)].2H₂O, [Cu(FIN)(OAc)(H₂O)].2H₂O, [Cu(FMB)₂(H₂O)₂].H₂O (Table 7.3) shows high toxicity in all concentration against 3T3-L1 cells. Complexes [Cu(FBH)(H₂O)(OAc)].H₂O, [Cu(FMBH)₂(H₂O)₂].2H₂O, [Cu(FMN)(OAc)].H₂O and [Cu(FMIN)(OAc)(H₂O)].H₂O shows mild toxicity in 50,100 ,150 μM.

Table 7.3 The percentage cell viability of Cu (II) complexes against 3T3-L1 cells by MTT assay

Compounds	Cells	10 μ M	50 μ M	100 μ M	150 μ M
[Cu(FB)(OAc)].H ₂ O (9)	3T3-L1	12	0	0	0
[Cu(FBH)(H ₂ O)(OAc)].H ₂ O (10)	3T3-L1	45	34	21	13
[Cu(FN)(OAc)].2H ₂ O (11)	3T3-L1	8	0	0	0
[Cu(FIN)(OAc)(H ₂ O)].2H ₂ O (12)	3T3-L1	15	8	0	0
[Cu(FMB) ₂ (H ₂ O) ₂].H ₂ O (13)	3T3-L1	12	0	0	0
[Cu(FMBH) ₂ (H ₂ O) ₂].2H ₂ O (14)	3T3-L1	53	24	12	8
[Cu(FMN)(OAc)].H ₂ O (15)	3T3-L1	38	20	11	7
[Cu(FMIN)(OAc)(H ₂ O)].H ₂ O (16)	3T3-L1	58	50	42	37

Cell viability results of zinc complexes (Table 7.4) indicates that [Zn(FB)(OAc)].2.5H₂O, [Zn(FN)(OAc)].H₂O, [Zn(FIN)(OAc)] and [Zn(FMB)₂].2H₂O exhibited 100% cell viability against normal 3T3-L1 cells. [Zn(FBH)(OAc)], [Zn(FMBH)(OAc)], [Zn(FMN)(OAc)].H₂O and [Zn(FMIN)(OAc)].0.5 H₂O showed mild toxicity at higher concentration.

Table 7.4 The percentage cell viability of Zn (II) complexes against 3T3-L1 cells by MTT assay.

Compounds	Cells	10 μ M	50 μ M	100 μ M	150 μ M
[Zn(FB)(OAc)].2.5H ₂ O (17)	3T3-L1	100	100	100	100
[Zn(FBH)(OAc)] (18)	3T3-L1	100	100	100	96
[Zn(FN)(OAc)].H ₂ O (19)	3T3-L1	100	100	100	100
[Zn(FIN)(OAc)] (20)	3T3-L1	100	100	100	100
[Zn(FMB) ₂].2H ₂ O (21)	3T3-L1	100	100	100	100
[Zn(FMBH)(OAc)] (22)	3T3-L1	100	100	89	71
[Zn(FMN)(OAc)].H ₂ O (23)	3T3-L1	100	100	100	98
[Zn(FMIN)(OAc)].0.5 H ₂ O (24)	3T3-L1	100	100	98	91

7.4 Conclusion

The cytotoxicity of hydrazones and their metal complexes have been evaluated by MTT assay against normal 3T3-L1 cells. All ligands exhibited 100% cell viability against normal 3T3-L1 cells. [Ni(FBH)(H₂O)(OAc)].2H₂O, [Ni(FN)(OAc)].H₂O, [Zn(FB)(OAc)].2.5H₂O, [Zn(FN)(OAc)].H₂O, [Zn(FIN)(OAc)] and [Zn(FMB)₂].2H₂O also showed 100% cell viability. [Cu(FB)(OAc)].H₂O, [Cu(FN)(OAc)].2H₂O, [Cu(FIN)(OAc)(H₂O)].2H₂O, [Cu(FMB)₂(H₂O₂)].H₂O showed high toxicity in almost all concentration against 3T3-L1 cells. Mild toxicity was observed for other complexes in concentration dependent manner.

References

- [1] J. Nordenberg, A. Novogrodsky, E. Beery, M. Patia, L. Wasserman, A. Warshawsky, *Eur. J. Cancer*, 26 (1990) 905.
- [2] A. Y. Shen, S. N. Wu, C. T. Chiu. *J. Pharm. Pharmacol.*, 51 (1999) 543.
- [3] S. Zhai, L. Yang, Q. C. Cui, Y. Sun, Q. P. Dou, B. Yan, *J. Biol. Inorg. Chem.*, 15 (2010) 259.
- [4] B. S. Tovrog, D. J. Kitko, R. Drago. *J. Am. Chem. Soc.*, 98 (1976) 5144.
- [5] A. A. El-Sherif, M. R. Shehata, M. M. Shoukry, M. H. Barakat, *Spectrochim. Acta A*, 96 (2012) 889.
- [6] T. M. Aminabhavi, N. S. Biradar, S. B. Patil, V. L. Roddabasanagoudar, W. E. Rudzinski, *Inorganica Chim. Acta*, 107 (1985) 231.
- [7] R. Hernandez-Molina, A. Mederos, Acyclic and macrocyclic Schiff base ligands. In: Mc Cleverty J. A. Meyer T. J., editors. *Comprehensive Coordination Chemistry*. 2nd edition. Vol. 1. London, UK: Elsevier; 2005.

- [8] I. S. MacPherson, M. E. P. Murphy, *Cell. Mol. Life Sci.*, 64 (2007) 2887.
- [9] D. J. Kosman, *J. Biol. Inorg. Chem.*, 15 (2010) 15.
- [10] K. Jomova, M. Valko, *Toxicology*, 283 (2011) 65.
- [11] M. Riha, J. Karlickova, T. Filipisky, K. Macakova, R. Hrdina, P. Mladenka, *J. Inorg. Biochem.*, 123 (2013) 80.
- [12] P. Talukder, A. Datta, S. Mitra, G. Rosair, *Z. Naturforsch, B. Chem. Sci.*, 59 (2004) 655.
- [13] V. V. Bon, *Acta Cryst. C*, 66 (2010) 300.
- [14] C. P. Pradeep, P. S. Zacharias, S. K. Das, *J. Chem. Sci.*, 117 (2005) 133.
- [15] N. Raman, S. Ravichandran, C. Thangaraja, *J. Chem. Sci.*, 116 (2004) 215.
- [16] M. M. Kamel, H. I. Ali, M. M. Anwar, N. A. Mohameda, M. Soliman, *Eur. J. Med. Chem.*, 45 (2010) 572.
- [17] B. S. Creaven, B. Duff, D. A. Egan *Inorganica Chim. Acta*, 363 (2010) 4048.
- [18] S. J. Soenen, B. Manshian, J. M. Montenegro, F. Amin, B. Meermann, T. Thiron, M. Cornelissen, F. Vanhaecke, S. Doak, W. J. Parak, *ACS Nano*, 6 (2012) 5767.
- [19] L. Wejia, Z. Jing, X. Yuyin, *Bio. Med. Rep.*, 3 (2015) 617.
- [20] V. P. Gaundarov, G. I. Kavalerov, *Med. Takh.*, 35 (2001) 4.
- [21] V. K. Chityala, K. K. Sathish, R. Macha, P. Tigulla, Shivaraj, *Bioinorg. Chem. Appl.*, 2014 (2014) 691260.
- [22] N. El-wakiel, M. El-keiy, M. Gaber, *Spectrochim. Acta A Mol. Biomol. Spectrosc.*, 147 (2015) 117.
- [23] B. Anupama, A. Aruna, V. Manga, S. Sivan, M. V. Sagar, R. Chandrashekar, *J. Fluoresc.*, 27 (2017) 953.

- [24] K. S. Kumar, V. K. Chityala, N. J. P. Subhashini, Y. Prashanthi, Shivaraj, ISRN Inorganic Chemistry, (doi.org/10.1155/2013/562082).
- [25] P. Krishnamoorthy, P. Sathyadevi, A. H. Cowley, R. R. Butorac, N. Dharmaraj, Eur. J. Med. Chem., 46 (2011) 3376.
- [26] D. S. Raja, N. S. P. Bhuvanesh, K. Natarajan, J. Biol. Inorg. Chem., 17 (2012) 223.
- [27] T. Mossman, J. Immunol. Methods, 65 (1983) 55.
- [28] G. Repetto, A. del Peso, J. L. Zurita, Nat. Protoc., 3 (2008) 1125.
- [29] P. Nymark, J. Catalan, S. Suhonen, H. Jarventaus, R. Birkedal, P. A. Clausen, K. A. Jensen, M. Vippola, K. Savolainen, H. Norppa, Toxicology, 313 (2013) 38.
- [30] G. Fotakis, J. A. Timbrell, Toxicol. Lett., 160 (2006) 171.
- [31] D. T. Vistica, P. Skehan, D. S. Cudieo, A. Monks, A. Pittman, M. R. Boyd, Cancer Res., 51 (1991) 2515.
- [32] P. Senthilraja, K. Kathiresan, J. Appl. Pharm. Sci., 5 (2015) 80.
- [33] S. B. ernadette, D. Brian, A. E. Denise, K. Kevin, R. Georgina, R. T. Venkat, W. Maureen, Chim. Acta, 363 (2010) 4048.

.....✂.....

SUMMARY AND CONCLUSION

Coordination chemistry is a challenging field in inorganic chemistry and has evolved as an important subject area in current research activities. Coordination compounds have been known for well over a century and the scientific interest in these compounds increased dramatically. The field of coordination chemistry has been widely explored. The recent surge in the popularity of coordination compounds is their perceived applications in many areas such as catalysis, analytical chemistry and medicine. Werner's coordination theory in 1893 was the first attempt to explain the bonding in coordination complexes. This theory and his painstaking work over the next 20 years won Alfred Werner the Nobel Prize for Chemistry in 1913. There has been much work done in attempting to formulate theories to describe the bonding in coordination compounds and to rationalize and predict their properties.

Coordination complexes show diversity in structures depending on the metal ion, its coordination number and the denticity of the ligands used. Therefore, the selection of the ligand is crucial in determining the properties and structures of coordination compounds. The presence of nitrogen and oxygen atoms attached to ligands increases their denticity

and thereby enhancing coordinating possibilities. Moreover, presence of these atoms in the coordination sphere leads to their biological activity. Hence the coordination chemistry of nitrogen-oxygen donor ligands is an interesting area of research. In this aspect, a great deal of attention has been focused on the complexes formed by transition metal ions with hydrazones. In view of their applicability in various fields, hydrazones, with triatomic $>C=N-N<$ linkage, takes the forefront position in the development of coordination chemistry.

Metal complexes have played an important role since the early days of coordination chemistry. Indeed, a great deal of work has been carried out on the synthesis and characterization of transition metal compounds, mainly due to their applications in various fields. However, the ability of the metal ion to participate in bonding to all possible coordination sites depends in part on its preferences for the donor atoms of the coordinated ligand, the flexibility and conformational adaptability of the ligand used, as well as on the competition from other Lewis acids and different entities capable of occupying a coordination pocket.

The work presented in this thesis is divided into eight chapters.

Chapter 1

Chapter 1 describes the general introduction of 3-formyl chromone hydrazones and their transition metal complexes. A brief discussion about the application of hydrazones and their metal complexes in various fields such as antimicrobial, anti-cancer agents etc. and its relevance and importance of enzyme inhibitors, the structure of DNA and its interactions with small molecules. The scope of the present work and

various physicochemical methods employed in the characterization of ligands and complexes are included.

Chapter 2

In this chapter we deal with synthesis and characterization of the hydrazones of 3-formyl chromone and benzhydrazide (FB), 3-formyl chromone and 4-hydroxybenzhydrazide (FBH), 3-formyl chromone and nicotinic hydrazide (FN), 3-formyl chromone and isonicotinic hydrazide (FIN), 6-methyl-3-formyl chromone and benzhydrazide (FMB), 6-methyl-3-formyl chromone and 4-hydroxybenzhydrazide (FMBH), 6-methyl-3-formyl chromone and nicotinic hydrazide (FMN), 6-methyl-3-formyl chromone and isonicotinic hydrazide (FMIN). All hydrazones were characterized by physicochemical methods such as elemental, FT-IR spectra, UV-Vis., ESI-MS spectra and $^1\text{H}/^{13}\text{C}$ NMR spectra.

Chapter 3

This chapter describes the synthesis and characterization of Ni (II), Cu (II) and Zn (II) complexes of 3-formyl chromone hydrazones. The analytical data suggest that all Ni (II), Cu (II) and Zn (II) complexes are mononuclear. A low molar conductance value indicates that all Ni (II), Cu (II) and Zn (II) complexes are non electrolyte in nature. Thermo gravimetric analysis revealed that all the complexes are found to be thermally stable. Magnetic moment values of nickel complexes $[\text{Ni}(\text{FB})(\text{OAc})(\text{H}_2\text{O})].2\text{H}_2\text{O}$, $[\text{Ni}(\text{FBH})(\text{H}_2\text{O})(\text{OAc})].2\text{H}_2\text{O}$, $[\text{Ni}(\text{FIN})(\text{OAc})(\text{H}_2\text{O})].\text{H}_2\text{O}$, $[\text{Ni}(\text{FMB})_2(\text{H}_2\text{O})_2].\text{H}_2\text{O}$, $[\text{Ni}(\text{FBH})_2(\text{H}_2\text{O})_2].2\text{H}_2\text{O}$ and $[\text{Ni}(\text{FMIN})(\text{OAc})(\text{H}_2\text{O})].1.5\text{H}_2\text{O}$ lies within the region 2.32-3.12 B.M expected for octahedral stereochemistry of the complexes. Ni (II) complexes $[\text{Ni}(\text{FN})(\text{OAc})].\text{H}_2\text{O}$

and Ni(FMN)(OAc)].2H₂O were 3.69 and 3.85 B.M which is consistent with the tetrahedral complexes. This was also confirmed by electronic and IR spectral studies. Magnetic moment values of all copper complexes gives an indication of distorted octahedral, square pyramidal or square planar structure. The physicochemical and spectral data reveals tetrahedral structure for all Zn (II) complexes.

Chapter 4

The antibacterial activity of synthesized 3-formyl chromone hydrazone as well as their Ni (II), Cu (II) and Zn (II) metal complexes was tested against Gram positive (*Staphylococcus aureus* and *Bacillus subtilis*), Gram negative bacteria (*Escherichia coli* and *Pseudomonas aeruginosa*) and fungus (*Candida albicans*) using disc diffusion method. The quantitative antimicrobial activity of the test compounds was evaluated using resazurin based microtiter dilution assay. Chloramphenicol and nystatin were used as standard antibiotics against bacteria and fungus respectively. Compounds individually exhibited varying degrees of inhibitory effects on the growth of the tested bacterial/fungus species. Metal complexes exhibited higher antimicrobial activity than the free ligands. Antibacterial activity difference is due to the nature of metal ions and also the cell membrane of the microorganisms.

Chapter 5

The present investigations were considering the binding behaviour of different chromone hydrazones and their Ni (II), Cu (II) and Zn (II) complexes towards CT-DNA. The important findings are - upon electronic absorption spectral titrations, all the synthesized metal complexes showed

hypochromism. DNA-binding studies with CT-DNA indicate that metal complexes bind to DNA by intercalation mode. Observed intrinsic binding constant (ranging from 10^4 - 10^5 M^{-1}) is comparable to other intercalators. Result from viscosity measurements clearly reveals that binding of DNA with metal (II) complexes is through intercalation. Among the complexes, copper (II) complexes $[Cu(FN)(OAc)].2H_2O$, $[Cu(FMB)_2(H_2O)_2].H_2O$ and $[Cu(FMIN)(OAc)(H_2O)].H_2O$ have higher relative viscosity values than standard intercalators ethidium bromide.

Chapter 6

In this chapter we evaluate 3-formyl chromone hydrazones and their Ni (II), Cu (II) and Zn (II) complexes for α -amylase and α -glucosidase inhibitory activity. All the synthesised compounds were screened for α - amylase and α -glucosidase inhibitor activity, α -glucosidase inhibitory activity was found in copper complexes are higher than that of standard drug acarbose. Nature of inhibition was found to be competitive inhibition for ligands FMB, FMBH and their Ni (II), Cu (II) & Zn (II) against α -amylase and for α -glucosidase ligands FN, FMB and their Ni (II), Cu (II), Zn (II) complexes inhibit also by competitively. All other ligands and complexes are inhibiting both α - amylase and α -glucosidase by non-competitively. Inhibitory activity of α -amylase and α - glucosidase against enzymes suggested its potential in prevention and therapy of obesity. It can also be used as drug designing targets for treatment of diabetes.

Chapter 7

The cytotoxicity of hydrazones and their metal complexes have been evaluated by MTT assay against normal 3T3-L1 cells. All

ligands exhibited 100% cell viability against normal 3T3-L1 cells. [Ni(FBH)(H₂O)(OAc)].2H₂O, [Ni(FN)(OAc)].H₂O, [Zn(FB)(OAc)].2.5H₂O, [Zn(FN)(OAc)].H₂O, [Zn(FIN)(OAc)] and [Zn(FMB)₂].2H₂O also showed 100% cell viability. [Cu(FB)(OAc)].H₂O, [Cu(FN)(OAc)].2H₂O, [Cu(FIN)(OAc)(H₂O)].2H₂O, [Cu(FMB)₂(H₂O)₂].H₂O showed high toxicity in almost all concentration against 3T3-L1 cells. Mild toxicity was observed for other complexes in concentration dependent manner.

Future outlook

- Molecular docking studies-In the field of molecular modeling, docking is a method which predicts the preferred orientation of one molecule to a second when bound to each other to form a stable complex. Knowledge of the preferred orientation in turn may be used to predict the strength of association or binding affinity between two molecules. The associations between biologically relevant molecules such as proteins, nucleic acids, carbohydrates, and lipids play a central role in signal transduction. Furthermore, the relative orientation of the two interacting partners may affect the type of signal produced. Therefore, docking is useful for predicting both the strength and type of signal produced. Molecular docking is one of the most frequently used methods in structure-based drug design, due to its ability to predict the binding-conformation of small molecule ligands to the appropriate target binding site. Characterisation of the binding behaviour plays an important role in rational design of drugs as well as to elucidate fundamental biochemical processes.

- *In-vivo* studies-testing effects of synthesized biological entities on whole, living organisms or cells.
- Synthesis of new ligands and metal complexes with different substituent groups for enhancing the biological activity.
- Development of the pharmacophores in to commercially viable cells.

.....❧.....

||| List of Publications |||

Publications

- [1] *Design, synthesis, antimicrobial and antioxidant activity of 3-formyl chromone hydrazone and their metal (II) complexes.* **Jessica Elizabeth Philip**, Shanty A. A., Sneha J. E., Kurup M. R. P. and Mohanan P. V., *Inorganica Chimica Acta* 469 (2018) 87-97 [IF: -2.046].
- [2] *Metal based biologically active compounds: Design, synthesis, DNA binding and antidiabetic activity of 6-methyl-3-formyl chromone derived hydrazones and their metal (II) complexes.* **Jessica Elizabeth Philip**, M. Shahid, M. R. P. Kurup, M. P. Velayudhan, *Journal of Photochemistry & Photobiology, B: Biology* 175 (2017) 178-191 [IF: - 2.673]
- [3] *Synthesis, characterization and biological studies of Schiff bases derived from heterocyclic moiety.* A. A. Shanty, **Jessica Elizabeth Philip**, E. J. Sneha, M. R. P. Kurup, S. Balachandran, P. V. Mohanan, *Bioorganic Chemistry* 70 (2017) 67-73 [IF: - 2.187].

Paper Presented (International)

- [1] *6-methyl-3-formyl chromone based hydrazones as inhibitors of α -glucosidase: Synthesis, characterization, in vitro evaluation.* **Jessica Elizabeth Philip** and Puzhavorparambil Velayudhan Mohanan, *Prof. K V Thomas Endowment International Symposium on New Trends in Applied Chemistry (NTAC - 2017)*, Sacred Heart College (Autonomous), Thevara.
- [2] *Synthesis, characterization and biological activities of some heterocyclic Schiff base derived from 3-carbaldehyde chromone.* **Jessica Elizabeth Philip**, P. V. Mohanan Presented at *International Conference on Materials for the Millennium (MatCon2016)* Cochin University of Science and Technology, Cochin, Kerala, India.

Paper Presented (National)

- [1] *Synthesis and DNA Binding Studies of Cu (II), Zn (II) and Ni (II) Chelates Based on tri-dentate ONO imine Ligand.* **Jessica Elizabeth Philip** and P.V. Mohanan, presented at *National seminar on Current Trends in Chemistry (CTriC-2017)*, Cochin University of Science and Technology, Cochin, Kerala, India.
- [2] *Synthesis and Anti-Diabetic Activity of 3-Formyl Chromone Derived Hydrazone and their Zinc (II) Complex.* **Jessica Elizabeth Philip** and Puzhavorparambil Velayudhan Mohanan, Presented at *29th Kerala Science Congress-2017* Marthoma College Thiruvalla.
- [3] **Jessica Elizabeth Philip**, P. V. Mohanan, Presented *14th Prof. K V Thomas Endowment National Seminar on “Molecular Approach to Current Advances in Chemistry” (Dec 2015)* at Sacred Heart College (Autonomous), Thevara .
- [4] *Synthesis and Antioxidant Activity of Some Heterocyclic Schiff Base Derived from Formylchromone.* **Jessica Elizabeth Philip**, S. Balachandran, P. V. Mohanan, Presented at *National seminar on Modern Trends in Chemistry (Nov 2015)* at Sree Kerala Varma College, Thrissur, Kerala, India.
- [5] *Synthesis, characterisation and antioxidant activity of new chromone derivatives.* **Jessica Elizabeth Philip**, S. Balachandran Nair, P. V. Mohanan, Presented at *National Conference on Recent Trends in Bio-Inorganic & Organometallic Chemistry (NCBOC-2015)*, Sri Shakthi Institute of Engineering & Technology, Coimbatore.
- [6] *Antioxidant activity of chromone hydrazones.* **Jessica Elizabeth Philip**, S. Balachandran Nair, P. V. Mohanan, Presented at *National seminar on Chemistry in Cancer Research (CCR 2015)*, St. Albert's College, Ernakulam, Kerala, India.

- [7] *Synthesis and Spectral Characterization of (E) -N'- (thiophen-2-ylmethylene) nicotinohydrazide.* **Jessica Elizabeth Philip**, S. Balachandran, P. V. Mohanan Presented, at *National Conference Current Trends in Chemistry (CTriC 2014)*, Cochin University of Science and Technology, Cochin, Kerala, India.
- [8] *Synthesis, Characterization and Antioxidant Activity of Hydrazones.* **Jessica Elizabeth Philip**, S. Balachandran, P. V. Mohanan, Presented at *National Conference 23rd Swadeshi Science Congress-2013*, Mahatma Gandhi University, Kottayam, Kerala, India.
- [9] *Antioxidant Activity of Hydroxy Derivatives of Benzaldehyde Schiff Base.* **Jessica Elizabeth Philip**, S. Balachandran, P. V. Mohanan, Presented at *National Seminar Current Trends in Chemistry (CTriC 2013)*, Cochin University of Science and Technology, Cochin, Kerala, India.

Workshops attended

- [1] Participated in the workshop on *Micro scale Experiments in Chemistry* at School of Chemical Sciences, Mahatma Gandhi University, Kottayam, Kerala, India [15-17 March 2018].
- [2] Participated *Science Academics three day Lecture workshop on Computational Quantum Chemistry* at Sacred Heart College (Autonomous), Thevara [5-7 January 2017].
- [3] Participated a workshop on *Computational Chemistry and Applications* by Srinivasa Ramanujan Institute for Basic Sciences, Kottayam-01, [30 December 2016-1 January 2017].
- [4] Participated a training programme on *Antimicrobial studies of metal complexes* conducted by Central Institute of Fisheries Technology, Indian Council of Agricultural Research, Willington Island, Matsyapuri, Cochin-29 [25-30 April 2016].

List of Publications

- [5] Participated Two Days workshop on Recent Trends in Inorganic-Organic Hybrid Materials at AMMRC, Mahatma Gandhi University, Kottayam, Kerala, India [27-28 January 2015].

....❧....

List of Abbreviations

A	- Adenine
AAS	- Atomic Absorption Spectroscopy
AIDS	- Acquired Immune Deficiency Syndrome
ANOVA	- Analysis of Variance
ATCC	- American Type Culture Collection
B.M.	- Bohr Magnetron
C	- Cytosine
Calc.	- Calculated
CFU	- Colony Forming Unit
Conc.	- Concentration
CT	- Calf Thymus
Cu	- Copper
DM	- Diabetic Mellitus
DMF	- Dimethyl Formamide
DMSO	- Dimethyl Sulphoxide
DNA	- Deoxyribonucleic Acid
DNS	- Dinitrosalicylic Acid
DPPH	- 2, 2-diphenyl picryl-hydroxyl
dsDNA	- Double Stranded DNA
DTG	- Differential Thermogravimetry
EB	- Ethidium Bromide
EI	- Enzyme Inhibitor
EPR/ESR	- Electron Paramagnetic Resonance/Electron Spin Resonance
ESI	- Electron Spray Ionization
FB	- Hydrazone derived from 3-formyl chromone and benzhydrazide
FBH	- Hydrazone derived from 3-formyl chromone and 4-hydroxybenzhydrazide
FIN	- Hydrazone derived from 3-formyl chromone and isonicotinic hydrazide
FMB	- Hydrazone derived from 6-methyl-3-formyl chromone and benzhydrazide

List of Abbreviations

FMBH	- Hydrazone derived from 6-methyl-3-formyl chromone and 4-hydroxybenzhydrazide
FMIN	- Hydrazone derived from 6-methyl-3-formyl chromone and isonicotinic hydrazide
FMN	- Hydrazone derived from 6-methyl-3-formyl chromone and nicotinic hydrazide
FN	- Hydrazone derived from 3-formyl chromone and nicotinic hydrazide
FT-IR	- Fourier Transform Infrared Spectroscopy
G	- Guanine
HIV	- Human Immunodeficiency Virus
I	- Inhibitor
IC ₅₀	- The concentration required to produce 50% inhibition
K _b	- Intrinsic Binding Constant
KBr	- Potassium Bromide
K _i	- Inhibition Constant
K _m	- Substrate concentration at which the velocity of the reaction is half-maxima.
LPS	- Lipopolysaccharide
M	- Molar
MHB	- Mueller-Hinton Broth
MIC	- Minimum Inhibitory Concentration
MLCT	- Metal to Ligand Charge Transfer
mM	- Millimolar
MTT	- (3-(4, 5-dimethylthiazol-2-yl)-2,5-diphenyltetrazolium bromide
Na ₂ HPO ₄ .2H ₂ O	- Disodium hydrogen phosphate
NaH ₂ PO ₄ .2H ₂ O	- Sodium dihydrogen orthophosphate
Ni	- Nickel
Obsd.	- Observed
pH	- Hydrogen ion concentration
p-NPG	- p-nitrophenyl-β-D-glucopyranoside
PPHG	- Postprandial Hyperglycemia
ppm	- Parts Per Million
RMDA	- Resazurin based Microtiter Dilution Assay
RT	- Room Temperature

[S]	-	Substrate Concentration
ssDNA	-	Single Stranded DNA
T	-	Thymine
TCNE	-	Tetracyanoethylene
TG	-	Thermogravimetry
TMS	-	Tetramethylsilane
Tris HCl	-	Tris (Hydroxymethyl)aminomethane
UV-Vis	-	Ultraviolet -Visible
V _{max}	-	Maximum Velocity of Reaction
XRD	-	X-Ray Diffraction
Zn	-	Zinc
ε	-	Molar Extinction Coefficient
η	-	Relative viscosity
λ _{max}	-	Maximum Wavelength
μM	-	Micro Molar
¹³ C NMR	-	Proton Decoupled Carbon Nuclear Magnetic Resonance
¹ H NMR	-	Proton Nuclear Magnetic Resonance.

.....❧.....